KWAME NKRUMAH UNIVERSITY OF SCIENCE AND TECHNOLOGY, KUMASI, GHANA

SOIL EROSION RISKS AND FARMERS' ADAPTATION STRATEGIES IN ANAMBRA STATE, NIGERIA

BY

CHRISTOPHER UCHE EZEH

(BSc. Geography, MSc. Climatology/GIS)

A Thesis submitted to the Department of Civil Engineering, College of Engineering in partial fulfillment of the requirements for the award of the degree of

DOCTOR OF PHILOSOPHY

in

Climate Change and Land Use

August 2023

CERTIFICATION

I hereby declare that this submission is my work toward the PhD degree in Climate Change and Land Use and that, to the best of my knowledge and belief, it contains no material previously published by another person nor material that has been accepted for the award of any other degree or diploma at Kwame Nkrumah University of Science and Technology, Kumasi or any other educational institution, except where due acknowledgement has been made in the thesis.

Christopher Uche Ezeh (PG9989719) Signature…………… Date…………..

(Student Name & ID)

Certified by:

Prof. Kwasi Preko Signature.................. Date...................
(Main Supervisor's name)

Prof. Kwaku A. Adjei Signature.................. Date......................
(Co-Supervisor's name)

Dr. Sarah Schönbrodt-Stitt Signature................... Date...................
(Co-Supervisor's name)

Prof. O. Igwe Signature.. ..... Date..................
(Co-Supervisor's name)

Certified by:

Prof. Sampson Oduro-Kwarteng Signature.................. Date.....................
(Head of Department's name)

DEDICATION

To my wife and children, and to all who were instrumental to my progress, and to the loving memory of my parents and uncle, who I lost while on this journey.

ABSTRACT

Soil erosion is a major land degradation problem in Anambra State, Nigeria. Research attention has focused mainly on gully erosion to the neglect of interrill erosion. Farmers' response to manage erosion menace is also scarcely studied. The study investigated soil erosion risks and farmers' adaptation strategies. The study objectives comprised the following: 1. Assessed the variability in rainfall in Anambra State, 2. Assessed soil characteristics and determined the in-situ soil loss, 3. Modelled soil erosion using the RUSLE model and 4. Appraised the farmers' adaptation strategies in Anambra State. The variations in rainfall were assessed using trend analysis, extraction of climate change indices following the ETCCDI, and the climatic water balance. Regression and correlation were used to determine the relationship between rainfall, and soil moisture with soil loss. The in-situ assessment was done during the 2022 rainy season at Isu-Aniocha, Aguleri, and Oko using runoff plots. The RUSLE model was used to determine the mean annual soil erosion rate in Anambra State. Then, the farmers were purposively surveyed using questionnaire to elicit information on their perception of soil erosion risks and their adaptation strategies. The results show that there was an increasing trend in the monthly, annual, and seasonal rainfall except for the MAM season. A significant positive correlation exists between soil loss and soil moisture. However, at Aguleri, it is not significant. High permeability of the soil suppressed the impact of soil moisture. Soil loss from the bare fallow was 6 to 11 times higher than that from the vegetated plot depending on the plot size. The mean annual soil loss in the field was 27.76 t $ha^{-1}yr^{-1}$ and that from the model was 25.25 t $ha^{-1}yr^{-1}$. The models' performance had a mean bias error (MBE) of -3.00 t ha^{-1} yr^{-1}, MAE of 9.34 t ha^{-1} yr^{-1}, and correlation coefficient of 0.88 indicating an underestimation of the soil erosion but with a good performance. This showed that the RUSLE model is good for erosion modelling and soil conservation planning in the State. Soil erosion increased from 2017 to 2022 (21.32 to 25.25 t ha^{-1} yr^{-1}) and to 31.22 and 31.79 t ha^{-1} yr^{-1} in 2060 under the SSP245 and SSP585 scenarios. The results showed that interannual changes in soil loss were highly influenced by the C-factor more than the erosivity. This does not necessarily imply that erosivity is unimportant but rather that its role in interannual variation was outweighed by the dynamics of the C-factor. The farmers perceive soil erosion as an environmental problem. However, their adaptation strategies were low. Thus, due to the rising soil erosion and poor adaptation by farmers in the State, the authority should embark on mass awareness creation by engaging the farmers on the need for the implementation of soil conservation measures.

TABLE OF CONTENTS

Contents

LIST OF TABLES

LIST OF FIGURES

LIST OF ABBREVIATIONS AND ACRONYMS

(R)USLE:	(Revised) Universal Soil Loss Equation
ACF:	Autoregression function
AGWA:	Automated Geospatial Watershed Assessment Tool
AnnAGNPS:	Annualised Agricultural Non-Point Source Model
ANSWERS:	Areal Nonpoint Source Watershed Environmental Response
BD:	Bulk density
C-factor:	Management factor
$CaCO_3$:	Calcium tetraoxocarbonate (iv)
CC:	Climate Change
CCA:	Climate Change Adaptation
CCI:	Climate Change Indices
CEC:	Cation Exchange Capacity
CHIRPS:	Climate Hazards Group InfraRed Precipitation with Station data
CO2:	Carbon dioxide
CPT:	Cone Penetration Test
CREAMS:	Chemicals, Runoff, and Erosion from Agricultural Management
cT:	Tropical continental air mass
CV:	Coefficient of Variation
CWBAL:	Climatic water balance
DEM:	Digital elevation model
DJF:	December January February season
DP:	Disturbed plot
EEA:	European Environmental Agency
EPIC:	Environmental Policy Integrated Climate model
EQM:	Empirical quantile mapping
ETCCDI:	Expert Team on Climate Change Detection and Indices
EUROSEM:	European Soil Erosion model
FAO:	Food Agricultural Organization
FTS:	Flat tillage system
GIS:	Geographic Information Systems
GUI:	Graphical user interface
IPCC:	Intergovernmental Panel on Climate Change
JJA:	June July August season
K factor:	Erodibility factor
KINEROS:	KINematic runoff and EROSion model
LGA:	Local Government Area
LL:	Liquid limit
LS-factor:	Length-slope factor
LULC:	Land Use and Land Cover Change
MAE:	Mean absolute error

MAM:	March-April-May season
MDD:	Maximum dry density
MMF:	Morgan-Morgan-Finney model
mT:	Tropical maritime air mass
NDVI:	Normalised Difference Vegetation Index
NEWMAP:	Nigerian Erosion and Watershed Management Project
NGO:	Non-Governmental Organization
NIMET:	Nigerian Meteorological Agency
NIR:	Near-Infra Red
OMC:	Optimum moisture content
P-factor:	Conservation practice factor
PBIAS:	Percentage of bias
PCP:	Precipitation
PERFECT:	Productivity, Erosion and Runoff Functions to Evaluate Conservation Techniques
PESERA:	Pan-European Soil Erosion Risk Assessment
PET:	Potential Evapotranspiration
PI:	Plastic index
PL:	Plastic limit
QGIS:	QGIS previously referred to as Quantum GIS
R-factor:	Rainfall erosivity
RMSE:	Root Means Square Error
SEAGIS:	Soil Erosion Assessment using GIS Service Simulation model
SLR:	Soil loss ratio
SOC:	Soil organic matter
SOM:	Soil organic matter
SON:	September October November season
SPL:	Stream Power Law
SSP:	Socioeconomic Shared Pathways
SWAT:	Soil and Water Assessment Tool Systems
TAMSAT:	Tropical Applications of Meteorology using SaTellite data and Ground-based Observations.
TOPOG:	TOPOGraphy model
UP:	Undisturbed plot
USCS:	Unified Soil Classification System
USDA-ARS:	United States Department for Agriculture-Agriculture research
USPED:	Unit Stream Power-based Erosion and Deposition
WASCAL:	West African Science Service Centre on Climate Change and Adapted land use
WaTEM/SEDEM:	Water and Tillage Erosion Model and Sediment Delivery
WEPP:	Watershed Erosion Prediction Project

ACKNOWLEDGEMENTS

My sincere gratitude to my Maker; the Alpha and Omega for His love and grace that enabled me to be part of the WASCAL family and be able to bring this journey to a fruitful end.

I also sincerely acknowledge the financial support provided by the German Ministry of Education (BMBF) for this research which was granted through the WASCAL Doctoral Research Programme on Climate Change and Land Use via the Graduate Research Programme on Climate Change and Land Use (GRP CCLU) in Kwame Nkrumah University of Science and Technology, Kumasi Ghana. I am profoundly appreciative of this immense support and generosity.

This journey was tough but with my ebullient supervisors' support, I could navigate to the end. I earnestly acknowledge and thank my principal supervisor, Prof. K. Preko for the moral, spiritual, academic and psychological support that kept motivating and inspiring me to persevere. He sacrificed his time and all in reading and supporting me to the end. I sincerely appreciate him and pray to God to keep blessing him.

It is with great pleasure and a heart full of appreciation that I acknowledge and thank the co-supervisory team members that included Prof. K.A. Adjei, Prof. O. Igwe, and Dr. S. Schönbrodt-Stitt. They are wonderful people to work with and their effort in re-shaping my life through this experience will forever be remembered.

I am also grateful to my mentor, Dr. Y. M. Asare for his time in guiding me through this journey. He devoted his time to seeing that I succeeded in this work. May you be blessed. I also acknowledge the support of Mrs Beatrice Osei Konadu of the Geoinformatics Department of KNUST Kumasi, Ghana. I also acknowledge the support from Mr Desmond Kemeh during the analysis stage of the work.

My special thanks to the jury members for their willingness to review and evaluate my thesis. Their comments and suggestions were critical and very much instrumental in improving the standard of the thesis. I also acknowledge the indefatigable and amiable Director of WASCAL KNUST, Prof. W. A. Agyare and his deputy, Prof. E. Forkuo for their inspiration and all the time they devoted to put up several trainings, workshops and seminars to improve our skills and knowledge towards achieving our goals as PhD researchers.

Finally, I extend my gratitude to all my wonderful colleagues (WASCAL CCLU 4th batch), all my friends, siblings, and all my relatives too numerous to mention here. I cannot end this section without acknowledging my wife, Jane and children who stood behind me and prayed endlessly for my success.

I also acknowledge the support from all the people who assisted me in one way or the other as I journeyed through the programme. I also thank Assoc. Prof. Surv. R.U. Ayadiuno, Prof. T.C. Nzeadibe, Rev. Fr. Michael of MTMSS Aguleri, and Director of Physical Planning, Federal Polytechnic Oko, Anambra State, Nigeria. I thank all my friends out there, too numerous to mention here.

1. INTRODUCTION

1.1 Background

Soil erosion is the dislodgement of topmost soil particles, their movement, and deposition. Soil erosion is a physical process driven by natural factors and it is often called geological erosion. However, accelerated soil erosion is induced by anthropogenic factors which have exacerbated the problem thereby posing risks to the environment and man. Risk is the potential of the occurrence of hazards, where a hazard is the likelihood of an external event or stress to occur in a given area within a specific time interval (de León, 2006). Adaptation refers to the ability to live with or adapt to a change in the environment which is irreversible.

Soil erosion is a severe environmental problem (Romshoo *et al*., 2012) and is nearly ubiquitous in all climatic belts (Mondal *et al*., 2015). Almost 1642 million hectares of global land are under attack by soil erosion (Li and Fang, 2016; Issaka and Ashraf, 2017). It is an environmental disaster with both on-site and off-site damages (Kou *et al*., 2016; Ayele *et al*., 2016). The on-site damages include deterioration of the soil's physical, chemical and biological properties and reduction of its productivity (Li and Fang, 2016). The off-site problems comprise sediment transportation and deposition, channel siltation (Mullan, 2013) and flooding. The financial loss associated with soil erosion is also enormous. For instance, in Nigeria, soil erosion gulps a huge amount from ecology funds to the tune of billions of Naira annually (Ifesinachi *et al*., 2015). Soil erosion degrades the soil thereby leading to soil quality and soil fertility decline (Francaviglia *et al*., 2023; Pimentel and Burgess, 2013). With world population expected to hit 9.3 billion, more food is required to feed them, yet erosion causes the loss of about 10 million ha of cropland annually (Pimentel and Burgess, 2013). Thus, effort should be intensified at soil conservation to stem the tide and save humanity from food insecurity. However, for an effective soil conservation, a firm understanding of the soil erosion dynamics is required.

The mechanism of soil erosion involves quite many natural and anthropogenic forces. That is, it involves the interplay of soil (Parras-Alcántara *et al.*, 2016) in terms of bulk density, porosity, and shear strength, topography in terms of the curvature, aspect and slope angle, rainfall in terms of its volume, intensity (Lanckriet *et al*., 2015) and temporal distribution, vegetation (Rahmati *et al.*, 2016) in terms of its composition, humus and biomass, roots' penetration, geology (Conforti *et al*., 2011) and anthropogenic activities.

The above-named factors of erosion can be grouped into three major classes, which are the conveyance force (energy), resistance (friction), and protection (Morgan, 2009). That is, some act to favour erosion while some counter its development. For instance, under natural conditions, agents of weathering and rainfall via gravitational forces and slopes tend to induce erosion, while the soil shear strength and vegetation offer resistance to erosion initiation. Erosivity factors induce erosion, while erodibility factors offer resistance due to soil attributes (Morgan, 2009). For instance, tillage may decrease the erodibility of clay soil but may accelerate that of sandy soil (Morgan, 2009). The binding forces of the plants' roots hold the soil together; the vegetation canopy counters the force of gravity by reducing the potential energy of the raindrop via interception. Also, the root system and accumulated organic matter slow down the kinetic energy of the overland flow or prevent its build-up by permitting much infiltration. Additionally, the vegetal cover might form dense cover for micro-organisms and rodents that facilitate soil formation. Also, their burrowing actions creates aeration and porosity which increase infiltration. Topography also acts as a force that promotes erosion. Steep slopes facilitate erosion, while flat terrains do not. Therefore, when the amount of resistance balances the force promoting it, erosion ceases or no change occurs in the landform.

Hence, soil erosion is initiated when the force of erosion is greater than the force opposing it. Thus, the movement of earth materials marks the beginning of a geomorphic activity. The initiation of geomorphic work leads to landform formation or transformation such that a given landform is traceable to the processes at work to shape it. Under natural conditions devoid of human impact, this geomorphic process is a slow, gradual process that will naturally balance itself. That is, under unchanged soil properties through time, soil formation rates usually balance the erosion rates (Morgan, 2009). Humans are a part of the natural system and has dominion over the other components of the system. Hence, human beings modified the other subsystems to their benefit, but their actions have strained them beyond the limit, and thus, it is now negatively impacting him. Under natural conditions, the rate of soil loss is generally in the range of 0.004 - 0.4 t $ha^{-1}yr^{-1}$ on moderate to steep relief, respectively (Morgan, 2009). But for man's influence, the rate has increased such that the rate of soil loss in agricultural land is 45 – 450 t $ha^{-1}yr^{-1}$ (Morgan, 2009). Thus, the amplified erosion results from man's influence owing to land cover and land use change.

The accelerated land degradation by man's action brings us to the gravest issue facing humanity- climate change. Thus, an enhanced runoff implies reduced soil moisture due to low infiltration and invariably low groundwater. This alters the hydrologic cycle and aggravates soil erosion. This is because infiltrated and percolated water is not a direct erosion hazard but promotes groundwater table. Again, the pattern of rainfall events in the future is still uncertain, including how it will affect erosion dynamics in the future. However, one certain thing is that the rate of erosion is increasing in many locations of the globe ,even in semi-arid regions (Arabameri and Pourghasemi, 2019).

Therefore, the challenge to scientists includes finding a way to reduce soil erosion or at least recover much of the land lost to erosion. Of more importance, therefore, is the development of management options that could minimise soil loss in the era of environmental change. The adaptation options should also be explored and the best approach developed. Achieving this requires a sound understanding of the processes that interact in a given location and the spatial variations among diverse locations. For instance, though vegetation protects the soil, its effectiveness varies with the type of vegetation. Thus, rainforest offers much more protection to the soil than savanna. Roose (1971) observed that soil loss ranges from 0.03 for rainforest belts to 0.1 (open grassland) to 0.20 $tha^{-1}yr^{-1}$ (dense grassland). However, with the vegetation removal for agriculture, the rate of soil loss became astronomically higher in the rainforest belt such that soil loss decreased from 90 (rainforest) to 8 (open grassland) to 26 t ha^{-1} in dense savanna (Morgan, 2009). Therefore, the presence of rainforest offers the highest protection to soils, yet its removal results in the worst soil loss. This is due to the interplay of the high erosive capacity of the convective rains of the tropics and the absence of tree cover which takes a long time to regrow, unlike grasslands that regrow quickly.

The changes in soil erosion over time due to the changing dynamics of land cover in the Anambra State are yet to be explored in detail by the scientific communities. Also, soil erosion assessment in-situ in the State is yet to receive adequate attention. Thus, this study investigated the variations in soil erosion in the State under varying soil conservation measures in the field and diverse degrees of land cover and rainfall over the years using the RUSLE model.

1.2 Objectives

The thesis' main aim was to assess the spatiotemporal patterns and changes in the soil erosion risks and farmers' adaptation strategies in Anambra State Nigeria.
The specific objectives are to:

- assess the variations in rainfall in the study area.
- assess the soil characteristics and determine the in-situ soil loss by water erosion.
- model soil erosion rates using the RUSLE model.
- assess the adaptation strategies of farmers.

1.3 Research questions

- o Have there been any variations in the seasonal and annual rainfall of Anambra State?
- o What is the rate of erosion?
- o Can the soil erosion rate be determined with a RUSLE model and to what extent have the erosion features changed over the years?
- o What are the farmers' adaptation strategies to soil erosion?

1.4 Research problem

Soil erosion is a major land degradation problem in Anambra State. Soil erosion degrades the soil and causes low crop productivity (Gupta, 2019), thus increasing the risk of famine and food insecurity. It is a major problem that gulps huge sums of money (Ifesinachi *et al.*, 2015), yet it seems to have defied the efforts aimed at tackling it. The problem is caused by the area's geomorphic characteristics such as the topography owing to the dip slope of the Awka-Orlu escarpment and the friable nature of the soils (Igwe, 2018). It is exacerbated by anthropogenic activities such as unsustainable agriculture and construction works (Igwe and Egbueri, 2018).

The problem was first observed in the early 20th century as mere gullies (Grove, 1951). However, due to increasing pressure on land by population explosion, urbanization, and development, it has expanded such that some are assuming ravine-like nature or becoming badland environments (Igwe, 2018; Egbueri and Igwe, 2020). The gullies have displaced many communities and still threaten others as they are still expanding.

There are several approaches to soil erosion studies such as plot measurement, modelling, tracing, and simulations. Modelling is the fastest approach that accelerates decision-making. Studies involving in-situ measurement or modelling are still nascent in the State. There are few to no studies implementing long-term soil erosion modelling with data that span decades. One of the few studies that employed long-term data albeit from remote sensing in Eastern Nigeria was Iro's study (Iro, 2018). It failed to estimate soil loss rather it assessed the dimensions of gully change. Nonetheless, these aspects are also critical to the efficient management of soil erosion. Also, much attention has been on gullies to the neglect of interrill erosion studies in the State.

However, soil erosion being a global problem requires a full understanding of its dynamics to proffer adequate solutions (Shruthi *et al.*, 2015). An understanding of its dynamics requires its study in the field and via modelling. However, there is little information on soil erosion dynamics from field measurements or using models in Anambra Nigeria. For instance, most of the studies were on geotechnical assessment or remote sensing (Igwe and Egbueri, 2018; Okoyeh *et al.*, 2014). Meanwhile, remote sensing hardly captures sheet and interrill erosion or does so at a very high cost. Soil erosion has been studied in the field (Mounirou *et al.*, 2022) and with models (Ganasri and Ramesh, 2016; Koirala *et al.*, 2019) in many parts of the world. However, such studies are limited in Anambra, especially in relation to land cover changes. Several soil erosion models exist such as AnnAGNPS (Young *et al.*, 1989), USPED (Mitas and Mitasova, 1998), and WEPP (Nearing *et al.*, 1989) among others. Many of them have limited applications in the developing world. However, RUSLE is easily adaptable in every region and is the most widely used erosion model (Alewell *et al.*, 2019; Kinnell, 2019). Hence, soil erosion was studied in-situ in the field and with the RUSLE model to improve our knowledge of soil erosion and conservation efforts in the State.

1.5 Scope of the study

The study covers Anambra State of Nigeria. It focused on water erosion but does not include fluvial erosion. It also excludes channel erosions like gullies and rills. The study conducted a thorough assessment of soil erosion risks resulting from interrills in Anambra State using runoff plots in the field and using the RUSLE model. It studied the impacts of vegetation, tillage, slope, and geology/soil on soil erosion. The impact of climate and land use dynamics on soil erosion was assessed using the RUSLE model. The model was used to forecast soil erosion rates in the future under the moderate and worst-case scenarios of greenhouse gas emission under climate change in the 2060s. I assessed the farmers' perception and awareness of soil erosion risks through questionnaires and interviews. The strategies employed by farmers to adapt to soil erosion risks were investigated. The study also identified the barriers that hinder farmers from adopting soil conservation measures.

1.6 Limitations of the study

The fieldwork was hampered by insecurity in eastern Nigeria, especially in the southern parts of Anambra State. This limited the fieldwork to the chosen locations. Another limitation is the insufficient time for a prolonged field experiment due to timeline. Also, the inability to secure automatic rain gauge for recording rain intensity limited the data to daily instead of minutes or hourly intensities so the study could not quantitatively account for the impact of rainfall intensity on soil loss.

The RUSLE model showed good performance in soil erosion prediction over Anambra State, Nigeria. However, the model's erosivity estimation was based on the mean annual rainfall. Also, the LS-factor was estimated from a coarse DEM of 30 m resolution but the estimation could have improved with a finer DEM resolution. Thus, estimation of erosivity using 30 mins intensity or DEM with finer resolution would improve the result.

The regression model's dependence on rainfall is a handicap because erosion is affected by multivariate factors. Model built on runoff better accounted for soil loss than the one based on rainfall and is recommended where runoff are available.

1.7 Organisation of the thesis

The thesis has six chapters. Chapter 1 focused on the overall introduction, scope, and objectives of the study. Chapter 2 was on the review of the literature related to soil erosion risks and adaptation strategies of farmers. Chapter 3 focused on the methodology that dealt with the description of the geography of the study area, the research methods, the description of the datasets used, and their preprocessing and processing methods. The results are presented in Chapter 4. Chapter 5 dealt with the general discussion while the last chapter, Chapter 6 comprised the conclusions and recommendations.

2. LITERATURE REVIEW

2.1 Introduction

Soil erosion is a severe environmental problem (Fernández-Raga *et al.,* 2017). It is caused by numerous factors including natural and human factors. These factors can be summed into energy factors (climate and topography), protective factors (vegetation cover and conservation practices), and resistance (geology/soil erodibility) (Borrelli, 2011) while the accelerated erosion is propelled by anthropogenic impact. The percentage contribution to soil erosion due to human impact vary from 43 % (deforestation), 29 % (overgrazing), 24 % (non-existence of conservation measures), to 4 % (over-exploitation of vegetation) (Borrelli, 2011). Soil erosion leads to ecosystem function degradation, poor agricultural yield, displaces communities and swallows farmlands (Ezeh *et al.*, 2021; Gupta, 2019; Sherka, 2023).

Soil erosion has been studied around the world by diverse disciplines employing diverse approaches. Qualitative and quantitative approaches from direct observations in the field to laboratory experiments (Stroosnijder, 2005; Tamta *et al.*, 2023). Others indirectly estimated soil erosion from sediments in outlets or reservoirs (Vanmaercke *et al.*, 2012). Remote sensing has also gained prominence in soil erosion monitoring and estimation (Iro, 2018). Also, several models have been developed to study erosion and aid soil conservation (Arnold *et al.*, 2012; Karydas *et al.*, 2014; Renard *et al.*, 1997; Young *et al.*, 1989).

Additionally, farmers' adaptation to soil erosion has been studied (Choudhury *et al.*, 2022; Huynh *et al.*, 2020). The adaptation measures employed by farmers comprise measures such as reduced tillage, cover crops, crop rotation, changes in cropping pattern, agroforestry (Choudhury *et al.*, 2022; Huynh *et al.*, 2020; Mitter *et al.*, 2014). Agriculture is considered one of the most climate-sensitive economic sectors (Mitter *et al.*, 2014). The vulnerability of a sector rises with increasing sensitivity and exposure but decreases with increasing adaptive capacity (Smit and Wandel, 2006). Yet, the stakeholders are unaware of the systems' complexity, the inherent uncertainties, and effectiveness of adaptation measure (Olesen *et al.*, 2011) which lead to inaction (Mitter *et al.*, 2014). Engaging farmers and other stakeholders is crucial in developing workable concepts and determining effective adaptation options (Webb and Stokes, 2012). An understanding of this complex dynamics of soil erosion will aid conservation planning in Anambra State.

2.2 Physicochemical soil characteristics

2.2.1 Physical properties

Slope materials are bound to fail due to shearing stresses caused by the force of gravity, water flow, and other triggers such as tectonic, seismic or construction activities. Soil strength increases with increasing use of farm machines due to compaction which decreases the moisture content (Hamza and Anderson, 2005). This is worsened by low SOM and overgrazing with the attendant poor vegetal cover that decrease soil fertility. Therefore, machine use in agriculture can alter the soil physicochemical properties, worsen runoff generation, and erosion (Hamza and Anderson, 2005; Woldeyohannis *et al.*, 2022). Also, soil compaction increases soil strength, thereby increasing soil resistance to root penetration and reduces infiltration (Hamza and Anderson, 2005). It affects soil health and increases runoff generation that may aggravate soil erosion. Soil strength reduces as the degree of saturation increases (Farooq *et al.*, 2016). Just as Gupta and Paul (2016) posited that slope geometry and strength of materials are the main factors that control slope stability. This can be described using the Mohr-Columb theory (Coulomb, 1773; Reeher *et al.*, 2023). The factor of safety for a shear surface is simply the ratio of shear strength to shear stress required for equilibrium (Duncan *et al.*, 2014). This relationship between these stresses was established by Mohr-Columb (eq. 2.1) (Hanbing Liu *et al.*, 2020).

$$\tau = c + \sigma \tan(\varphi) \qquad 2.1$$

where τ represents the shear strength, σ represents the normal stress to the shear surface, φ represents the angle of internal friction, and c represents the cohesion force of the material. Sticky soils like clays and silts under undrained conditions have an internal friction angle of zero. Their shear strength depends on the cohesive force while the angle of internal friction is critical in non-cohesive soils.

The Atterberg test distinguishes four soil states and is used to determine the consistency index of soils (Casagrande and Fadum, 1940). The liquid limit (LL) defines the water content at which the soil flows viscously in a cup when under a series of blows. The plastic index is expressed in equation 2.2. Clayey soils are usually associated with high plasticity but reduce with increasing silt content and tend to zero for soils with very little to no fines (Sowers and Sowers, 1970). Soils with a liquid limit of 25 % and above are likely to fail due to the likelihood of expansion (Mugagga *et al.*, 2012). A description of the plasticity ranges is given by Bell (2004) (Table 2. 1).

Table 2. 1. Ranges of plasticity

Range of Liquid Limit	Plasticity
<35	Low
35-50	intermediate
50-70	High
70-90	Very high
>90	Extra high

Source: Bell (2004).

Liquidity index is a measure of soil consistency such that when it is 100 %, the soil behaves like a liquid but when it is zero, it has reached its plastic limit but tends to negative values when the soil becomes drier than the plastic and takes the behaviour of a solid and become brittle under intense pressure (Arora, 2008).

$$PI = LL - PL \qquad 2.2$$

where LL is the liquid limit, PL is the plastic limit, PI is the plasticity index.

Compaction aims to improve the dry density of the soil. MDD has a negative relationship with LL, PL and PI but OMC has a positive correlation with them (KS *et al.*, 2015). Isikwue *et al.* (2012) showed that low moisture content reduces the cohesiveness of soils, hence making them easily detachable. Again, high rainfall also increases the pore water pressure of soils, thereby making them dispersible if clayey. Gao *et al.* (2016) opined that there is a relationship between hydro-mechanical behaviour and soil microstructure. Additionally, a linear relationship holds between shear strength and void ratio (Chen *et al.*, 2020). Understanding the soil compaction changes with moisture-content variations is vital for scheduling farm traffics and cultivation operation at suitable moisture content (Hamza and Anderson, 2005). Also, changes in dry density correlate with changes in macropore distribution (Yu *et al.*, 2019). Thus, the maximum permissible ground pressure of farm machines to allow satisfactory crop production decreases with a decrease in bulk density and rising soil moisture (Hamza and Anderson, 2005). Thus, soil compaction increases with rising moisture until the optimum moisture content (OMC) is reached. Above the OMC, rising moisture content leads to a decrease in compaction as the soil increasingly becomes plastic-like (Hamza and Anderson, 2005). The physical properties like soil compaction, bulk density, moisture content, and grain size of soils have a direct relationship with soil erodibility (Regazzoni *et al.*, 2008). Erodibility is affected by soil texture, structure, density, moisture content, swell, clay mineral, and pore pressure (Al-Madhhachi *et al.*, 2013). The grading of maximum dry density (MDD) according to Emesiobi (2000) is shown in Table 2. 2. Measures to improve soil quality by reducing compaction include; addition of SOM, controlled traffic, mechanical loosening such as deep ripping, and crop-pasture rotation (Hamza and Anderson, 2005). A strong relationship exists between soil compaction and SOM, SOC, and total nitrogen (Woldeyohannis *et al.*, 2022).

Table 2. 2. MDD grading

MDD(g/cm^3)	Remark
>2.1	Excellent
1.9 – 2.1	Good
1.7 – 1.9	Fair
1.6 – 1.7	Poor
1.1 – 1.6	Very poor

Source. Emesiobi (2000).

Permeability describes the capacity of soil material to transmit water when pressure is applied. It is obtained in the laboratory by observing the percolation rate of water via samples of known length and cross-sectional area in a known difference in the head (Johnson, 1963). Permeability is a vital property that relates to seepage which determines the movement of moisture within soil pores (Terzaghi *et al.*, 1996). The soil permeability coefficient (k) directly correlates with the square of its particle size (D) (Nelson, 1994). Arora (2008) derived a table of the coefficient of permeability (Table 2.3). Highly permeable soils have low moisture contents and reduced cohesiveness (Isikwue *et al.*, 2012). Darcy's law states that the rate of flow of water is proportional to the hydraulic gradient (eq. 2.3) (Johnson, 1963; Keller, 2017).

$$Q = kiA \qquad 2.3$$

where Q is the discharged quantity per unit time, A is the cross-sectional area of the permeable medium, i is the hydraulic gradient (i.e. the difference in head (h) divided by the flow length, (l)), and k is the coefficient of permeability.

Table 2.3. Classification of permeability coefficients

S/N	Soil type	Coefficient of K (mm/sec)	Remark
1	Clean gravel	10^{+1} to 10^{+2}	Very good
2	Coarse and medium sands	10^{-2} to 10^{+1}	Good
3	Fine sand, loose silt	10^{-4} to 10^{-2}	Fair
4	Dense silt	10^{-5} to 10^{-4}	Poor
5	Silty clay, clay	10^{-8} to 10^{-5}	Very Poor

Source. Arora (2008).

The permeability coefficient varies with soil type due to structure, grain size and degree of sorting (Johnson, 1963). Thus, it is lowest for clay and other fine-textured soils or highly compacted soils or soils with high bulk density but high for coarse-grained soils and gravel (Casagrande and Fadum, 1940; Johnson, 1963). Hence, soils with high permeability have good drainage and thus have low runoff generation and reduced soil erosion (Miller, 1994).

Particle size analysis and bulk density

Knowledge of the particle size distribution is vital in so many areas of research such as hydrology and thermal properties (Farhadi-Machekposhti *et al.*, 2020), erosion vulnerability (Borrelli, 2011; Fernández-Raga *et al.*, 2017), and microbiological soil activities (Frąc *et al.*, 2020). It is a basic physical property of the soil being a permanent and characteristic quantity and forms the foundation for determining other measures such as air-water relationship, pore size distribution, and moisture movement in the soil profile (Polakowski *et al.*, 2021).

The bulk density is related to soil compaction and greatly depends on soil mineral composition. Soils high in organic matter used to have a low bulk density. It is shown that higher bulk densities are associated with soils with slope stability (Tan, 2006). Soil bulk density which simply refers to soil weight per its unit volume (eq. 2.4) is a key physical property of soil that affects biomass productivity and invariably influences root growth and expansion (Lal and Kimble, 2001). It affects soil aeration, soil water regime, runoff, and erosion (Lal and Kimble, 2001). Soil bulk density is influenced by grain size distribution, soil organic carbon content (SOC), organic matter content, cation exchange capacity (CEC), exchangeable cations, flora and fauna, and climatic factors (Lal and Kimble, 2001). Soils rich in high-activity clays tend to have high bulk densities than soils low in clay and SOCs (Lal and Kimble, 2001). It is a property with which to calculate other physical properties like porosity, water retention, heat capacity, and compressibility (Ruehlmann and Körschens, 2009). It is also required to convert weight-based measures to volume- and area-based data (Ruehlmann and Körschens, 2009). The tensile strength of soils decreases with decreasing bulk density and rising moisture content (Zhang *et al.*, 2001). Soil strength affects soil erosion as it describes the resistance of soils to erosion (Zhang *et al*., 2001). Soil bulk density is negatively correlated with organic matter and carbon contents (Al-Shammary *et al.*, 2018; Chaudhari *et al.*, 2013).

$$BD = D/VD \qquad 2.4$$

where BD is bulk density, D is the dry weight of the soil core, VD is the volume of the dry soil core.

2.2.2 Chemical soil analysis

Soil erosion adversely impacts water resources and the net primary productivity of the land that stocks SOC (Olson *et al.*, 2016). Soil erosion leads to loss of SOC (Grahmann *et al.*, 2020; Olson *et al.*, 2016). SOC is vital for the aggregate stability of mollisols (Rubio *et al.*, 2021). Land use change significantly affects SOC stock, especially in fast-eroding landscapes (Olson *et al.*, 2016). Also, locations of low SOC stock correlated with eroding/eroded portions (Arunrat *et al.*, 2022) while areas of deposition are associated with high SOC stocks (Hancock *et al.*, 2019). More carbon is held in soils than in the atmosphere and vegetation, and so a little variation in soil carbon may alter atmospheric CO_2 concentration (Minasny and McBratney, 2018). Quantifying and understanding SOC and its dynamics is critical to soil conservation (Hancock *et al.*, 2019). Soil organic matter (SOM) is useful in nutrient storage and soil aggregation (McCauley *et al.*, 2009). SOM is a sink for CO_2 and it is a key indicator of soil health (McCauley *et al.*, 2009; Sharma, 2022). A decrease in SOM leads to decreased infiltration and increased soil erosion such that soil with less than 3.5 % organic matter is considered highly erodible (Efthimiou, 2020, 2018).

Soils can be acidic, neutral, or alkaline depending on their pH values. Thus, soil pH measures the degree of acidity or otherwise of a given soil (McCauley *et al.*, 2009). Soil is influenced by the mineral ions in the soil. Soils with high CECs will tend to be basic, and clay and SOM usually have higher CECs (McCauley *et al.*, 2009). The shear strength of clay soils varies with the constituent mineral contents. Thus, clay-rich kaolinite is more stable than montmorillonite as they resist expansion when wetted and has low erodibility (Efthimiou, 2018). The soil's shear strength determines its cohesiveness and resistance to shearing forces of water and mechanical loads and often describes the detachability of soil particles to the erosive impact of raindrops and runoff (Efthimiou, 2018).

2.3 Physical process of soil erosion

Soil is the basic resource for life sustenance (Wu *et al.*, 2022) including food production, medicines, ecosystem services, and fuel. About 19.65 M km^2 of global land is under human-induced land degradation of which water erosion is a major contributor (Eswaran *et al.*, 2019). Soil erosion by water has affected the world differently, with the worst affected continents being Asia and Africa (Oldeman, 1994) (Table 2.4).

Table 2.4. Soil erosion rates across different continents

Continent	Asia	Africa	Europe	South America	North America
Soil loss (Mha)	317	169	93	77	46

Source: Lal (2003).

Soil erosion is a dynamic process that comprises three main processes; detachment, transportation, and deposition (Morgan, 2009). The detachment is initiated by the potential energy of the falling raindrops and then transported by the kinetic energy of the moving runoff. The transportation is initiated once the runoff energy surpasses the interstitial forces binding the soil particles together or soil erodibility (Harmon *et al.*, 2001). The detached materials are transported from higher to lower ground due to the combined effects of gravity, soil properties, relief, lithology, climate, vegetation, climate, geomorphology and morphometry, and man (Morgan *et al.*, 1998; Morgan, 2009).

The forms and shapes on the earth's surface are a reflection of the denudation process at work in the area. Hence, the erosive agents corrode and carve the surface into rills, interrills and gullies depending on the competence of the overland flow (Bryan, 2000). The occurrence of the three processes is dependent on the stage of the erosional cycle according to the Davisian cycle of erosion. That is, whether at the upper, middle or lower stage. The upper stage is associated with detachment, the middle stage with transportation and corrasion, and the lower stage with deposition.

The most important detaching agent is the rain splash (Fernández-Raga *et al.*, 2017) which is dependent on its potential energy (rain intensity), rainfall amount and frequency (duration). A majority of detached soils during an erosion process are due to the rain splash effect (Borrelli, 2011).

In the transporting stage of erosion, the overland flow does a lot of work. However, to initiate the flow, certain conditions must be met. The falling rain is first absorbed via infiltration (Kirkby, 1985) and percolation until the soil becomes saturated, and the flow begins. However, in some cases, it can be generated when the falling rain overcomes infiltration. This infiltration-excess overland flow also called the Hortonian flow (Horton, 1933) is prevalent in places where the rainfall intensity exceeds the infiltration capacity. It is predominant on steep bare surfaces with high intensity such that the rain splash rearranges the soil particles reducing the pore spaces or areas with superficial crust (Cerdan *et al.*, 2002) such that runoff generates quickly without the soil being saturated.

However, the saturation-excess process (Dunne and Leopold, 1978) is common in places where the Hortonian process is rare, like in densely vegetated, gentle, and permeable soils. Vegetation promotes pore spaces and reduces the potential energy of the falling rain via interception such that the hydraulic conductivities are high (Dunne and Leopold, 1978). Runoff generation is also controlled by the antecedent soil moisture content (Dunne and Leopold, 1978). Thus, it is common in locations with very low elevations, such as plains, valley bottoms and convergent topography (Beven, 2001) and on very permeable soils. Nevertheless, the generation of runoff from either process is not mutually exclusive in any watershed (Walter *et al.*, 2003). Hence both can occur in the same watershed at different locations or at different times depending on the driving factors such as rainfall intensity, prior soil disturbance, its erodibility, and surface configuration.

The transport capacity of runoff is the maximum amount of load that it can carry without losing strength or deposition (Morgan, 2009). In a given flow, the detachment and transport are interlinked and their interaction is a reflection of the erosion or deposition dynamics (Hudson, 1995). The condition where one exceeds the other gives rise to a detachment-limited or transport-limited erosion process (Foster, 1982). Thus, detachment-limited erosion manifests when the flow is greater than the available load detached by the rain impact or overland flow. The transport-limited erosion is when the detached load possesses higher energy than that of the overland flow (Borrelli, 2011; Zerihun *et al.*, 2018).

Aside the rainfall erosivity and soil erodibility, there are still many other factors that influence soil erosion. These other factors might be considered spatial variables (Symeonakis, 2001). These variables can be grouped into two, namely the terrain and the ground cover variables. The terrain includes the geomorphic features or its surface configurations such as the altitude, hillslopes and slope length, aspect, and profile curvature among others. The ground cover variables include biomass canopy cover, and species diversity (Symeonakis, 2001).

However, the soil erosion menace is worsened by man's unsustainable exploitation of natural resources and poor land use. Additionally, to feed the world's burgeoning population, indiscriminate deforestation has compounded the problem. Therefore, erosion is at present majorly a product of man's actions rather than a natural factor (Castillo and Gómez, 2016; Chen *et al.,* 2018). This view contrasts earlier consensus held by old geomorphologists that soil erosion is mainly due to natural factors (Ofomata and Egboka, 1986). It is man's activities that have removed the vegetal cover, replacing it with crops and impermeable surfaces, thereby exposing the topsoil to various agents of mass wasting and erosion.

It has been asserted that rainfall will increase in some regions like the temperate regions but decrease in others (Trenberth, 2011; Dosio and Panitz, 2016). Guinean coast of Africa has been projected to experience increased extreme rain events (Bichet and Diedhiou, 2018; Faye and Akinsanola, 2022) though with uncertainties over some areas (Dosio *et al.*, 2020). The uncertainty with regards to the exact nature of precipitation such as changes in the patterns like onset, volume and intensity still limit intervention strategies and planning. Yet what is certain is that climate change accelerates erosivity and erosion in many places like the USA (Nearing *et al.*, 2004) and Africa.

Furthermore, climate factors are very critical to soil loss and the flow of matter on a slope of which the most significant is rainfall (Budnik, 2019). The variations in these factors reflect the variations in the dimensions or extent of transport of matter. The variations of rainfall in time have been recognised in literature where Stefenson (1986) cited by Budnik (2019) noted that the highest rainfall intensity occurs in the first half of the rain event (ie the first 30 mins) (Budnik, 2019). It is also observed that the rainfall comes with higher intensity at the periods of the onset of the rainy season (Budnik, 2019) at which soil erosion is also highest (Fang *et al.*, 2015). However, the amount of rain from a single event increase as the rainy season progresses. The highest intensity in the rainforest region occurs around the onset and toward the end of the rainy season (Ezeh *et al.*, 2016).

Therefore, Shruthil *et al.* (2015) called for soil erosion research to fully understand its dynamics which will facilitate mitigation and management. Since multivariate environmental factors affect soil erosion, it is pertinent to understand and recognise the relationships among these factors and the erosion to predict erosion-prone areas which will form critical steps for soil conservation and management (Zabihi *et al.*, 2018). Modelling is a fast approach to studying these dynamics to aid soil conservation.

Several models were developed for soil erosion assessment with varying strengths and weaknesses (Karydas *et al.*, 2014), some of which are listed in Table 2.5. They range from simplistic to complex robust ones that utilise huge data to generate several parameters that interact to yield results.

Table 2.5. Different models, their scales, outputs, and sources

Model	Type	Spatial scale	Temporal scale	Outputs	Source
USLE	Empirical	Hillslope	Annual	Erosion	(Wischmeier and Smith, 1978)
RUSLE	Empirical	Hillslope	Annual	Erosion	(Renard *et al.*, 1997)
USPED	Empirical/ conceptual	Watershed	Event/ annual	Erosion/ deposi-tion	(Mitas and Mitasova, 1998)
AGNPS	Conceptual	Small wa-tershed	Event/ conti-nuous	Runoff, peak rate, erosion, sediment yield	(Young *et al.*, 1989)
ANSWERS	Physical	Small wa-tershed	Event/ conti-nuous	Runoff, peak rate, erosion, sediment yield	(Beasley *et al.*, 1980)
CREAMS	Physical	Plot/field	Event/ conti-nuous	Erosion/ deposi-tion	(Foster *et al.*, 1981)
WEPP	Physical	Hillslope/ wa-tershed	Continuous	Runoff, sediment yield, soil loss	(Nearing *et al.*, 1989)
EUROSEM	Physical	Small wa-tershed	Event	Runoff, erosion, sediment	(Morgan *et al.*, 1998)
KINEROS	Physical	Hillslope/ small watershed	Event	Runoff, peak rate, erosion, sediment	(Smith, 1981)
SWAT	Conceptual	Watershed	Continuous	Runoff, peak rate, erosion, sediment yield	(Arnold *et al.*, 2012)

AGWA	Concep-tual/ physi-cal	Watershed	Continuous	Runoff, peak rate, erosion, sediment yield	(Miller *et al.*, 2007)
PERFECT	Physical	Plot/field	Continuous	Runoff, erosion	(Littleboy *et al.*, 1992)
TOPOG	Physical	Hillslope		Erosion hazard	(O'loughlin, 1986)
EROSION-3D	Physical	Watershed	Event	Runoff, erosion, sediment	(Schmidt *et al.*, 1999)
MMF	Empirical/ conceptual	Hillslope/wa-tershed	Annual	Runoff/erosion	(Morgan *et al.*, 1984)
THORNES	Concep-tual/ empi-rical	Hillslope/wa-tershed	Annual	Runoff, erosion	(Francis and Thornes, 1990)
EPIC	Physical	Hillslope/wa-tershed	Continuous	Erosion	(Williams *et al.*, 1983)
SE-DEM/Wa-TEM	Conceptual	watershed	Annual	Erosion	(Van Rompaey *et al.*, 2001)
SEAGIS	Empiri-cal/concep-tual	watershed	Annual	Erosion, sediment yield	(DHI, 1999)
PESERA	Physical	Hillslope/regio-nal	Continuous	Runoff, erosion, sediments	(Kirkby *et al.*, 2004)
SPL	Empirical/ conceptual	Watershed/ri-ver	Annual	Fluvial erosion, ri-ver incision	(Stock and Montgomery, 1999)

Source: Merrit *et al.* (2003); Borrelli (2011); Bormann (2013); Karydas *et al.* (2014).

However, most of these models have limited applications in the developing world. This is due partly to the too-robust data requirement and the difficulty of parameterisation and integration of all the factors of erosion (Arabameri *et al.*, 2019b). Additionally, the dearth of data compounds the problem of model application in the developing world (Arabameri *et al.*, 2019a). Thus, RUSLE which is easily adaptable to diverse regions and is the most widely used model (Alewell *et al.*, 2019; Benavidez *et al.*, 2018; Kinnell, 2019) is used in the study.

Nevertheless, most studies have focused on using imageries and UAVs to assess the effects of land use change on erosion. These technologies do not capture small erosion features such as interrill and rill erosion. Thus, it is pertinent to carry out an in-depth study of soil erosion in many parts of southeastern Nigeria as notable areas of severe erosion (Lal, 1990). Only a very few studies have assessed soil loss rates in Anambra State (Ajibade *et al.*, 2020; Egbueri *et al.*, 2022; Fagbohun *et al.*, 2016). Again, these studies were done using the RUSLE model with no data to validate the result. Only Egbueri *et al.* (2022) attempted to validate their results albeit using Multi-criteria decision analysis which simply entails validating soil erosion susceptibility zones rather than soil loss. Additionally, only very few studies exist that assessed the adaptation strategies of farmers in the area. Hence, the current study estimated soil loss and runoff in the field, predicted soil erosion using the RUSLE model and assessed the adaptation strategies of the farmers in the State.

2.4 Soil erosion in Anambra State

Anambra State is notable for soil erosion and several studies abound on its dynamics. For instance, Osadebe *et al.* (2014) looked at the stability of the gully walls in the Agulu-Nanka-Oko gully erosion complex using an empirical approach. Their interest was mainly in the gully wall profiles and how they can be predicted. Onyeka *et al.* (2019) added that the menace requires a target-oriented and structured procedure which comprises erosion identification, assessment and hazard handling. Okoli also working from the engineering perspective and employing Saburo's equation found that the area is highly susceptible to erosion due to very intense rainfall and weak cohesive soil (Okoli, 2014). Igbokwe *et al.* (2008) employed remote sensing and GIS to map the gully locations in the area. They attempted to model soil loss but was not validated due to the paucity of data.

Away from the engineering perspective, Okoyeh *et al*. (2014) and Igwe and Egbueri (2018) utilised geomorphologic, hydrologic and geophysical data to investigate the underlying causes of gully erosion. Their result shows that the soil bulk density and organic matter range from 1610 to 1740 kgm^{-3} and 0.32 % to 0.46 %, respectively which shows the area is dominated by porous, poorly cemented coarse materials (Okoyeh *et al.*, 2014). They showed that the States in the Southeast with the majority of gully locations are Anambra with 700 and Enugu with 600 (Igbokwe *et al.*, 2008; Okoyeh *et al.*, 2014). Thus, Okoyeh *et al.* (2014) add that 37 %, 28 % and 35 % of the Anambra's landmass is severely, moderately and mildly gullied, respectively. The increasing gully sizes are due to weak soil, bare surface and dip slope of the area (Igbokwe *et al.*, 2008; Okoyeh *et al.*, 2014; Igwe and Egbueri, 2018). The highly gullied area (the Nanka axis) has a low soil moisture content, an indication of unsaturation, low cohesion and low angle of particle friction (Igwe and Egbueri, 2018).

Also, Gobin *et al.* (1999) employed a biophysical and participatory research approach to erosion study in the Southeast focusing mainly on the Udi-Nsukka Cuesta. They reveal that measured runoff and infiltration rates were at variance with reported runoff and soil loss. They used the modified Universal Soil Loss Equation to model soil loss in the area. Soil loss on the escarpment was 10 to 100 times higher than that on the plateau (Gobin *et al.*, 1999). They add that ravine and gully formations result from a combination of infrastructure, geohydrology, topography, vegetation and land use (Gobin *et al.*, 1999). Their findings did not differ from previous and later studies in the area such as those by Egboka and Okpoko (1984); Egboka *et al.* (2019) and Igwe and Egbueri (2018). The complex interaction among diverse factors that drive soil erosion evolution was not explored. Also, the participatory approach utilised was not different from that of Simpson (2010). It did not elicit information from the participants beyond practices of land tenure and spatial land use patterns as it regards soil erosion.

The majority of other studies were reviews of the State of soil erosion in the region. Such studies include Egboka and Okpoko (1984); Obiadi *et al.* (2011) among others. Obiadi *et al.* (2011) advised a specific and multidisciplinary approach to gully intervention in the area. Egboka *et al.* (2019), combining a mix of review and remote sensing, assert that rainfall and geology are the major causes of soil erosion in the area. Also, Egboka and Okpoko (1984) reported that the gully growth rate is about 20-50 m per year. They add that the erosion menace began in the 1850s and the British colonial

Office endeavoured to control it by constructing dams and planting trees, which failed just like current engineering measures by State and National government is failing (Egboka and Okpoko, 1984). Egboka and Okpoko (1984) suggested the declaration of the affected areas as disaster areas with human movement and agricultural activities restricted or controlled and the stoppage of the structural control measures.

Using a qualitative study approach, Nwobodo *et al.* (2018) found that farmers in Anambra are disposed to use erosion control measures. They also found from the respondents that the major causes of erosion in the area are rainfall and poor road construction. In a similar vein, Angela and Ezeomedo (2018) found that the majority of farmers in the Akpo region of the State are highly tied to their land as a majority have below tertiary education. Yet, gully erosion has degraded their land resulting in low yield. Chinweze (2017) argued that the causes of erosion in the area are mainly climate change, anthropogenic activities such as poor farming practices, road construction and laterite mining. Also, nearly 1769.52 km^2 of the State is severely eroded, 1316.58 km^2 is moderately eroded and 1416.12 km^2 is mildly eroded (Chinweze, 2017, 2019). The consequences of gully erosion include displacement of communities, loss of lives, loss of farmland, and destruction of houses and highways (Chinweze, 2017, 2019).

Additionally, Egbueri and Igwe (2020) employed hydro-geomorphologic characteristics to study the gullies in Anambra State where they found that hydrogeomorphology and soil engineering properties significantly influence gullying processes in the area. However, the gullies are more in the area underlain by the Nanka formation than the areas underlain by the Ogwashi formation, a reflection of the varying hydro-geomorphologic characteristics. It was found that the gullies have inclination angles of over 30^o which induce landslides (Egbueri and Igwe, 2020). They also indicate that the upland region dominated by Nanka sand has slopes in the range of 30^o to 85^o with a mean of about 60^o. This is one of the most current studies that covered the whole State from a hydrogeomorphic perspective, however, it was not comprehensive as they too admitted, that further studies should incorporate remote sensing, GIS and soil loss modelling.

Additionally, less attention was accorded to interrill erosion in the State which threatens food security. Thus, this study assessed interrill erosion in the field, also with a model and engaged the farmers to learn their adaptation strategies.

2.5 Methodological approaches

Several approaches have been adopted in soil erosion research. Where data are available, estimation and prediction of soil loss have been conducted using diverse models. However, in data-scarce areas, the utilisation of remote sensing and GIS have been explored to assess soil erosion. Nevertheless, this does not remove the necessity for fieldwork in a geomorphic study rather it reinforces and reemphasizes its importance and place in geosciences (Chorley and Kennedy, 1971; Mentlik and Stacke, 2015). Hence, a combination of remote sensing, GIS, and fieldwork are used to assess the spatiotemporal dynamics of soil erosion.

Soil loss measurement or estimation is a very herculean task and it is usually estimated with less accuracy (Bosco *et al.*, 2015). It seems difficult to measure directly in the field using experimental plots, erosion markers (137Cs) or even river sediment yield at outlets (Bosco *et al.*, 2015). In recent times though, there have been few successes, especially with 137Cs (Evans *et al.*, 2017). It is also financially expensive and difficult (Fernández-Raga *et al.,* 2017; Khaledi Darvishan *et al.,* 2014). Further, the accuracy of the assessment with tracers has been questioned (Evans, 2017; Evans *et al.*, 2017). Due to this difficulty, measurement in the field is rare and often replaced with sediment yield measurement in reservoirs (Bosco and de Rigo, 2013). Nevertheless, sediment yield is not a true representation of soil erosion estimated with the USLE family of models (Vanmaercke *et al.*, 2014).

Most often it is estimated with empirical equations based on linear relationships such as USLE or RUSLE, and INTERO (Prasuhn *et al.*, 2013; de Hipt *et al.*, 2019) as they offer viable options and are less data-demanding (Bosco and de Rigo, 2013). Additionally, remote sensing is another option that has aided soil erosion research. However, it has its limitations in that for soil erosion studies, very high-resolution images are required, which are limited and very expensive (Bosco *et al.*, 2015). Furthermore, there is no standardised operational erosion assessment using satellite data due to the complexity and variability of soil erosion processes (Vrieling, 2006). More so, its use in very humid regions is hampered by cloud cover and it hardly captures sheet and interrill erosion.

Though the robust physically distributed models like AnnAGNPS, SWAT, WEPP, PESERA etc offer scientifically sound methods for predicting soil loss, however; they are input-data-intensive which most often are difficult to acquire (Bras *et al.*, 2003). For these challenges, the lumped regression-based models perform best in several case studies than the complex physically distributed models (Bosco and de Rigo, 2013; De Vente *et al.*, 2013).

Hence, it is opined that robust empirical models could provide vital support for risk managers or researchers involved in decision-making processes (Bosco *et al.*, 2015). However, a key limitation of empirical models is that they do not necessarily model the right process and might only be used for the purpose for which they were developed (Bosco *et al.*, 2015). Therefore, increasingly needed, is for the computational methods to be integrated with reproducible open-source software as it is with QGIS and R.

Most of the models have been integrated with open-source software, especially GIS. However, the family of models based on USLE have the added advantage of having been applied to different regions and climatic belts and yet have performed practically well (Bosco *et al.*, 2009, 2015). The RUSLE are the most widely used erosion models (Alewell *et al*., 2019; Benavidez *et al*., 2018; Kinnell, 2019).

2.6 In-situ soil erosion assessment in the field

The need for field experiments/fieldwork in geosciences cannot be overemphasized. It has been argued that there cannot be geography without fieldwork (Chorley *et al.*, 1984; Mentlik and Stacke, 2015). Stroosnijder (2005) added that it is an illusion to assume that the importance of fieldwork can be overtaken by the application of technology to erosion studies. This is because the technologies require measured data for their calibration and/or validation to ensure their reliability. Field plots are one of the most effective approaches to assessing management effects on runoff and soil loss under varying cover management, and natural and simulated rainfall (Evelpidou *et al.*, 2013; Wendt *et al.*, 1986). The dynamics of runoff and erosion under varying degrees of treatment underscore the fact that field plots are associated with high variability in runoff and soil loss (Mounirou *et al.*, 2022; Wendt *et al.*, 1986). Such variations confine the interpretation of the data (Wendt *et al.*, 1986). Sources of such variations abound ranging from differences in rainfall intensity and raindrop sizes, surface water films, aggregate stability, formation and break-up of debris dams during events, tillage-induced plot differences, slope angles and length, soil type to issues of technicalities (Wendt *et al.*, 1986; Fiener *et al.*, 2019; Mounirou *et al.*, 2022). Highly porous soils have high infiltration capacity and good drainage but low runoff output (Miller, 1994). Also, for its fine drainage, soil loss is minimal due to a higher time for runoff concentration.

Field plots studies are divided into experiment and observation (Roels, 1985). It is an experiment when one or more factors of erosion are controlled but observation when the measurement is made under a natural condition without interference.

Soil loss is found to be minimal in land with soil conservation measures but worse in intensively tilled and cropped soils (Grahmann *et al.*, 2022; Keesstra *et al.*, 2016). Erosion is found to be worse in soils undergoing land cover changes and vegetation losses (Borrelli *et al.*, 2018, 2016). Runoff and soil loss are found to be higher on bare soils than on covered soils (Oza *et al.*, 2022). Of the several factors of erosion, hydrology, soil erodibility and soil transportability are impractically controllable (Choi *et al.*, 2005) and so are unmodified in erosion studies and management. Soil loss estimation from runoff plots and erosion pins is higher than those from sediment yields from catchments (Vanmaercke *et al.*, 2012; Millington and Cleland, 2017). However, the variations are higher for larger basins such that the smaller the catchments, the closer to agreement the results became with the soil loss from plots (Vanmaercke *et al.*, 2012). Also, soil losses generated in closed plots decline with time such that less to no sediment is got after several years (Boix-Fayos *et al.*, 2006). The threshold initiating soil loss increased with time but remained the same for runoff generation (Boix-Fayos *et al.*, 2006).

Further, Duley and Ackerman (1934) found that on many occasions, runoff and soil loss from plots with shorter slope lengths surpassed those from plots with longer slope lengths though soil loss results were not significant statistically. Zingg (1940) added that doubling the slope angle increases soil loss 2.8 times while doubling the slope length leads to a 3.03 times increase in soil loss.

It should be noted that the dominant erosion type in the plots is sheet erosion. Plots are designed to mimic the original USLE plots as the model was developed for soil conservation and management in agricultural lands. Thus, it has been stated that the original plots upon which the USLE model was based, the plots were often tilled to eliminate rill and so no record of rill occurrence is available in the USLE database (Kinnell, 2016). Additionally, it is argued that when installing experimental plots they are on bare fallow conditions to use some of the factors in the USLE model (Kinnell, 2016). When this is done, then soil losses can be determined by considering that erodibility values are constant across the fallow landscapes with management factors and practice factors being assigned unity (C =1, P =1) (Kinnell, 2016). The optimum model should be based on duplicate plots. However, this assumption is not faultless as it is shown that relationships between duplicate plots are imperfect (Wendt *et al.*, 1986). This is due to spatial variations of soil properties with locations. That is, soil attributes across plots or landscapes are rarely homogenous (Kinnell, 2016) as some degrees of variations are expected in their texture, bulk density, and organic matter content among others. Despite considerable efforts at managing replicates, variations in event soil losses are unavoidable (Bagarello *et al.*, 2011).

Detachment of soil materials increases with rainfall intensity (Ma *et al.*, 2014). That is, the potential and kinetic energies of raindrops/runoff are critical to soil detachment and dislocation (Fernández-Raga *et al.*, 2021, 2017).

Additionally, higher soil losses have been recorded on tilled lands (Biddoccu *et al.*, 2014; Cerdà, 2000). However, Fang *et al*'s (2017) study found a contrasting result in that higher soil losses were found on bare lands followed by cropland. It is shown that soil loss sharply increases as slopes become steeper (Ziadat and Taimeh, 2013). Thus, Wischmeier and Smith (1978) opined that soil loss is much more rapid than runoff. Most of the variations in soil loss have been attributed to the slope (Fagbohun *et al.*, 2016; Ziadat and Taimeh, 2013). However, this is also dependent on the soil properties and surface roughness (Mah *et al.*, 1992). Soil erosion has a positive correlation with slope and vegetal cover (Shi *et al*., 2022). Also, Vanmaercke *et al.* (2014) find that strong relationships exist between sediment yield and slope and lithology but not with climate variables. Land use and land cover change also significantly impact soil loss as it increases more on agricultural lands than scrubland (Cerdà, 2000). Organic matter content increases the aggregate stability of the soil and infiltration rate which in turn are enhanced by a dense vegetal cover (Cerdà, 2000). Consequently, scrublands and agricultural lands with sustainable land management practices experience low soil erosion rates and pose less danger to ecosystem health (Fernández-Raga *et al.*, 2017; López-Vicente *et al.*, 2017; Prosdocimi *et al.*, 2016). Against this background, it is vital to increase knowledge and understanding of erosion processes through research (field studies and modelling) to proffer appropriate conservation practices most suitable to a specific site. This is because understanding soil erosion dynamics and processes is key to applying suitable management techniques that control soil erosion risks (Keesstra *et al.*, 2016; Shruthi *et al.*, 2015).

Soil loss characteristics have been studied using different methods such as runoff plots, photogrammetry, rainfall simulator and radioactive dating/tracing. However, rainfall simulation does not completely replicate a truly natural environment and so the experiment is carried out in a controlled but modified environment (Lassu *et al.*, 2015). Also, it can be quite costly. It is difficult to reproduce rainfall intensities with similar

kinetic energy as that observed in the open field during natural rainstorms (Fernández-Raga *et al.,* 2017; Lassu *et al.,* 2015). It requires the movement of soil materials to the laboratory which leads to soil disturbance unlike measurements taken in a natural open environment. Also, the use of radioactive tracing involves an individual determination of the trajectories that particles run which requires an objective photographic treatment and analysis. The process is complex, laborious and very expensive (Fernández-Raga *et al.,* 2017; Khaledi Darvishan *et al.,* 2014). Furthermore, it has been noted that erosion pins give low rates of erosion (Hancock *et al.*, 2015). Also, tracers are associated with over-estimation of erosion (Evans *et al.*, 2017). Furthermore, it has been recommended to use erosion pins in areas of substantive soil loss and badlands (Boardman and Favis-Mortlock, 2016).
Thus, runoff plots remain the most viable and used method of soil loss estimation which are utilised for model validation, designing soil conservation measures and planning purposes. However, measurement under natural conditions is costly and difficult to control the factors involved (Fernández-Raga *et al.,* 2017).

Soil loss estimations in the field are critical as scholars contend that sediment yield from rivers is unsuitable for use to model soil erosion in a catchment (Vanmaercke *et al.*, 2012). This is because soil loss estimates are generally ten times lower than the sediment yield (Vanmaercke *et al.*, 2012).

2.7 Description of the RUSLE model

The RUSLE model is the most widely used soil erosion model (Alewell *et al*., 2019; Benavidez *et al.*, 2018; Ghosal and Bhattacharya, 2020; Kinnell, 2019). It is an empirical model that estimates soil loss by integrating six main risk factors of erosion (eq. 2.5). These factors include rainfall erosivity (R-factor), soil erodibility (K factor), Slope steepness and length factors (together referred to as topographic factor) (LS-factor), Cover management factor (C-factor), and conservation practice factor (P-factor). RUSLE estimates a long-term average of annual soil loss from interrill erosion (Ghosal and Bhattacharya, 2020; Kinnell, 2019; Renard *et al.*, 1997).

$$As = R \times K \times LS \times C \times S \qquad 2.5$$

where A_S is the mean annual soil loss in metric tonnes per hectare per year (t/ha/yr), R is rainfall erosivity in megajoule millimetres per hectare per hour per year (MJ mm ha^{-1} h^{-1} yr^{-1}), K is soil erodibility in metric tonnes hours per megajoules per millimetre t ha h $(ha \cdot MJ \cdot mm)^{-1}$, LS is the topographic factor, C is the cover management factor, and P is conservation/support practice.

The last three factors are dimensionless (Andreoli, 2018; Benavidez *et al.*, 2018; Wischmeier and Smith, 1978). The mean annual soil loss ranges between 0 and infinity and in practice, it varies between 0 and 5 t $ha^{-1}yr^{-1}$ for interril erosion but can reach over 1000 t $ha^{-1}yr^{-1}$ in areas with gullies (Andreoli 2018).

The original version of the model is the Universal Soil Loss Equation USLE developed in the USA at a farm plot scale to assess agricultural land (Benavidez *et al.*, 2018; Kinnell, 2019; Wischmeier and Smith, 1978). It has gained wider acceptance and is now applied in many other climatic regions (Benavidez *et al.*, 2018). The original plot comprises a 22.1 m long and approximately 1.83 m wide on a slope of 9 % (Wischmeier and Smith 1978). The USLE was developed for plot scale study and performs best on medium textured soils, on slope ranges of 3 – 18 % and length of 400 feet with managed consistent cropping (Benavidez *et al.*, 2018; Wischmeier and Smith, 1978). Its use outside this definition requires some careful parameterisation with the attendant uncertainty. As a result, the model was upgraded and revised, and thus the RUSLE was developed (Benavidez *et al.*, 2018; Renard *et al.*, 1997).

The preference for the RUSLE model over others stems from its simplicity of use, low data requirement, adaptability to diverse climates and regions, and its integration into the GIS environment. However, the model faces some challenges such as its inability to estimate soil loss from gullies, landslides, and mass movements (Benavidez *et al.*, 2018; Ghosal and Bhattacharya, 2020). Another challenge is the abuse of its use (Kinnell, 2010) and the lack of data for validating the model in several studies.

2.7.1 Rainfall erosivity (R) factor

The R-factor accounts for the effects of rainfall on soil erosion which reflects the impact of the kinetic energy of rainfall-runoff on soil erosion. In the absence of other factors or holding them constant, the rate of erosion is directly proportional to erosivity (Shamshad *et al.*, 2008). The R-factor is expressed as 30-min intensity EI_{30} which reliably accounts for rainfall-erosion potential (Ghosal and Bhattacharya, 2020). Thus, the total annual EI value is the rainfall-erosion index. However, due to data unavailability with detailed temporal scales, alternative equations have been developed that correlate the R-factor with the available monthly or annual data (Alewell *et al.*, 2019; Benavidez *et al.*, 2018; Diodato *et al.*, 2013; Ghosal and Bhattacharya, 2020; Roose, 1975). The R-factor of Wischmeier and Smith (1958) works fine in temperate regions but not so in the tropics (Nill *et al.*, 1996). More so, the intensities of rain in the tropics can be excessively high reaching 340 mm/h to 800 mm/h as observed, respectively, in Southern Africa and Jamaica (El-Swaify and Dangler, 1982; Nill *et al.*, 1996).

Most of these intensities occur within the first minutes of most storms (Budnik, 2019; Nill *et al.*, 1996). The R-factor has been criticised for overestimating large storms from which only little runoff results and underestimating small storms associated with high runoff (Foster, 1982; Foster *et al.*, 1981). Thus, several algorithms have been devised to estimate rainfall erosivity based on monthly and annual rainfall data. Hurni (1985) devised one for Ethiopia. In West Africa, an erosivity equation based on annual rainfall was devised (eq.2.6) (Morgan *et al.*, 1998; Roose, 1977).

$$R = 0.5 \times AP \qquad 2.6$$

where R is erosivity, and AP is annual rainfall/precipitation.

It is the rainfall aggressiveness factor that varies from 0 to infinity. In humid tropical climates, it reaches above 1000 MJ mm $(ha\cdot h\cdot year)^{-1}$ and can exceed 3000 MJ mm $(ha\cdot h\cdot yr)^{-1}$ (Andreoli, 2018; Dumas *et al.*, 2010).

2.7.2 Erodibility K factor

The erodibility factor expresses the average soil loss occurring per unit of erosivity (Kinnell, 2019). That is, it accounts for the influence of soil properties on slope susceptibility to soil erosion (Renard *et al.*, 1997; Römkens *et al.*, 1997). The K factor value was originally estimated as the ratio of the event soil loss from a unit plot to the maximum 30-min1utes rainfall intensity (Wischmeier and Smith, 1978). It is estimated from soil loss and runoff plot attributes.

However, due to the technicalities and difficulties associated with it, the K factor values are estimated from soil properties (Wischmeier and Mannering, 1969). As a result, equation (2.7) was developed to estimate the K factor where soil properties of permeability, organic matter, and silt content are available (Wischmeier and Johnson 1971). To facilitate its use, Wischmeier and Smith (1978) developed a nomograph for K factor values.

$$K = \left[2.1\left(10^{-4}\right)\left(12 - OM\right)M^{1.14} + 3.25\left(s - 2\right) + 2.5\left(\rho - 3\right)\right]/100 \qquad 2.7$$

where K is the erodibility factor, OM is the percentage of organic matter, M is the percentage of silt, s is soil structure and ρ is permeability class.

A higher value of soil erodibility is an indication of the high susceptibility of the soil to erosion (Adornado *et al*., 2009). However, other equations have been devised to estimate the k factor due to the unavailability of some properties like structure and profile permeability. Some estimated the K factor value using the information on soil colour (Phinzi and Ngetar, 2019), while others used the textural classes, and a combination of some other attributes (Williams *et al.*, 1983). Thus, with the availability of soil carbon and textural classes, the erodibility can be determined (eq. 2.8) (Williams *et al.*, 1983). Soil erodibility estimation is still a subject of tests and verifications as the most suitable estimation method remains an open question (Kruk, 2021). However, the algorithm presented in equation (2.10) (Wawer *et al.*, 2005) is widely used in literature too. It is widely used in the tropics and has been shown to estimate the K factor value reasonably well (Tsige *et al.*, 2022). Furthermore, models that employ both textural classes and soil organic matter/carbon or other attributes perform better than those that consider only particle sizes (Adhikary *et al.*, 2014). Some researchers employed textural classes of soil and the climate condition of the given location to estimate soil erodibility (Borselli *et al.*, 2012). However, despite the recognition that climate exerts some control on soil erodibility, the prediction based on climate yields poor values of soil erodibility (Borselli *et al*., 2012).

$$K = \left(0.2 + 0.3 \times \exp\left(-0.0256 \times S_a \times \left(1 - \frac{S_i}{100}\right)\right)\right) \times \left(\frac{S_i}{C_L + S_i}\right)^{0.3} \times \left(1 - \frac{0.25c}{c + \exp(3.72 - 2.95c)}\right)$$

$$\times \left(1 - \frac{0.75 S_N}{S_N + \exp(-5.51 + 22.9 S_N)}\right) \qquad 2.8$$

where S_a is sand (%), S_i is silt (%), C_L is clay (%), C is organic carbon,

$$S_N = 1 - (S_a / 100) \qquad 2.9$$

$$K f_{csand} \times f_{cl-si} \times f_{orgC} \times f_{hisand} \qquad 2.10$$

where

$$f_{csand} = 0.2 + 0.3 \exp\left[-0.256 m_S \left(1 - \frac{m_{silt}}{100}\right)\right] \qquad 2.11$$

$$f_{cl-si} = \left(\frac{m_{silt}}{m_c - m_{silt}}\right)^{0.3} \qquad 2.12$$

$$f_{orgC} = \frac{0.25 \times orgC}{orgC + \exp[3.72 - 2.95 orgC]} \qquad 2.13$$

$$f_{hisand} = 1 - \frac{0.7\left(1 - \frac{m_S}{100}\right)}{1 - \frac{m_S}{100} + \exp\left[-5.51 + 22.9\left(1 - \frac{m_S}{100}\right)\right]} \qquad 2.14$$

Other methods are equation (2.15) (David, 1988) which uses pH, organic matter, carbon, and textural classes, and equation (2.17) which uses textural classes and is tested on volcanic soils in subtropical Hawaii soils (El-Swaify, 1990).

$$K = \left[0.043 \times pH + \frac{0.62}{SOM} + 0.0082 \times S - 0.0062 \times C \right] \times Si \qquad 2.15$$

where pH is soil pH (acidity or alkaline level), SOM is soil organic matter, SOC is soil organic carbon, S is the percentage of sand, C is clay ratio (eq. 2.15), Si = silt content

$$C = \frac{\%\ clay}{\%\ sand + \%\ silt} \qquad 2.16$$

$$K = -0.03970 + 0.00311_{X_1} + 0.00043_{X_2} + 0.00185_{X_3} + 0.00258_{X_4} + 0.00823_{X_5} \qquad 2.17$$

where X_1 is the unstable aggregate fraction less than < 0.25mm in %, X_2 is modified silt content in % (0.002-0.1 mm) multiplied by modified sand in % (0.1 – 2 mm), X_3 is base saturation, X_4 is the silt fraction in % (0.002-0.05 mm), and X_5 is the modified sand fraction in % (0.1-2 mm) (Tsige *et al*., 2022). Organic matter is critical to enhancing soil structure and aggregation, soil pore distribution and permitting infiltration (Fasinmirin *et al.*, 2018). The greater the clay contents of a given soil, the higher the resistance to detachment and soil translocation because they have low erodibility and are sticky (Ganasri and Ramesh, 2016). However, with increasing silt content, erodibility becomes higher even when clay and sand content are high (Mhangara *et al.*, 2012).

There are yet other methods for estimating soil erodibilty (K factor) in the literature. They include those for the EU (Panagos *et al.*, 2014), India (Olaniya *et al.*, 2020), China (Hua Liu *et al.*, 2020; Wang *et al.*, 2016, 2012), US ((Corral-Pazos-de-Provens *et al.*, 2023; Lee *et al.*, 2022; Wischmeier and Smith, 1978), Middle East (Ebrahimi *et al.*, 2021; Ostovari *et al.*, 2017, 2019, 2022), Italy (Bagarello *et al.*, 2012), Uruguay (Beretta and Carrasco-Letelier, 2017), Greece (Efthimiou, 2020), and Brazil (Cassol *et al.*, 2018). It is estimated based on the laboratory analysis of generic soil types (Merchán *et al.*, 2023). The initial nomograph (Wischmeier and Smith, 1978) was revised, updated and improved upon which becomes very useful for locations with silt contents and fine sands not exceeding 70 % (Corral-Pazos-de-Provens *et al*., 2023). It is recommended that the use of any of the methods for estimating the k factor should be dependent on the conditions or purposes for which they were conceived and should not significantly differ from those of its development (Corral-Pazos-de-Provens *et al.*, 2023).

2.7.3 Topographic LS-factor

The LS-factor often referred to as the topographic factor is a combination of two factors of the RUSLE model; the slope steepness factor and the slope length factor. It expresses the soil loss from a given area due to the effect of slope angle and its length. Hence, steepness depicts the soil loss ratio to a 9 % slope under similar conditions (Tsige *et al.*, 2022). Slope length expresses the distance from where overland flow is initiated to where deposition begins or where the runoff enters a defined drainage channel (Wischmeier and Smith, 1978). Soil loss increases with increasing slope steepness (Gwapedza *et al.*, 2018; Ziadat and Taimeh, 2013). However, soil loss is of higher sensitivity to slope steepness than length (Roose, 1975). In the same vein, the LS-factor is the most sensitive of all the factors of RUSLE (Hrabalikova and Janeček, 2017; McCool *et al.*, 1987; Tetzlaff and Wendland, 2012). Despite being a very critical factor, it is very difficult if not impossible to derive the LS method of a large-scale study from ground-based measurement (Oliveira *et al.*, 2015; Risse *et al.*, 1993). The LS-factor was originally designed for a unit runoff plot (Wischmeier and Smith, 1978). The LS calculation assumes slopes have uniform gradients with any irregular terrain or slope treated as a unique segment to yield accurate results (Wischmeier and Smith, 1978). However, it has been extended in RUSLE to a one-dimensional hill slope scale, using different equations that depend on the steepness of the slope (Renard *et al.*, 1997).

This extension uses flow accumulation on a DEM in a GIS environment. However, the DEMs of which the highest resolution of the most widely used is 30 m are still insufficient for a more detailed study at catchment or hillslope level as it does not capture important details at micro-topography (Tsige *et al.*, 2022). Thus, with a decreasing resolution (about 100 m), it fails to capture accurately the flow network of a catchment (Duraes *et al.*, 2020; Panagos *et al.*, 2015a). It has been shown that low-resolution DEMs tend to overestimate the LS-factor and therefore soil loss (Yang, 2015). Thus, using a high-resolution image for soil loss prediction is appropriate and desirable (Duraes *et al.*, 2020; Michalopoulou *et al.*, 2022; Panagos *et al.*, 2015c; Yang, 2015). The degree of variations increases as elevation approaches 1000 m (Michalopoulou *et al.*, 2022). The method of using flow accumulation has gained popularity and wide application due to its ability to account for divergence and convergence of flow thereby capturing complex topographies (Tsige *et al.*, 2022). It has been shown that at small scales, the manual method of using slope length and steepness performed well at finer resolutions but its accuracy decreases as the scale becomes larger like a watershed or field scale (Benavidez *et al.*, 2018). The slope length factor is expressed as (eq. 2.18).

$$L = \left(\frac{\lambda}{\lambda_l}\right)^m \qquad 2.18$$

where λ is the slope length, λ_l is the unit plot length (22.13 m), also defined as the horizontal projection of the slope length (Kinnell, 2010; Mitasova *et al.*, 1996; Tsige *et al.*, 2022). There are diverse equations for estimating the LS-factor (eqs. 2.19 – 2.23). However, it has been shown that equations employing slope in percentage yield more accurate values when used in soil loss estimation than the ones that use a slope in degrees (Nakil and Khire, 2016). Also, at hillslope levels, the original manual method, the Moore and Burch method, and the McCool *et al.* 1996 methods perform best in the Czech Republic (Hrabalikova and Janeček, 2017; Karásek *et al.*, 2022). The original S factor was derived simply as (eq. 2.19) (Smith and Wischmeier, 1957).

$$S = 0.43 + 0.30s + 0.043s^2 \qquad 2.19$$

where S is the slope factor, s is the slope steepness in percent

$$LS = \left(\frac{\lambda}{22.13}\right)^m \left(65.41\sin^2\theta + 4.56\sin\theta + 0.065\right) \quad 2.20$$

where λ is the slope length in metres, θ is the slope angle, and m is the exponent which depends on the degree of slope. Thus, m is 0.5 if the slope exceeds 5 %, 0.4 if between 3.5 and 4.5 %, 0.3 if the slope is between 1 % and 3 %, and 0.2 if the slope is less than 1 %. This was developed by Wischmeier and Smith (1978).

Also, McCool *et al*. (1987) devised equation (2.21).

$$LS = \left(\frac{\lambda}{22.13}\right)^m \quad 2.21$$

where λ is slope length in metres, m is a dimensionless parameter that depends on the slope,

$$m = \frac{\beta}{1+\beta} \quad 2.21a$$

$$\beta = \frac{\frac{\sin\theta}{0.0896}}{3.0 \times (\sin\theta)^{0.8} + 0.56} \quad 2.21b$$

$S = 10.8 \times \sin\theta + 0.03$ if the slope is less than 9 % 2.21c

$S = 16.8 \times \sin\theta - 0.5$ if the slope is above or equal to 9 % 2.21d

$S = 3.0 \times (\sin\theta)^{0.8} + 0.56$ if the slope length is less than 4.6 m 2.21e

where and θ is the slope angle in degrees.

In Britain, a similar algorithm was used to estimate the LS-factor (eq. 2.22) Morgan (2005) cited by Tsige, Malcherek and Seleshi (2022)

$$LS = \left(\frac{\lambda}{22.13}\right)^{0.5} \times \left(0.065 + 0.045s + 0.0065s^2\right) \quad 2.22$$

where s is the slope in percent.

Moore and Burch (1986) developed equation (2.20) taking into account unit stream theory.

$$LS = \left(\frac{\lambda}{\lambda_l}\right)^m \times \left(\frac{\sin\beta}{0.0896}\right)^n Z \quad 2.23$$

where λ is the flow path length in metres also equals flow accumulation multiplied by the cell size of the DEM. This is easily computed in a GIS environment. λ_l =22.13 m, β is the slope angle in radians, and Z = $(c/e)^a$ which is a rilling factor. The rilling factor is used to modify the slope length factor (Ghosal and Bhattacharya, 2020). Thus, for sheet flow, the Z is 1 because a, c, and e have the value of 1. In the presence of five parabolic rills per unit length, each having a width of 10 cm, then Z will be 1.12 as a is 5, c =2/3, and e is 0.5, if there are no parabola-like rills per unit length of a contour, then Z is 1.62 because a will be 1, c=2/3, and e = 0.2. The values of m and n are 0.4 and 1.3 respectively according to Moore and Burch (1986a, 1986b).

Many researchers have also used a modified LS-factor in their studies (Wu *et al.*, 2021; Zhang *et al.*, 2017a, 2017b, 2013). Zhang *et al.* (2013) developed the LS-Tool which performs relatively well in the Xiannangou watershed in China. The estimated soil loss differs depending on the LS-factor method used (Hrabalikova and Janeček, 2017; Karásek *et al.*, 2022; Panagos *et al.*, 2015b).

2.7.4 Cover C- factor

The cover or simply the C-factor accounts for the effect of vegetal cover on soil erosion. The C-factor is defined as the ratio of soil loss from a plot with a given cover and management to that from a field under tilled continuous fallow but on the same soil, slope steepness and length, and having the same rainfall events (Kinnell, 2019; Wischmeier and Smith, 1978). Vegetation in association with topographic factors plays a significant role in soil erosion (Ben-Kobi *et al.*, 1994). The vegetal cover acts as a roughness factor or frictional force that counters the effect of slope and erosivity on the soil surface. Thus, while erosivity and topographic factors favour or induce soil erosion, the C- and P-factors oppose and counteract them. That is, the C-factor acts to prevent erosion such that a land use that lacks this protection, has a C-factor value of 1 but then decreases to zero as the power of this protection increases. Hence, a land cover with a C-factor of 0 implies total protection against soil erosion. Therefore, the

C-factor is considered the most significant factor of the RUSLE model (Fenta *et al*., 2021, 2016; Prasuhn, 2022; Toy *et al.*, 1999) but its estimation is very tasking.

The value of the C-factor varies with the nature and type of vegetal cover such that dense forests have the lowest C-factor value. The C-factor is computed with the knowledge of soil loss ratio (SLR). The SLR is derived from a combination of management, canopy cover, land cover/roughness, and antecedent soil moisture (Renard *et al.*, 1997). Such computation requires rigorous fieldwork and a working knowledge of the area's cover attributes including agricultural management (Benavidez *et al.*, 2018), a condition that limits its application to small-scale studies. For this limitation, the C-factors are usually determined from reported values of studies on similar cover and land uses (Benavidez *et al.*, 2018). Examples from such look-up tables are shown in Table 2.6 and Table 2.7 (USDA_ARS, 2004; Wischmeier and Smith, 1978). Several researchers have applied the table values (Gashaw *et al.*, 2018; Kalambukattu and Kumar, 2017; Rozos *et al.*, 2013).

Another approach is estimating it from the Normalised Difference Vegetation Index (NDVI) (Abdelsamie *et al.*, 2022; Durigon *et al.*, 2014; Hagras, 2023; Halder, 2023; Yigez *et al.*, 2021). McFarlane *et al.* (1991) devised the following equation (eq.2. 24) for estimating the C-factor value from the NDVI.

$$C\ \ factor = 1.02 - 1.21 \times NDVI \qquad 2.24$$

where

$$NDVI = (NIR - RED)/(NIR + RED) \qquad 2.25$$

where NIR is near-infrared, and RED is red in the electromagnetic spectrum.
Several researchers have employed this method in their studies (Pal and Shit, 2017; Samanta *et al.*, 2016). There are yet other methods of estimating the C-factor which can be found in Halder (2023).

Table 2.6. C-factor values of the USDA-SCS

Land use/land cover class	C-factor value
Built-up	0.00
Agricultural land	0.40
Dense vegetation	0.004
Sparse vegetation	0.03
Barren land	1.00
Waterbody	0.00

Source: USDA-SCS (2004)

The NDVI approach has been criticised for not reflecting the content of the C-factor (Tanyaş *et al.*, 2015) and as such provided some adjustments to its usage (Alexakis *et al.*, 2021; Chen *et al.*, 2011; Wang *et al.*, 2023). Van et al. (2000) cited by Ghosal and Bhattacharya (2020) argued that the C-factor decreases exponentially with NDVI and thus they added alpha and beta to the NDVI exponent (see (Ghosal and Bhattacharya, 2020; Saha *et al*., 2022; Wang *et al.*, 2019). It is also argued that since it is based on reference to the chlorophyll content of vegetation, grassland might have higher NDVI values than forest (Tanyaş *et al.*, 2015). In such a case, if utilised would result in an output where a forested area is shown as being more prone to erosion than a grassland which is erroneous (Tanyaş *et al.*, 2015). Moreover, the method has been criticized for overestimating the C-factor values and invariably overestimating soil erosion rates (Ayalew *et al.*, 2020; Jones *et al.*, 2022). Thus, Bircher *et al.* (2021) devised a new tool called CP-Tool for estimating the C- and P-factor values which they argue produces a nice fit. Rescaled C-factor (Cr2) and precipitation correction (C-PC) have been used to modify the NDVI-based C-factor estimation (Almagro *et al.*, 2019; Macedo *et al.*, 2021).

Therefore, there are variations in the C-factor values used in different studies even for the same location. Such variations lead to different results for a given location. For instance, many studies assign different values to bare land, water, built-up or urban land uses. A compact urban space with little to no spaces or bare areas should have a value different from an urban area with many land spaces and cropland. A related table (Table 2.8) was published by Mahamud *et al.* (2021).

Table 2.7. Cover C- factor values

Land cover class	C-factor value
Inland marshes	0.00
Salt marshes	0.000
Sclerophyllous vegetation	0.005
Broad-leaved forest	0.001
Coniferous forest	0.001
Mixed forest	0.001
Cultivation with significant areas of natural vegetation	0.050
Non-irrigated arable land	0.050
Moors and heathland	0.050
Transitional woodland shrub	0.050
Sparsely vegetated areas	0.050
Discontinuous urban fabric	0.050
Industrial or commercial units	0.050
Mineral extraction sites	0.050
Orchard	0.080
Olive grove	0.080
Complex cultivation patterns	0.080
Natural grasslands	0.100
Burnt areas	1.000
Beaches, dunes, and sands	1.000
Shrub	0.014

Source: Wischmeier and Smith **(**1978**)**, Mengie *et al.* **(**2022**)**

A comprehensive review of the C-factor and P-factor values of the RUSLE was carried out by Ebabu and his team (Ebabu *et al.*, 2022). It was a good attempt to highlight the use of both factors of RUSLE in different countries and continents (Ebabu *et al.*, 2022). They found that soil management practices are more effective than crop cover factors in reducing soil loss in semi-arid areas (Ebabu *et al.*, 2022). The global average of the C-factor varies from 0.34 for cropland to 0.03 for forest land, with maize (0.42) and potato (0.40) having the highest values (Ebabu *et al.*, 2022). Finally, though there are significant improvement in the C- and P-factor values estimation using remote sensing, there is no satisfactory methodology for their estimation (Phinzi and Ngetar, 2019).

Table 2.8. Cover C-factor values for different land uses

Cover class	C-factor value
Quarrying areas	1.00
25 % forest cover	0.42
50 % forest cover	0.39
75 % forest cover	0.36
100 % forest cover	0.03
Agricultural plants	0.38
Horticulture/traditional mixed plants	0.25
Cocoa/tea/coffee	0.20
Coconut/oil palm/Rubber	0.20
Paddy	0.01
Flower/Fruit	0.30
Low-density urban space (50 % green area)	0.25
Medium density (25 % green area)	0.15
High density (5 % green area)	0.05
Impervious (Parking lot, road)	0.01
Waterbody	0.01

Source: Mahamud *et al.* (2021).

2.7.5 Practice P- factor

The support practice factor expresses the ratio of soil loss under a given conservation measure to the soil loss on a field with up- and down-slope cultivation (Renard *et al.*, 1997). It describes the management practices put in place by the farmer to attenuate the impact of runoff on soil thereby holding back sediment from being washed away. The most common conservation practices include contouring, strip cropping, solid bund, or terracing (Renard *et al.*, 1997).

The effectiveness of support practices to weaken erosion increases with decreasing rainfall or increasing aridity (Ebabu *et al.*, 2022; Jia *et al.*, 2019). This is due to the super-saturated nature of the soils in high-rainfall areas that fail to infiltrate much of the runoff (Jia *et al.*, 2019). This is in agreement with the assertion that soil loss rates are lower in the arid zones than in the humid tropics and temperate zones with heavy rainfall (Xiong *et al.*, 2019). The effectiveness or otherwise of the support practices depends on rainfall and elevation (Taye *et al.*, 2018). Effective conservation practices have low values (Bagherzadeh, 2014).

There are two main approaches to assigning the P-factor values. The first is through intensive fieldwork to assess the conservation practices put in place in the agricultural areas. However, when the area under investigation is very large, it becomes impractical to achieve. Thus, like the C-factor values, the P-factor can be obtained from the literature (Table 2.9, Table 2.10) (Benavidez *et al.*, 2018). In the absence of information on conservation practice or under natural conditions, the P-factor value assumes unity (Adornado *et al.*, 2009; Bensekhria and Bouhata, 2022; Dumas *et al.*, 2010; Ghosal and Bhattacharya, 2020).
Due to the difficulties in modelling P-factors, Wener (1981) derived an equation for estimating the P-factors based on its relationship with slope (eq. 2.26).

$$P = 0.2 + 0.03 \times S \qquad 2.26$$

where P is the P-factor (conservation practice), and S is the slope in percent.

Table 2.9. Conservation P-factor values

Conservation practices	P-factor
Up and down the slope	1.00
Cross slope	0.75
Contour farming	0.50
Strip cropping, cross slope	0.37
Strip cropping, contour	0.25

Source: Stone and Hilborn **(2011)**

Table 2.10. Conservation P- factor values

Land use/land cover type	Slope %	P-factor value
Agricultural land use	0-5	0.10
	5-10	0.12
	10-20	0.14
	20-30	0.19
	30-50	0.25
	> 50	0.33
Non-agricultural land	all	1.00

Source: Wischmeier and Smith (1978) in Mengie *et al.* (2022)

2.8 Limitations and uncertainty

The USLE model suffers from certain limitations and uncertainties (Tiruwa *et al.*, 2021). One of the issues is the overt dependence of the model on C and P parameters which are critical to the model like all the other factors (Vieira *et al.*, 2018). Yet, these parameters are estimated by simple assignment of non-uniform weights across spatial scales.

Thus, the Revised USLE (RUSLE) (Renard *et al.*, 1997) was developed to take care of most of the shortcomings of the USLE. The RUSLE can effectively deal with slopes of diverse shapes (Mello *et al*., 2016; Wang *et al.*, 2019). The model's simplicity ensures it can be used on diverse topographic surfaces and regions and possess a significant positive correlation between input and output variables (Kebede *et al.*, 2021; Kumar *et al.*, 2022).

However, the RUSLE model is still bedevilled by two main uncertainties: the uncertainty in the input data and uncertainty due to model inadequacies (Bamutaze *et al.*, 2021). The model was originally predicated on slopes of under 18 % and 91.4 m long (Hammad *et al*., 2004) such that beyond this range, the accuracy of the LS-factor becomes uncertain. However, this problem has been investigated by researchers (Hrabalikova and Janeček, 2017; Nakil and Khire, 2016). They opined that for medium to steep terrain, the LS methods based on percentage slope give accurate soil loss estimation (Nakil and Khire, 2016). The RUSLE has the capacity of handling effectively soil simulation on slopes of up to 300 m (Kumar *et al.*, 2022; Renard *et al.*, 1997).

Furthermore, the LS-factor does not take into account the terrain shape of the upslope area (Alewell *et al.*, 2019). The model does not account for the sedimentation or deposition process, and cannot simulate gullies and mass movement (Alewell *et al.*, 2019; Koirala *et al.*, 2019; Kumar *et al.*, 2022; Thapa, 2020; Wischmeier and Smith, 1978). Another limitation is its poor performance due to its reliance on the kinetic energy of raindrops rather than utilising runoff which is critical to soil dislocation (Kinnell, 2019; Kumar *et al.*, 2022). Its inability to isolate factors that influence soil loss such as plant biomass, decomposition, runoff, infiltration, soil detachment, and movement (Alewell *et al.*, 2019).

The model does not simulate soil loss on an event basis (Kumar *et al*., 2022; Mello *et al.*, 2016). Additionally, the utilisation of process-based models like WEPP, PESERA or AGNPS does not necessarily result in lower uncertainties in comparison to simple empirical models like the USLE family of models (Alewell *et al.*, 2019).

2.9 Validation of the model

Validation simply entails testing or comparing the output of a model with the observed to see if it fits well or not (Fishman and Kiviat, 1968; Trucano *et al.*, 2006). It has been argued that direct validation of a model should prove that a model replicates the reality it represents and in which case it works for closed systems (Alewell and Manderscheid, 1998). In line with this, therefore, an open system may not require validation (Alewell *et al.*, 2019). However, validation is possible following Martin's (1996) definition of validation in accord with its Latin meaning of strong, healthy, or robust.
Against this background, it points to the well-known dictum attributed to Box and Draper (1919) that all models are wrong but some are useful. Thus, Foster *et al*. (2001) and Batista *et al*. (2019) reported that a model's success is intricately connected to its usefulness. Thus, a RUSLE2 model with perfect erosion estimates but fails to provide adequate conservation planning decisions does not meet its objective (Yoder *et al.*, 2001).

Usually, validation entails splitting data set where one set is for calibration and the other set is for validation. However, in open systems, it was suggested that a model can be validated if it was not calibrated (Sverdrup *et al.*, 1995). This simply implies that the estimated output from the model is directly compared with the measured target values forgoing any inverse process step (Alewell *et al.*, 2019). The USLE family of models fall into this class where the model derives its input parameters from measured data and devoid of calibration, the modelled erosion is compared with the measured data (Alewell *et al.*, 2019).

The challenge faced in validating RUSLE with measured data is that while RUSLE estimates gross erosion rates, measurements usually provide net erosion rates (Alewell *et al.*, 2019). Thus, comparing sediment yield and results from RUSLE is a mismatch as long as RUSLE is unconnected with erosion and deposition, for the modelled and the observed represent different fluxes (Alewell *et al.*, 2019; Ghosh *et al.*, 2023; Vanmaercke *et al.*, 2014). Trimble and Crosson (2000) asserted that USLE predicts soil dislocated in a field (gross erosion), and not necessarily the amount of soil eroded from a field (net erosion).

To be useful, a model result is supposed to compare well to field-measured data (Castillo *et al.*, 2012). This entails a model replicating areas of erosion severity identified via field survey (Evans and Brazier, 2005). Nevertheless, there are cases where this does not hold. Several studies have reported disagreement between model output and field erosion patterns (Evans and Brazier, 2005; Hessel *et al*., 2006). Furthermore, erosion risk assessment maps from USLE-type models or decision trees like AHP have shown near-agreement with field data (Bufalini *et al.*, 2022; Egbueri *et al.*, 2022; Ganasri and Ramesh, 2016; Prasuhn *et al.*, 2013). Such an approach is a validation of erosion risk zones rather than soil loss validation. Moreover, model testing is less rigorous in such cases, and when compared with actual erosion rates the results turn out less satisfactory (Prasuhn *et al.*, 2013).

Others have simply adopted the scientific approach (Biondi *et al.*, 2012) where findings are merely compared with results from other publications from experts or scientific projects (Haregeweyn *et al.*, 2017; Sinshaw *et al.*, 2021). Again, due to the difficulty in validating soil erosion, some scholars proposed a validation method based on visual evaluation (Bosco *et al.*, 2015).

2.10 Risks and vulnerability

According to the Sendai Framework for addressing risk, risk management requires two basic approaches. The first is to avoid creating new risks and the second is to systematically reduce the existing ones (McGlade *et al.*, 2019). The people's adaptive strategy must be strengthened to withstand and bounce back from stressors and transform through crises (McGlade *et al.*, 2019). Risk is a term in disaster management that is dependent on two components; hazard and vulnerability (Birkmann, 2007). A hazard is a likelihood of an external event or stress occurring in a given area within a specific time interval that impacts the environment, economy and society (de León *et al*., 2006; Diaz-Saracaga and Jato-Espino, 2020). Hazards can be divided into natural (Erosion; flooding; earthquake), technological (oil spill, toxic pollution) and human-induced (civil riots, terrorist attacks) (de León, 2006). Risk describes the potential effects of an imminent hazard. It is simply denoted as a function of hazard and vulnerability (eq. 2.27)

$$Risk = Hazard \times Vu \ln erability \qquad \ldots\ldots\ 2.27$$

However, Cutter (1996) described risk as the potential occurrence of hazard which differs from the above viewpoint. Some scientists argue that other factors like coping (White *et al.*, 2007), deficiencies in preparedness (de León, 2006) and/or exposure (Dilley *et al*., 2005) should be integrated into defining risk. Thus, a hazard becomes a disaster when a society or population is unable to cope with its occurrence thereby resulting in disruption of their normal function and leading to extensive losses (EEA, 2018 cited by Diaz-Sarachaga *et al.* (2020). Over the years, these factors have instead been integrated into defining vulnerability. Just as the statement by O'Keefe *et al.* (1976) and Thomas *et al.* (2019) that the occurrence of natural hazard events was on the increase could not be substantiated. Thus, it might be inferred that the vulnerable population to disaster events is increasing based on the above-noted dimensions of vulnerability. However, the impact natural hazards have on people varies considerably with the socioeconomic characteristics of the exposed people (Zakour and Gillespie, 2013).

Thus following Volpe *et al*. (2021), soil erosion risk assessment comprises assessing its susceptibility where susceptibility is the likelihood of erosion occurring in a given location based on its terrain conditions. It encompasses an estimate of 'where' or the likely places erosion may occur. Thus, soil erosion risk assessment entails susceptibility (S) analysis to find the likely areas of hazard (H) of different magnitudes, and the vulnerability (V) assessment that accounts for the people and infrastructures that might be affected or involved. However, this study considered the first dimension of risk (susceptibility analysis) and peripherally dealt with the vulnerability by considering how the affected farmers adapt to soil erosion.

Adaptation herein used refers to the ability to cope, live with or adapt to the change in the environment in which one cannot reverse or revert to its previous state. It should be highlighted that the words; vulnerability, resilience and adaptation are interrelated. They conceptually overlap (Engle, 2011; Nelson *et al.*, 2019) such that decreasing vulnerability is often viewed as increasing resilience (Bahadur *et al.*, 2010). It has been defined and used differently in many contexts (Chen and Zha, 2016). Some scholars view vulnerability as a subset of resilience metrics (Baroud *et al.*, 2014).

Adaptive capacity simply refers to the ability to be in a prepared state and respond to disturbance (Engle, 2011). According to Nelson (2018), the concept of adaption is less developed, unlike those of vulnerability and resilience or sustainability. The IPCC defined adaptation as the ability of a people or system to modify its attributes to effectively cope with actual or imminent external stresses (Hameso, 2015).

3. MATERIALS AND METHODS

3.1 Geography of the study area

3.1.1 Location

Anambra is located between latitudes 5.60 ^{o} and 7.00 ^{o} N, and longitudes 6^{o} 45$^{'}$ and 7.45 ^{o} E (Figure 3. 1). Its landmass is about 4844 km^{2}. It lies in the rainforest zone (Okoyeh *et al.*, 2014). It is located in eastern Nigeria. It has a very high population density. It is also known for its high ecological problems including flooding and erosion especially gullies (Igbokwe *et al.*, 2008; NEWMAP, 2015). Anambra State was chosen for the study due to its location on the lower Niger and Anambra floodplains which makes it strategic for agricultural productivity in eastern Nigeria. Also, its high erosion susceptibility makes it a good site for a study like this in order to aid planners and stakeholders in mitigating soil erosion risks in Anambra State.

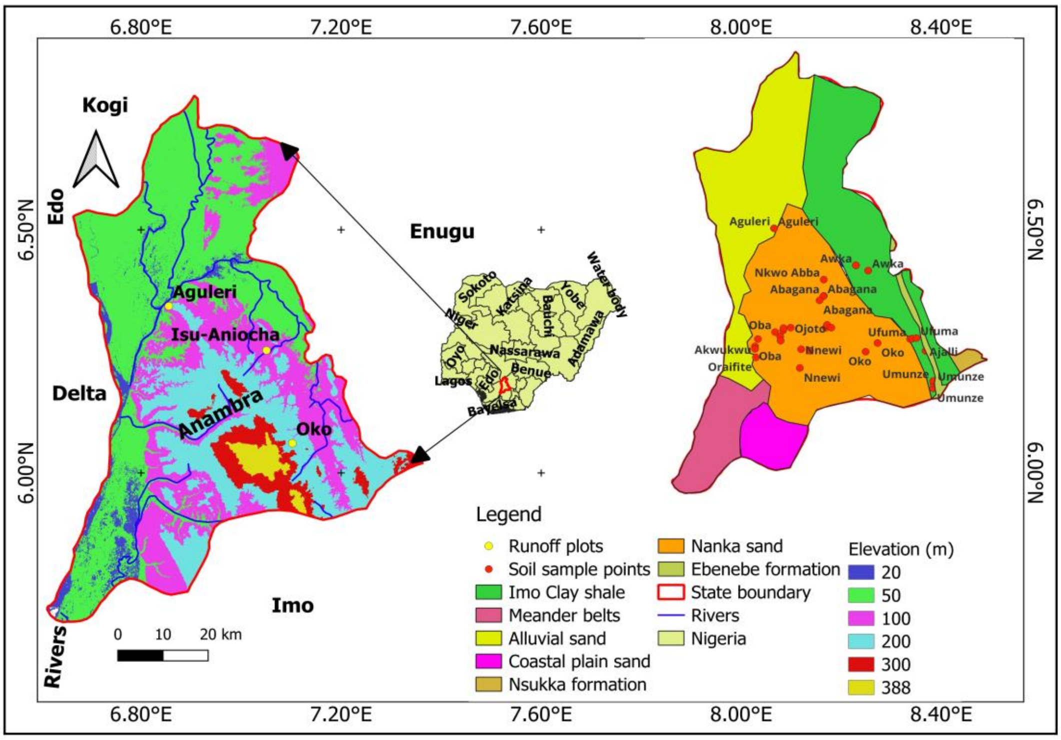

Figure 3. 1. Study area (Anambra State) and the geology
Source: Adapted from Egbueri *et al.* (2022)

3.1.2 Climate and geology of Anambra State

The area has the Aw climate of Koppen's climate classification (Koppen, 1936). The summer rainy season lasts seven or eight months. The rainy season starts from March to October with a mean annual rainfall of about 1850 mm (Ogungbenro and Morakinyo, 2014; Chinweze, 2017). The mean temperature is 27^{o}C, ranging from 25 to 32^{o}C (Chinweze, 2017, 2019). The climate change phenomenon that has affected the rainfall pattern also exacerbated the gully situation in the area (Farauta *et al.*, 2012; Okoyeh *et al.*, 2014). The geology of the area comprises the Nanka formation (Figure 3. 1) which is a friable unconsolidated sand deposit of part of the Eocene. The area is also underlain by the Imo clay shale of the Palaeocene and overlain by the Ogwashi formation of the Oligocene. The elevation of the area varies from 20 m to 388 m above sea level with the southern upland predominated by Nanka sand and the eastern lowland on the Imo shales. The Nanka sand is classed as a family of the Ameke formation (Onyeka *et al.*, 2019). The dominant soils are the ferruginous and the hydromorphic soils. The uplands run from the Awka-Orlu Cuesta which also forms the headwater for many Rivers (Ofomata, 2002). The major River draining the area is River Niger and its tributary, the Anambra River (Figure 3. 1). Other rivers that drain the area include the Nkisi, Idemili, Mamu, Ezu, Aghomili and Orashi (Okoyeh *et al.*, 2014). There are also lakes like the Agulu, Uchu and Ulasi lakes. The gullies' dimensions range from 25 m to 2.9 km in length and from 2m to 300m in width Okoye *et al*. (2014). It has a higher width in the upstream section which gives a characteristic fan shape (Okoyeh *et al.*, 2014).

3.1.3 Administrative and economic attributes of Anambra State

Anambra State is one of the 9 States in the east of the country and one of the 5 core Igbo states. It has 22 Local Government Areas with 127 communities (Chinweze, 2017) with the administrative headquarters at Awka. It is the most densely populated State in the eastern part of the country (Chinweze, 2017) and second to Lagos State in Nigeria. It is highly urbanised with several commercial centres such as Onitsha market and Nnewi Auto-Spare parts market among others.

3.2 Materials and Methods

3.2.1 Introduction

The outline of the thesis' methodology is shown in Figure 3. 2. It is a flowchart of the approaches employed to achieve the objectives of the study. The procedures (materials and methods) used to achieve the aim are presented in the following subsections.

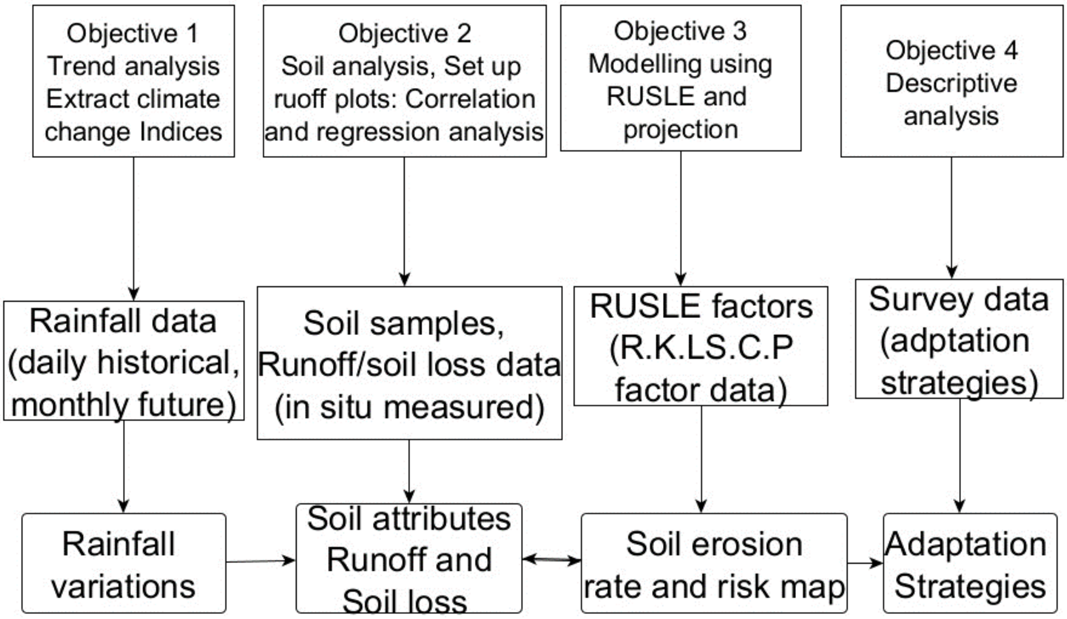

Figure 3. 2. Flowchart of the thesis methodology

3.2.2 Climate data and land cover data

The data used in the study comprise daily rainfall data from the Nigeria Meteorological Agency (NIMET) for Awka covering the period 1991 to 2020. Due to the unavailability of conventional data for the other points in the area, more daily rainfall and soil moisture data were obtained from the Climate Hazards Centre InfraRed Precipitation with Station data (CHIRPS*)* at https://data.chc.ucsb.edu/products/CHIRPS-2.0/africa_daily/tifs/p05/. They have been validated and are widely used in the tropics in hydroclimatic studies (Funk *et al.*, 2015; Atiah *et al.*, 2020; Ayanlade *et al.*, 2021). The Tropical Applications of Meteorology using SaTellite data and ground-based observations (TAMSAT) daily rainfall data were used. They are reliable and widely used in hydroclimatic studies over Africa (R. Maidment *et al.*, 2017; R. I. Maidment *et al.*, 2017).

However, due to poor spatial distribution of the station data (only in Awka), satellite data were used. The CHIRPS data provides quasi-global rainfall data from 1981 to near-present at a 0.05 × 0.05 degrees (~5.3 km by 5.3 km) and the TAMSAT data provides daily climate data for Africa from 1983 to the delayed present at 0.0375 × 0.0375 degrees (~ 4 by 4 km) spatial resolution were used.
The land cover maps were downloaded from the ESRI website at https://livingatlas.arcgis.com/landcoverexplorer/#mapCenter=7%2C6.177%2C10&mode=step&timeExtent=2017%2C2022&year=2022&downloadMode=true for the years 2017 to 2022. They are very high-resolution (10 m) data that are classified at country levels and merged to produce the global land cover map. The Land cover maps of 2017, 2020 and 2022 were used to predict the 2060 land cover map using the Clark University Terrset software. The key driver of change in the area is the forest-to-built environment and so the forest-to-built submodel was used to predict the 2060 map using the Multilayer Perceptron (MLP). It had a Kno and Kstandard accuracy of 63 % and 90 %, respectively. The 30 seconds MIROC6 Worldclim data for 2041-2060 were downloaded from https://www.worldclim.org/data/cmip6/cmip6_clim30s.html. The Shared Socio-economic Pathway SSP245 and SSP585 representing the moderate and extreme case scenarios, respectively, were used in the study.

3.2.2.1 Data preprocessing and preparation

The NIMET data were homogenized using the RHtest GUI interface in the R environment (Vincent *et al.*, 2012; Wang *et al.*, 2010). The data had 2 significant change points. Based on this information, they were harmonized using the Quantile mapping adjusted and mean-adjusted precipitation approach. The mean-adjusted approach was finally used. The CHIRPS data were bias-corrected using empirical quantile mapping (EQM) in the R environment. Due to the paucity of conventional data at Aguleri and Oko, TAMSAT data with a lower variance compared with NIMET data was used to adjust the CHIRPS data. The output is shown in Table 3.1, and the accuracy assessment metrics are in Table 3.2. When transformed into monthly data (Awka), the correlation between the adjusted CHIRPS and homogenised data increased to 0.75 but between TAMSAT and the homogenized data was 0.79. Based on the performance, the CHIRPS data were used since they had a better daily distribution than the TAMSAT, unlike the monthly distribution. In Ethiopia, CHIRPS and TAMSAT outperformed other compared data (Fenta *et al.*, 2018).

Table 3.1. Mean annual rainfall data for Awka station

Raw data				homogenised			
year	PCP	year	PCP	year	PCP	year	PCP
1991	2095	2006	1910.3	1991	1519.1	2006	1950.2
1992	1804.9	2007	2026.8	1992	1331.2	2007	2066.2
1993	1654.1	2008	2056.2	1993	1184.0	2008	2093.9
1994	2081.7	2009	2157.6	1994	1552.8	2009	2197.5
1995	2478.5	2010	1585.9	1995	1874.6	2010	1621.2
1996	1826.7	2011	1957.5	1996	1337.8	2011	1994.7
1997	2277.4	2012	1986.1	1997	1764.4	2012	2031.4
1998	1375.3	2013	1447.3	1998	976.5	2013	1720.9
1999	2101.2	2014	1499.5	1999	1593.9	2014	2036.7
2000	2069.1	2015	2499.4	2000	1537.7	2015	2501.1
2001	1516.6	2016	2084.8	2001	1076.3	2016	2072.0
2002	1928.1	2017	3526.2	2002	1409.7	2017	3518.9
2003	1671.1	2018	3665.4	2003	1231.7	2018	3658.7
2004	1861.5	2019	3821.5	2004	1604.8	2019	3816.6
2005	1914.7	2020	2777.6	2005	1951.0	2020	2770.0

Table 3.2. Accuracy metrics for the corrected daily rainfall data

Isu	CHIRPS	Aguleri	CHIRPS	Oko	CHIRPS
MAE	7.58	MAE	4.48	MAE	5.24
PBIAS	-1.25	PBIAS	-2.01	PBIAS	2.34
R	0.20	R	0.47	R	0.47

3.2.2.2 Trend analysis

The Mann-Kendall test (Hamed, 2011; Hamed and Rao, 1998; Kendall, 1975; Mann, 1945) was applied to determine the trends in the rainfall of the area at Isu-Aniocha, Aguleri and Oko. The Mann-Kendall test has the advantage of being independent of data outliers. It is a non-parametric test and therefore free from assumptions of the parametric test. It has a null hypothesis which is posited thus: 'There is no monotonous trend in rainfall over the period'. The test involves the calculation of the variance V, the standardized statistic Z, correlation tau, the S, and Sen's slope test to determine the magnitude of the trend (eqs 3.1 – 3.5).

$$S = \sum_{i=1}^{n-1} \sum_{j=i+1}^{n} sig(x_j - x_i) \qquad 3.1$$

$$\mathrm{sgn}(x_j - x_i) = \begin{cases} +1 \; if \; (x_j - x_i) > 0 \\ 0 \; if \; (x_j - x_i) = 0 \\ -1 \; if \; (x_j - x_i) < 0 \end{cases} \qquad 3.2$$

$$V(S) = \frac{1}{18}\left[n(n-1)(2n+5) - \sum_{p=1}^{q} t_p (t_p - 1)(2t_p + 5) \right] \qquad 3.3$$

$$Z = \begin{cases} \frac{S-1}{\sqrt{VAR(S)}} & if \; S > 0 \\ 0 & if \; S = 0 \\ \frac{S+1}{\sqrt{VAR(S)}} & if \; S < 0 \end{cases} \qquad 3.4$$

where x_i and x_j are observations in the time series. A positive Z value indicates a rising trend but negative Z is a downward trend in the distribution.

Sen's slope estimator (Sen, 1968) is also a non-parametric method applied to time series data to determine the magnitude of its trend. It is expressed by the equation shown below (eq. 3.5).

$$Ss = \frac{x_i - x_j}{i - j} \qquad 3.5$$

where Ss is Sen's slope estimator, x_i and x_j are data values at times i and j respectively.

Auto-correlation lag 1 was checked using the ACF ( ) function in R and where serial correlation existed, the modified Mann-Kendall test (Hamed, 2011; Yue and Wang, 2004, 2002) was used. The modified Mann-Kendall package in R (modifiedmk) was used with the appropriate function called depending on whether there was autocorrelation or not (Patakamuri *et al*., 2021; Pohlert, 2020).

3.2.2.3 Climate change indices (CCI)

The climate change indices were selected from the 27 indices listed by the Expert Team on Climate Change Detection and Indices (ETCCDI). The online version of Climpact and R-Instant (R-Instant, 2022; Stern *et al*., 2020; Zhang and Yang, 2004) were used and can be assessed from https://ccrc-extremes.shinyapps.io/climpact/ and https://r-instat.org/. Out of the 27 indices, 7 were selected for the study. These included: extreme one-day rain (rx1day), annual number of days when precipitation is above 10 mm (r10 mm), annual number of days when precipitation is above 20 mm (r20 mm), annual sum of daily precipitation above 1 mm (prcptot), Annual total precipitation divided by the number of wet days (when precipitation is above 1 mm) (SDII), annual sum of daily precipitation above 95th percentile (r95p), annual sum of daily precipitation above 99th percentile (r99p), and maximum 5-day precipitation total (rx5day).

3.2.2.4 Climatic water balance

Climatic water balance (CWBAL) is simply the difference between precipitation depth and the depth of potential evapotranspiration (PET) at a given location (eq. 3.6). It was estimated using the Standardised Precipitation-Evapotranspiration Index (SPEI) package (Miró *et al.*, 2023; Vicente-Serrano *et al.*, 2010). It gives an indication of the fraction of rainfall that remains when evapotranspiration has been accounted for. The balance is usually higher in areas or seasons of sufficient rainfall. Thus, it is a highly variable factor in time and space. The amount of rain that remains after PET is an indication of the possibility of flood or erosion, as antecedent moisture content is a precursor of these extreme events.

$$CWBAL = PCP - PET \quad 3.6$$

where CWBAL is climatic water balance, PCP is precipitation, and PET is potential evapotranspiration.

3.2.3 Soil samples and data

3.2.3.1 Soil sampling procedure

The soil samples were collected in two batches. The first soil samples (30) were collected during the fieldwork of 2021. They were collected at gully locations in the State. The GPS locations of the soil sample points were taken (Figure 3. 1). About 9.5 kg of soil was collected at each point at a 0-10 m depth. Additional 8 soil samples were collected in 2022 from the field plots and the neighbouring areas. The 30 samples were subjected to physical laboratory analyses including the Atterberg test, permeability tests, triaxial tests, compaction, and particle size analysis. The other 8 samples were subjected to particle size analysis, organic matter content, soil carbon content, soil pH, calcium carbonate, and bulk density. Soil samples meant for the bulk density determination were collected with a 5 cm diameter ring at locations within the plots.

3.2.3.2 Laboratory soil samples analysis

Physicochemical characteristics of the soils

Soil strength parameters

The geotechnical properties comprising Alterberg or consistency tests, compaction, permeability, and shear strength of materials (triaxial tests) were carried out. The samples were subjected to oven drying at the appropriate temperature according to the relevant American Society of Testing Material (ASTM) standard for soil tests (ASTM, 2005, 1996, 1987).

The procedures for measuring the shear strength are the direct shear and triaxial tests. The results are usually plotted on a Mohr circle where sand usually starts from the origin, but finer soils like clay cut an intercept on the y-axis. The Direct Shear box test was conducted on three samples with much sands while others were subjected to triaxial test (unconsolidated undrained). Thus, the cohesion, angle of internal friction, and the weight were determined.

The Atterberg test is used to determine the consistency index of soils (Casagrande and Fadum, 1940). The tests distinguish four states of soils with high fines based on their moisture content; liquid, plastic, semi-solid or solid. The liquid limit (LL) defines the water content at which the soil flows viscously in a cup when under a series of blows. The device allows the cup with the soil in which a small opening is cut to be lifted and dropped a little distance. Thus, the test involves counting the number of blows at which the groove closes at differing moisture contents while the moisture content at which the groove closes following 25 blows is the LL. The results of the experiment are then plotted on a graph. The PI is the water content for which small threads of the soil crumble when rolled to a 3 mm diameter.

Compaction test was done to determine the optimum moisture content (OMC) and the maximum dry density (MDD) of the soils. One of the most widely used tests for compaction is the cone penetration test (CPT) which agrees with field results (Elhakim, 2016). Thus, the CPT was used in the study. Figure 3. 3 shows some of the machines for the physical analysis in the laboratory. The falling head method was used for the permeability tests.

Figure 3. 3. Physical laboratory analysis showing the shear box test machine and others.

Particle size analysis and bulk density

The sieve analysis was done following the IS:2720 (part 4, 1985). The soils were oven dried at the temperature of 105ºC and then sieved using the different sieve sizes. The sizes included 100, 75, 19, and 4.75 mm. The sieve was shaken in such a way as to ensure there was no distortion or breakage of any soil particle by allowing each sieve to trap the proportional sizes. The mass of the material retained in each sieve was therefore recorded against the percentage passing through each sieve. According to the Unified Soil Classification System (USCS) of the US Army Corps of Engineers, US Bureau of Reclamation, and American Society of Testing of Materials, the percentage of each soil texture class is given in Table 3.3 and the standard US sieve sizes are shown in Table 3.4.

Table 3.3. The percentage passing for each soil class

% of soil class	% passing
Gravel	76.2 mm – 4.75 mm
Sand	4.75 mm – 0.075 mm
Silt and clay	0.075 mm

Table 3.4. US standard sieve sizes

Sieve no.	Opening (mm)	Sieve no.	Opening (mm)
4	4.75	35	0.500
5	4.00	40	0.425
6	3.35	50	0.355
7	2.80	60	0.250
8	2.36	70	0.212
10	2.00	80	0.180
12	1.70	100	0.150
14	1.40	120	0.125
16	1.18	140	0.106
18	1.00	170	0.090
20	0.850	200	0.075
25	0.710	270	0.053
30	0.600		

Source: Hamad and Younis (2016)

The mass of soil retained on each sieve is noted including the total mass of the soil. Then, the cumulative mass of retained soils above each sieve is recorded, as the mass of soil passing on each sieve, and the percentage of soil passing.

Chemical soil analysis

The SOC was analysed using a hot plate, cool flash, 10 ml pipette, 20 ml pipette, 250 ml beaker, 200 ^{o}C thermometer, 50 ml burette, and 1000 ml flask where reagents such as Potassium dichromate (vi), tetraoxosulphate (iv) acid, iron sulphate, deionized water and phenolphthalein indicators were mixed and result obtained (eq. 3.7).

$$SOC = \frac{0.003 \times 0.4N \times 20 \times \left(1 - \frac{T}{S}\right) \times 100}{W} \qquad 3.7$$

where N is the normality of Potassium dichromate (vi), T is the volume of 0.4 normality of iron sulphate in the sample, S is the volume of 0.4 normality of iron sulphate in a blank, and W is the weight of the oven-dry sample.

The pH was determined using 10 g of sample weighed and dissolved in deionized water constituting 50 ml to prepare the required emulsion solution. Thereafter, the pH was determined using a pH meter (H19813-6) Hanna Instrument USA. After dipping the probe into the sample, the pH is displayed on the LED screen. The initial samples were cleaned with iodised or distilled water to avoid cross-contamination.

The SOM was determined using the Walkley-Black chromic acid wet oxidation method. It was oxidized by 20 ml of 1 mole of potassium dichromate (vi) ($K_2Cr_2O_7$), and mixed in a concentrated sulphuric acid solution. The remaining dichromate is titrated with iron sulphate where the titre is inversely related to the amount of carbon present. Figure 3. 4 shows some of the laboratory equipment for the chemical analysis.

The Calcium carbonate was determined with the X-ray fluorescent (XRF) method. It comprised a sample cup with propylene thin film, ensuring smoothness of the film. Pulverised sample was poured into thin film covered cup with sample filled to a third of the sample cup (~ 5 g). The lid of the sample cup was covered permitting no leakage or loose particles on the thin film layer. The lids are tightened. The sample was then inserted into sample turret of Genius-IF Xenometric XRF sample chamber. The X-ray lamp was then powered and allowed to stabilize in two minutes on the run tab, Voltage and emission current values were set to ensure that observed dead times is between 35 – 40 kv. The analysis was then Run to obtain spectrum data. XRS-FP crossroad scientific software was then opened and the Master Oxide.tfr file was uploaded. Then the obtained Spectra sample file was processed and saved.

Figure 3. 4. Chemical laboratory analysis

3.2.4 Field plots

The runoff plots were set up to monitor soil loss by water erosion at three different locations. Three locations were chosen considering diversities in the soil, geology, and geo-political space. Hence, runoff plots were set up in the Imo clay Formation, the alluvium sands, and the Nanka Formation (Figure 3. 1). The site at Isu-Aniocha in Awka North local government area (LGA) (herein referred to as Isu plot) is on the Imo clay shale and is in the Anambra Central senatorial zone of the State. The site at Otu-

Aguleri in Anambra East LGA is on the alluvial sands and is in the Anambra North senatorial zone while the site at Federal Polytechnic Oko in Orumba North LGA is on the Nanka sand formation in the Anambra South senatorial zone (Figure 3. 1). The three areas are in the agricultural zones of the State.

The plots help to find the differences in soil loss generated over the different geologic formations. The geologic zones have been reported to be high soil erosion risk zones in the State (Egbueri *et al.*, 2022; Fagbohun *et al.*, 2016). Thus, the findings of the field plots on similar vegetal cover and slope lengths help to determine the part of the State with a higher soil loss rate. The premise is based on the belief that when all factors are controlled, the differences in soil erosion are attributed to the isolated factor (Hayward, 1967). For instance, if all factors except geology or vegetation are comparable, then the differences in soil loss and runoff can be attributed to geology or vegetation (Hayward, 1967).

3.2.4.1 Description of the field plots

Isu

The field plots include a 5 by 20 metres plot each on bare fallow agricultural land (herein also referred to as disturbed plot) and vegetated fallow agricultural land (herein referred to as undisturbed plot) (Plate 3.1). However, a shorter length of 5 by 10 m plot was constructed to account for the effect of slope length on soil loss in the area, each on bare fallow and vegetated fallow. The disturbed plots were levelled once at the inception of the experiment while the undisturbed plots were left fallow with vegetation. The disturbance occurred once to minimize temporal variations in erodibility according to Kinnel (2016). The tillage system used in the previous year was heaps and mounds for growing root crops, a common practice in the eastern part of Nigeria. The mounds have furrows in between 4 mounds (Plate 3.1). The disturbed plots were cleared of grasses using herbicides and clear-cutting on 4 occasions throughout the rainy season. The plots were built with planks, sealed on the edges with cellophane bags enclosed with a small board of wood to prevent leakage. It was fitted with a 4-inch diameter pipe through which the runoff drains into collection containers inside a pit. The pipes had collection bags to trap the sediments while permitting runoff to pass through and enter the containers in the pit (Figure 3. 5). The collection points were covered with tarpaulin (cellophane materials) to prevent direct rainfall into the collection points. However, frequent wear and tear led to the changing of the tarpaulin fortnightly which became uneconomical and then were changed with zinc (corrugated) sheets (Figure 3. 6). The big disturbed agricultural land had 3 collection points while the other three plots had a collection point each. The big disturbed plot had a 60-litre container each in two pits and one 120-litre container in the third pit, the small disturbed plot had an 80-litre container, the big undisturbed plot had a 50-litre container while the small undisturbed plot had an 18-litre container for collecting the runoff.

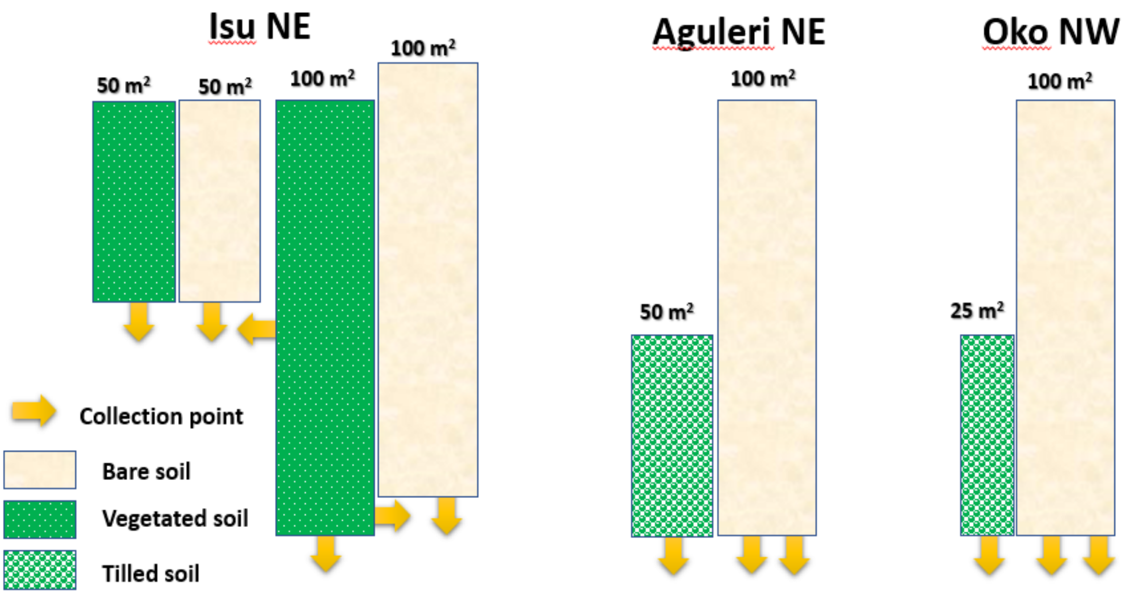

Figure 3. 5. Hypothetical representation of the runoff plots. *NE and NW are Northeast Northwest direction of flow, respectively.

Figure 3. 6. The runoff plots: a. Oko, b. Aguleri, and c. Isu

Aguleri

Two plots were set up at Aguleri: a big fallow plot and a tilled small plot. The big plot is 5 by 20 metres while the small plot is 5 by 10 metres. The big plot was cleared of vegetation and left bare. The small plot was tilled and corn planted (Figure 3. 6). A flat tillage system (FTS) was used. Only very few seedlings survived as pests comprising guinea fowls plucked them from the ground as they germinated. The big plot had 2 collection points of 140 litres and 120 litres. The small plot had a collection point of a 100-litre container.

Oko

Two plots were set up at Oko, a big one of 5 by 20 metres and a small one of 2.5 by 10 metres (Figure 3. 6). These were the last plots set up and were completed on July 27th 2022. The big plot was kept bare of vegetation but the small plot was tilled and corn planted. The area was very bushy before it was cleared of vegetation and kept bare throughout the study (Figure 3. 6). The collection points for the big plot were two but one for the small one. However, there were no containers installed to measure runoff. The soil loss data were collected weekly.

The attributes of the plots were shown in Table 3.5. The plots' slopes fall in the very gentle (2-5 %) and gentle slopes (5-9 %) classes.

Table 3.5. Attributes of the plots

Site	Plot type	Lat	Long	Slope	Aspect	length
Isu	DBP	6.2520337, 6.2520727 6.2520337, 6.2520015	7.05073530, 7.0509224 7.0509224, 7.050747	1.6	NE-SW	20
"	DSP	6.2520733 6.252117 6.2520999, 6.2520554	7.0509024,7.050892, 7.0508006, 7.0508083	"	NE-SW	20
"	UBP	6.2520038, 6.25219539 6.2520539, 6.2520035	7.0507852, 7.0508061 7.0510148, 7.051038	"	NE-SW	10
"	USP	6.2520926, 6.2521095 6.2521554, 6.252141	7.0508035, 7.0508926, 7.0508816, 7.0507916	"	NE-SW	10
Aguleri	Big plot	6.3426649, 6.3426204 6.3426204, 6.3426649	6.8556337, 6.855634 6.855808, 6.855808	2.4	NE-SW	20
"	Small plot	6.3426643, 6.342709 6.342709, 6.3426643	6.8556363, 6.8556363 6.855723, 6.855723	"	NE-SW	10
Oko	Big plot	6.06125, 6.06127 6.06125, 6.06127	7.10226, 7.10208 7.10226, 7.10208	3.8	NW-SE	20
"	Small plot	6.06125, 6.06125 6.06123, 6.06123	7.10213, 7.10224 7.10213, 7.10224	"	NW-SE	10

Rain gauge

A rain gauge was installed at each of the sites. It was installed at a height of 42 cm above the ground. The data were collected after every rain event in Isu and Aguleri but weekly in Oko.

3.2.4.2 Data collection and measurements

The soil loss and the runoff were measured daily in Isu and Aguleri but weekly in Oko. The runoff was measured in litres in-situ each day there was rainfall while the soil loss was collected in a white polythene bag, and labelled accordingly. They were oven dried for 24 hours under a temperature of 105 °C and then brought out and kept open for air drying. When dried, they were weighed on a weighing scale in grams and recorded.

Annual soil loss estimation

The collected data were organised and further analysed using regression analysis (eqs. 3.8-3.10). It is a powerful statistical tool used to determine the relationship between an independent (predictor) and a dependent variable. It is also used to predict the dependent variable in statistics. This was done following the works of other researchers (Hsieh *et al.*, 2009; Mohamadi and Kavian, 2015; Todisco *et al.*, 2015).

$$y = a + bx + \varepsilon \qquad 3.8$$

Where

$$a = \frac{\left(\sum y\right)\left(\sum x\right) - \left(\sum x\right)\left(\sum xy\right)}{n\left(\sum x^2\right) - \left(\sum x\right)^2} \qquad 3.9$$

$$b = \frac{n\left(\sum xy\right) - \left(\sum x\right)\left(\sum y\right)}{n\left(\sum x^2\right) - \left(\sum x\right)^2} \qquad 3.10$$

where y is the dependent variable, a is the intercept, b is the slope, x is the independent variable, and ε is the error term.

With the regression analysis, the coefficient of determination was obtained, which also helps to estimate the correlation between the dependent and independent variables without necessarily running a correlation analysis. Hence, the regression was used to fit a model for the relationship between rainfall and runoff, rainfall and soil loss, and runoff and soil loss.

Arithmetic estimation of annual soil loss and runoff.

The soil loss and runoff data were collected for six months in Isu, five months in Aguleri, and four months in Oko. The rainy season in the area is 7 months a year. Thus, simple arithmetic was used to convert the collected data into annual data. If the data in a year is y, the length of the rainy season is a, and the sum of the data collected in n months is summation x, then the data for a year is (eq. 3.11). The import of this assessment is to have a relative comparison between its result and that of the output from the regression model above.

$$y = \frac{a}{n} \times \left(\sum x\right) \qquad 3.11$$

where y is the annual soil loss, a is the length of the rainy season, n is the number of months the data were collected and Σx is the summation of the collected data.

The conversion rate from g/m^2 to kg/m^2 to t/ha is shown in equations 3.12 and 3.13 (Evelpidou *et al.*, 2013). Also, runoff is converted to litres per metre square (l/m^2) by dividing the runoff by the area of the plot which is also equivalent to runoff in mm while kg/m^2 is the soil loss divided by the area of the plot (Evelpidou *et al.*, 2013; Hudson, 1993).

$$a = b \times 0.001 \qquad 3.12$$

$$c = a \times 10 \qquad 3.13$$

where a is the data in kg/m2, b in g/m2, c is t/ha

Accuracy assessment

The linear model is used to estimate soil loss and runoff as earlier stated. The chosen model was selected based on its performance on the error metrics which include the mean absolute error MAE), and the root mean square error (RMSE) (equations 3.14 – 3.17). The model was tried on the relationship between rainfall and soil loss, rainfall and runoff, and the relationship between runoff and soil loss. Based on that, the model with the lowest error margin was selected. However, for data unavailability, the rainfall-soil loss model was used, though the runoff-soil loss model outperformed it. The data were analysed in R statistical software.

$$MAE = \sum_{i=1}^{n} \frac{y_i - \overline{y}}{n} \qquad 3.14$$

$$RMSE = \sqrt{\frac{\sum_{i=1}^{n} y_i - \overline{y}^2}{n}} \qquad 3.15$$

$$MAPE = \frac{1}{n} \times \sum \left(\frac{y_i - \bar{y}}{y_i} \right) \times 100 \qquad 3.16$$

where $| y_i - \bar{y} |$ is absolute deviation, y_i is the i-th measurement, $\bar{y}$ is the prediction value, n is the number of observations, and δ is the standard deviation.

A MAPE value of less than 10 % is good but values between 10 and 25 % are acceptable (Swanson, 2015). Thus, Chang *et al*. (2007), Kumar and Vasantha (2015), and Olatunji *et al*. (2019) added that MAPE of less than 10 % is excellent, between 10 and 20 % is good, and between 20 and 50 % is acceptable but MAPE of over 50 % is considered unacceptable. The choice of these metrics is based on their wide application in forecast and prediction studies (Olatunji *et al.*, 2019). The lower the values of the RMSE or MAE, the better is the performance of the model (Tiwari and Chong, 2019).

3.2.5 Revised Universal Soil Loss Equation model

The RUSLE is a widely used model for soil erosion rate assessment (Kinnel 2019; Alewell *et al*. 2019; Ghosal and Bhattacharya, 2020). It simply estimates soil erosion of a given area as a product of five key factors. These factors include the rainfall erosivity, soil erodibility, Slope steepness and length, the cover factor, and the conservation practices factor.

3.2.5.1 Rainfall erosivity (R) factor

Data and analysis

The data comprised daily rainfall data from 2015 to 2022. The data were aggregated into mean annual rainfall for each year. The data was subjected to further analysis in QGIS using the raster calculator module from the Map Algebra Toolbox to derive the erosivity using equation 3.17.

The erosivity factor is determined by the product of the storm's total kinetic energy and its maximum 30-minute intensity (I_{30}) which is linearly related to soil loss

(Wischmeier and Smith, 1958). The method developed by Roose who worked much on West African soil erosion considers the annual rainfall and a constant of 0.5 (eq. 3.17) (Adediji *et al.*, 2010; Luvai *et al.*, 2022; Roose, 1977; Rozos *et al.*, 2013) were used.

$$R = 0.5 \times P_a \times 1.73 \qquad 3.17$$

where R is erosivity, and P_a is annual precipitation.

The erosivity values range from 0 to infinity, such that under tropical climates, the R-factor can reach 1500 to over 3000 MJ mm $(hahyr)^{-1}$ (Andreoli, 2018; Dumas *et al.*, 2010). The variations in erosivity were assessed for the periods 2017-2022. It has been argued that about 75 % of variations in soil loss are explained by variations in erosivity and slope steepness (Doetterl *et al.*, 2012). They also represent natural factors in the RUSLE model as they can very minimally be modified by direct human influence (Borrelli, 2011) and also are triggers of soil erosion since they supply the energy required to erode the soil (Naipal *et al.*, 2015). The erosivity trend is reported to be on the increase (Qin *et al.*, 2016; Wang *et al.*, 2017), slowly decreasing trend in Iran (Sadeghi and Hazbavi, 2015) while Diodato *et al.* (2020) reported a slowly increasing trend.

3.2.5.2 Soil erodibility (K) factor

Data and analysis

The data comprised soil data from the iSDA comprising properties such as percentage silt, sand, clay, and the organic matter content.

The algorithm presented in equation (3.18-3.22) (Williams (1995) cited by Wawer *et al.* (2005) is used. It is widely used in the tropics and has been shown to estimate the K factor value reasonably well (Tsige *et al.*, 2022).

$$K = f_{csand} \times f_{cl-si} \times f_{orgC} \times f_{hisand} \qquad 3.18$$

where

$$f_{csand} = 0.2 + 0.3\exp\left[-0.256 m_s\left(1 - \frac{m_{silt}}{100}\right)\right] \qquad 3.19$$

$$f_{cl-si} = \left(\frac{m_{silt}}{m_c - m_{silt}} \right)^{0.3} \quad 3.20$$

$$f_{orgC} = 1 - \frac{0.25 \times orgC}{orgC + \exp[3.72 - 2.95 orgC]} \quad 3.21$$

$$f_{hisand} = 1 - \frac{0.7\left(1 - \frac{m_s}{100}\right)}{1 - \frac{m_s}{100} + \exp\left[-5.51 + 22.90\left(1 - \frac{m_s}{100}\right)\right]} \quad 3.22$$

where K is the erodibility factor, and f is the fraction of soils' attributes (clay, silt, sand, and carbon).

3.2.5.3 Topographic (LS) factor

Data and analysis

The DEM obtained from the USGS was used. It is a 30 m resolution data.

Several algorithms have been developed for estimating the LS-factor (Wischmeier and Smith, 1978; Moore and Nieber, 1989; Desmet and Govers, 1996; McCool *et al*., 1997). However, based on the study by Nakil and Khire (Nakil and Khire, 2016), equation 3.23 by Wischmeier and Smith (1978) was used.

$$LS = \left(\frac{\lambda}{22.13} \right)^{0.5} \times \left(0.065 + 0.045s + 0.0065s^2\right) \quad 3.23$$

where s is the slope in per cent, λ is flow accumulation multiplied by the spatial resolution of the DEM.

With increasing slope steepness and length, so erosion also increases (Pitt, 2004; Ziadat and Taimeh, 2013; Sinshaw *et al*., 2021; Merchán *et al*., 2023). Longer slopes increase the runoff accumulation and soil movement (Wischmeier and Smith, 1978; Jones et al., 2012; Selmy *et al*., 2021).

3.2.5.4 Management C-factor

The Land cover map from the ESRI were used. They are land cover of 2017, 2020, and 2022. They are 10 m resolution land cover maps with high accuracy (Karra *et al*.

2021). The land cover of 2060 was generated using the Multilayer Perceptron method in the Terrset software. The simulation was based on vegetation-to-settlement submodel as the driver of change in the study area. The land cover had a kno and klocation accuracies of 63 and 90 % respectively.

Thus, the C-factor values were estimated based on the look-up tables from the literature. Seven-class land use and land cover of the area were used while the appropriate C-factor value was assigned to each. Rangeland was assigned 0.15 (Barman *et al.*, 2020), settlement or urban 0.8 close to 0.7 by Egbueri *et al*.(2022), bare land 1.0 (Conforti *et al*., 2016; Egbueri *et al*., 2022; Zanchin *et al*., 2021), forest 0.08 (Merchán *et al*., 2023), cropland 0.38 (Benavidez *et al*., 2018; Ebabu *et al.*, 2022; Koirala *et al.*, 2019; Wischmeier and Smith, 1978), and water 0.0 (Tsegaye and Bharti, 2021; Zanchin *et al*., 2021). The settlement in most of the urban areas is a mix of built spaces and bare ground. Untarred streets dominate most of the places and these bare surfaces are highly susceptible to surface flows generated by corrugated roofs and other impervious surfaces. They form a major source of sediment for runoff during rain events. Due to the effect of erosion on some of the bare streets, they are unusable or difficult to use by vehicles and pedestrians (Figure 3. 7). Hence, it was assigned 0.8. The forest areas are mainly found in the riparian zones and so were assigned 0.08 following earlier studies as shown above. The C-factor was assessed for the periods 2017, 2020, 2022, and 2060. This is to permit assessment of the variations in soil erosion due to the variations in C-factors (land cover) and erosivity (climate). They were used to predict the land cover and C-factor for 2060.

Figure 3. 7. Street erosion in Awka town

3.2.5.5 Conservation P-factor

The P-factor is the conservation factor. However, due to data unavailability on soil conservation practices in the area, the value of unity was used in line with other studies (Ajibade *et al.*, 2020; Borrelli, 2011; Fagbohun *et al*., 2016; Ghosal and Bhattacharya, 2020).

3.3 Materials and Methods

3.3.1 Purposive sampling

The study involved 128 farmers who were purposively selected. The communities were purposively selected from the main agricultural Local Government Areas (LGAs) in Anambra State. Among the 4 main farming regions: the north, east, south, and southwestern parts of the State, 3 were purposively selected which are the north, east, and south. From these, the main farming LGAs were selected purposively and thus in the north, Anambra East was selected, in the east, Awka North, and in the south, Orumba North LGA was selected. From them, 5 communities were chosen. Thus, in Anambra East, Aguleri and Enugu Otu were selected, in Awka North, Ebenebe and Ugbenu were selected, and in Orumba North, Ndiowu was selected. One community was selected in the south due to increasing insecurity in the southern part of the State.

Purposive sampling was used because it helped to achieve the objective of the study. Again, the State is cosmopolitan with commerce/trade as the major economic activity of the people. Thus, only a very few percentage of the population are farmers. Hence, most of the communities have an urbanising part where the inhabitants comprise people with different occupations. Therefore, in each of the communities, those who are farmers were sampled as many as could be reached. It was difficult to get the farmers' consent to respond to our questions because they were very busy with their farm activities. After much pleas, some obliged while some agreed to attend to us only if we would meet them on Sundays when they were free. Besides, many of them were unhappy and frustrated due to the destruction of their farmlands and houses by the 2022 flood.

A semi-structured questionnaire (Appendix 1) was used to garner information from the farmers. It permitted the exploration of their perceptions of soil erosion, the causes of soil erosion, pieces of evidence of soil erosion in their farms, and adaptation options they employ to withstand and live with the impact of soil erosion. It also allowed flexibility by enabling respondents to reflect on the issues properly (Lange *et al.*, 2015).

3.3.2 Analysis

The data were analysed following an inductive approach where a systematic analysis of the data is guided by the research objectives. The results were summarized in tables and percentages. The results showed the socioeconomic characteristics of the farmers, their perception of soil erosion risk, its causes, their adaptation measures, and the barriers to adopting soil conservation measures.

4. RESULTS AND DISCUSSIONS

4.1 Variations in rainfall in Anambra State

4.1.1 Nature and distribution of rainfall

The rainy season begins in March and ends in November, with an annual rainfall of about 1725.2 mm (Aguleri), 1940.8 mm (Isu), and 2031.7 mm (Oko). The southern part of the State is wetter than the northern part (Figure 4. 1). The State has double maxima which is more pronounced in the northern part. The highest rainfall occurred in September in the north but in July in the southern part (Figure 4. 1). The southern part has the highest mean annual rainfall. This concurs with the fact that rainfall decreases from south to north (Okoloye *et al*., 2013). Also, the mean monthly rainfall was 176.4 mm in the south but 146.1 mm in the north. The south had the highest recorded monthly rainfall. It was 517.1 mm (Aug 1987) in the south but 477.5 mm (Aug 1987) in the north. The least monthly rainfall was 0 in the State. However, it was more in the north than in the south. It occurred in Dec 1981, 1986, 1999, and 2015 and Jan 1983, 89, 91, 92, 2002, 07, 11, 18, and 20 in the north. In the south, it occurred in Jan 1983, 84, 89, 2007, 20 and Dec 1999, 2009 and 2019. That was 13 months of no rain in the north but 8 months in the south within the period of study. The lowest mean annual rainfall occurred in 1983 (1140.4 mm, north and 1366.3 mm, south). The highest mean annual rainfall occurred in 1995 (2096.5 mm, north and 2586 mm, south) (Table 4.1). Oko recorded higher rainfall and experienced the earliest retreat of the cT wind thus making the Harmattan wind milder than the northernmost part.

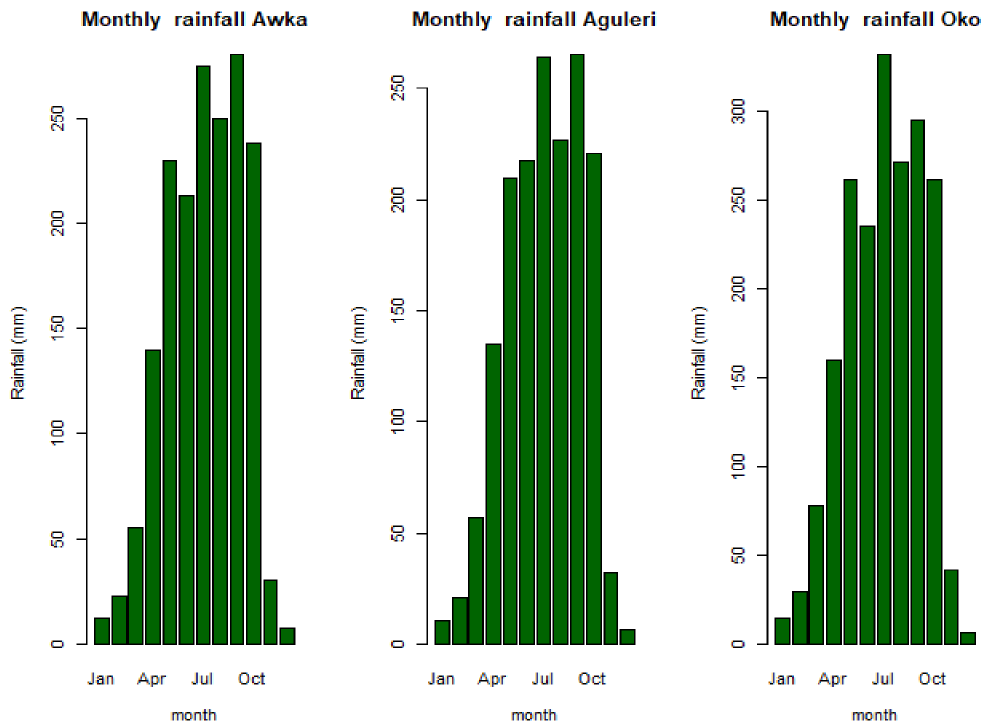

Figure 4. 1. Monthly rainfall distribution in Anambra State

Table 4.1. Summary statistics of the rainfall

Daily	Isu (mm)	Aguleri (mm)	Oko (mm)
Min	0.0	0.0	0.0
Median	0.0	0.0	0.0
Mean	4.8	4.6	5.4
Max	106.6	85.6	113.3
CV	1.71	1.74	1.68
Monthly	Isu (mm)	Aguleri (mm)	Oko (mm)
Min	7.7 (Dec)	6.2 (Dec)	6.3 (Dec)
Median	176.7	172.4	197.7
Mean	146.1	138.9	165.7
Max	279.9 (Sept)	265.0 (Sept)	331.9 (Jul)
CV	0.77	0.76	0.75
Annual	Isu (mm)	Aguleri (mm)	Oko (mm)
Min	1212.2 (1983)	1140.4 (1983)	1366.3 (1983)
Median	1780.3	1694.9	1992.5
Mean	1940.8	1725.2	2031.7
Max	2309.4 (1995)	2096.5 (1995)	2586.4 (1995)
CV	0.12	0.11	0.12

4.1.2 Variations in rainfall in the area

The rainfall in the area varied spatially and temporally. Rainfall was higher in southern locations than in northern parts (Table 4.1, Table 4.2). The rainfall also varied temporally, such that the driest months were December, January, and February (Figure 4. 2). The highest amount of rainfall was recorded in the months of June-September (Figure 4. 1, Figure 4. *2*, Table 4.1). However, the amount varied from 1940.8 mm (north) to 2031.7 mm (south). This was in line with Okoloye *et al*. (2013) that rainfall decreased from south to north. Figure 4. 2 showed that December to February was very dry with little to no rain. That showed that soil erosion was at its barest minimum or non-existent at this period of the year as little or no rain was experienced. However, from March the rains are expected. That is, the onset of the rainy season when rain is expected as the humidity is higher and the cloud is usually overcast from this period.

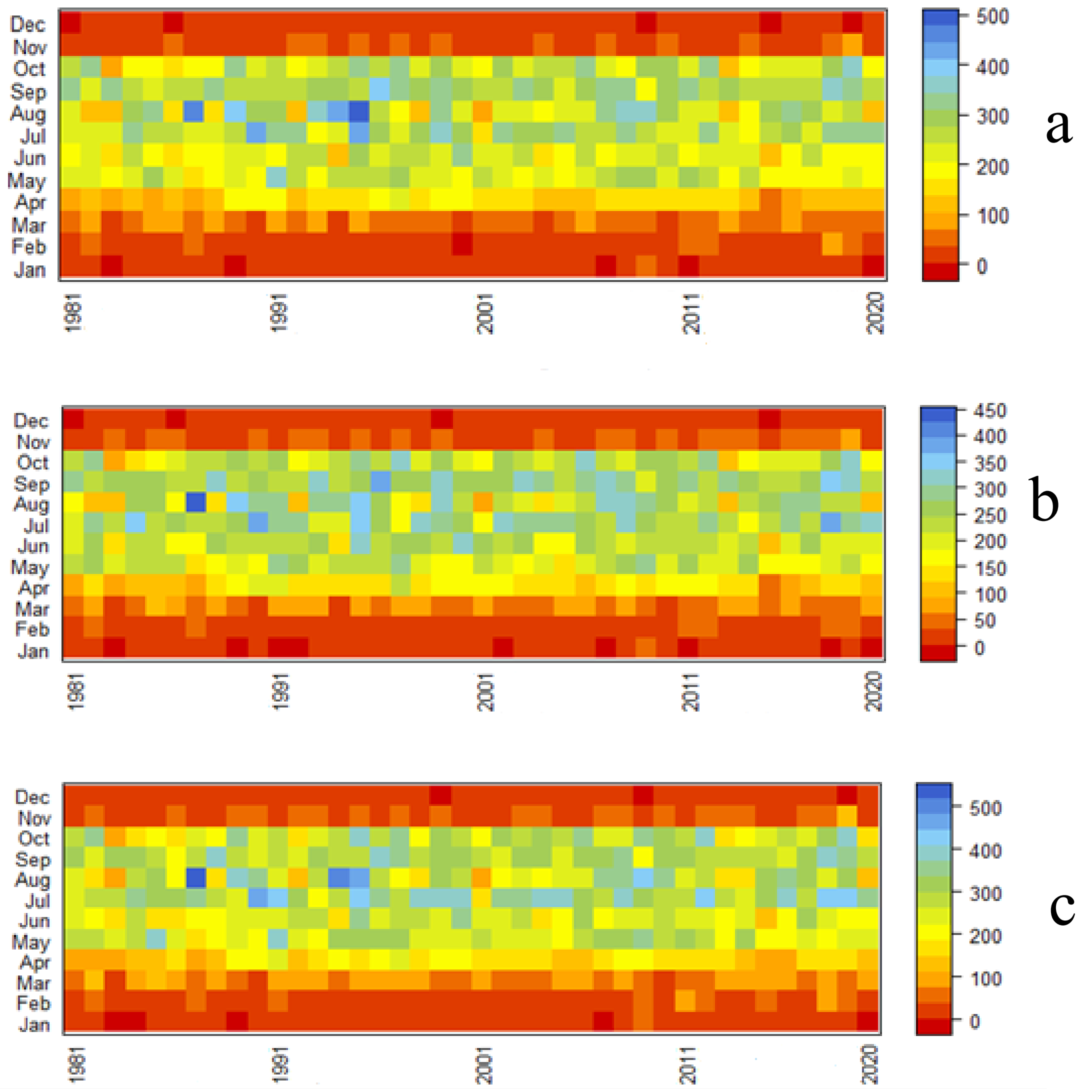

Figure 4. 2. Interannual rainfall variations in rainfall values (mm/month): a. Isu, b. Aguleri, and c. Oko

The seasonal rainfall distribution was higher in the south than in the north (Table 4.2). The highest amount of rainfall was recorded in the season of June-August followed by September-November. This showed that soil erosion would likely be high within these two seasons. This is because due to sparse vegetation cover, runoff and erosion increase with increase in rainfall, and second, at this time the soil is at field capacity or saturated because antecedent soil moisture significantly influences soil loss (Roose, 1977; Ziadat and Taimeh, 2013).

Table 4.2. Seasonal distribution of rainfall

Seasonal	Isu (mm)	Aguleri (mm)	Oko (mm)
DJF	43.1	37.8	50.7
MAM	424.7	401.7	499.6
JJA	737.4	708.6	838.8
SON	547.8	518.2	598.0

The coefficient of variation in annual rainfall in the area is 12 % for Isu and Oko but 11 % for Aguleri (Table 4.1). However, the coefficient of variation was higher for the daily rainfall followed by the monthly rainfall and the least was the annual rainfall (Table 4.1). This showed that there were much more variations in daily rainfall than there were in annual rainfall. The month of December had the highest coefficient of variation in the area, 89 % for all locations. The degree of variations in rainfall is relatively similar in all locations in the State.

The CV in rainfall also shows that the variations in rainfall is higher for daily events than the monthly and annual events. This is because rainfall is a highly variable climate element but when expressed in months and annually, the variability is hidden in the climatology/aggregation.

4.1.3 Possibilities of extremes

The northern part has a lower mean of such events than the southern part (Figure 4.3). A higher than the mean was experienced from 2005 to 2017 (Figure 4.3). The trend is positive but not significant (0.63 in Aguleri, 0.30 in Isu, and 0.26 in Oko). The rate of increase was 0.7 mm (Aguleri), 2 mm (Isu), and 2.4 mm (Oko) per decade. It showed that extreme rainfall was highest in 2005 followed by 2010 and 2015 in the three locations. In the 1980s, the maximum annual one-day rainfall recorded was below or barely above the average. It then increased in the 1990s, however, it became very pronounced in the 2000s as it reached the highest level in this decade and the following one (Figure 4.3). The maximum one-day rainfall was vital in influencing runoff and soil erosion. All things being equal, days with the highest rainfall were usually associated with the highest erosion. However, this varies with time and rainfall intensity. This is because, soil erosion varies with season, antecedent moisture, and time (either the onset or the end) of the rainy season.

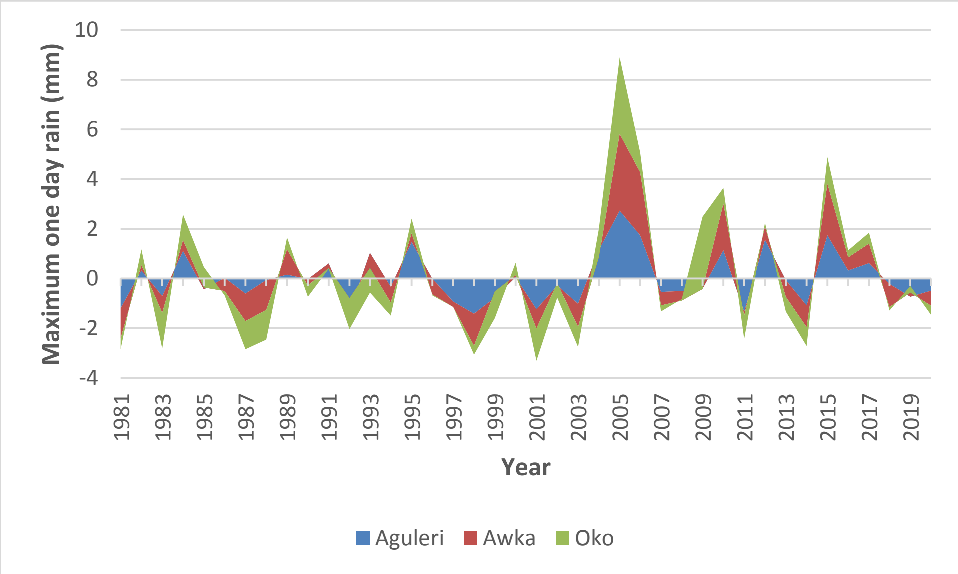

Figure 4.3. Normalised maximum extreme one-day rain (mm) in Anambra State.

The plot of the number of rainy days with rainfall above 20 mm each year is shown in Figure 4.4. It showed that the southern part had a higher number of days with rainfall of above 20 mm. It also shows that 1981 and 2013 were very dry in the north and south as they had a little above 10 days when rainy days had above 20 mm. The southern part in those two years had a mean of 14 days while the northern part had a mean of 11 days (Figure 4.4). The trend shows that it is significantly rising in Oko (P-value 0.01) but is not significant in Isu (0.38) and Aguleri (0.39) though they are all increasing. The rate of increase is 0.3 in Oko but 0.09 in Isu and 0.06 in Aguleri. The increasing trend might likely lead to an increase in runoff and soil loss in the area.

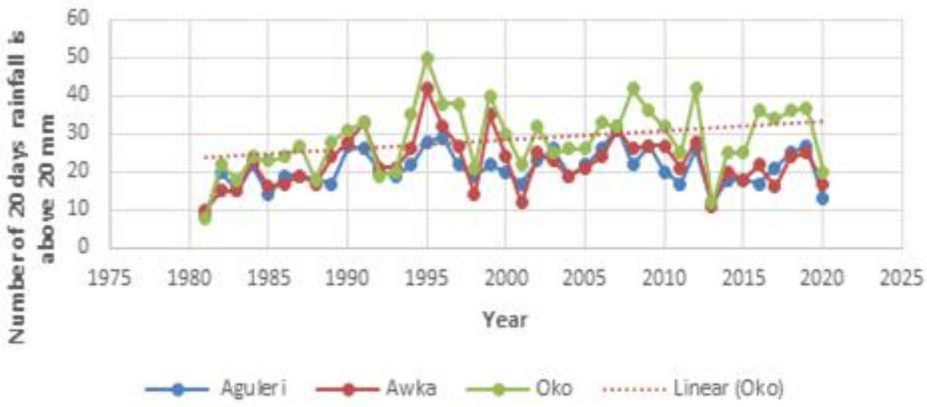

Figure 4.4. Number of rainy days with or above 20 mm of rainfall in each year

The plot of the 95th percentile rainfall occurrences in the area was shown in Figure 4.5. It can be deduced that there was a higher likelihood of extreme event occurrence in Oko than in the other locations. Thus, the southern part experienced heavier rainfall events than the northern part (Figure 4.5). Heavy rainfall events were the suppliers of the force that erode the surface. It offers competence to the runoff and induces infiltration-excess runoff that has a greater force to erode. This is in line with Ziadat and Tiemah's (2013) assertion that intensity is one of the most important factors that drive soil loss. Also, Roose (1977) agreed to this that intensity and antecedent soil moisture drive erosion in tropical Africa. At this, it can be inferred that soil loss was greater in the south than in the north. The trends of the 95th percentile of rainfall in the area are shown in Table 4.3. It showed that they are all increasing in the area but none was significant at a 0.05 confidence level. However, there was a higher chance for an increase in Oko as there was a higher confidence in the p-value than in other locations (Table 4.3). There was about 82/83 % confidence in the likelihood of an increase in the trend in Oko. This foretells more soil degradation in the south.

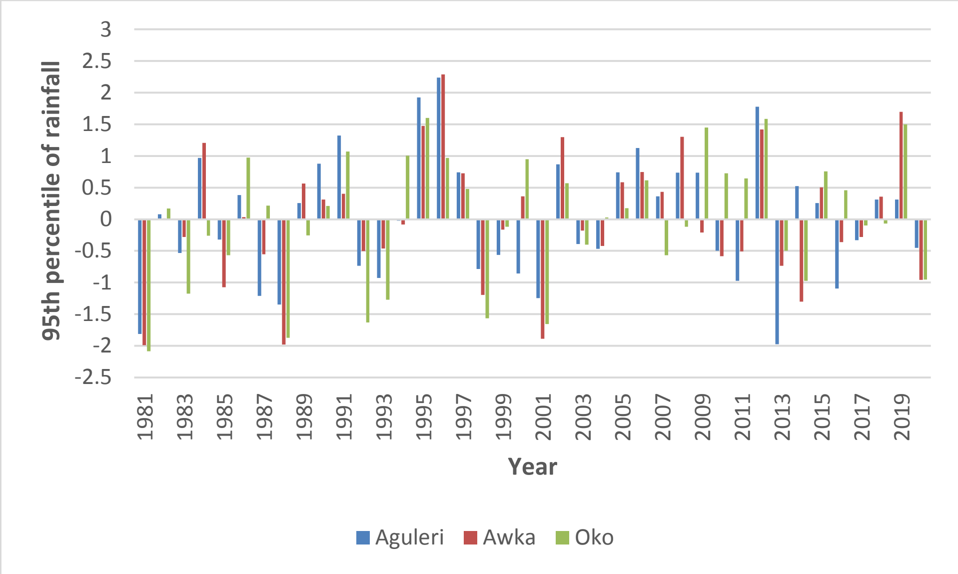

Figure 4.5. Plot of rainfall above the 95th percentile (extreme rains)

Table 4.3. Magnitude of the trend in the 95th percentile of rain

	Sens slope	P-value	Sens slope	P-value	Sens slope	P-value
	95th % sum daily rain		95th % of total rain		99th percentile total rain	
Isu	0.80	0.60	0.03	0.74	0.01	0.62
Aguleri	0.32	0.90	0.02	0.88	0.00	0.69
Oko	2.58	0.17	0.12	0.18	0.05	0.18

It (Figure 4.6) shows that the percentage of extreme rainfall has been high from 2003 to 2020. It also shows that the mid-1990s, mid-2000s, and later periods (2015-2019) witnessed higher increases in extreme events (Figure 4.6). This indicated that the erosivity and the competence of runoff would be high. The contribution from the very extreme rainfall (Figure 4.6) showed that it has an increasing trend but it was not significant. However, the significance level was higher in Oko as it can be said that at 82 % confidence level (Table 4.3), the very extreme rainfall is rising. This indicated that there was a higher chance for high rainfall in the southern part and consequently a higher erosivity. The rising trend was a warning signal for intensified conservation efforts. This is because projections point to an increase in rainfall extremes on the Guinea Coast of West Africa (Bichet and Diedhiou, 2018; Faye and Akinsanola, 2022;

Sanogo *et al.*, 2015). Again, it was established that intense rainfall and storms lead to high soil erosion (Boix-Fayos *et al.*, 2007). On this account, Roose (1977) adds that 10-20 % of such storms cumulated control the level of erosion in tropical Africa.

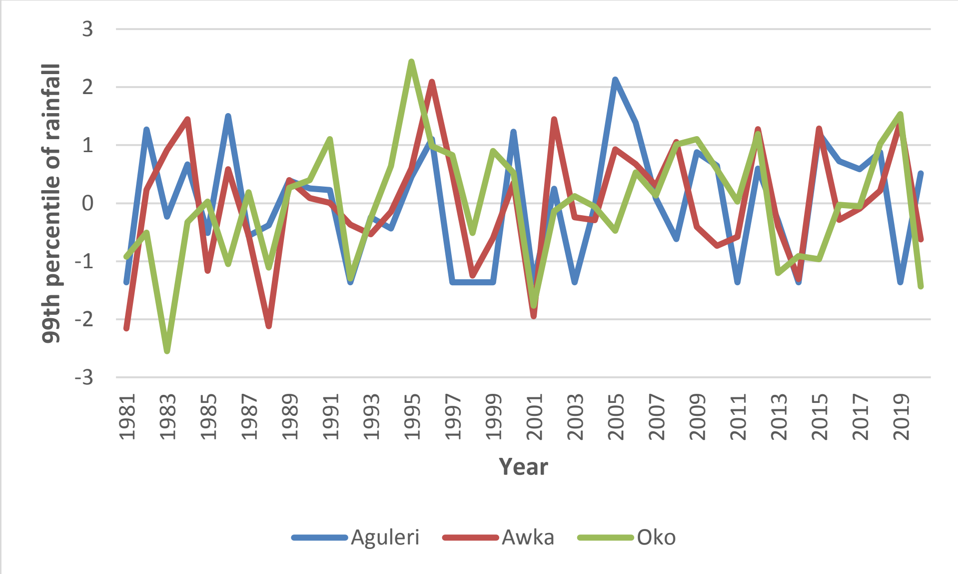

Figure 4.6. Plot of the 99th percentile contribution from the rainfall

The daily rainfall intensity was displayed in Figure 4.7. It revealed that the pattern of the daily rainfall intensity was similar in all stations, though the likelihood of occurrence of daily rainfall intensity was slightly higher in the south than in the north. It showed that low intensity (below average) persisted in the 1980s until around 1990, from when it became higher than average till around 2019 though with minor fluctuations (Figure 4.7). The simple daily intensity index (SDII) also showed a positive trend in all stations but was higher in the south (Oko). The trend is not significant as the p-values were higher than the alpha value (Isu-0.52, Aguleri-0.97, Oko-0.20). The rate of increase was also low (Isu 0.01, Aguleri-0.002, Oko- 0.02). The SDII was obtained by dividing the total annual precipitation by the number of rainy days. It shows that erosivity could be higher in the south than in the north since intensity influences soil loss (Fang *et al.*, 2015; Ziadat and Taimeh, 2013).

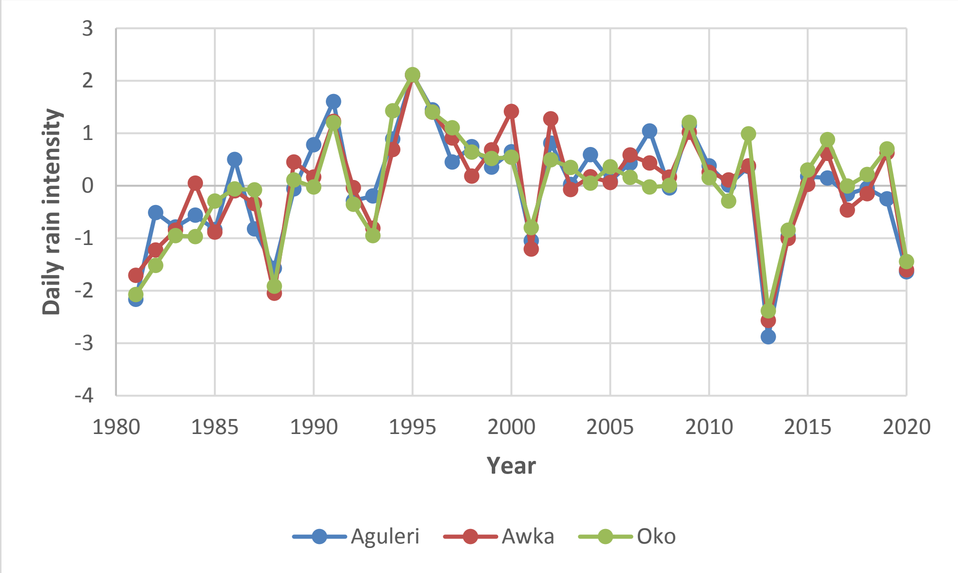

Figure 4.7. Plot of the simple daily rainfall intensity (SDII)

4.1.4 Extreme five-day rainfall

The extreme 5-day rainfall in the area shows an increasing trend which is more pronounced in the 2000s, from 2005 to 2018 (Figure 4.8). This rising trend indicate high soil erosion as extreme events are associate with severe erosion. It shows a rate of change of 2.5 mm (Aguleri), 1.5 mm (Isu), and 2.2 mm (Oko) per decade but they are not significant. The trend is higher in Aguleri followed by Oko.

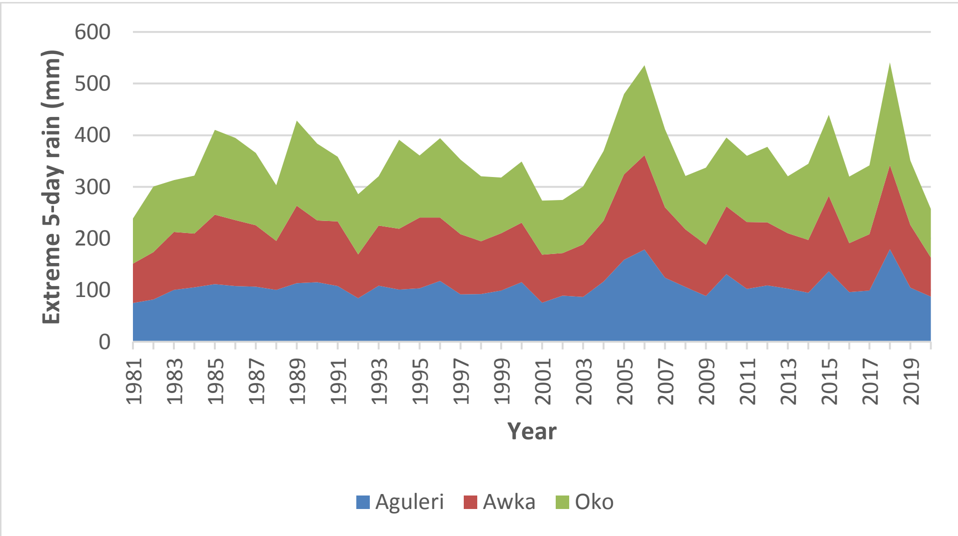

Figure 4.8. Extreme 5-day rainfall (mm) in Anambra State

Monthly rainfall anomaly, climatic water balance CWBAL, and soil moisture

The deviations from the monthly mean rainfall over the years showed that the dry season months November to March and April, the month of the onset of the rainy season had negative deviations. It showed that their mean rainfall was less than the overall mean for the months while the core rainy season months were positive (May to October). This nearly coincided with the period the soil was at field capacity or saturated when the climatic water balance is positive (Figure 4.9). Thus, the rainfall was above the potential evapotranspiration (PET). The climatic water balance revealed that it was positive during the peak of the rainy season. It had a near-zero value for April, the month of the onset of the rainy season. This means that the quantity of rain accumulated in April was barely more than the potential evapotranspiration in the area. The highest water balance occurred in September in the north but in July in the south (Figure 4.9). There was a very strong positive correlation between rainfall and climatic water balance in the area (0.998). It was an expected relationship as moisture content increases with increasing rainfall which climaxes at the peak of the rainy season. Runoff increases during the wet seasons in the humid tropics (Feddema, 1998). At the peak of the rainy season and toward the end of the season due to super-saturation of the soil, saturation-excess runoff and soil loss predominate. There is a significant strong positive correlation between CWBAL and soil loss, and between soil moisture and soil loss in Isu and Oko but not significant in Aguleri (Table 4.4). Feddema (1998) added that estimated water balance might yield skewed results, so soil moisture estimates should be used where possible. Therefore, soil moisture data was correlated with soil loss and it yielded similar results. This shows that CWBAL data can be used as proxy soil moisture data in the absence of actual soil moisture data. Thus, it implied that as CWBAL or soil moisture increased, so did soil erosion increase in the area. However, it was not significant in Aguleri indicating that other factors like permeability suppressed the impact of CWBAL. The alluvial soil of the area is highly permeable and erosion was very highly reduced in the area until very much later in the season when the soil became super-saturated toward the end of the season.

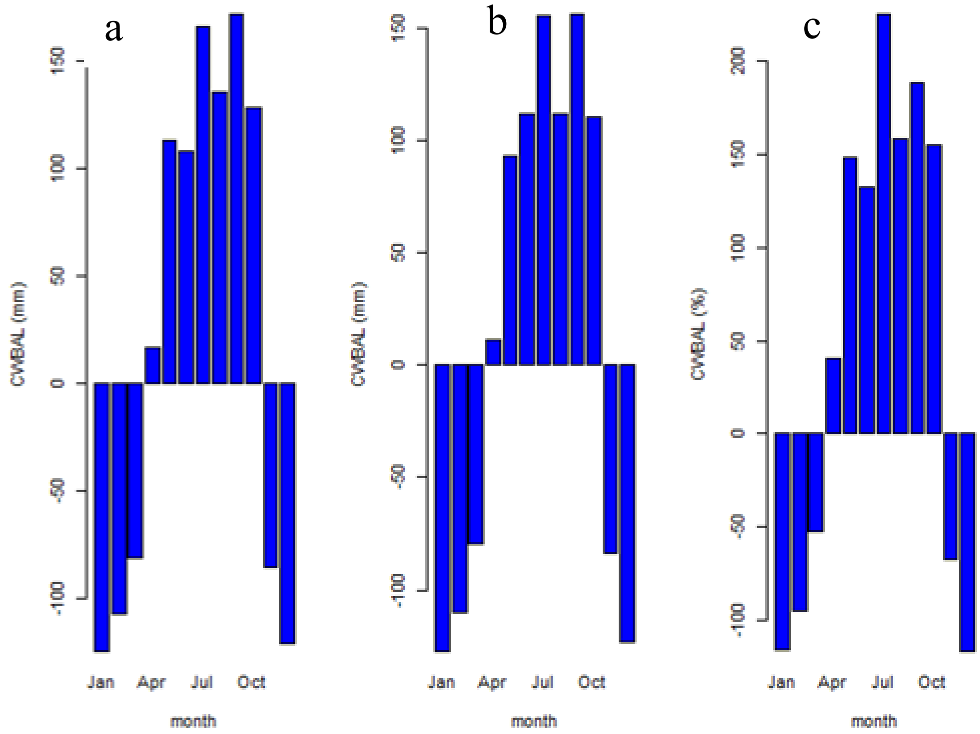

Figure 4.9. Climatic water balance in Anambra State: a. Isu, b. Aguleri, and c. Oko

Table 4.4. Correlation between CWBAL/soil moisture and soil loss

Location	CWBAL		Soil moiture	
	r	p-value	r	p-value
Isu	0.66	0.02*	0.59	0.04
Aguleri	0.39	0.21	0.38	0.22
Oko	0.84	0.00*	0.68	0.01

*significant at 0.05 significance level

Also, for the positive deviations, Oko had higher peaks than Isu and Aguleri which shows that the southern part had heavier rainfall than the northern part. The high atmospheric water balance entails high soil moisture due to net gain in moisture over evapotranspiration in the area. All things being equal, the net gain will increase soil moisture. As Feddema (1998) added, runoff increases with increasing water balance during the wet season. Additionally, water surplus conditions increase with a decreased soil's ability to absorb excess rainfall (Feddema, 1998). Thus, the antecedent soil moisture will be higher in the south than in the north. The higher the soil moisture content the higher the likelihood of saturation-excess erosion. Therefore, saturation-excess runoff/soil erosion would likely be higher in the south than in the north.

The soil moisture in the area reflected the rainfall pattern (Figure 4.10). A weak positive correlation exists between soil loss and soil moisture in the vegetated fallow plots in Isu. However, a significant positive correlation exists between soil loss and soil moisture (0.59 with a p-value of 0.04) in the 100 m^2 bare fallow plot. In Oko, it had a significant strong positive correlation with soil loss in the big (0.68) and small plots (0.72) with a p-value of 0.01 in both plots at Oko. However, at Aguleri, the correlation was weak and not significant statistically (0.38 for the big plot) and (0.41 for the small plot) with p-values of 0.22 and 0.19, respectively. This showed that an increase in soil moisture was accompanied by an increase in soil erosion in the area though with a lower confidence in Aguleri. The Aguleri area was affected by high permeability which implied that an increase in soil moisture might not always be accompanied by a corresponding increase in soil erosion due to other local conditions. However, once the soil reached saturation, the soil erosion became increasingly severe. This was confirmed by field experiments in Aguleri. This was in line with studies that antecedent soil moisture leads to an increase in soil erosion and runoff (Li and Fang, 2016; Sachs and Sarah, 2017; Sadeghi *et al.*, 2016; Ziadat and Taimeh, 2013).

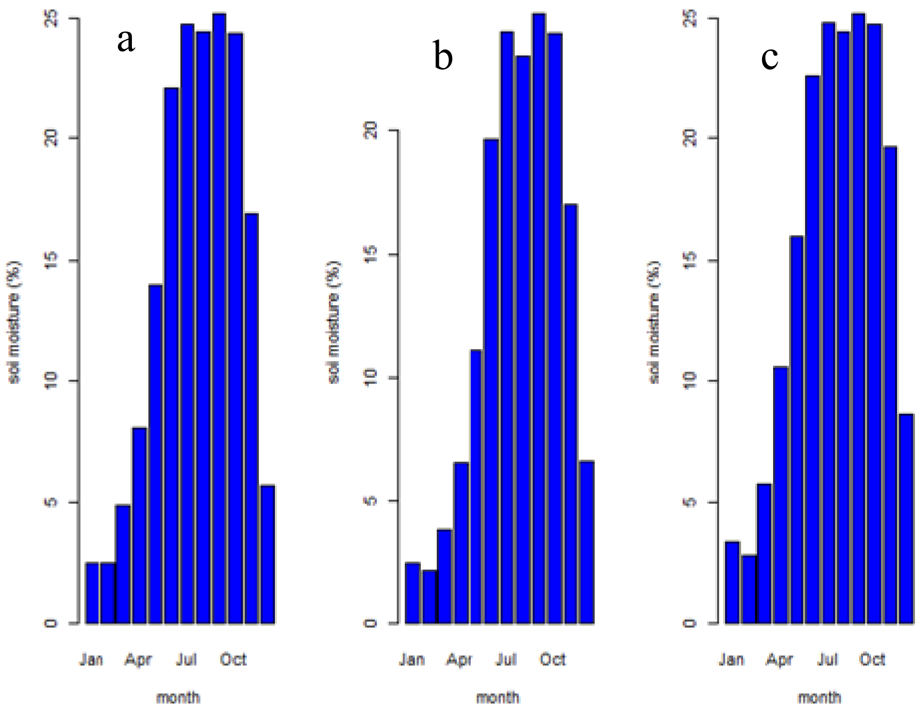

Figure 4.10. Soil moisture distribution in Anambra State: a. Isu, b. Aguleri, and c. Oko

4.1.5 Start and end of the rainy season

The mean start date of the rainy season in Isu was 2nd April, 9th April in Aguleri, and 19th March in Oko. The mean end date of the rainy season was 29th October in Isu and Aguleri but 1st November in Oko. The mean length of the rainy season was 210 days in Isu, 203 days in Aguleri, and 227 days in Oko. The start dates and end dates of the rainy season were critical to soil degradation due to the intensity of the rain during this period of the year. The rains at these times were usually torrential and often accompanied by thunderstorms. Thus, the erosivity of the rain was high and the generated runoff had high power or competence and therefore has the potential to erode. However, the susceptibility of the soil to erosion was always higher toward the end of the rainy season than at the onset in the equatorial belt. This is because at the start of the season, the soils are usually compact while at the end of the season, the soil is highly disturbed due to harvest, saturated and so is more vulnerable to erosion. This is in contrast to the findings of Fang *et al*. (2015) and Mounirou *et al*. (2022) findings that erosion is higher at the onset of the rainy season. However, they worked in semi-arid areas where soils are highly disturbed and bare during the dry season. In addition, Nill *et al*. (1996) opined that erosion is higher on wet soils than on dry soils and soils at the end of the rainy season are super-saturated. Thus, little intense rain generates runoff and soil erosion as infiltration is drastically at its minimum due to super-saturation. Thus, antecedent soil moisture is important in driving soil erosion and runoff as intensity alone might be not enough to cause severe soil loss.

The start of the rainy season in the area tends towards later dates (Table 4. *5*, Figure 4.11). That means that the rainy season starts later than it did previously. This portends danger to agriculture and soil degradation. At a 99 % confidence level, the rising trend in start dates of the rainy season is significant in Isu but Aguleri (94 %) and was not significant in Oko (Table 4. *5*).

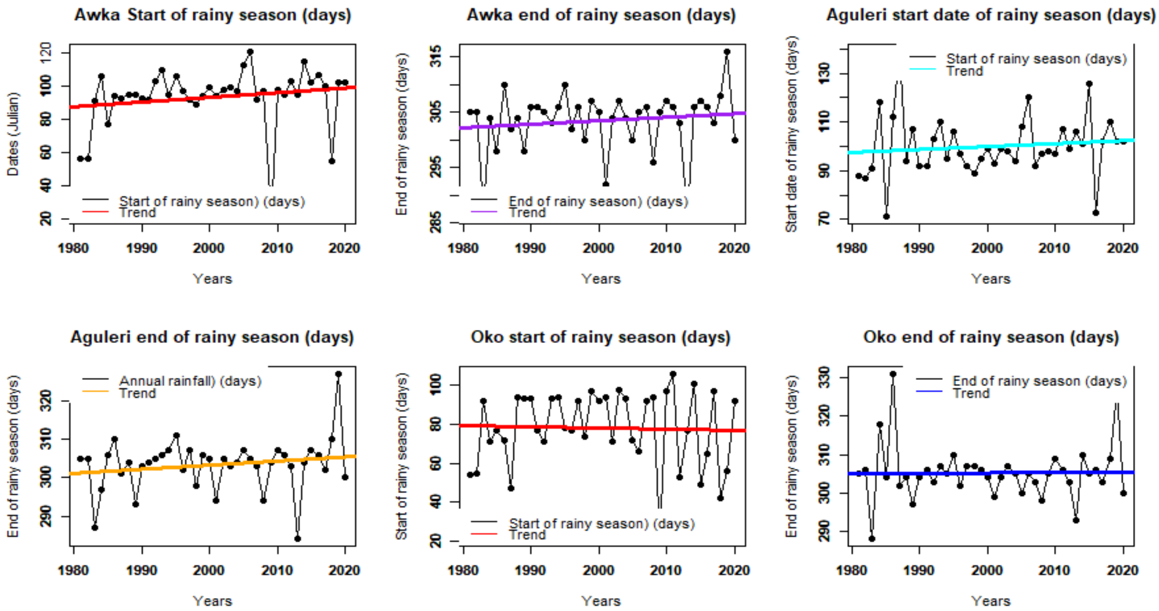

Figure 4.11. Start and end of the rainy season in Anambra State

The end dates of the rainy season had rising trends; however, they were all not significant. This means that the rainy season ends at later dates nowadays than in the past. The later end of the rainy season is not good for agriculture and soil erosion. The later end of the rainy season will impact erosion as rain of higher intensities is expected toward the end of the season and hence, much more havoc is expected with such a trend.

Table 4. 5. Trend test for the start, end and length of the rainy season

Isu	Z	tau	Sens slope	p-value	S	var
Start	2.67	0.29	0.29	0.01	230.00	7329.33
End	1.14	0.13	0.05	0.25	98.00	7245.33
Aguleri	Z	tau	Sens slope	p-value	S	var
Start	1.87	0.21	0.27	0.06	161.00	7341.00
End	0.74	0.08	0.03	0.46	64.00	7276.67
Oko	Z	tau	Sens slope	p-value	S	var
Start	0.47	0.05	0.05	0.64	41.00	7315.67
End	0.16	0.02	0.00	0.87	15.00	7283.67

The earliest start date of the rainy season in the area was 21st January (Isu, 2009), 21st January (Oko, 2009), and 12th March (Aguleri). The latest start dates of the rainy season were the 30th of April (Isu, 2006), the 15th of April (Oko, 2011), and the 18th of May (Aguleri). The most recurring start dates of the rainy season were 14th April (Isu), 11th April (Oko), and (Aguleri). The most recurring end dates of the rainy season were 2nd November (Isu), 1st November (Oko), and 1st November (Aguleri). The later date of the end of the rainy season impacts soil erosion as the rainfall in the area experiences higher intensities toward the end of the rainy season. It generates more soil loss given that the soil is saturated at this period of the year. For it is reported that soil erosion is higher on wet soils (Nill *et al.*, 1996). Additionally, most soil losses occur with rainfall of high intensities (Fang *et al.*, 2017; Yuan *et al.*, 2021; Ziadat and Taimeh, 2013). The late onset has implications on the runoff and soil loss. It has been argued that soil loss is higher at the onset of the rainy season (Fang *et al.*, 2015). However, this does not hold in all environments as erosion at this stage is detachment-limited except where the soil is disturbed. However, the generated runoff is expected to be high due to the high rainfall intensity at this time owing to soil sealing and the associated low infiltration. Therefore, knowledge of the start and end dates of the rainy season is vital for erosion and soil conservation planning.

4.1.6 Rainfall trend

The test for autocorrelation shows that there was no autocorrelation in the annual and seasonal rainfall except for the monthly distribution (Figure 4.12Figure 4.13Figure 4.14). Thus, the modified Mann-Kendall package and test were used for the monthly data applying the pwmk ( ) function in R (Yue and Wang, 2004, 2002).

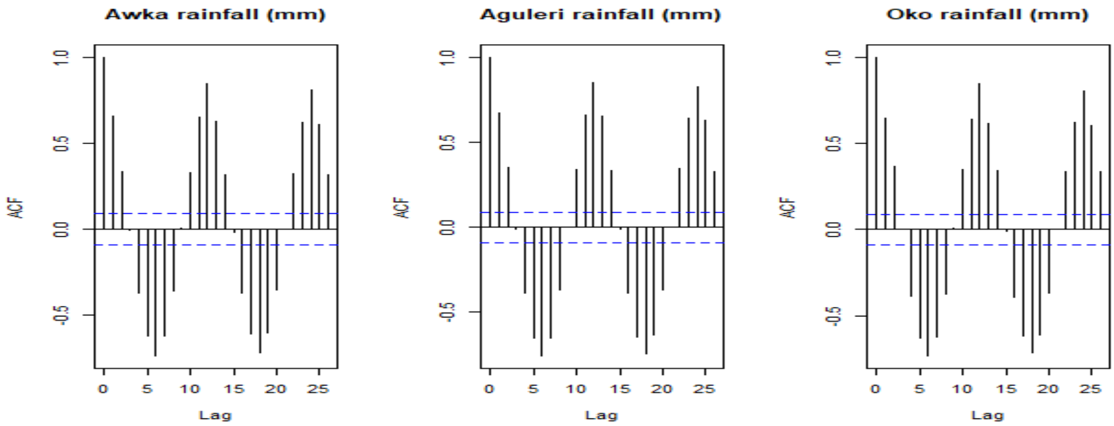

Figure 4.12. Autocorrelation plots of the monthly rainfall data in Anambra State

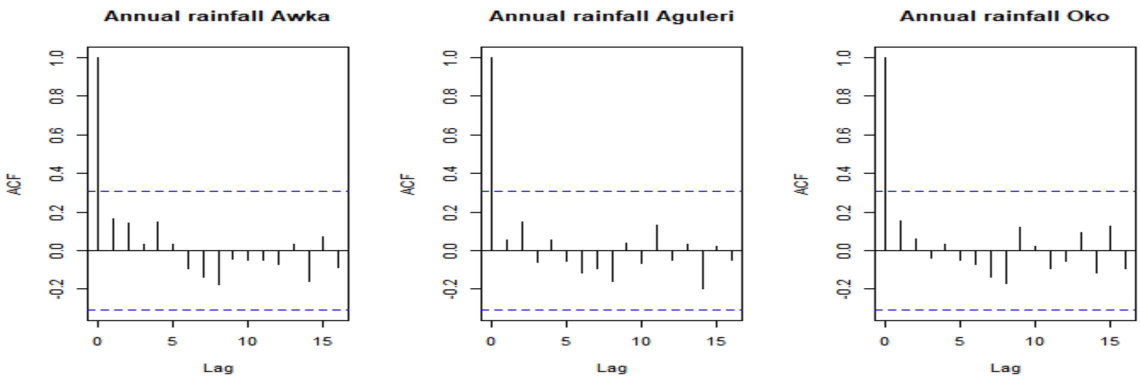

Figure 4.13. Autocorrelation plots of the annual rainfall in Anambra State

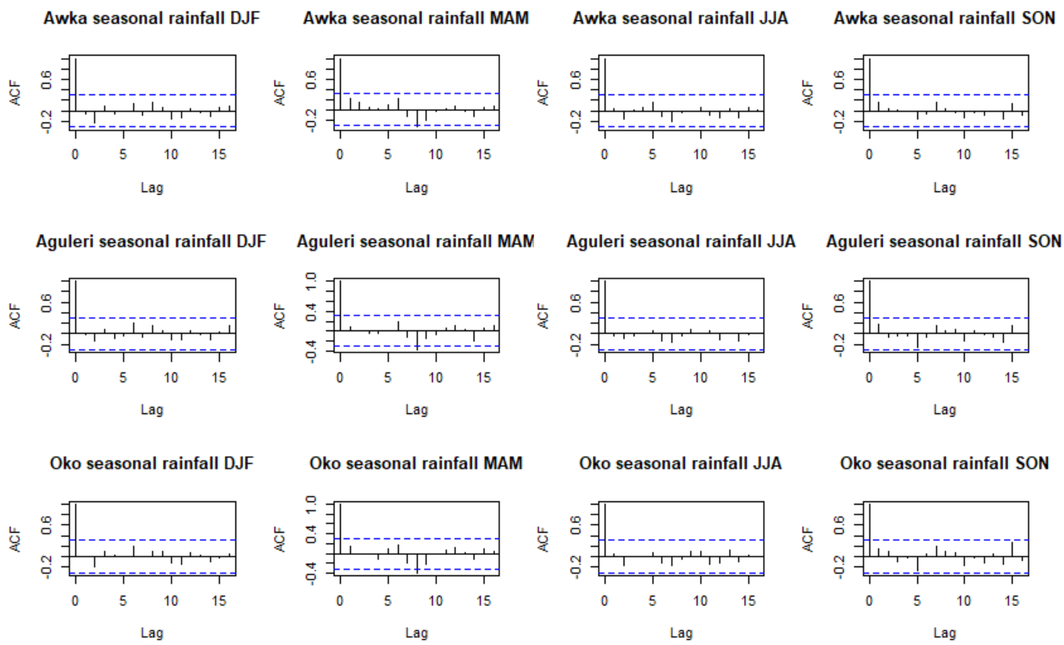

Figure 4.14. Autocorrelation plots of the seasonal rainfall in Anambra State

The trends were run for the monthly, seasonal and annual rainfall of the area (Tables 4.6; 4.7). The trends were not significant for the rainfall distribution irrespective of the temporal scale. The monthly trend was positive for all locations. The rate of increase in the monthly rainfall was 0.01 mm in Isu and Oko but 0.002 mm in Aguleri. The annual rainfall trend was positive at all the locations with a rate of increase of 16.3 mm (Aguleri), 18.6 mm (Isu) and 42 mm (Oko) (Table 4. 6). The rate of increase was higher in the annual than in the monthly trend. In any case, the trends for both monthly and annual rainfall were not significant.

Table 4. 6. Trends of monthly, and annual rainfall in the area

Monthly	Z	tau	O Sen	N Sen	p-value	var
Isu	0.37	0.011	0.01	0.01	0.71	12249467.00
Aguleri	0.07	0.002	0.01	0.002	0.94	12249467.00
Oko	0.32	0.01	0.02	0.01	0.75	12249467.00
Annual	Z	tau	Sens slope		p-value	var
Isu	0.45	0.05	1.86		0.65	7366.67
Aguleri	0.55	0.06	1.63		0.58	7366.67
Oko	1.25	0.14	4.20		0.21	7366.67

*O Sen is old Sens's slope, N Sen is new Sens's slope, var is variance

Table 4. 7. Trend analysis in seasonal rainfall

DJF	Z	tau	Sens slope	p-v	var
Isu	1.03	0.11	0.39	0.31	7365.67
Aguleri	1.31	0.14	0.12	0.19	7363.67
Oko	1.14	0.13	0.54	0.25	7365.67
MAM					
Isu	-0.36	-0.04	-0.46	0.72	7366.67
Aguleri	-0.69	-0.08	-0.17	0.49	7366.67
Oko	-0.09	-0.01	-0.12	0.93	7365.67
JJA					
Isu	-0.15	-0.02	-0.20	0.88	7366.67
Aguleri	0.20	0.02	0.09	0.84	7366.67
Oko	0.57	0.06	1.86	0.57	7366.67
SON					
Isu	1.15	0.13	1.37	0.25	7366.67
Aguleri	0.55	0.06	0.29	0.58	7366.67
Oko	1.39	0.15	2.00	0.17	7366.67

**Z is the test statistic, tau is a correlation, p-v is the P-value, and var is variance.

The trend test indicated a rising trend for rainfall in all the seasons except March-April-May (MAM), though none of the trends was statistically significant at a 95 % confidence level. Several studies have reported declining March to May rainfall elsewhere in the tropics (Gebrechorkos *et al.*, 2023, 2019; Nicholson, 2018). This might result in less erosion severity during this period. However, the SON season had a higher trend with a higher confidence level (83 %). The slope indicates that the SON rainfall of Isu and Oko increased by 13.7 and 20 mm per decade, respectively while the Aguleri SON rainfall increased by 2.9 mm per decade (Table 4. 7). The rate of increase in the JJA season was 18.6 mm in Isu and Oko per decade but 0.9 mm per decade in Aguleri (Table 4. 7). The increase in rainfall in these two seasons had a lot of implications on the seasonal erosion patterns. The JJA is the peak of the rainy season, a period when the soil is at field capacity or saturated. The SON is the post-little dry season and marks the end of the rainy season. It is a season associated with intense storms and high rainfall that implies more severe erosion in the area. The seasonal rainfall pattern indicated that attention should be given to the seasonal patterns of rainfall in the management of soil erosion in the area.

Anambra State is one of the States with the highest density of road networks, high population density and other artificial surfaces that service the urban population. As such, the rate of urbanization is negatively influencing the climate and land cover of the area as well as the magnitude of soil erosion. It is the State with the worst soil erosion scenario in Nigeria (NEWMAP, 2015) and the trend needs to be arrested before the whole area is eaten up by soil erosion and degradation. With the acknowledged impact of erosivity on soil erosion, the increasing trend is an indication of increasing soil degradation. It has been asserted that soil erosion increases with increasing rainfall intensity and duration (Zhao *et al*., 2021; Ziadat and Taimeh, 2013). Thus, increasing rainfall in the area points to increasing soil erosion for it has been shown that most of the soil erosion in Africa is attributable to high erosivity (Roose, 1977).

4.2 Soil characteristics and in-situ soil loss measurement in the field

4.2.1 Soil characteristics

4.2.1.1 Soil strength parameters.

The results of shear strength parameters indicate low to moderate strength. The Mohr-Coulomb failure envelope (Figure 4.15, Appendix 4), was used to represent the shear strength of soils. Both the angle of internal friction and cohesive forces are critical to determining the shear strength of the soils in the area though they vary spatially across the area. The Mohr circles of sands and gravels pass through the origin due to high permeability and they are cohesionless and well-drained (Figure 4.15b). From the result, location one has more fines, and so the effective stress/shear strength envelope cut an intercept away from the origin. However, locations 6, 7, 10, 12, and 27 have very low quantities of fines and so their effective shear strength envelopes pass very close to the origin (Figure 4.15b, Appendix 4). Such soils with little fines have a cohesion of 0 – 1 kpa and their shear strength parameter of interest is their internal angle of friction. Locations 11, 16, and 18 are non-plastic. That shows they have no or insignificant quantities of fines. Thus, they are soils with good aeration and high permeability. They too have increased soil strength due to their high infiltration rate.

The soils in locations 1 and 3 (Umunze) are more cohesive than the other areas. The shear strength is shown to correlate with bulk density, and permeability according to Duncan *et al*. (2014). An apt understanding of the soil strength is critical to a veritable slope stability analysis (Duncan *et al.*, 2014). The locations with high cohesion are also locations of high dry density, high moisture content and compact soil texture. This corroborates Wei *et al.* (2018) and Horn and Albrechts (2002) that soil strength is influenced by moisture content, soil texture and structure. The higher cohesive soils have higher quantities of fines than the cohesionless soils whose cohesive force is close to zero. Soils of poor strength are at the liquid limit (Arora, 2008). This shows that locations 12 and 27 and others with low fines and cohesion are at the liquid limit. Thus, locations 1 and 3 have high fines and high plasticity (Appendix 4) according to Sowers and Sowers (1970). This shows that locations 1, 2, 3 and others with high fines are cohesive soils and so are associated with problems due to their expansive nature (Mugagga *et al.*, 2012). Thus, they are highly erodible soils especially when wetted.

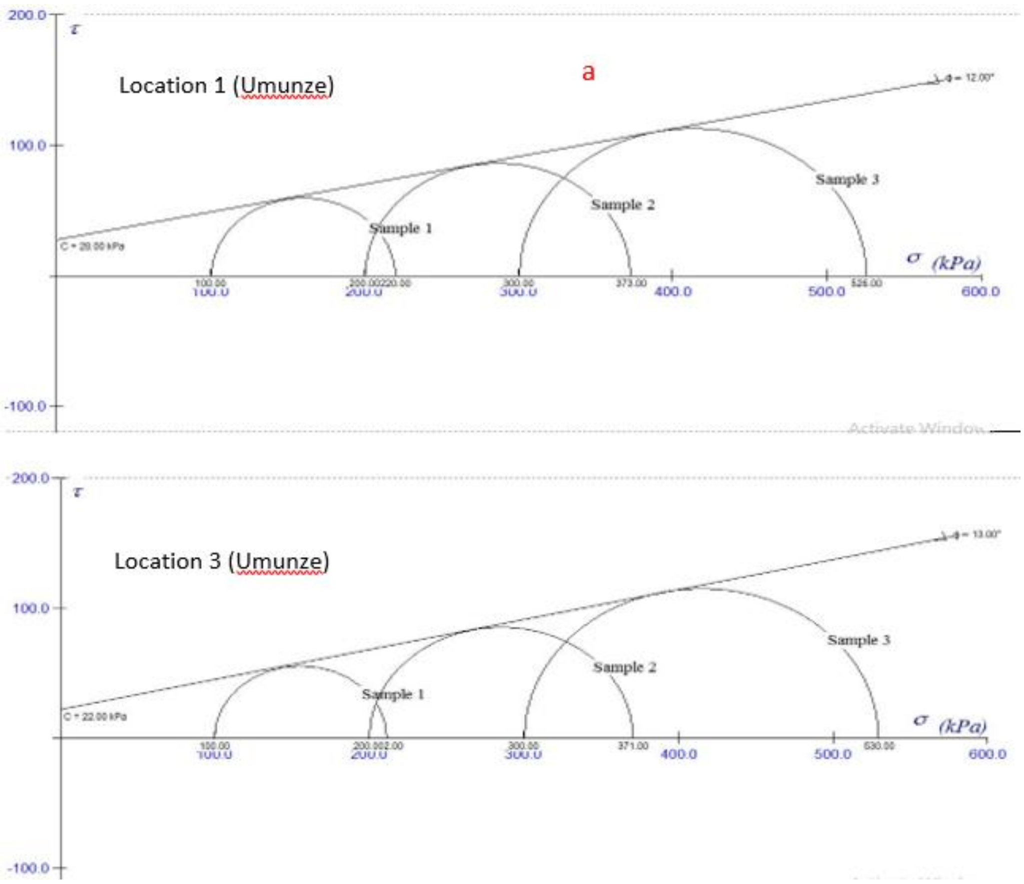

Figure 4.15a. Linear relationship between soil cohesion and angle of internal friction

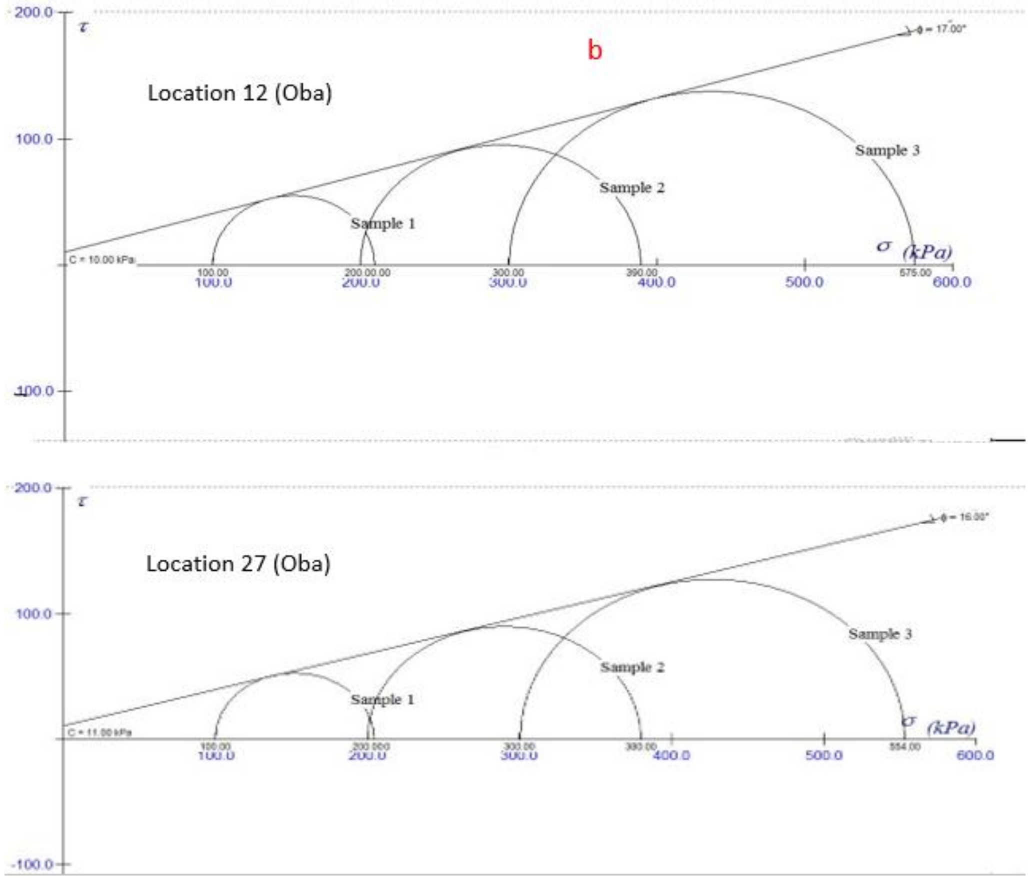

Figure 4.15. Linear relationship between soil cohesion and angle of internal friction

The Atterberg limits of soils are affected by the presence of clay minerals and other dynamic factors such as pH, temperature, cation exchange capacity, and quantity of cations (Polidori, 2007). Increasing salt concentration leads to a decrease in the LL of montmorillonite minerals (Polidori, 2007). Soil strength is also influenced by moisture content (Fasinmirin *et al.*, 2018; Han *et al.*, 2020). The LL in the area varies from 27 to 38 % which indicates they are likely to fail as posited by Mugagga *et al.*(2012) that soils with LL above 25 % are more likely to fail due to the expansive nature of such soils. According to Casagrande's (1932) Plasticity chart, most of the soils in the area are inorganic clay of low to medium plasticity (Casagrande and Fadum, 1940). Appendix 2 shows that the soils in the area have the potential to fail as they possess an expansive nature. Also, a positive correlation exists between high plasticity and fine-grained inorganic clay (Cerato, 2001). According to Bell's (2007) classification, the soils in the area fall in the low category of plasticity. However, the southern part has higher plasticity. Soils with high PI tend to be clayey but those with lower PI are likely silty and those with zero PI are non-plastic (Sowers and Sowers, 1970). The vulnerability of soils with clay is worsened by their low permeability (Wati *et al.*, 2010). As a result, pore pressure builds up during the rainy season. Again, as soil saturates, shear strength reduces due to a rise in pore pressure and loss of cohesion (Biscontin *et al.*, 2004; Rao, 1996). Thus, soils in the southern and central parts of the area are more susceptible to failure and erosion due to their high quantities of fines, especially during the rainy season when pore pressure increases. Compaction increases soil strength due to farm machines use which decreases the moisture content (Hamza and Anderson, 2005). This is worsened by low SOM and overgrazing with the attendant poor vegetal cover that decreases soil fertility. Hence, machine use in agriculture alters the soil's physicochemical properties, worsens runoff generation and erosion (Hamza and Anderson, 2005; Woldeyohannis *et al.*, 2022). Thus, farmers' use of tools and machines for ploughing and weeding affects the soil strength, and might aggravate erosion.

4.2.1.2 Moisture content, dry density and permeability

Compaction improves the dry density of the soil. Figure 4.16 and Appendix 3 show the compaction curves of the soils. The soils of the area have very poor to fair MDD while locations 1-3 (Umunze) have the poorest MDD. The soils at locations 1, 2,3,21, 24, and 27 have high moisture retention and so have high fines. Low moisture content reduces cohesion and makes such soils detachable (Isikwue *et al.*, 2012). This is because cohesion is correlated with porosity and thus invariably influences the shear strength of soils (Chen *et al.*, 2020). Expansive soils are known to be low in alkaline, dry density but high in fines and moisture content and directly correlate with erodibility (Regazzoni *et al.*, 2008). The OMC suggests that the soil has moderate to high moisture-holding capacity (Figure 4.16, Appendix 3). Thus, most of the soils of the area are highly erodible. Location 1 (Umunze) as shown below has the highest OMC but lowest MDD and is thus more likely to fail (Figure 4.16). Thus, soils with more clay content tend to have higher OMC. As the degree of saturation increases at a given dry density, the shear strength decreases (Yoshida *et al.*, 1991). Thus a decrease in MDD is an indication of soil weakness (Eltaif and Gharaibeh, 2008). Further, MDD has a negative relationship with liquid limit (KS *et al.*, 2015). This supports the earlier statement that locations 1-3 are more likely to fail. Since changes in dry density correlate with macropore distributions (Yu *et al*., 2019). According to Emesiobi (2000), the soils of the southern part fall in the poor class of MDD but elsewhere, it is in the fair class. Thus, compaction improves soil's MDD, minimizes the moisture content and so improves its strength and therefore makes them more resistant to erosion. This is because factors like dry density, grain size and moisture content influence the erodibility of soil (Al-Madhhachi *et al.*, 2013; Regazzoni *et al*., 2008).

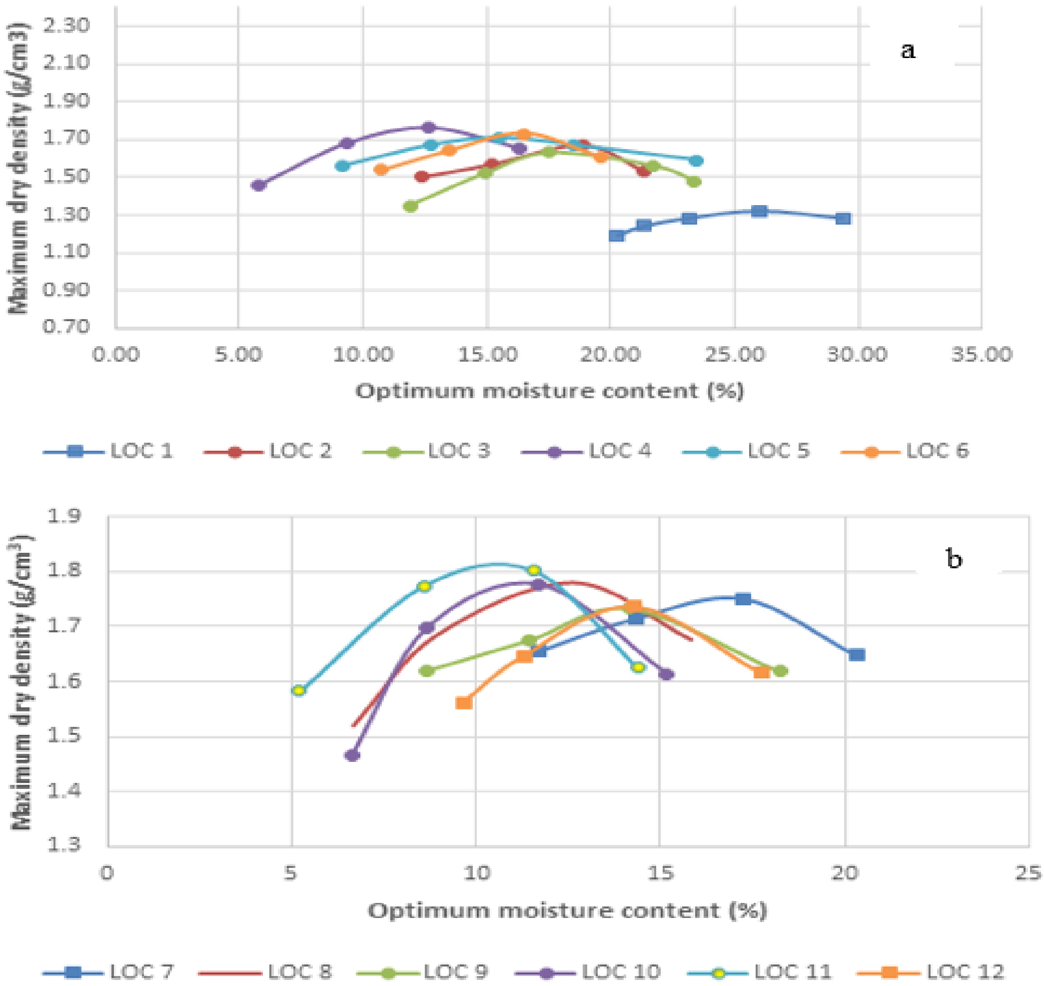

Figure 4.16. Relationship between OMC and MDD in Anambra State.

Permeability describes the relative ease or otherwise for which soil can transmit water under pressure. High permeability is associated with soils with low moisture content and reduced cohesion (Isikwue *et al*., 2012). Following the permeability coefficient classification of Arora (2008), the soils of the area fall under the fair class except for location 1 (Umunze) which is poor (Table 4. *8*). The ranges of the coefficients indicate most of the soils have high quantities of sand (Elhakim, 2016). Soils with much fines are more likely to fail due to the high water retention capacity (Mugagga *et al*., 2012). The larger the grain size, the higher the permeability of such soils. This is because permeability correlates with the square of soil particle size (Nelson, 1994). The soil at location 1 (Umunze) has the lowest permeability coefficient (Table 4. *8*) followed by those of locations 2 and 3. Permeability determines how water moves within soil pores (Terzaghi *et al.*, 1996). Thus, soils with high permeability have a low moisture content and so, are less cohesive when moist (Isikwue *et al.*, 2012). Permeability varies with soils and is lowest for soils rich in fines and clay (Casagrande and Fadum, 1940; Johnson, 1963). Thus, soils in locations 1-3 are highly susceptible to erosion and failure due to their high water retention capacity which is in line with Mugagga *et al.* (2012) findings.

Table 4. 8. Soils, their classes and the permeability

S/No.	SOIL PHYSICAL DESCRIPTION.	K - (mm/Sec)
1	GRAYISH BROWN CLAYEY SOIL.	9.97E-05
2	REDDISH BROWN SANDY SOIL.	0.001273
3	REDDISH BROWN SANDY SOIL.	0.001333
4	LIGHT BROWNISH SANDY SOIL.	0.001692
5	REDDISH BROWN SANDY SOIL.	0.001437
6	REDDISH BROWN SANDY SOIL.	0.001633
7	REDDISH BROWN SANDY SOIL.	0.001292
8	LIGHT REDDISH BROWN SANDY SOIL.	0.00178
9	REDDISH BROWN SANDY SOIL.	0.001948
10	DARK BROWNISH SANDY SOIL.	0.001681
11	BROWNISH SAND.	0.010086
12	YELLOWISH SANDY SOIL.	0.004807
13	BROWNISH SANDY SOIL.	0.002449
14	REDDISH BROWN SANDY SOIL.	0.001792
15	REDDISH BROWN SANDY SOIL.	0.002585
16	BROWNISH SAND.	0.010498
17	REDDISH BROWN SANDY SOIL.	0.002956
18	YELLOWISH SHARP SAND.	0.013537

19	BROWNISH SANDY SOIL.	0.002450
20	REDDISH BROWN SANDY SOIL.	0.001791
21	REDDISH BROWN SANDY SOIL.	0.002585
22	BROWNISH SAND.	0.030497
23	REDDISH BROWN SANDY SOIL.	0.002955
24	REDDISH BROWN SANDY SOIL.	0.002438
25	REDDISH BROWN SANDY SOIL.	0.001676
26	REDDISH BROWN SANDY SOIL.	0.001805
27	REDDISH BROWN SANDY SOIL.	0.002307
28	DARK BROWNISH SANDY SOIL.	0.001680
29	BROWNISH SAND.	0.010087
30	YELLOWISH SANDY SOIL.	0.004810

4.2.1.3 Particle size distribution, dry bulk density and chemical attributes

The particle size distribution (PSD) tests show the soils have high sand content. High sand content of the soil with low fines favours failures in the area. The soils have much sand, little gravel, and a fair quantity of fines. However, the particular fines could not be distinguished for most of the soils as the analysis method was sieve analysis and so could not isolate the finest materials.

From Figure 4.17, we see that the dominant soils in the area are variants of loamy soils with high quantities of sand. The soil at Ufuma is nearly poorly graded as it has very few quantities of fines (Figure 4.17).

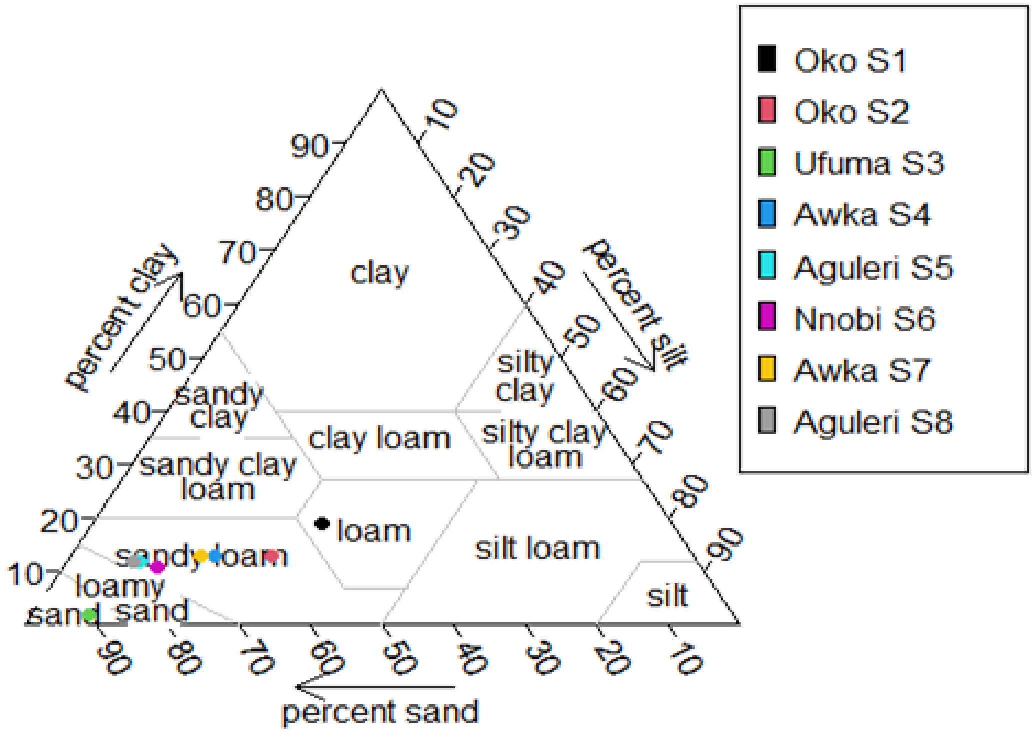

Figure 4.17. *1*Soil texture triangle for Anambra State

This shows that the soils of the area have moderate resistance to erosion. The soils at Oko are loamy to sandy loam (Figure 4.17). At Ufuma, it is loamy sand while other locations have sandy loam (Figure 4.17). However, the soils at Oko have a higher percentage of fines than those at the other locations (Figure 4.17).

The bulk density of the soils varies with location and organic matter content. The bulk density ranges from 1.34 to 1.40. This shows that the soils are mainly sand to sandy loam intercalated with fines (Figure 4.17). The areas with higher bulk densities are areas of low organic matter content, carbon content, and low infiltration (Chaudhari *et al.*, 2013). These are areas that are highly compacted and impervious and are thereby likely to generate higher runoff that aggravates erosion (Saffih-Hdadi *et al.*, 2009). However, the contrary holds in the area in that soil erosion is higher in the locations with lower bulk densities and high SOM. The high bulk density areas might generate higher runoff but lower soil loss due to less erodible geology.

Table 4. 9. Physico-chemical results of soil samples in the area

PARAMETER	UNIT	1	2	3	4	5	6	7	8
pH	-	8.3	8.5	8.4	8.4	8.3	8.6	8.3	8.2
Organic matter	g kg^{-1}	12.66	16.71	16.53	10.31	12.41	14.35	10.31	12.44
Carbon	g kg^{-1}	8.41	9.46	9.36	6.21	7.28	7.24	6.3	7.31
$CaCO_3$	%	1.03	1.03	0.89	0.70	0.23	0.71	0.70	0.23
Bulk density	g/cm^3	1.34	1.35	1.38	1.39	1.4	1.4	1.4	1.4

The chemical analysis showed that Oko soils have high quantities of CaCO3 followed by Ufuma. This shows that soils in the south have higher quantities of alkaline minerals than the other parts. Alkaline content, SOM, and SOC influence soil texture and erodibility (F Hassan, 2012; Nill *et al*., 1996; Ostovari *et al*., 2022). This is also confirmed by the results of the pH (Table 4. 9). Soil organic matter content (SOM) is higher in the southern soils than in the other parts (Table 4. 9). There is a positive correlation between SOM and soil loss (Table 4. 10). A positive correlation exists between SOM and SOC. Also, studies show the existence of a correlation between SOM and OMC and SOC (Holtz and Krizek, 1970) but the MDD decreases (Abdi *et al*., 2018). More on the relationships between soil losses and soil attributes are shown in Table 4. 10.

Table 4. 10. Correlation between soil attributes and soil loss

	pH	SOM	SOC	CaCO3	S. loss	slope
pH						
SOM	0.53					
SOC	0.44	0.95*(0.004)				
CaCO3	0.66	0.37	0.50			
S. loss	0.05	0.91*(0.01)	0.86*(0.03)	0.53		
BD.	-0.49	-0.63	-0.81* (0.05)	-0.85* (0.03)	-0.87* (0.02)	-0.89* (0.02)

*significant at 0.05 confidence level. The p-value is in bracket for the significant ones.

The results (Table 4. 10) contrast the findings from the literature that soil loss decreases with increasing SOM, SOC, and CaCO3 (Borrelli *et al.*, 2016; Sakin, 2012). For increasing SOM and SOC leads to improved soil structure, and infiltration but reduces the bulk density (Carter, 2002; Sakin, 2012). Also, increased SOC is correlated with porosity and so leads to a decrease in soil erosion (Borrelli *et al*., 2016). This holds when each plot was considered. For instance, at Oko, the bare plot (S1) had a lower erosion rate at the inception of the experiment due to the high SOM but with time, the top organic matter became depleted and erosion became accelerated. Unlike on the small tilled plot (S2) where the erosion was intense right from the onset of the experiment because tillage disturbed the soil and upturned the SOM. However, considering the whole State, soil loss was lower on Isu plots but runoff was high which is due to its location on the less erodible Imo clay shale and low slope. In Aguleri, the soil loss and runoff generation were very low from inception due to its high permeability but when it reached saturation towards the end of the season, the soil erosion became severe. In all, it shows that differences in slope played a stronger role in influencing soil erosion than the SOM in Anambra State. This is because, the high slope of Oko had higher soil loss irrespective of having higher SOM while the low slope of Isu-Aniocha had a lower SOM and lower soil loss. Therefore, the role of SOM on soil loss is better appreciated when comparison is for plots on similar slopes.

The BD had a negative correlation with SOC, SOM, CaCO3, slope, and erosion. It had a statistically significant relationship with CaCO3, slope, SOC, and soil loss but a non-significant relation with SOM. This is in line with related research (F Hassan, 2012; Ostovari *et al.*, 2019). Also, in a related study, BD was found to have a negative relationship with erodibility (Chaudhari *et al*., 2013; Deng *et al*., 2016; Peng *et al.*, 2022; Zhu *et al.*, 2022). That is, high BD was accompanied by low erodibility and vice versa. Peng *et al.* (2022) showed that soil detachment decreased exponentially with increasing bulk density and aggregate stability. The result of the BD showed that soils in the eastern and northern parts are less erodible compared to southern soils. However, a counter-argument shows that soils with high BD are more erodible because increased

BD was accompanied by low SOM, poor soil structure, and compact soil with low porosity and vegetation cover (Al-Shammary *et al.*, 2018; Keesstra *et al.*, 2016; Tanveera *et al*., 2016). This was supported by the study that bulk density has a negative relationship with soils with much fines like silt and clay (Khan *et al*., 2013; Wang and Shao, 2013). Silt soils are known to be highly susceptible to erosion, and bulk density negatively correlates with soils with high quantities of fines. It implies that the relationship of bulk densities to soil loss is complex and varies with locations. This variation might be partly because density changes temporally (Kodiwo *et al.*, 2014*)*. The presence of SOM and SOC increases surface roughness and it is associated with low densities, improved infiltration, and less runoff and soil loss (Chaudhari *et al*., 2013; Du *et al.*, 2022). This is location-dependent and also depends on the factors at work in the area, so it should be interpreted with caution for it can be influenced by the area's geology, soil and slope. Thus, the locations with high BD are on Imo clay shale which was less erodible compared to the more erodible friable Nanka sands which dominate the southern and central parts of the study area. Bulk density is a dynamic property. For instance, tillage may increase soil porosity and reduce bulk density, however; in the long run, cultivation will lead to increased bulk density (Arunrat *et al.*, 2022; Villarino *et al*., 2017). This is because, tillage depletes SOM, and aggravates soil structure thereby leading to low porosity and high bulk density (Lyon *et al*. 1952 cited by Murphy *et al*.(2004).

4.2.2 In-situ soil loss measurement

4.2.2.1 Soil Loss from the runoff plots: overview

The runoff generated in the bare fallow agricultural land is much higher than that from the vegetated fallow agricultural land in Isu (Figure 4.18, Table 4. 11). The estimated soil loss from the bare fallow big plot was 0.09 $kgm^{-2}mon^{-1}$ (0.49 kg m^{-2}) while the vegetated fallow big plot was 0.01 $kgm^{-2}mon^{-1}$ (0.007 kg m^{-2}) (Figure 4.18). Also, the runoff from the bare fallow big plot was 4.02 mm mon^{-1} (21.69 mm) compared to 0.67 mm mon^{-1} (3.62 mm) from the vegetated fallow big plot (Figure 4.18, Table 4. 11).

The soil loss from the bare fallow small plot was 0.12 $kgm^{-2}mon^{-1}$ (0.30 kg m^{-2}) while it was 0.01 $kgm^{-2}mon^{-1}$ (0.003 kg m^{-2}) from the vegetated fallow small plot. The runoff from the bare small plot was 3.00 mm mon^{-1} (15.64 mm) while from the small vegetated fallow plot was 0.22 mm mon^{-1} (1.14 mm) (Table 4. 11).

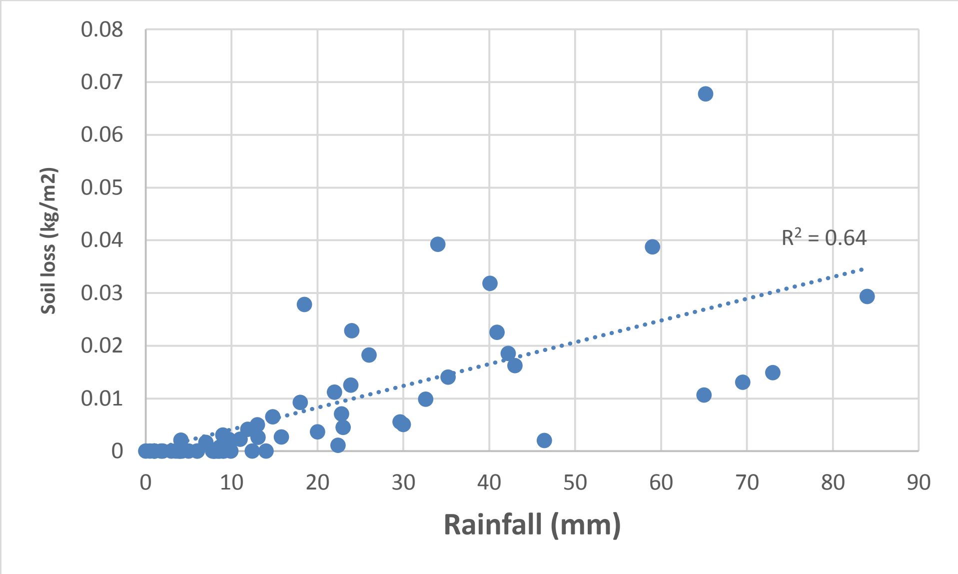
Soil loss (kg/m2)
R² = 0.64
Rainfall (mm)

a

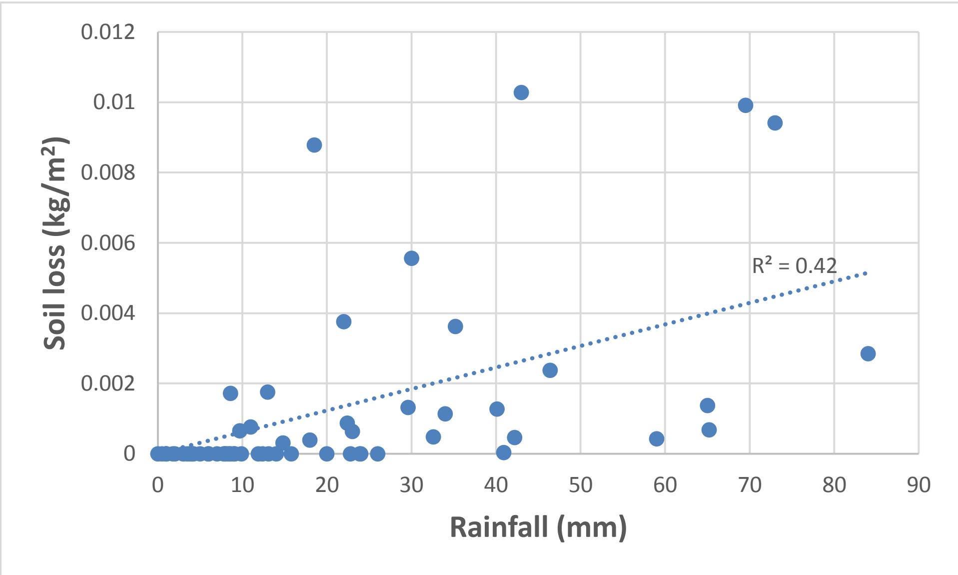
Soil loss (kg/m²)
R² = 0.42
Rainfall (mm)

b

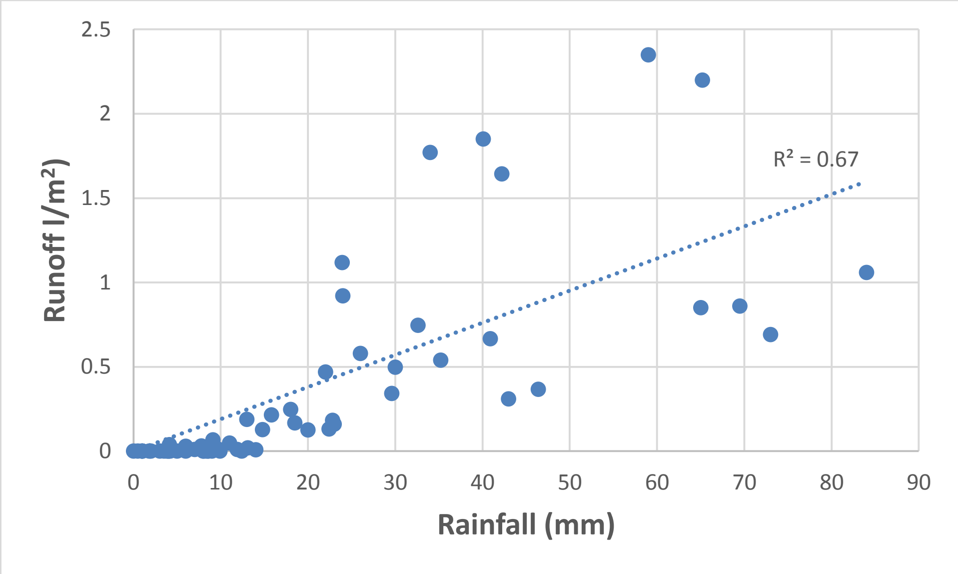

c

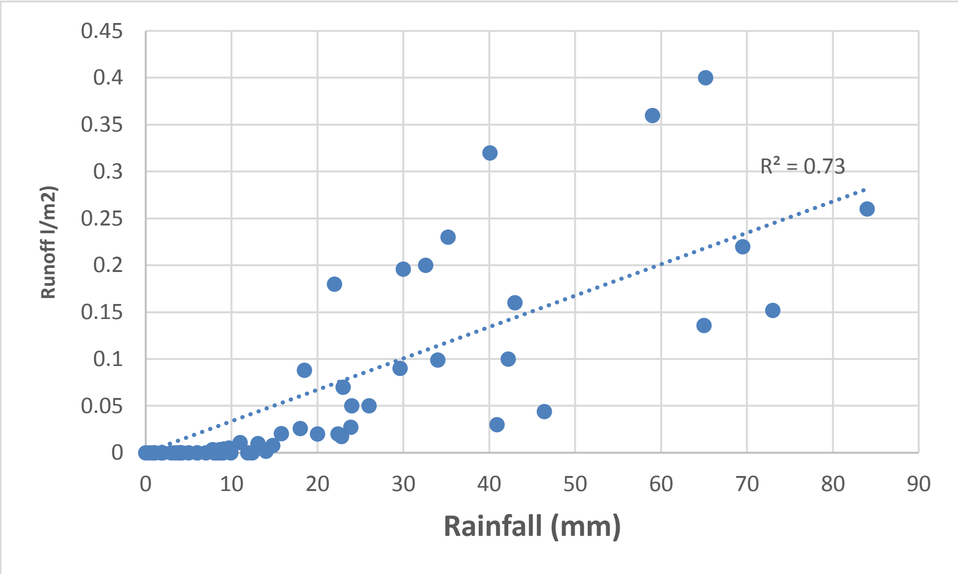

d

Figure 4.18. Linear relationship between rainfall and soil loss/runoff at Isu.

Soil loss in Isu 100 m^2 a. bare plot, b. vegetated plot, Runoff in Isu 100 m^2 a. bare plot, and d. vegetated plot

The rainfall generated in the plots within the study frame was 1286.6 mm in Isu (big plots) (Table 4. 11). The correlation between rainfall and soil loss was 0.80, and runoff with rainfall was 0.82 for the Isu big bare fallow (Figure 4.12). The runoff and soil loss for the same plot has a correlation coefficient of 0.91 (Table 4. 12). The small plots are shown in Figure 4.19 and Table 4. 12.

The soil loss per millimetre (mm) of rain in the big bare fallow was 0.04 kg/mm, 1.69 l/mm of runoff per unit of rain, and 0.02 kg/l of soil loss per unit runoff. It was 0.01 kg/mm of soil loss per unit of rain in the vegetated fallow, 0.28 l/mm for runoff per unit of rain, and 0.02 kg/l of soil loss per unit of runoff. In the small plots, it was 0.03 kg/mm for soil loss per unit of rain, 0.64 l/mm of runoff per unit of rain, and 0.04 kg/l of soil loss per unit runoff for the bare fallow plot. In the vegetated small plot in Isu, it was 0.002 kg/mm of soil loss per unit of rain, 0.05 l/mm of runoff per unit of rain, and 0.05 kg/l of soil loss per unit runoff.

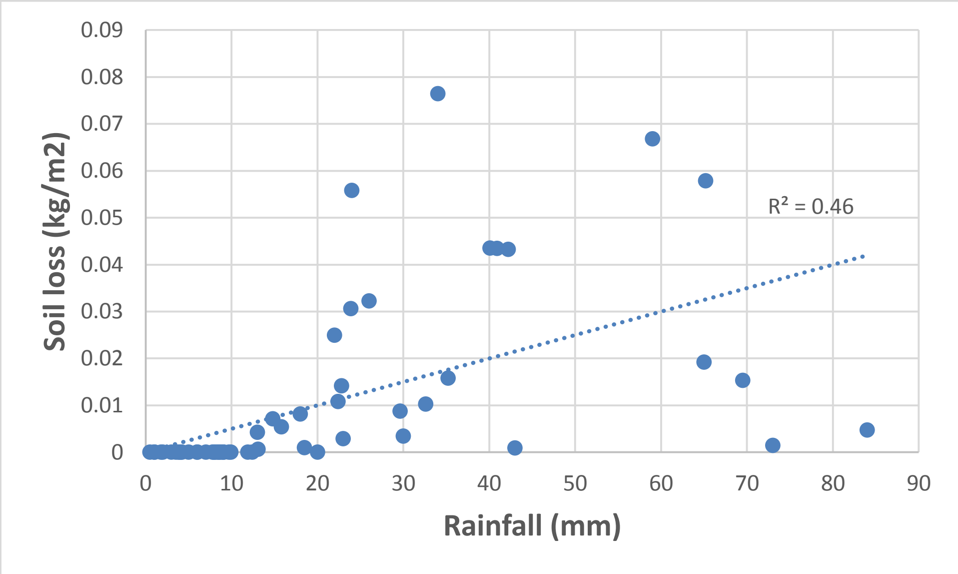

a

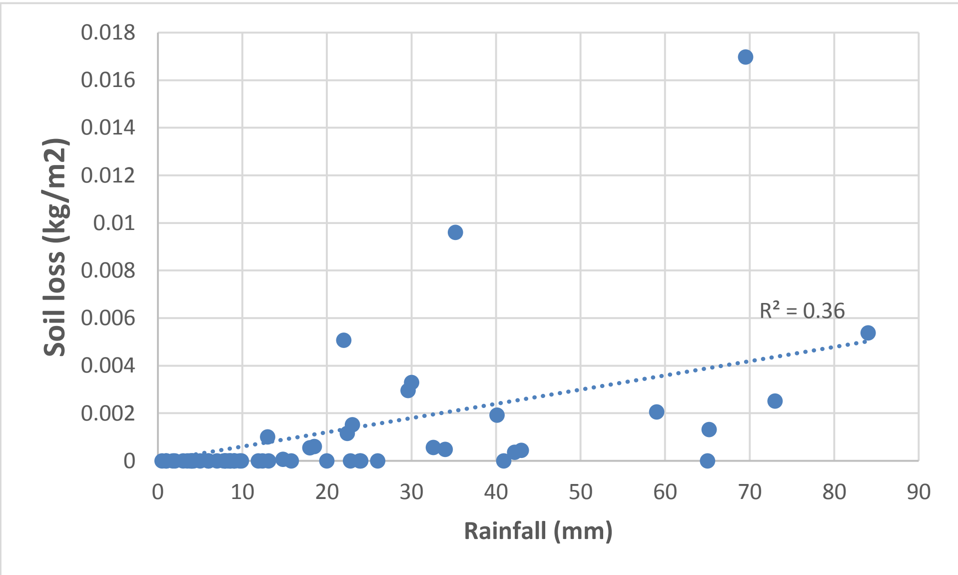

b

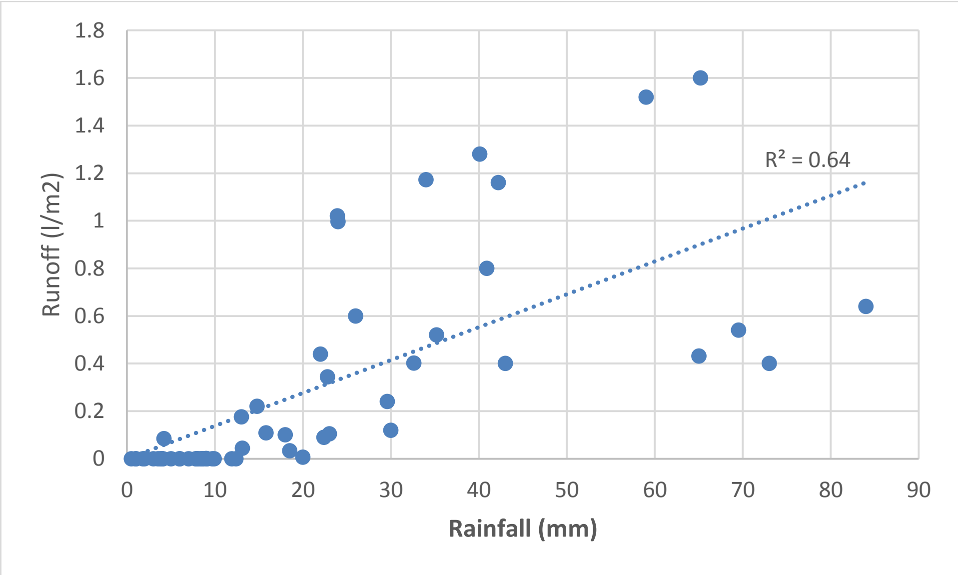

c

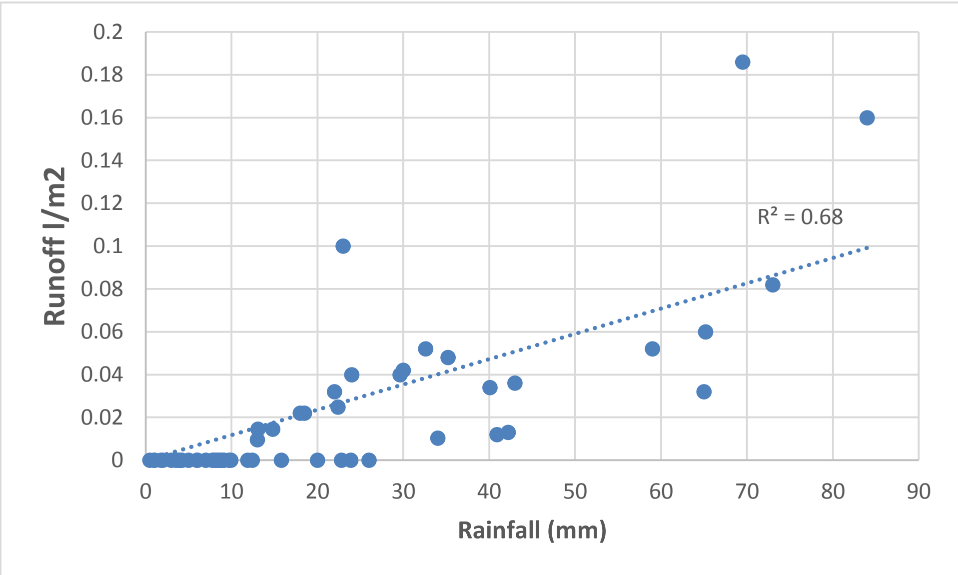

d

Figure 4.19. Linear relationship between runoff and soil loss in the small plots at Isu.

Soil loss in Isu 50 m^2 plot: a. bare plot, b. vegetated plot. Runoff in Isu 50 m^2 plot c. bare plot, d. vegetated plot

Table 4. 11. Soil loss and runoff generated in the plots during the 2022 rainy season

plot	Rainfall (mm/mon)	Soil loss (kg m^{-2} mon^{-1})	Runoff (mm mon^{-1})
Isu big DP	238.2	0.09	4.02
Isu big UP	238.2	0.01	0.67
Isu small DP	233.4	0.12	3.00
Isu small UP	233.4	0.01	0.22
Aguleri big plot	439.5	0.36	4.19
Aguleri small plot	517.6	0.46	2.52
Oko big plot	200.5	0.74	-
Oko small plot	200.5	1.24	-

Table 4. 11 shows the mean soil loss and runoff per month for the period of the experiment. The runoff and soil loss from the plots at Aguleri also varies with the plot's size (Figure 4.19). The runoff and soil loss from the big plot were 4.19 mm/mon (1843.25 litres) and 0.36 $kgm^{-2}mon^{-1}$ (1.60 kg m^{-2}), respectively (Table 4. 11). The relationship between soil loss, runoff and rainfall is shown in Table 4. 11. The soil loss per unit of rain in the Aguleri big plot is 0.08 kg/mm, 0.95 l/mm of runoff per unit of rain, and 0.09 kg/l of soil loss per unit of runoff. In the small plot, it is 0.04 kg/mm of soil loss per unit of rain, 0.24 l/mm of runoff per unit of rain, and 0.18 kg/l of soil loss per unit runoff.

Table 4. 12. Correlation between rainfall and soil loss, and runoff

Isu 100 m²	r	p-v	Adj r^2	**Isu 50 m²**	r	p-v	Adj r^2
DP_runoff	0.82	2.2e-16	0.63	DP_runoff	0.80	2.2e-16	0.59
DP_soil loss	0.80	2.2e16	0.59	Dp_soil loss	0.68	2.2e-16	0.39
UP_runoff	0.85	2.2e-16	0.70	UP_runoff	0.82	2.2e-16	0.65
UP soil loss	0.65	1.65e-15	0.35	UP soil loss	0.60	1.43e-13	0.33
Aguleri 100 m²	r	p-v	Adj r2	**Aguleri 50 m²**	r	p-v	Adj r2
Runoff	0.79	2.2e-16	0.57	Runoff	0.72	2.2e-16	0.46
Soil loss	0.59	5.77e-11	0.32	Soil loss	0.56	8.21e-09	0.25
Oko 100 m²	r	p-v	Adj r2	Oko 25 m²	r	p-v	Adj r2
Soil loss	0.69	0.065	0.19	Soil loss	0.76	0.018	0.33

*DP is disturbed plot, UP is undisturbed plot, p-v is P-value, r is correlation coefficient, Adj r^2 is coefficient of determination.

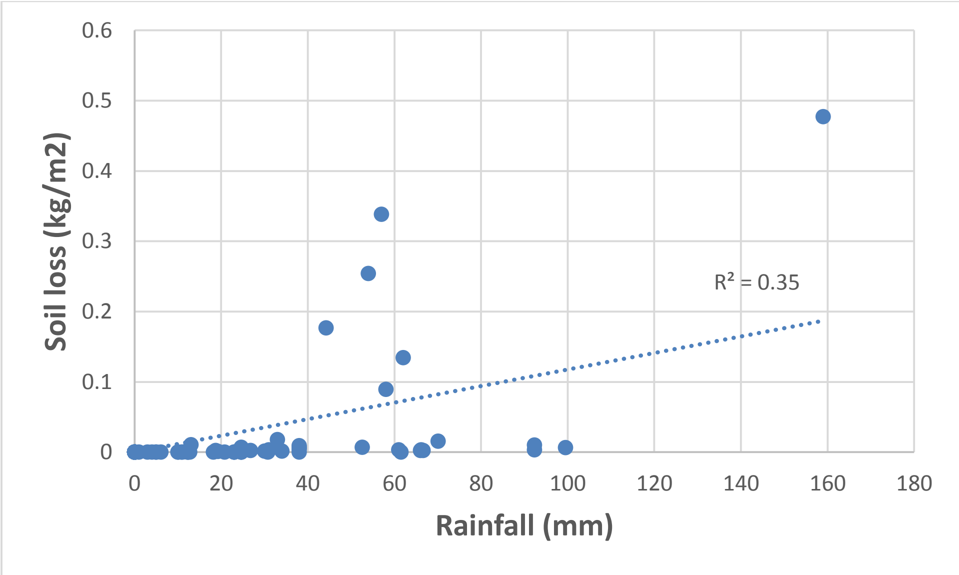
0.6
0.5
0.4
0.3
0.2
0.1
0
Soil loss (kg/m2)
R² = 0.35
0
20
40
60
80
100
120
140
160
180
Rainfall (mm)

a

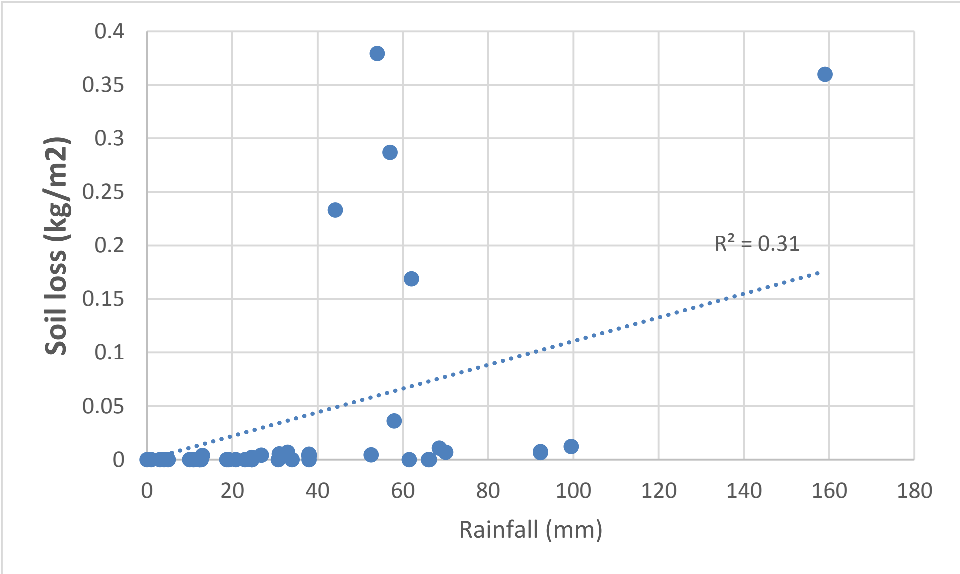
0.4
0.35
0.3
0.25
0.2
0.15
0.1
0.05
0
Soil loss (kg/m2)
R² = 0.31
0
20
40
60
80
100
120
140
160
180
Rainfall (mm)

b

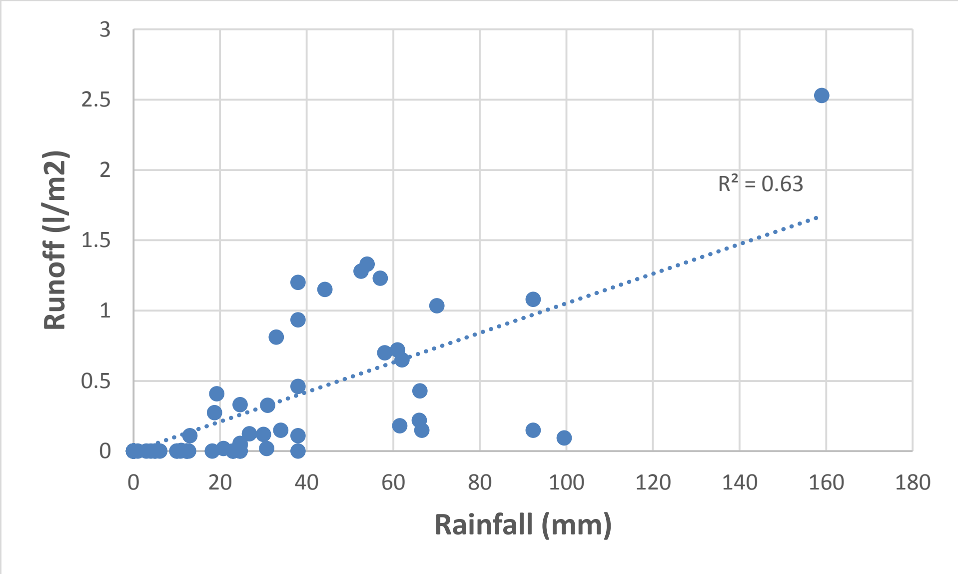

c

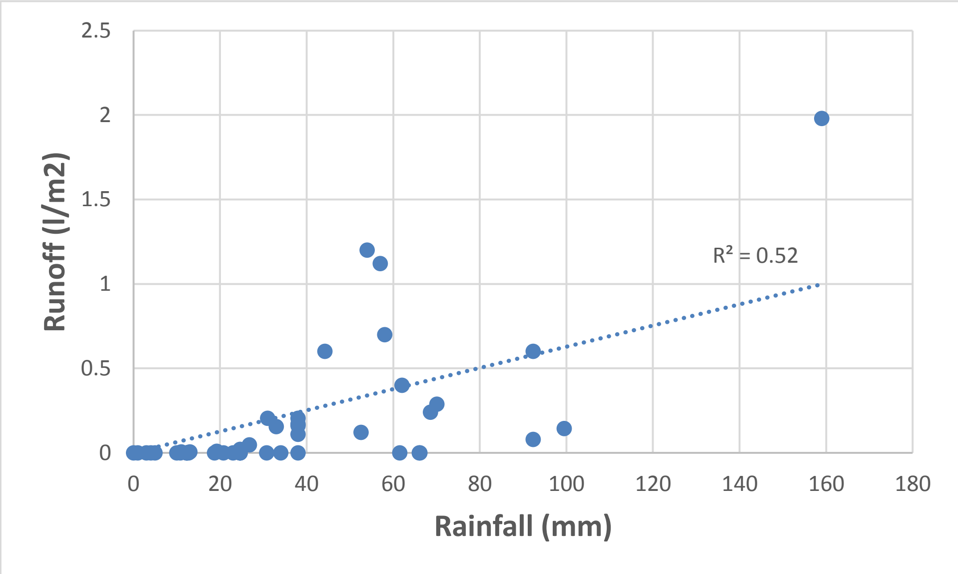

d

Figure 4.20. Linear relationship between rainfall and soil loss/runoff in Aguleri

*Soil loss in Aguleri: a. 100 m^2 plot, b. 50 m^2 plot, Runoff in Aguleri: a. 100 m^2 plot, d. 50 m^2 plot

The estimated soil loss from the Oko big plot was 0.74 kgm^{-2}mon^{-1} (2.50 kg m^{-2}) (Table 4. 11). The quantity of soil loss per unit of rain in the Oko big plot was 0.37 kg/mm, but 0.15 kg/mm for the small plot. The relationship between rainfall and soil loss is in Figure 4.21.

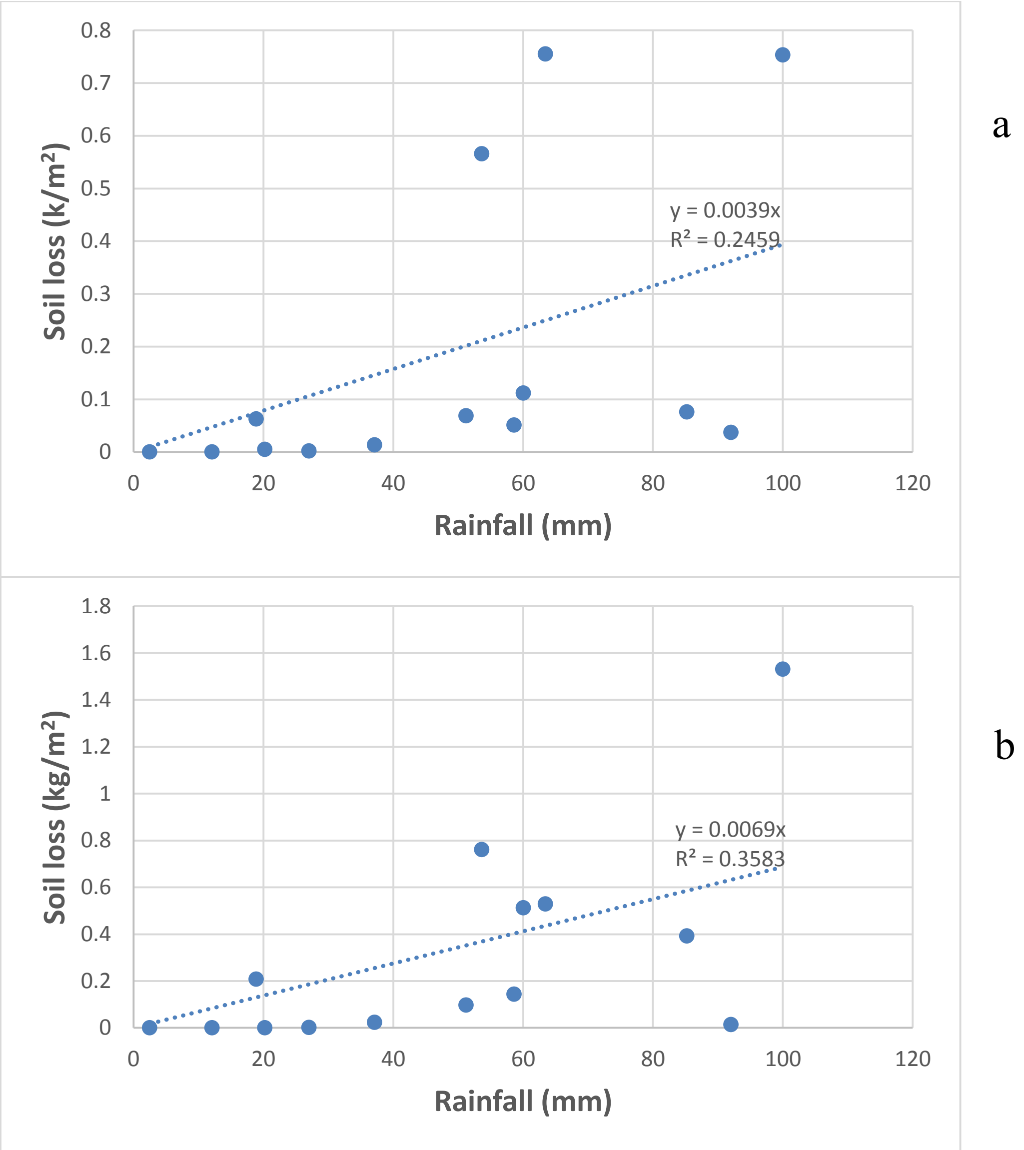

Figure 4.21. Linear relationship between rainfall and soil loss in Oko: *a. 100 m^2 plot, b. 25 m^2 plot*

4.2.2.2 Assessment of soil loss from the rain events that generated erosion

The rainfall amount per day was cross-checked for the events that generated runoff, and the events that generated soil loss. This was done to understand the impact of the rainfall amount per day on the dynamics of soil loss in the area. Therefore, the rain events that did not produce runoff and soil loss were isolated. Those that generated runoff but had no soil loss were isolated. Thereafter, the rain events that generated runoff and soil loss in each plot were known.

4.2.2.3 Isu 100 m^2 plots (the big bare fallow and vegetated fallow).

The daily rainfall events that generated runoff and soil loss was 59.38 % of the rain events. Then, 6.25 % produced runoff and trace soil loss. It generated runoff of 13.5 litres from 30.8 mm while 34.38 % of the rains produced no runoff and, therefore no soil loss as well. None of the rains that generated no runoff was above 10 mm except 12.4 mm on 10/9 which was likely due to the 4-day dry spells that preceded it. Other related events were 9.9 mm rain and 9 mm rain on September 16th and 26th, respectively, followed by 4 days of dry spells. Antecedent moisture content played a role in their inability to generate runoff. The 22 rainfall events that produced no runoff had 113.5 mm of rainfall. The rain events that generated runoff but trace soil loss was small in amount to produce soil loss. For instance, 2 events on July 29th had 6 mm of rain but were preceded by 65 mm of rain the previous day. It supposedly had antecedent soil moisture enough to generate runoff and soil if the rain had been of substantial quantity. The event on September 21st with 7.8 mm had 40.9 mm of rain preceding it, yet it could not produce soil loss. The one on September 4th with 9.1 mm did not produce soil loss because it was preceded by rainfall of only 7.9 mm. It was likely insufficient to wet the soil as it was itself preceded by 3 days of dry spells. The highest soil loss generated was in October (47.66 %). It was 16.43 % in June, but decreased to 13.62 % in July, 11.74 % in August, and further decreased to 10.54 % in September. The soil loss here clearly followed the rainfall pattern of the year. The rainfall of the year was small in Isu compared to previous years and its dynamics differed too. For instance, it used to rain heavily in late August and September after the end of the little dry season. However, the little dry season prolonged this year such that the rainfall in September was smaller than that of August, unlike previous years. The runoff generated was 12.09 % in June, 14.50 % in July, 10.21 % in August, 8.94 % in Sept, and 54.25 % in October. In all, 42.98 g/mm (of soil loss per mm of rain) was generated in the bare fallow plot while it had 22.77 g/litre due to its accompanying runoff.

In the vegetated fallow, 40.63 % of the rains produced runoff and soil loss. 42.19 % had no runoff or soil loss while 17.19 % generated runoff with trace soil loss. Most of the rains above 10 mm generated runoff except on 10/9 (12.4 mm) and 31/7 (11.9 mm). The 10/9 event had 3 days' dry spells before it while the 31/7 event had no dry event but the rain events that preceded it were too small to wet the soil (6mm and 3 mm). The soil loss per rain here was 7.45 g/mm with 20 g/litres of soil loss per unit runoff in the class that generated soil loss. The 11 rainfall events that generated runoff but no soil loss had 184.4 mm of rain with a runoff of 20.64 litres. The rains that generated no runoff had 151.5 mm of rain. The soil loss decreased from June to October. It was 56.15 % (June), 32.49 % (July), 2.11 (Aug), 0.06 (Sept), and 5.62 % (October). The soil loss was least in September followed by August, and October. It shows it nearly followed a similar pattern to that of the bare fallow. However, the effect of vegetation on soil loss is apparent. The soil loss decreased with time as the vegetation blossomed with time. It was less in September due to decreased rainfall amount this September 2022 unlike what is usual for the month and also due to protection from vegetation. September and late August used to have high intensity rain as they are post-little dry season months that do have intense storms but this year was unusual. Also, October had reduced runoff despite increased rain storms due to protection from the vegetation. The runoff also decreased from June to September and then increased in October. Thus, June had 23.90 %, July (23.29 %), August (14.46 %), Sept (0.88 %), and October (37.47 %) in Isu vegetated big plots. Although, vegetation limits erosion, this ability is weakened at certain rainfall intensities (Chen *et al.*, 2018; Ge *et al*., 2023; Wu *et al*., 2020). Again, in line with Boix-Fayos *et al.* (2006) assertion that soil loss reaches exhaustion over the years in a given plot, exhaustion can be reached within a year on less erodible soils because soil erosion is load-limited, and devoid of any serious disturbance, soil loss decreases over time. Thus, on weak and erodible soil, the exhaustion might not hold even after a long while. However, this calls for more research to validate it on very weak and resistant soils over longer periods.

4.2.2.4 Isu 50 m^2 plots (the small bare fallow and vegetated fallow).

In the bare fallow plot, all rains above 10 mm had runoff except 11.9 mm (31/7) event despite the previous days having rain. However, the rain was too small to wet the soil as it was 3 mm of rain. On 10th September, there was 12.4 mm of rain but did not generate runoff because it was preceded by three days of dry spells. About 25 rain events had no runoff with total rainfall of 176.4 mm, about 44.64 % of the rain events. The 3 events that had runoff but trace soil loss produced runoff of 4.58 litres. The rains that produced runoff and soil loss are 50 % of the rain events. The rain events that generated runoff and soil loss had a 30.44 g/mm (of soil loss per mm of rain). It also had 39.29 g/litres (of soil loss per litre of runoff).

The rainfall events that generated runoff but no soil loss is attributed to the effect of antecedent soil moisture on soil erosion. For instance, 65 mm recorded 1.6 litres of runoff but no soil loss because it was preceded by two days' dry spells from 25th – 28th July. Again, rainfall of 40.9 mm on 20th September had no soil loss due to a low runoff of 0.6 litres as it was preceded by a 3-day dry spell from 17th -20th September. This year's rainy season was peculiar and different from the usual temporal pattern. The later period of the year, that is, the post-little dry season is usually accompanied by rain events of high intensity. However, this year's little dry season prolonged beyond what was usual for the area. From June to 27th August, 56.07 % of rain, 28.74 % of runoff, and 21.14 % of soil loss were generated. From 29th August to 24th October, it generated 43.93 % rain, 71.25 % runoff, and 78.86 % of soil loss. This shows the impact of antecedent moisture and the intensity of rain on the generation of runoff and soil loss. A 56.07 % of rain generated less soil and runoff than 43.93 % of rain. The variables increased from June to July; rain from 217.1 mm to 227.1 mm, runoff from 64.9 litres to 109.9 litres, and soil loss from 921.3 g to 4516.5 g. It decreased in August to 162.5 mm, 70.32 litres, and 1545.9 g respectively. In September, rainfall decreased to 80.7 mm, but runoff increased to 95.25 litres, and soil loss increased to 5233.2 g which also increased in October to 313.2 mm of rain, 434.8 litres runoff, and 18242.5 g of soil loss. This is a clear manifestation of the effect of rainfall intensity and soil moisture on runoff and soil loss. The rain that generated the huge runoff and soil loss in September occurred on three days. There was no rain sufficient to generate runoff from 30th August to 20th September, the next rain was on 24th September, and then on 29th September. The intensity was high, and higher runoff and soil loss were generated despite the rain amount. And it continued with a high intensity into October, such that one-third of all the soil loss was obtained in October.

In the vegetated fallow, 57.14 % of the rains had no runoff or soil loss, 35.71 % had runoff and soil loss and 7.14 % had runoff but trace soil loss. The 22 events with no runoff had a rain of 319.4 mm while the events with runoff but trace soil loss had a rain of 143 mm and runoff of 4.93 litres. A 3.77 g/mm is soil loss per unit mm of rain in this class of rainfall events with runoff and soil loss. A 55.68 g/litres of soil loss per unit litre of runoff was recorded. The rain events of 22.8 mm (24th October), 23.9 (14th October), 26.0 mm (7th October), 15.8 mm (September 29th), 20 mm (September 6th) had no runoff and soil loss in the undisturbed plot because there were two days or more dry spells before the event while 13.1 mm (30th August), 13 mm (10th July), 14.8 mm (19th August) had runoff and soil loss because there were consecutive two to three days' wet spells. It shows the significance of antecedent soil moisture in runoff and soil loss generation in an area despite the influence of vegetation on infiltration and runoff.

Additionally, the plots had low soil loss from mid-August to the end of the season due to the impact of vegetation. For instance, the last two months of the rainy season produced 53.6 % of the rainfall but had a corresponding runoff of 42.56 % and 24.01 % of soil loss while the initial period had 46.39 % of the rain with a corresponding runoff of 57.44 % and soil loss of 75.99 %. Also, the monthly rainfall decreased from June to July (217.1-162.1 mm) while soil loss increased from 568.5 – 1690.3 g and runoff decreased from 16.1 to 15.02 litres. The 3 variables decreased again in August to 149.4 mm, 12.43 litres, and 329.6 g. However, in September, there was no rainfall sufficient enough to generate runoff or soil loss in the vegetated plot. This shows that the friction exerted by the vegetal cover was high enough to suppress runoff in September. This also gives credence to the unusual rainfall in September this year. However, in October, the rain increased to 240.5 mm, runoff (8.47 litres) and soil loss (308.1 g). This is a manifestation of increased storms in October such that despite the frictional effect exerted on runoff by the vegetation, the storm event still produced some runoff.

4.2.2.5 Aguleri plots

Aguleri 100 m^2 plot

In the big plot, there was 53.70 % of rain events with runoff and soil loss while 9.26 % had runoff but trace soil loss. A 37.04 % had no runoff and soil loss. The 5-day rain events that produced runoff but trace soil loss had rain of 148.7 mm which generated runoff of 26.6 litres. The 20-day events with no runoff had 279 mm of rainfall. The rains that produced runoff and soil loss generated soil loss of 106.33 g/mm, that is, 106 grams of soil loss per unit mm of rain. It also had soil loss per unit litre of runoff of 88.25 g/litres. The rain, runoff, and soil loss increased progressively from June to October; however, the rate of increase varies with time as that of October is far higher than any other month. It increased from 125 mm of rain, 99 litres of runoff, and 686.3 g of soil loss in July to 262.8 mm, 361.65 litres, and 5080.4 g of soil loss in August. In September, it was 510.6 mm, 396 litres, and 13025.7 g and then 609.3 mm, 960 litres, and 141527.5 g in October for rain, runoff and soil loss respectively. The month of October yielded 88.28 % of all the soil loss, Sept (8.12 %), Aug (3.17 %), and July (0.43 %). Runoff had 52.84 % in October, 21.80 % (Sept), 19.91 % (Aug), and 5,45 % (July).

Most of the rains from July to mid-August had little to no runoff and soil loss. It rained but no runoff. However, from 13th August, it started raining almost daily or latest after a 2-day interval. The only 3-day intervals were between 15th and 18th August and between 20th and 23rd August. These were merely a gap of two days' dry spell. However, it ceased again by 13th October with dry spells of five days and began again to rain on 19th, 20th and 24th October.

Until 13th August, soil loss was as low as 2603.6 g and runoff was 245.5 litres but from 13th August to 24th October, soil loss was 157716.3 g and runoff was 1597.75 litres. The bulk of the soil loss occurred between 24th September and 24th October. It shows that the greatest chunk of the soil loss was derived in a month. It recorded soil loss of

152739.3 g and runoff of 1295 litres. Also, 70.26 % of runoff was derived between 24th September and 24th October while the soil loss was 95.27 %. Storms of 70 mm and above yielded soil loss of 51339.7 g (32.02 %) and 26.92 % of runoff from 34 % of rainfall. Storms of 50 mm and above yielded 62.79 % of the soil loss. This shows that intensity is critical to soil loss and runoff generation.

Aguleri 50 m^2 plot

In the small plot, there was a total of 46 days of rain events, out of which 47.83 % had rains with no runoff, 4.35 % had runoff but trace soil loss and 47.82 % had runoff and soil loss. The two days' events with runoff but trace soil loss had rain of 30.3 mm with a runoff of 0.65 litre. The 22 events with no runoff had rain of 516.2 mm. The rains with runoff and soil loss had 1214.6 mm of rain, 428.1 litres of runoff and 77681.9 g of soil loss. This produced a soil loss per unit mm of rain of 63.96 g/mm and soil loss per unit litre of runoff of 181.46 g/l. There was no soil loss till August 8th with 70.1mm of rain that generated 343.3 g of soil loss and 14.4 litres of runoff. Again, August 13th and 14th had rains of 31 mm and 33 mm, respectively, generating soil loss of 270.2 g and 340.4 g, respectively. For the next 14 rain events, from August 20th to September 18th, soil loss occurred in 2 events. The bulk of the soil loss was generated in the last month of the season from 24th September – 24th October. From 28th July to 18th August, the generated runoff was 33.6 litres and a soil loss of 1041.5 g. From 20/8 to 23/9, the runoff was 24.35 litres and soil loss were 1633.6 g. From 24th September to 24th October, the runoff was 370.8 litres and the soil loss was 75006.8 g.

There were occasions when heavy rainfall generated no runoff. For instance, 61.5 mm (16th September), and 66 mm (18th September) generated no runoff. This might not necessarily be due alone to dry spells that separated the events between 9th and 18th September but due to the high permeability of the alluvial soils of the area. The high infiltration led to little or no runoff in the area until deep late in the rainy season towards the end of the season. This might be due to two major reasons. One is that this might be the period when the soil has reached its saturation level and therefore saturation-excess runoff and soil loss became effective. The second reason is that the end of the rainy season is always a period of high intensity rainfall which contributed to a buildup of runoff competent enough to generate runoff. Both reasons seem to hold together or else the runoff might not be strong enough to produce soil loss. That is, if the rain was not intense, the soil might still be absorbing the rains if they rain calmly.

Thus, the soils are susceptible to erosion once the saturation point is reached and thus need to be protected especially towards the end of the rainy season for maximum conservation outcome. This is reflected in the soil loss in the last month of the season which was 96.56 % of the recorded soil loss and 77.56 % of the runoff. Storms of 70 mm and above constitute 42.25 % of the rain generating 36.11 % of the runoff and 25.31 % of the soil loss. Storms of 50 mm and above constituted 71.24 % of the rain yielding 80.26 % of the runoff and 82.38 % of the soil loss. Additionally, it varied temporally across the months. It had 158.7 mm of rain, 33.35 litres (runoff) and 1041.5 g of soil loss in August. It increased to 446.6 mm, 75.45 litres and 4112.1 g respectively in September. It increased in October to 609.3 mm, 319.3 litres, and 72528.3 g of rain, runoff, and soil loss respectively. This shows that October produced 93.37 % of the soil loss, Sept had 5.29 %, and August had 1.34 %. Runoff had 74.59 % in October, 17.39 % in September, and 7.79 % in August.

4.2.2.6 Oko plots

Two weeks had rains but no soil loss in the area. These events happened on the weeks of 26th August and 10th October. Other weeks had soil loss, out of which 375.17 g/mm (big) and 157.95 g/mm (small) are soil loss per unit mm of rain in the area. This also points to the low rain recorded this year in some parts of the State. The weeks of 4/8 to 17th September recorded soil loss of 13379.1 g (big) and 10822.4 g (small) but from 24th September to 24th October, a soil loss of 236937.2 g (big) and 94563.05 g (small) was generated. This shows that the bulk of the soil loss was recorded toward the end of the rainy season. This was 94.66 % of the soil loss recorded in the last month of the season. This shows that soil erosion is critical toward the end of the rainy season in the area.

4.2.2.7 Other characteristics

A summary of the daily characteristics of the runoff and erosion is presented in Table 4. 13. It shows that there is a relatively high variation in the daily soil erosion attributes in the area. The highest variation is in Aguleri big plot followed by Isu small vegetated fallow plot (Table 4. 13). This is characteristic of daily rainfall distribution too which has a high coefficient of variation and since rainfall is the driver of erosion in the area, it is expected to follow a similar pattern. Aguleri big and small plots had the highest daily mean soil loss (Table 4. 13). Also, soil loss per unit of rainfall is higher in the Aguleri plot too (82.83 g/mm for big and 41.11g/mm for small plots).

Table 4. 13. Summary of the Daily Characteristics

Plots	Mean (g)		Mean rgrsl (g)		CV		sloss per unit rain g/mm	Sloss per unit runoff g/l
	Sloss (g)	Run (l)	Sloss (g)	Run (l)	Sloss (g)	Run (l)		
Isu 100 m^2 DP	767.01	33.89	1291.88	56.73	1.64	1.67	38.16	22.63
Isu 100 m^2 UP	110.70	5.66	272.50	13.13	2.22	1.70	5.51	19.57
Isu 50 m^2 DP	507.66	5.73	1087.84	27.68	1.83	2.67	25.09	39.06
Isu 50 m^2 UP	48.28	0.95	144.83	2.60	2.77	1.92	2.39	50.86
Aguleri 100 m^2	2914.91	33.51	5528.27	62.64	3.02	1.53	82.83	86.98
Aguleri 50 m^2	1894.68	10.46	3531.00	19.46	2.58	1.93	41.11	181.18

*sloss is soil loss, the Run is runoff, rgrls is rain that generated soil loss, CV is coefficient of variation

4.2.2.8 Monthly attributes

The distribution of soil loss and runoff within the months is shown in Figure 4.22Figure 4.23. It shows that the distribution of soil loss is skewed to the right except for the vegetated plots which looked nearly like a normal distribution (Figure 4.22).

This shows that soil erosion increases with time on those plots peaking towards the end of the rainy season. However, on the vegetated plots, it increased during the initial period of installation due to some disturbances and the absence of grass cover but as the grasses regrew, the soil loss began to decrease. It decreased with increasing grass cover such that towards the end of the rainy season when the intensity of rain was high and the soil was near super-saturation, there was very low soil loss (Figure 4.22).

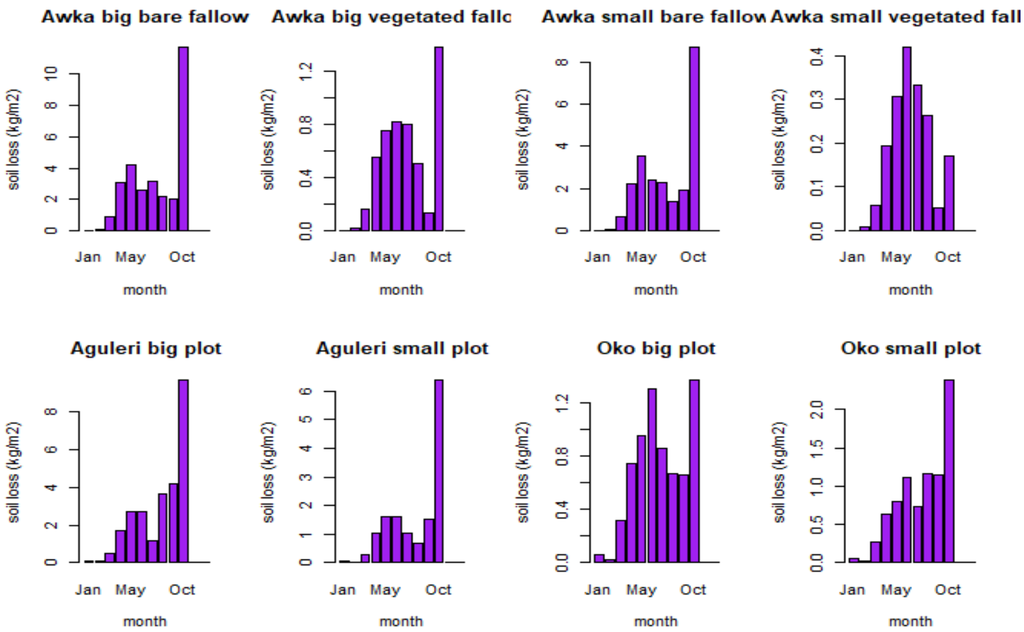

Figure 4.22. Soil loss distribution by months

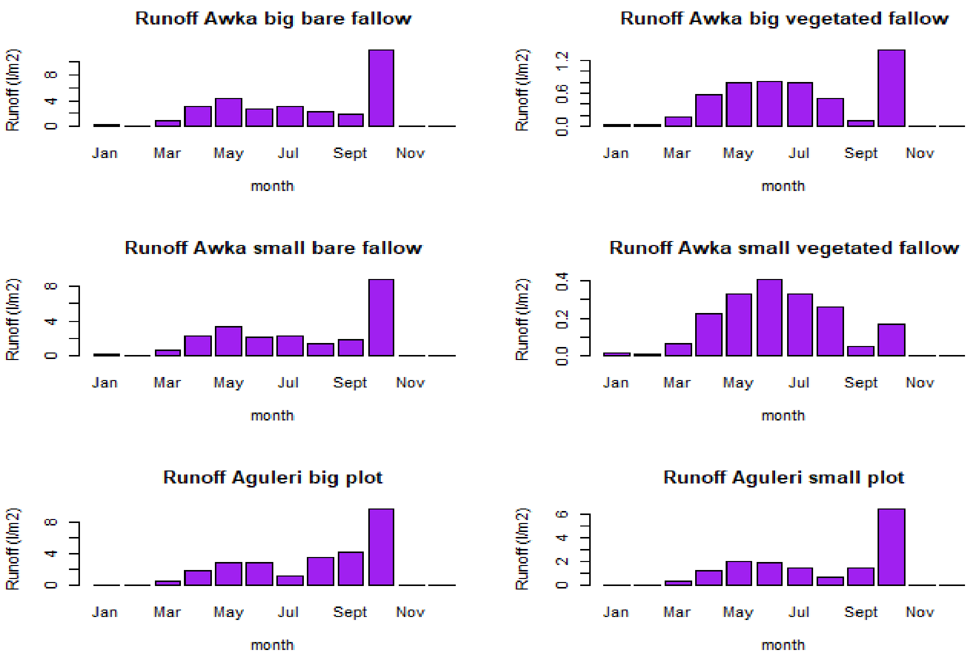

Figure 4.23. Distribution of runoff by months

Figure 4.22 shows that soil loss is highest in October at all locations except the Isu vegetated fallow plots. This is due to the moderation effect of vegetation on soil loss. Also, soil erosion is highest during the time of the cessation of the rainy season. That is, the intensity of rainfall is high and soil is super-saturated during the post-little dry season so soil erosion is highest during this period. The Oko plots have nearly bimodal erosion peaks which nearly mimic the annual rainfall distribution of the area which has its highest rainfall in Jun/July and Sept/October.

The runoff distribution is similar to that of the soil loss with the highest amount occurring in October. The vegetated plots at Isu have different shapes that nearly resemble a normal distribution which reflects the impact of vegetal cover on runoff generation (Table 4. *14*,

Table 4. *15* and Figure 4.23). This is a reflection of earlier studies that vegetation is an effective conservation measure that promotes aeration and soil pores, increases soil biomass and reduces runoff and soil loss (Diop *et al.*, 2022; Gongora *et al.*, 2022; Petito *et al.*, 2022; Trigunasih and Saifulloh, 2023).

Table 4. 14. Summary of monthly runoff

Statistic	Isu BDP (l/m^2)	Isu BUP (l/m^2)	Isu SDP (l/m^2)	Isu SUP (l/m^2)	Aguleri big (l/m^2)	Aguleri small (l/m^2)
Min	0.00	0.00	0.00	0.00	0.00	0.00
Median	0.09	0.33	1.66	0.11	1.43	0.85
Mean	2.12	0.42	1.93	0.15	2.19	1.88
Max	11.70	1.37	8.70	0.42	9.66	6.39

Table 4. 15. Summary of monthly soil loss

Soil loss	Isu BDP (kg/m^2)	Isu BUP (kg/m^2)	Isu SDP (kg/m^2)	Isu SUP (kg/m^2)	Ag BP (kg/m^2)	Ag SP (kg/m^2)	Oko BP (kg/m^2)	Oko SP (kg/m^2)
Min	0.00	0.00	0.00	0.00	0.00	0.00	0.00	0.00
Median	0.05	4.01e-03	0.04	0.004	0.05	0.07	0.66	0.68
Mean	0.06	9.75e-03	0.07	0.01	0.21	0.21	0.58	0.69
Max	0.23	3.98e-02	0.36	0.03	1.42	1.45	1.37	2.38

*Ag is Aguleri, B is big, S is small, P is plot, D is disturbed, U is undisturbed

4.2.2.9 Annual soil erosion rate and runoff

The annual rates in the plots were shown in equations 4.1 - 4.8. Below were equation 3.12 equivalents for soil loss in each plot (equations 4.1- 4.14).

$$SLBDP = 0.0004r \quad (4.1)$$

$$SLBUP = 0.00006r \quad (4.2)$$

$$SLSDP = 0.0005r \quad (4.3)$$

$$SLSUP = 6e - 05r \quad (4.4)$$

$$SLAgbig = 0.0012r \quad 4.5$$

$$SLAgsm = 0.0011r \quad 4.6$$

$$SLOk = 0.0039r \quad 4.7$$

$$SLOksm = 0.0069r \quad 4.8$$

where SLBDP is soil loss in Isu big disturbed (bare fallow) plot in kg, SLBUP is soil loss in Isu big undisturbed (vegetated fallow) plot, SLSDP is soil loss in Isu small (bare fallow) plot, SLSUP is soil loss in Isu small plot vegetated fallow, SLAgbig is soil loss in Aguleri big plot, SLAgsm is soil loss in Aguleri small plot, SLOk is soil loss in Oko big plot, SLOksm is soil loss in Oko small plot, r is rainfall in mm, soil loss is in kg.

Also, the equations for the runoff are shown below (eqs 4.9- 4.14)

$$RBDP = 0.019r \quad 4.9$$

$$RBUP = 0.0034r \quad 4.10$$

$$RSDP = 0.0138r \quad 4.11$$

$$RSUP = 0.0012r \quad 4.12$$

$$RAgb = 0.0105r \quad 4.13$$

$$RAgs = 0.0063r \quad 4.14$$

where RBDP is a runoff in Isu big disturbed plot, RBUP is the runoff in Isu big undisturbed plot, RSDP is the runoff in Isu small disturbed plot, RSUP is the runoff in Isu small undisturbed plot, RAgb is the runoff in Aguleri big plot, RAgs is the runoff in Aguleri small plot, r is rainfall in mm, runoff in litres/m2.

The performance of each of the models is shown in Table 4. 16. The results show that their performance is quite okay. The error values are very low except for those of Oko plots. However, the small plot at Oko is significant at a 0.05 confidence level, unlike the big plot. However, at a 90 % confidence level, it is significant. This shows that the models perform best on daily data.

4.2.2.10 Model accuracy

The performance of the model was assessed as shown in Table 4. 16.

Table 4. 16. Accuracy assessment of the linear models for soil loss estimation

Variables	MAE	MSE	RMSE	NRMSE.mean	R^2
Isu BDP soil loss- rain	0.5	0.769	0.877	1.14	0.64
Isu BDP runoff-rain	0.224	0.137	0.37	1.09	0.67
Isu BUP soil loss - rain	0.117	0.041	0.203	1.83	0.42
Isu BUP runoff - rain	0.036	0.003	0.056	0.992	0.73
Isu SDP soil loss - rain	0.474	0.592	0.77	1.53	0.46
Isu SDP runoff - rain	0.188	0.084	0.289	1.12	0.64
Isu SUP soil loss - rain	0.053	0.012	0.11	2.29	0.37
Isu SUP runoff - rain	0.013	0.0005	0.022	1.16	0.68
Isu BDP soil loss - runoff	0.332	0.326	0.571	0.745	0.84
Isu BUP soil loss- runoff	0.119	0.046	0.215	1.94	0.32
Isu SDP soil loss- runoff	0.179	0.11	0.331	0.658	0.90
Isu SUP soil loss- runoff	0.039	0.007	0.081	1.68	0.66
Oko big soil loss- rain	18.1	555	23.6	1.32	0.47
Oko small soil loss- rain	6.07	66.9	8.18	1.09	0.58
Aguleri big soil loss- rain	4.37	52.6	7.25	2.44	0.35
Aguleri big runoff - rain	0.257	0.135	0.368	1.08	0.63
Aguleri small soil loss - rain	2.39	16.1	4.01	2.38	0.32
Aguleri small runoff- rain	0.175	0.079	0.281	1.51	0.55
Aguleri big soil loss- runoff	3.55	32.4	5.7	1.92	0.60
Aguleri small soil loss- runoff	1.19	4.18	2.04	1.21	0.81

*DP is disturbed plot (bare fallow), UP is undisturbed plot (vegetated fallow), rainfall is in mm, soil loss in kg, and runoff in mm

The above table (Table 4. 16) shows that using runoff to estimate soil loss outperforms those modelled using rainfall. This is quite understandable given that it is not every rain event that causes soil erosion while most of the runoff is associated with soil erosion. The performance of the rainfall-erosion model worsens in areas with severe soil loss. Thus, it can be stated that the performance is weaker in locations with high soil loss. However, the runoff could not be used to predict erosion in the area due to the unavailability of runoff data that span the whole period. Hence, the rainfall-soil loss model was used instead. Nevertheless, wherever runoff data are available, the runoff-erosion model should be utilised.

4.2.2.11 Assessment of the 2022 rainfall, runoff and soil loss

The remaining part of the 2022 annual rainfall was completed with the CHIRPS data from January to when the experiment began. This part was then added to the collected rainfall for the months in each location and the annual rainfall was the sum of both. Thus, the mean annual rainfall for each location was 1731.7 mm (Isu), 2686.2 mm (Aguleri), and 1745.6 mm (Oko). The mean soil loss collected during the field experiment was estimated with equations 4.4 - 4.17 (Table 4. 17).

Table 4. 17. Linear model performance on soil loss (kg/m2)

Location	Field	Equation 3.12	difference
Isu big DP	0.49	0.51	-0.02
Isu big UP	0.07	0.08	-0.01
Isu small DP	0.61	0.61	0.00
Isu small UP	0.06	0.07	-0.01
Aguleri big	1.60	2.32	0.72
Aguleri small	1.55	1.94	0.39
Oko big	2.50	2.66	0.16
Oko small	4.22	4.70	0.48

MBE = 0.21 kg/m^2, MAPE = 15.37 %, RMSE = 0.34 kg/m^2, PBIAS = 16.13 %

The results (Table 4. 17) show that the performance of the linear model is relatively good and so can be used for soil loss prediction in Anambra State. However, it overpredicts the high erosion areas in Aguleri and Oko plots. This is its major weakness and might affect its use over severe erosion areas. The error metrics are within an acceptable range. For instance, MAPE values within the range of 10 and 25 are acceptable (Swanson, 2015). Also, lower values of the RMSE or MAE, indicate a better model performance (Tiwari and Chong, 2019). Since, their performance was good, the models including equation 3.11 were used to estimate the mean annual soil loss and runoff as shown in Table 4. 18. It shows that the highest runoff was in Isu and Aguleri's 100 m^2 plots. The mean annual soil loss and runoff rates are shown in Table 4. 18.

Table 4. 18. Mean annual soil loss and runoff from the plots

	soil loss kg m^{-2} yr^{-1}		Runoff mm yr^{-1}	
	Equation 3.11	Equation 3.12	Equation 3.11	Equation 3.12
Isu_BDP	0.64	0.69	28.12	32.9
Isu BUP	0.09	0.1	4.69	5.89
Isu SDP	0.82	0.87	21.40	23.9
Isu SUP	0.08	0.1	1.52	2.08
Aguleri big	2.55	3.22	29.32	28.21
Aguleri small	3.19	2.95	17.66	16.92
Oko big	5.15	6.81		
Oko small	8.69	12.04		

*BDP is big disturbed plot, BUP is big undisturbed plot, SDP is small disturbed plot, and SUPis small undisturbed plot

Thus, the mean annual soil loss rate for each location predicted with the equations 3.11 and 3.12 are shown in Tables 4.18. It shows higher mean annual soil loss rates in Oko and Aguleri than Isu bare plots. There is higher soil loss on bare soils than on vegetated plots (Table 4. 18). The mean annual soil loss on the big bare fallow plots was 0.64 kg ha^{-1} from the arithmetic model but 0.69 kg ha^{-1} with the linear model. This reflects an overestimation from the linear model.

4.2.2.12 Effects of vegetation on runoff and erosion

The effect of vegetation on runoff and soil loss was studied in the Isu plots. The results show that soil erosion and runoff are higher in unprotected agricultural lands than the protected ones. Vegetation impacts runoff and soil loss in different ways. It intercepts the rain droplets. Some will evaporate while many find their way to the ground via stem fall or direct from foliage as the wind blows. This way, they reach the soil at a reduced speed due to increased travel time and concentration time. Vegetation including its branches decelerates runoff and reduces the erosivity of the rainfall. The increased presence of plant remains and biomass close to the ground increases the soil's organic matter content, boosting infiltration, improving soil structure and limiting rainfall erosivity (Renard *et al.*, 1997). The effects of vegetal cover led to a very much reduced soil erosion in the vegetated plots. This showed that the absence of vegetation led to about 7 times higher erosion in the big plot and 10 times higher in the small plot. Again, the runoff increased 6 times higher in the bare fallow big plot than in the vegetated fallow plot. Also, in the small plots, the runoff was 14 times higher in the bare fallow small plot than in the vegetated small plot. This was in line with the statement that in agricultural lands with sustainable land management, soil erosion was very low (Fernández-Raga *et al.*, 2017; López-Vicente *et al.*, 2017). Borrelli *et al*. (2016) add that vegetation losses lead to high soil erosion. This showed that vegetation provides rough surfaces to the soil of which the biomass contributes to soil organic matter that helps to improve soil health, boost infiltration and minimize runoff. As Choi *et al*. (2005) added, soil erosion is worse on bare soils than on protected soils. This is because more vegetal cover implies more organic matter leading to low bulk density, increased infiltration, and reduced erosion (Diop *et al.*, 2022; Parras-Alcántara *et al.*, 2016; Zhu and Cheng, 2022). The finding is corroborated by Keestra and the team's work that runoff is higher on herbicide-treated plots and tilled plots than the vegetated plot (Keesstra *et al*., 2016)). Therefore, soil loss and runoff increase with a decrease in vegetal cover and vice versa. Hence, the vegetal cover is a good management strategy for soil and water conservation in agriculture.

4.2.2.13 Effects of slope angle and slope length on soil loss

The slope of the land to a large extent affects the erosion of the surface. Plots at Oko have steeper slopes followed by the Aguleri plots. The big plots in Isu, Aguleri, and Oko have similar surface attributes except for slope angle. They are all bare, 20 metres long and 5 metres wide but differ in soil attributes and slope. It has been stated that when every other attributes are similar except the isolated ones, then the differences in erosion among the compared areas are due to the isolated factors (Hayward, 1967). The soil erosion in the area was higher on the high slopes of Oko followed by Aguleri and least in Isu which had the lowest gradient. The correlation between slope and soil loss also showed a very strong significant positive relationship (0.91, p-value of 0.01). This indicates that soil loss increases with increasing slopes. The works of Ziadat and Teimah (2013) and Vanmaercke *et al*. (2014) corroborate this that soil erosion increases with increasing slope. Thus, less soil loss is expected on land with a gentle slope than on a steep one. However, Duley and Ackerman (1934) asserted that erosion and runoff were higher in plots with shorter slopes. This is true when the soil loss and runoff are considered in terms of output per unit area. Otherwise, the reverse is the case. The ability of soils to resist erosion reduces with increasing slope. This is because soil erosion has a positive relationship with slope (Shi *et al*., 2022). Also, Supandi *et al.* (2023) add that soil loss has a high positive correlation with erodibility and slope while Wang *et al*. (2023) adds that erosivity and slope are the key drivers of runoff and soil loss. Additionally, Panagos *et al*. (2015c) show that higher soil loss in some parts of the EU like Italy and Slovenia is due to high erosivity and steeper slopes in those countries. Thus, increasing slope steepness leads to an increase in soil loss. Hence, erosion is higher in areas of higher slopes and elevation in the central and southern parts (Figure 4.24).

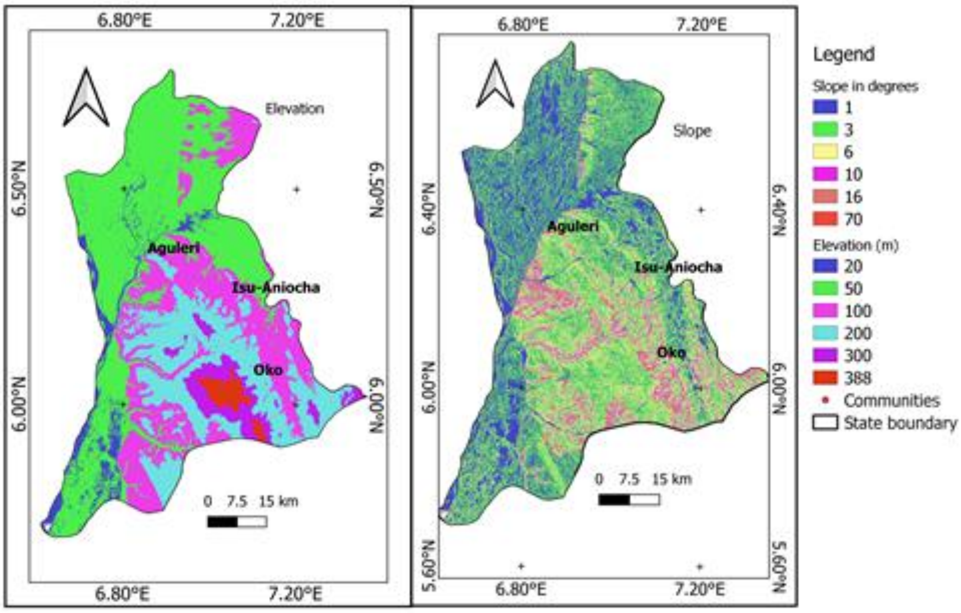

Figure 4.24. Elevation and slope maps of Anambra State

4.2.2.14 Effect of size (area) on Soil loss and runoff

The area has a moderate negative relationship with soil loss (-0.47). It shows that soil loss increases with decreasing areal size of the plot. Plot area has been shown to influence runoff generated in a plot (Kinnell, 2016). Also, the number of collection points of the runoff and soil loss from a plot affects the efficiency of its output. The greater the number of collection points, the higher the quantity of the variables trapped. This is because runoff flows through any area of descent on a plot but the plot's boundary restricts it to a common collecting point. This inhibition leads to forced infiltration as some of the runoff that could have left the plot in different directions is forced to redirect its flow towards the collection point. In the process, some of it is lost to infiltration except where infiltration capacity has been reached or on clay soils where infiltration is drastically reduced due to pore pressure resulting from a few voids. Soil erosion is affected by spatial scale since it is a spatially distributed phenomenon that encompasses sediment transfer along hill slopes (Figueiredo, 2013). The results show that increasing the area of a plot does not necessarily lead to increased output from the plot. Runoff and soil loss per unit area decrease with plot size (Mounirou *et al*., 2022) due to the long travelling time of runoff (Mutchler and Greer, 1980). They add that erosion measured at one scale does not necessarily represent erosion at other different scales (Mounirou *et al*., 2022). Additionally, the longer the flow stays in the watershed or plot, the more water, and soil can be held back in depressions, ponding, and infiltration (Nill *et al*., 1996). However, it has been suggested that such correlation should be cautiously interpreted as such relations might be due to inter-correlations of an area with other plots' properties (Vanmaercke *et al*., 2014). Thus, it shows that runoff and soil loss decrease with an increase in the area of the plot when the runoff and soil loss are considered based on output per unit area. However, when the gross output is considered, soil loss and runoff increase with increasing area. Therefore, the mean soil loss per plot depends on the size of the plots (Cerdan *et al*., 2019; Mounirou *et al*., 2022). Thus, increasing the size of the plot entails more catch of soil from it.

4.2.2.15 Tillage effect on runoff/soil loss

The impact of tillage is tested with the small plots at Aguleri and Oko. The results showed rapid erosion occurring on agricultural lands. The results from the small plot at Oko were 92.93 t/ha while from the big plot, it was 55.19 t/ha. At Aguleri, it was 41.17 t/ha in the small plot against 27.49 t/ha in the big plot. However, it has been argued that more erosion and runoff are recorded in the small plots due to less travel time and friction to overcome due to the short distance to cover before it reaches the outlet. Tillage causes soil disturbances by breaking the bonds that hold them together, thus making the soil susceptible to erosion. Thus, even though the big plots are bare of vegetation, the erosion rates are less on them than on the small tilled plots. For instance, at Oko, the soil loss was not very much in the big plot at the beginning of the experiment because the SOM reduced soil erosion. Also, the soil density measured in the big plot was lower than those collected on the agricultural small plot. However, over time, the SOM became depleted and thus it was followed by rapid soil erosion. Also, the runoff was slightly lower in the tilled plots but soil loss is higher compared to the bare plots in Aguleri. This agrees with the findings of Keesstra *et al*. (2016) that tilled soils show low runoff concentration but high sediment concentration. However, Mounirou *et al*. (2022) find a counter-result in a semi-arid environment in Burkina Faso. This might be due to the effect of slopes and soil types. They did their work on lower slopes, leading to more of a saturation-excess type of runoff and erosion. In that case, laminar flow persists which usually is initiated after much infiltration except where intensity is too high unlike on a higher slope where flow is often turbulent and initiated by infiltration-excess runoff. Also, Xiong, Sun and Chen (2019) assert that human-disturbed lands (cropland, orchards, and degraded grasslands) are more prone to soil erosion. Therefore, tilled soils yield more soil loss due to disturbances associated with agricultural lands such as the movement of tools, machines, weeding, and harvesting, especially in very humid regions where erosivity is very high. This is because tillage does not only modify the surface cover but also alters the soil structure and soil properties like SOC (Hassan *et al*., 2016), the biota's habitat (Costantini *et al*., 2015), and also some other soil chemical properties (Zornoza *et al*., 2015). Tillage is known to drive soil erosion in rainfed agriculture (Keesstra *et al*., 2016; Obia *et al*., 2020). Hence, minimal tillage should be encouraged in tropical agriculture as a sustainable soil conservation practice.

4.2.2.16 Effects of soils and geology

The soils and geology of a place exert influence on its response to soil erosion. Areas with impervious and hard rocks are less vulnerable to soil erosion, unlike areas with weak geology. However, the effect of geology could not be isolated quantitatively in this study. From the results, soil loss was less on the Imo clay shale but increased in Aguleri and is highest in Oko. The Aguleri soils were highly permeable such that little runoff was generated irrespective of the rainfall amount until very much later in the season. It showed that the alluvial soils were highly permeable with good drainage that offers protection from erosion. This was in line with Miller (1994) that highly porous soils are permeable and so have good drainage with limited soil erosion. However, as the rainy season advanced and with increased antecedent soil moisture, the soil became susceptible to erosion. That is, towards the end of the rainy season, the soil loss witnessed within the last month of the rainy season accounted for over 88 % of soil loss in the area. This implies, that the soil loss in the area likely increased due to increased soil moisture and intense storms which are characteristic of the area after the little dry season. It has been stated that soil loss increased as a result of high intensity storms on highly detachable soil with low infiltration (Wang and Shao, 2013). Thus, very permeable soils like the alluvial soils of Aguleri are less susceptible to erosion at the beginning of the rainy season but their resistance to erosion decreases as the rainy season progresses. This is because soil moisture and antecedent moisture are critical to soil loss and runoff (Ziadat and Taimeh, 2013).

4.3 Modelling soil erosion using the RUSLE model

Soil erosion rates was estimated with the RUSLE model for Anambra State, Nigeria. It was estimated for the year 2022 and also estimated for 2017 and predicted for 2060.

The prediction is necessary to aid planners towards the attainment of the AU's 2063 Agenda.

4.3.1 Current soil erosion rate as of 2022

Erosivity

The R-factor was estimated with the mean annual rainfall following equation 3.21. Due to little variations in the spatial distribution of rainfall across the State which is in line with the rainfall distribution of the area, there were little spatial variations in erosivity (Figure 4.25). The erosivity varied from 1300 MJ mm $ha^{-1}h^{-1}yr^{-1}$ in the north to 2135.02 MJ mm $ha^{-1}h^{-1}yr^{-1}$ in the south (Figure 4.25). The area has high erosivity due to its location in the humid tropics. This is in line with studies in the humid tropics that showed high erosivity of over 1000 MJ mm $ha^{-1}h^{-1}yr^{-1}$ (Andreoli, 2018; Fagbohun *et al.*, 2016; Talchabhadel *et al.*, 2020). Erosivity is highest in the extreme southern tips of the area followed by areas around Oko and decreased northwards in like manner (Figure 4.25). The erosivity has a very low variability across the area as its CV was 9.88 %. This implies that the mean erosivity is far above its standard deviation. The low degree of variation is due to the little variation in rainfall across the area (Figure 4. *1* and Figure 4.25).

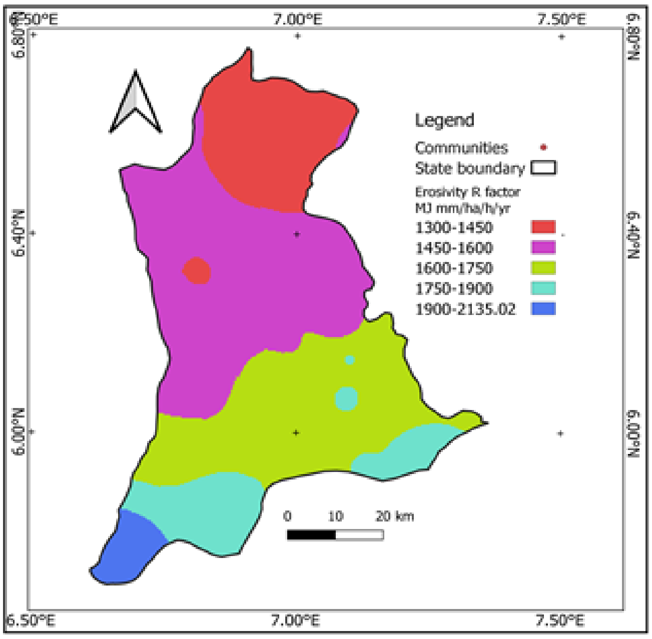

Figure 4.25. Erosivity map of Anambra State in 2022.

Soil erodibility

The soil erodibility indicates the soils of the area have low values that range from 0.03 to 0.041. This is due to the low silt content of soils in most locations and the high carbon content in the area. This is corroborated by studies that soils with low silt content have low erodibility (Emeribeole and Iheaturu, 2015). However, southern soils have low erodibility due to the high SOC, SOM, and carbonates. The northern part has high erodibility (Figure 4.26) due to the lower content of SOC and SOM. However, due to their high permeability, the soils are hardly eroded until later in the season toward the end of the season when the soils become super-saturated. Its high permeability conceals its susceptibility to erosion until later in the season when the soil must have reached its infiltration capacity and the rainstorm is intense. The soils of the southern part with higher quantities of fines have lower erodibility due to the moderating impacts of SOC and carbonates (Figure 4.26). It has been shown that SOM, SOC, and carbonate-rich soil soils have low BD, high infiltration, and low soil erosion (Al-Shammary *et al*., 2018; Chaudhari *et al*., 2013; Efthimiou, 2020, 2018; Nill *et al.*, 1996; Ostovari *et al.*, 2022). Soil erodibility has a CV of 2.70 % implying a low variability in the area.

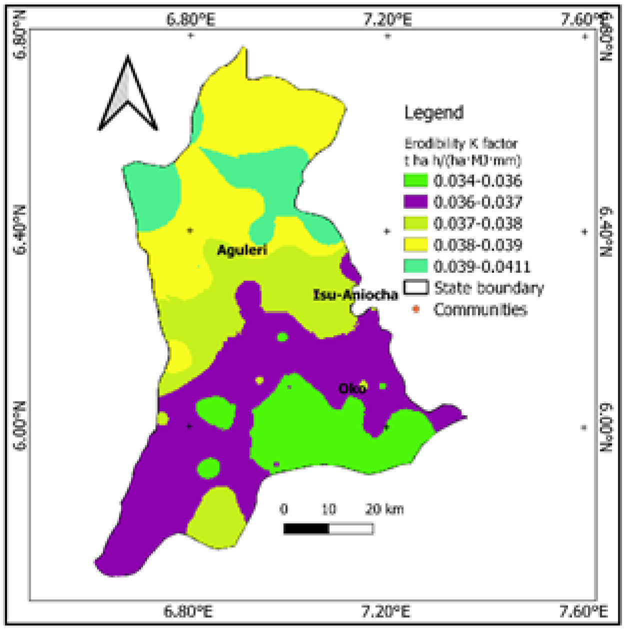

Figure 4.26. Erodibility (K) map of Anambra State

Topographic LS-factor

The LS-factor is a critical risk factor for soil erosion. It describes the impact of slope length and steepness on soil erosion (Figure 4.27). The slope of the area ranges from 0 to 68 degrees (Figure 4.24). However, a greater portion of the area is under a slope class of less than 16 degrees with the dominant slope class being 0 to 6 degrees (Figure 4.24). The steeper slopes occur in areas of higher relief in the southern and central parts of the State (Figure 4.24, Figure 4.27; Table 4. *19*). Table 4. *19* shows that three LGAs; Aguata, Anaocha, and Orumba South have the highest points in the State. These areas are located in the central and southern parts of the State. High slopes and elevation characterize the central and southern parts. Low slopes dominate the western parts of the State and eastern flank which are part of the Rivers Niger and Anambra/Mamu floodplains. The area is generally low with 99.75 % of the State being under slope class of 0-16 ^{o}. Also, low to moderate relief dominates the landscape as only 4.79 % of the area is on an elevation of 0 - 20 m above sea level. Also, 95.21 % of the State lies on a height of 20 m and above with only 6.69 % being on an elevation of 300-388 m. The slope has a CV of 101.59 % and the LS-factor has 201.59 %. This shows a very high variation in the slope and LS-factor in the area. This is in line with the statement that the LS-factor is one of the most sensitive factors of soil erosion (Hrabalikova and Janeček, 2017; McCool *et al.*, 1997, 1987; Tetzlaff and Wendland, 2012).

Table 4. 19. Mean slope and elevation in the local government areas (LGAs)

LGA	Mean slope degrees	Mean elevation m	Maximum slope	Maximum elevation
Aguata	3.35	244.21	28.85	388
Anambra East	2.89	51.58	31.48	187
Anambra West	1.14	25.01	39.18	78
Anaocha	3.29	229.33	26.23	377
Awka North	1.95	50.24	18.16	147
Awka South	3.69	112.54	28.09	286
Ayamelum	1.65	40.79	17.14	119
Dunukofia	3.10	121.15	20.21	194
Ekwusigo	2.73	62.24	30.16	171
Idemili North	3.44	130.02	20.32	242
Idemili South	3.05	110.86	22.57	262
Ihiala	2.37	85.13	28.49	188
Njikoka	3.74	160.78	27.39	269
Nnewi North	3.51	107.52	25.24	181
Nnewi South	4.00	82.08	34.55	181
Ogbaru	1.44	23.53	68.30	248
Onitsha North	2.23	42.81	31.28	139
Onitsha South	1.41	23.56	39.11	58
Orumba North	3.55	121.47	43.12	372
Orumba South	4.16	153.29	30.47	332
Oyi	4.39	108.51	31.11	206

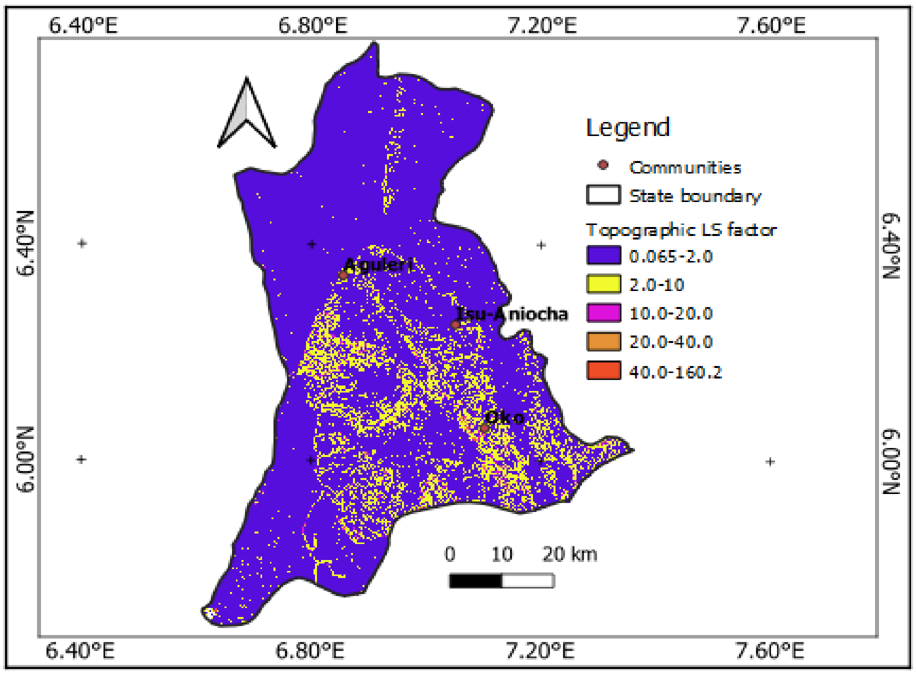

Figure 4.27. Topographic (LS) factor map of Anambra State

C- and P-factors

The land cover maps are derived from high-resolution 10 m images from the ESRI website. Details are in the Methods subsection. The scores assigned to each land cover class were described in the methods sub-section. Human occupation is higher in the central and southern parts than in other parts. The C-factor ranged from 0 to 1 with a mean of 0.33. There is a high variation in the C-factor value such that its CV is 90.91 %. Thus, it has been argued that the C-factor is the most significant in the RUSLE model (Fenta *et al*., 2017, 2016; Prasuhn, 2022; Toy *et al*., 1999).

The C-factor is a very important and critical risk factor of soil erosion which defines how protected or insulated a given soil is. Thus, the denser the vegetal cover in a given soil, the less its susceptibility to soil erosion and vice versa. Thus, it is reported that erosion is very sensitive to vegetation changes (Chen *et al*., 2018; Ge *et al*., 2023; Usman *et al*., 2023; Wu *et al*., 2020). The State is rapidly urbanising with a very high population density that has significantly impacted its vegetation cover. The State has major commercial centres such as Onitsha, Nnewi, and Ekwulobia. The town of Awka became the administrative capital of the State in 1991 which also spurred the growth of the urban area and other developmental projects in the State. Its vegetation has been described as poor and weak to provide the soil with enough cover from erosion (Egbueri *et al.*, 2022). The area lacks a large expanse of thick rainforest cover for they have been depleted by unrestricted and uncontrolled exploitation. Its vegetation is mainly shrubs and secondary regrowth and palm tree plantations. The sparse vegetation cover renders most parts of the State susceptible to soil erosion. The major areas with notable forest cover are the riparian areas on the western parts and a few portions on the eastern flank (Figure 4.28). The P-factor was chosen to be unity following the unavailability of data on conservation practices in the area. This was done following earlier researchers' recommendation on the choice of P-factor value when data on conservation is unavailable or in a natural environment (Ajibade *et al.*, 2020; Borrelli, 2011; Fagbohun *et al.*, 2016; Ghosal and Bhattacharya, 2020).

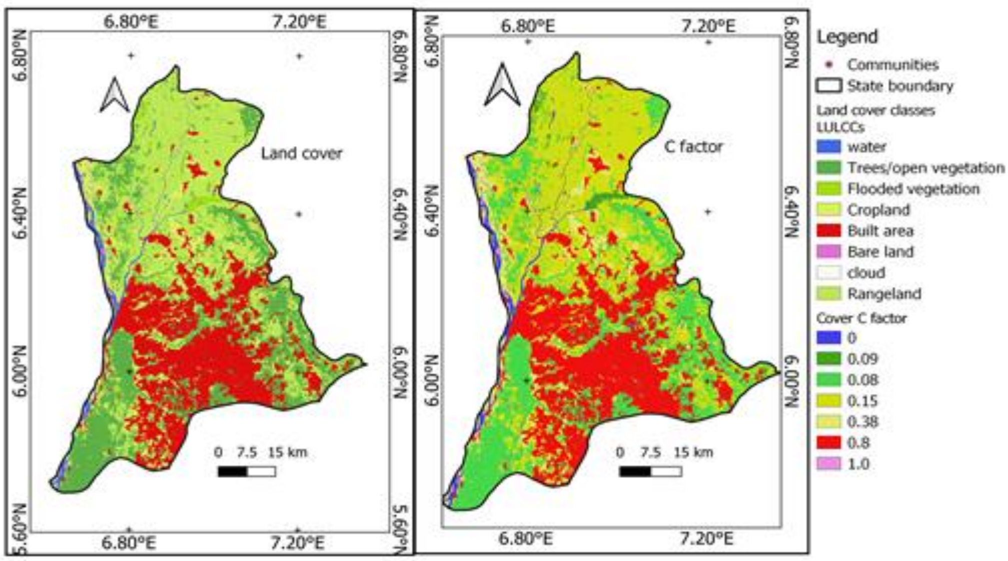

Figure 4.28. Land use and land cover classes of Anambra state

4.3.1.1 Mean annual soil loss

The mean annual soil loss in the State has wide spatial variations from north to south (Figure 4.29). Soil erosion is high in the area with a mean annual soil erosion rate of 25.25 t ha^{-1} yr^{-1}. The spatial variations in soil loss are shown in Figure 4.29 and Table 4. *20* with a CV of 241.43 %. Soil erosion is higher in the southern and central parts than in the western and northern parts (Figure 4.29, Table 4. *20*).

Soil erosion is severest on high slopes (Table 4. *20*). This is in line with studies that erosion increases with increasing slope (Fagbohun *et al.*, 2016; Huang *et al.*, 2020; Merchán *et al.*, 2023; Pitt, 2004; Sinshaw *et al.*, 2021; Ziadat and Taimeh, 2013). No LGA with a mean slope of less than 2 degrees has high soil loss (Table 4. *20*). However, Onitsha North and Awka North are experiencing high soil loss due to increasing urbanisation and bare surfaces (Table 4. *20*).

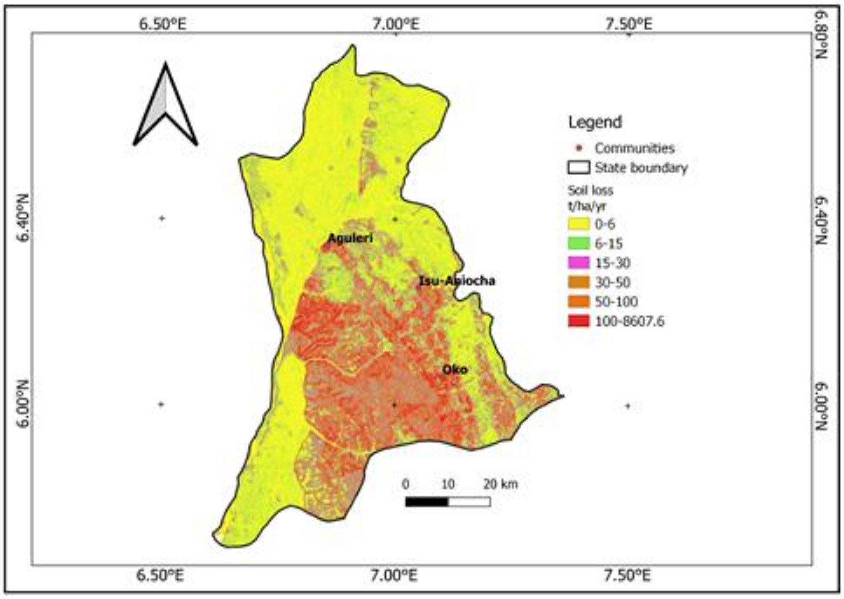

Figure 4.29. Soil loss rate of Anambra State

Table 4. 20. Mean soil loss per LGA in the State (t ha-1 yr-1)

LGAs	Mean slope degrees	Mean annual soil loss
Aguata	3.35	55.74
Anambra East	2.89	31.62
Anambra West	1.14	4.34
Anaocha	3.29	50.88
Awka North	1.95	11.19
Awka South	3.69	47.76
Ayamelum	1.65	5.75
Dunukofia	3.10	30.86
Ekwusigo	2.73	30.75
Idemili North	3.44	53.09
Idemili South	3.05	41.40
Ihiala	2.37	29.29
Njikoka	3.74	47.11
Nnewi North	3.51	59.99
Nnewi South	4.00	48.22
Ogbaru	1.44	6.78
Onitsha North	2.23	37.11
Onitsha South	1.41	5.66
Orumba North	3.55	34.45
Orumba South	4.16	33.25
Oyi	4.39	69.60

The soil loss map (Figure 4.29, Table 4. *20*) shows that soil erosion is higher in the central to southern parts, southeastern and northern tips of the State. These parts of the Anambra State are also areas with higher slopes and low vegetation covers due to increasing human occupation and agriculture. A classification of the soil erosion risk zones was done and presented in Table 4. *21*.

Table 4. 21. Soil erosion rates, their risk classes, and area in each class

Erosion rate	Km^2	%	Remark
0 - 6	2206.13	48.35	very low
6.01 – 15	830.02	18.19	low
15.01 – 30	562.23	12.32	moderate
30.01 – 50	346.53	7.59	high
50.01 – 100	356.89	7.82	severe
Above 100	261.33	5.73	very severe

It showed that the area under the low class of soil loss is 66.54 % while 5.73 % is under the very severe erosion class (Table 4. 20). Thus, a greater percentage of the State is under a low class of soil loss. Also, the severe class is worrisome as 13.55 % of the State is threatened by severe to very severe erosion. This calls for concerted efforts to combat and limit its growth and development.

4.3.1.2 Validation and uncertainty of the model

The mean annual soil loss for Anambra State from the field was 27.76 t ha^{-1} yr^{-1} but that from the RUSLE model was 25.25 t ha^{-1} yr^{-1}. The mean annual soil loss rates in Awka North LGA (Isu), Anambra East LGA (Aguleri), and Orumba North LGA (Oko) are shown in Table 4. 22. The model's performance against the field output had a mean bias error (MBE) of -3.00 t ha^{-1} yr^{-1} and MAE of 9.34 t ha^{-1} yr^{-1}, coefficient of determination of 0.77, and R of 0.88 indicating an underestimation of the soil erosion but with a good performance. This is in line with the literature that RUSLE underestimates soil erosion in areas with severe erosion but overestimates areas of low erosion (Behera *et al.*, 2023; Nearing, 1998). Thus, the model's performance was good in estimating the low to moderate erosion areas in Isu and Aguleri but underestimated the severe erosion area in Oko (Table 4. 22). That is, it had an absolute error (AE) of 4.84 and 6.17 t $ha^{-1}yr^{-1}$ in Isu and Aguleri respectively but an AE of -17.02 t $ha^{-1}yr^{-1}$ in Oko. In line with the model's weakness, it was unable to simulate the impact of rainfall intensity or extreme rainfall events on soil erosion (Yang *et al.*, 2023).

Table 4. 22. Comparison of soil loss rates from the model and from the field

LGA	RUSLE estimate (t $ha^{-1}yr^{-1}$)	Field estimate (t $ha^{-1}yr^{-1}$)
Anambra East	31.62	25.45
Awka North	11.19	6.35
Orunmba North	34.45	51.47

The model has shown that it can be utilised in soil erosion modelling and management in Anambra State, Nigeria.

4.3.2 Linking soil erosion to erosivity (climate) and land use and land cover

The RUSLE model was used to predict soil erosion rates in 2060. It involved estimating erosivity from GCM data of 2050-2060 from the Worldclim and C-factor 2060 simulated using the Multilayer Perceptron from the Terrset software. It showed the likely state of soil erosion in 2060 compared to 2022 should the current trend of vegetation-to-settlement conversion persist under the Shared Socioeconomic Pathways SSP245 and SSP585 climate scenarios.

4.3.2.1 Erosivity

Due to little variations in the distribution of erosivity across the State which is in line with the interannual rainfall distribution, there were few temporal variations (Figure 4.30). It changed from 1565.17 (MJ mm $ha^{-1}h^{-1}yr^{-1}$) in the first period of the study (2017), to 1599.76 (MJ mm $ha^{-1}h^{-1}yr^{-1}$) in the second period (2022). Also, the coefficient of variations (CV) shows that there are relatively small variations in the R-factor values: 11.29 % (2017) and 9.88 % (2022) (Figure 4.30). This indicates that there were little variations in the distribution of erosivity values over the periods. Studies have also reported a slow trend in erosivity (Diodato *et al*., 2020; Mondal *et al*., 2016; Wang *et al*., 2017). However, some scholars have reported a very rising trend (Qin *et al*., 2016; Wang *et al*., 2017) and others a slowly decreasing trend (Sadeghi and Hazbavi, 2015). It was reported that a greater percentage of the variations in soil loss was attributed to erosivity and slope (Doetterl *et al*., 2012; Zhao *et al*., 2021).

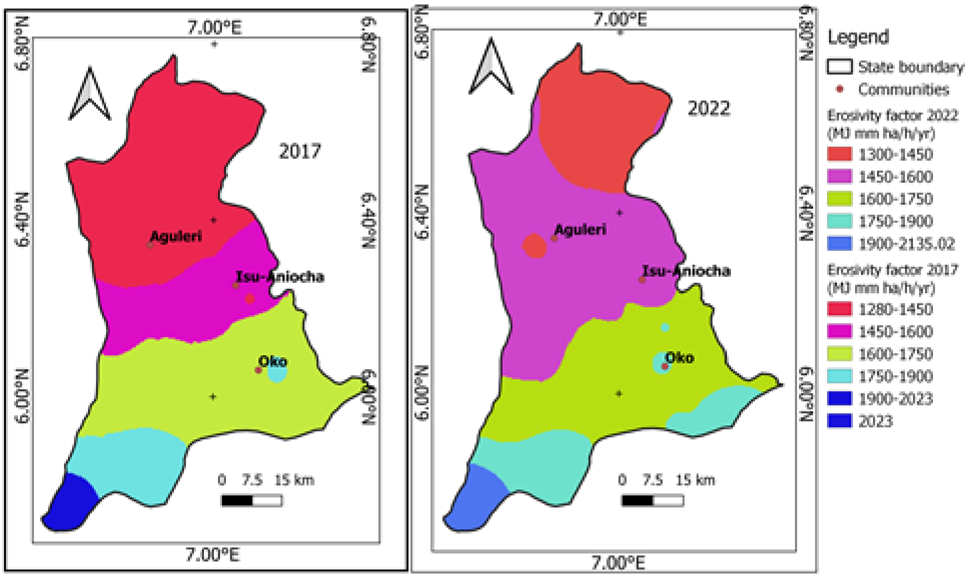

Figure 4.30. Erosivity maps of Anambra State for the periods 2017 and 2022.

4.3.2.2 Cover C-factors

The flooded vegetation cover (riparian forest) decreased from 2017 to 2022 while the urban land space increased (Table 4. *23*, Figure 4.31,Figure 4.32). The flooded vegetation which is the remaining thickets in the area decreased while the rangeland increased. Thus, there was about a 14 % loss in forest thickets (flooded vegetation) that led to an 8.89 % and 3.91 % increase (gain) in rangeland and built-areas respectively (Table 4. *23*). The C-factor ranged from 0 to 1 with a mean of 0.29 (2017) and 0.33 (2022). There were high variations in the C-factor values which were 103.45 % (2017) and 90.91 % (2022). The CVs reveal some high spatial variations in the C-factor values in the State. This implies that the C-factor plays a significant role in influencing variations in soil erosion in the area both temporally and spatially. It also shows that the central and southern parts have lost much of their vegetation and have also had much increase in human occupation in the State (Figure 4.28). Thus, soil erosion increases with increasing human occupation and vegetation cover loss. This is corroborated by earlier studies that the loss of vegetation to agriculture, grazing, and others led to increases in soil erosion (Ebabu *et al*., 2022; Ganasri and Ramesh, 2016; Kidane *et al*., 2019).

Table 4. 23. Percentage change in land uses and land cover LULC classes

LULC class	2017	2022	% change
Water	2.06	2.11	0.05
Flooded vegetation	39.36	25.19	-14.18
Open forest	0.62	1.13	0.51
Cropland	5.39	6.23	0.84
Built-areas	24.05	27.96	3.91
Bareground	0.34	0.35	0.01
Rangeland	28.13	37.02	8.89

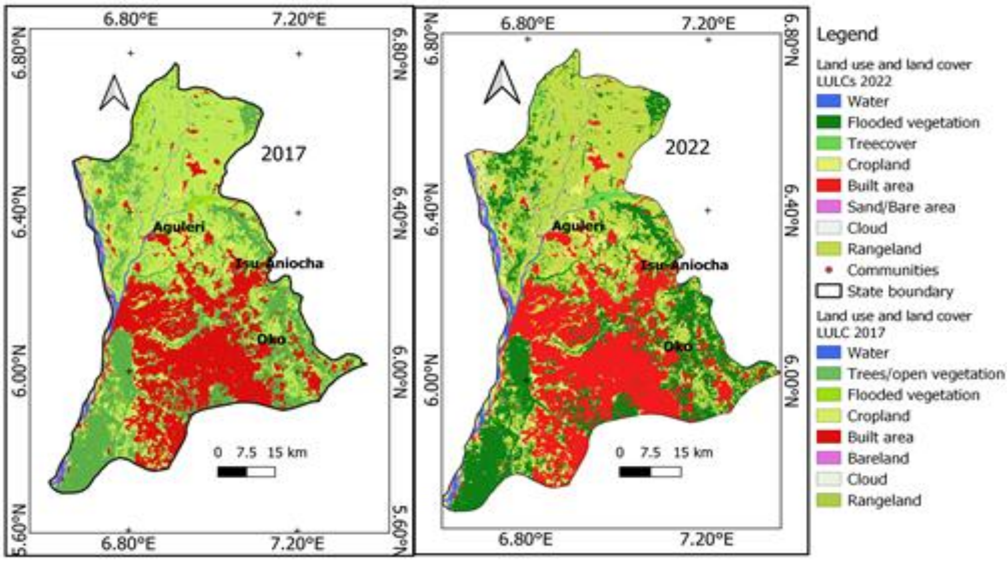

Figure 4.31. Land use and land cover classes of Anambra in 2017 and 2022

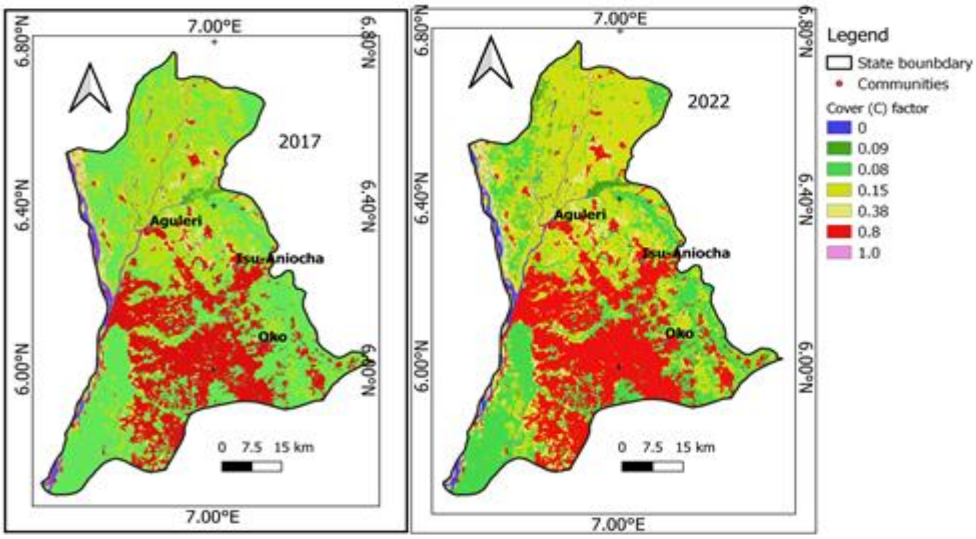

Figure 4.32. Cover C-factor maps of Anambra State in 2017 and 2022.

4.3.2.3 Mean annual soil loss

The mean annual soil loss in the State has wide spatial and temporal variations from north to south (Figure 4.33). Soil loss increased from 2017 to 2022 in the State. It showed that mean annual soil loss increased by 18.43 % from 2017 to 2022. The mean annual soil loss in 2017 was 21.32 t $ha^{-1}yr^{-1}$ but 25.25 t $ha^{-1}yr^{-1}$ in 2022. The spatiotemporal variations in soil loss are shown in Figure 4.33 and Table 4.24. There was higher soil erosion in 2022 than in 2017.

Soil erosion is severest in the local governments with high slopes (Tables 4.20 and 4.24). This is in line with studies that erosion increases with increasing slope (Fagbohun *et al*., 2016; Huang *et al*., 2020; Ziadat and Taimeh, 2013). None of the LGAs with a mean slope of below 2 degrees has high soil loss (Table 4.24).

Also, with the regression model (eq. 3.12), the predicted soil loss for 2017 was 34.39 t $ha^{-1}yr^{-1}$, 2020 was 29.02 t $ha^{-1}yr^{-1}$, and 2022 was 30.54 t $ha^{-1}yr^{-1}$. The regression model is overpredicting the soil erosion rates in the low to high erosion areas while the RUSLE underpredicts the high erosion area but slightly overpredicts the low erosion areas. The regression-based model follows the rainfall pattern of the year which is its sole predictor. This is its major weakness because several factors influence erosion.

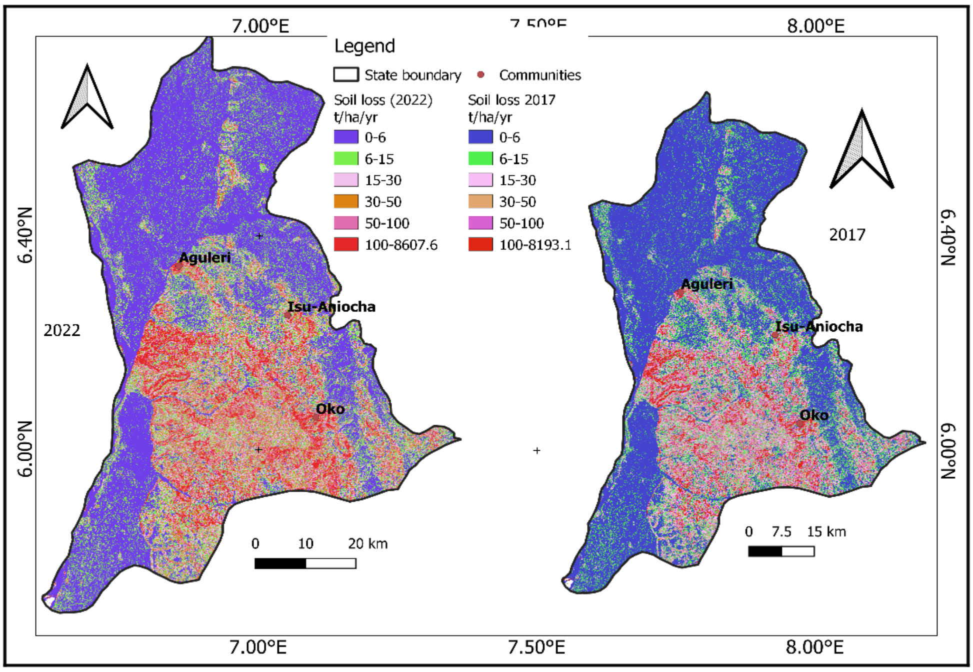

Figure 4.33. Soil loss maps of Anambra State in 2017 and 2022

Table 4.24. Mean soil loss per LGA in the State

towns	2017 t ha^{-1} yr^{-1}	2022 t ha^{-1} yr^{-1}	Changes
Aguata	46.72	55.74	9.02
Anambra East	26.55	31.62	5.07
Anambra West	3.73	4.34	0.61
Anaocha	45.72	50.88	5.17
Awka North	9.76	11.19	1.43
Awka South	38.59	47.76	9.17
Ayamelum	5.00	5.75	0.75
Dunukofia	28.05	30.86	2.81
Ekwusigo	27.77	30.75	2.98
Idemili North	43.74	53.09	9.35
Idemili South	37.58	41.40	3.82
Ihiala	25.27	29.29	4.02
Njikoka	38.73	47.11	8.38
Nnewi North	53.04	59.99	6.95
Nnewi South	40.51	48.22	7.71
Ogbaru	6.04	6.78	0.74
Onitsha North	39.15	37.11	-2.03
Onitsha South	5.38	5.66	0.28
Orumba North	28.74	34.45	5.71
Orumba South	25.46	33.25	7.78
Oyi	55.61	69.60	13.99

The soil loss map (Figure 4.33, Table 4.25) shows that soil erosion is higher in the central to southern parts, southeastern and northern tips of the State. These parts of the State are also areas with high slopes and low vegetation covers due to increasing human occupation and agriculture. These are areas with high increases in soil erosion in the State, unlike areas with much vegetation covers like Ogbaru, Ayamelum and others (Table 4.25, Figure 4.33). Additionally, the results show that soil loss is lowest under vegetation cover but severest under bare ground and built-areas followed by croplands (Table 4.25). Also, soil erosion increased with increasing slope (Table 4.25). In all slope classes, soil erosion rates increased from 2017 to 2022. However, the increase is higher on steeper slopes than on gentle slopes (Table 4.25). Furthermore, it shows that soil erosion increases as the slopes increase.

Table 4.25. Mean annual soil erosion rate per LULCC and slope

Soil erosion per Land use and land cover class				
		$t\ ha^{-1}\ yr^{-1}$		
Land cover class		2017	2022	changes
water		1.16	1.15	0.00
Flooded vegetation		3.18	1.94	-1.24
Open forest		9.14	10.12	0.99
cropland		16.59	19.84	3.25
Built-areas		59.17	63.84	4.68
Bare ground		85.36	70.91	-14.45
Rangeland		7.92	8.84	0.93
Soil erosion rate per slope class		$t\ ha^{-1}\ yr^{-1}$		
Slope class	Area in %	2017	2022	changes
1	38.54	4.38	4.90	0.53
3	37.39	16.63	18.74	2.11
6	16.51	41.79	49.11	7.32
10	5.68	72.89	91.89	19.00
16	1.64	109.53	145.81	36.28
70	0.24	242.90	266.44	23.54

A classification of the soil erosion risk zones was done as presented in Table 4. 26.

Table 4. 26. Erosion rate, the risk classes, and the area under each class

Erosion rate $t\ ha^{-1}\ yr^{-1}$	Erosion risk class 2017		2022		Changes		
	Km^2	%	Km^2	%	Km^2	%	class
0 - 6	2393.33	52.45	2206.13	48.35	-187.20	7.82	very low
6.01 – 15	807.79	17.70	830.02	18.19	22.22	2.75	low
15.01 – 30	536.33	11.75	562.23	12.32	25.90	4.83	Moderate
30.01 – 50	315.59	6.92	346.53	7.59	30.94	9.80	high
50.01 – 100	307.77	6.74	356.89	7.82	49.11	15.96	severe
Above 100	202.22	4.43	261.33	5.73	59.11	29.23	very severe

Hence, considering the periods (2017 and 2022), the State is experiencing an increasing trend in soil erosion. However, the rate of increase is higher in the central and southern parts of the State (Figure 4.33, Table 4.24) and on bare ground and croplands (Table 4.25). Table 4. *26* shows that the very low erosion class decreased in 2022 while other classes increased. The increase was such that the severe and the very severe classes had 15.96 % and 29.23 % increases, respectively. These increases in the severe erosion classes portend danger to agriculture and the environment in the State.

This increasing mean annual soil erosion rate with a slight increase in erosivity denotes that though it is important in driving soil erosion, it played a less role in determining the temporal change in erosion in the State. That is, soil erosion increased by 18.43 %, erosivity by 2.21 %, and C-factor by 13.79 % from 2017 to 2022. Hence, vegetation plays a more important role in the temporal variations in soil erosion in the State. This corroborates studies that vegetation and slope play critical roles in determining soil loss risk (Benkobi *et al.*, 1994; Prasuhn, 2022). That is, vegetation is a risk factor for erosion that majorly control the temporal variations in erosion in the State. All the risk factors of erosion (erosivity, erodibility, slope steepness and length, vegetation) contribute to its spatial variations. However, due to heavy rainfall over the State owing to its location in the same rainfall and climate regime, there is little spatiotemporal variation in erosivity. Yet, that does not imply a less role by erosivity but that the variations across the State are driven by other factors with wider variations like LULCs and slope. The erosion in the area shows that low to moderate soil erosion risks predominate the area but are decreasing while the severe categories are increasing (Table 4. 26). The increasing soil erosion with time is in line with several studies (Kayet *et al*., 2018; Kidane *et al*., 2019). Erosivity, vegetation cover, and slope are very critical to soil loss variations. Thus, it was asserted that 75 % of variations in soil loss were due to variations in erosivity and slope (Doetterl *et al*., 2012; Zhao *et al*., 2021). Although, vegetation limits erosion, this ability is weakened at certain rainfall intensities (Chen *et al*., 2018; Ge *et al*., 2023; Wu *et al*., 2020). Thus, erosion is high in the central and southern parts due to sparse vegetation, high slope, and rainfall erosivity, especially toward the end of the season.

4.3.2.4 Soil erosion in the future (2060).

The land use and land cover classes were projected to 2060 as discussed in the methodology and the 2050-2060 rainfall data were obtained from the Worldclim website for the Shared Socioeconomic Pathways (SSP) 245 and 585 scenarios.

Erosivity

The erosivity factor for the SSP245 scenario is slightly lower than the SSP585 scenario in the State. It has a mean erosivity value of 1602.00 MJ mm $ha^{-1}h^{-1}yr^{-1}$ (SSP245) and 1630.19 MJ mm $ha^{-1}h^{-1}yr^{-1}$ (SSP585). In line with the interannual rainfall distribution of the State, there was a small variation (Figure 4.34). Also, the coefficient of variations (CV) shows that there are relatively small variations in the R-factor values: 8.28 % (SSP245) and 7.87 % (SSP585) (Figure 4.34). This indicates that there will be little variations in the distribution of erosivity values in the 2060s.

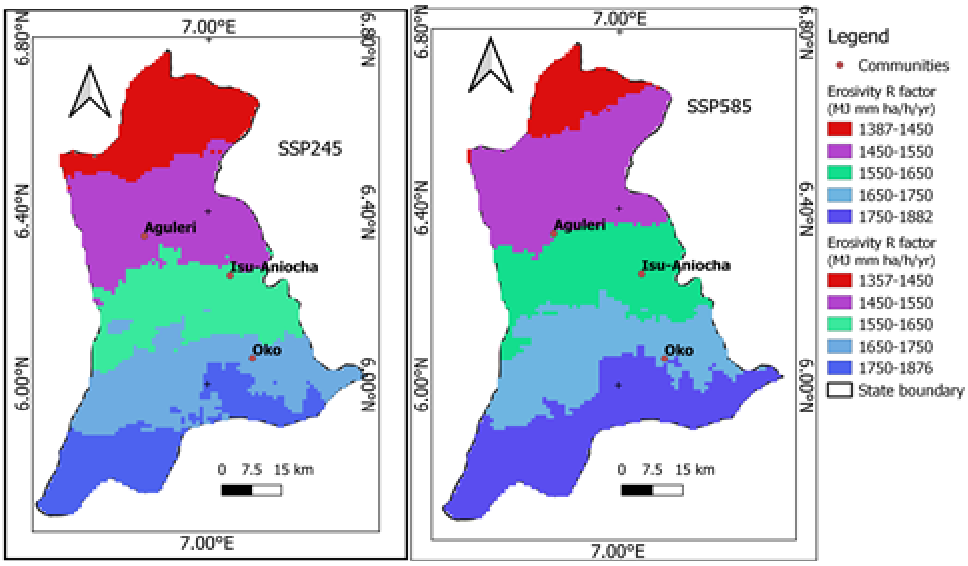

Figure 4.34. Erosivity of Anambra State for 2060

Cover C-factor

The land cover map was generated using the Clark Terrset software using the flooded vegetation to built-area submodel as it is the principal driver of land cover change in the State. The land cover classes and the C-factor values are presented in Figure 4.35.

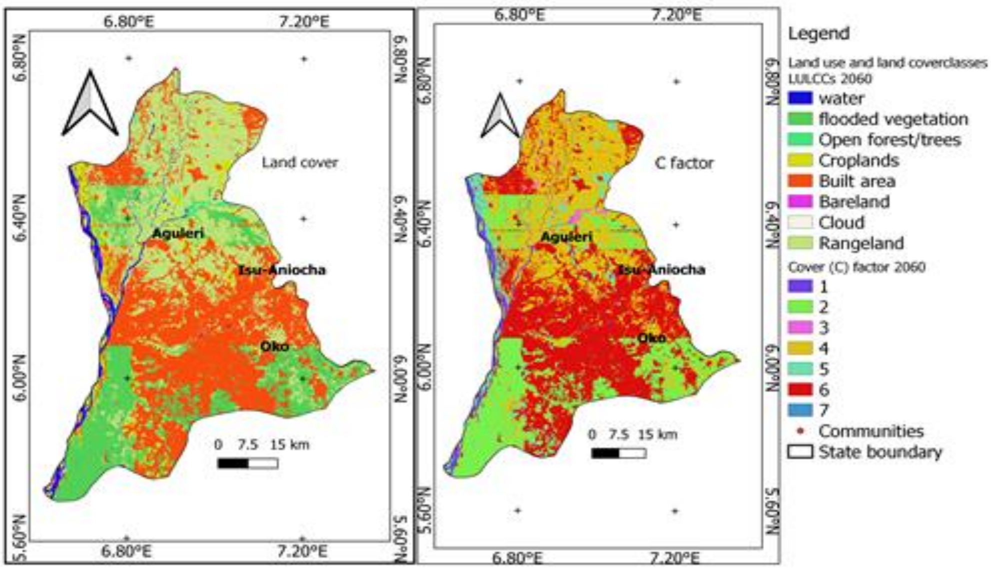

Figure 4.35. Land use and land cover classes and the C-factor for 2060

The land cover will experience a significant change in 2060 as the built-area will move from 27.96 % to 39.45 % (Table 4.27). Table 4.27 also shows that all other land cover classes will experience a decrease in 2060. This is because the State is highly urbanising and engages in services and commercial activities more than agriculture.

Table 4.27. Percentage change in land uses and land cover LULC classes

LULC class	2022	2060	% change
Water	2.11	1.98	-0.13
Flooded vegetation	25.19	20.55	-4.64
Forest	1.13	0.68	-0.45
Cropland	6.23	5.06	-1.17
Built-areas	27.96	39.45	11.49
Bareground	0.35	0.30	-0.05
Rangeland	37.02	31.98	-5.04

4.3.2.5 Annual soil loss

The mean annual soil loss rate in the State will be higher than the current state following the forest-built-area transition. Thus, the mean annual soil erosion rate will be 31.22 and 31.79 under the SSP245 and SSP585 scenarios respectively (Figure 4.36). This shows that the worst-case scenario (SSP585) has very little difference from the moderate scenario (SSP245). Thus, it can be said that the C-factor change will impact future soil erosion more than the climate (rainfall erosivity).

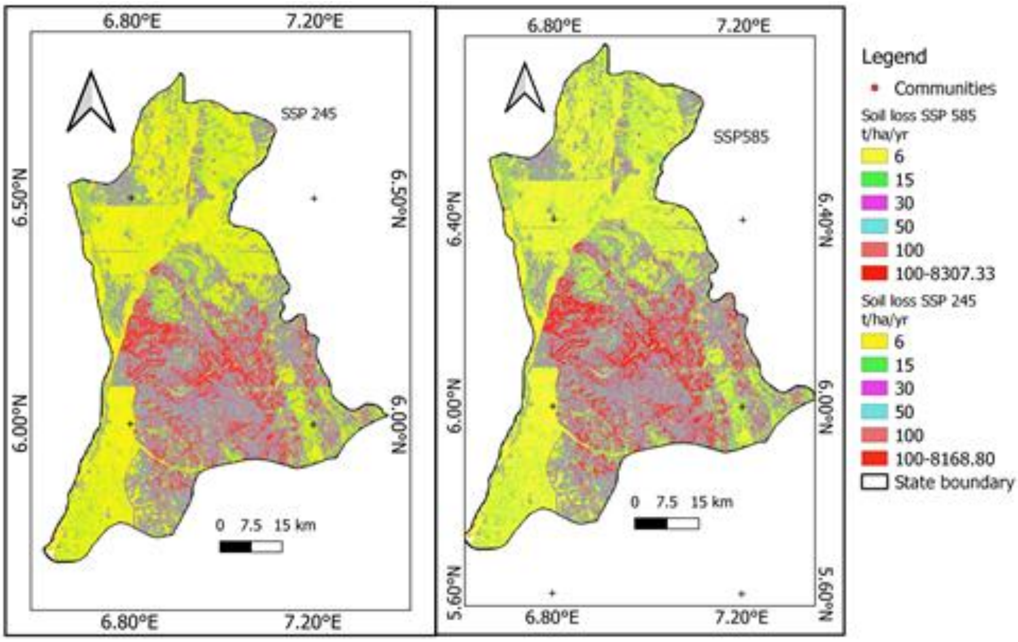

Figure 4.36. Mean annual soil loss of Anambra State for 2060

The soil loss rate per LGA is shown in Table 4. *28*. It shows that erosion will increase in most of the LGAs. The major susceptible areas comprising the southern and central parts of the State are the areas with higher rates of increase in soil erosion in both scenarios in 2060 (Table 4. *28*). These are LGAs with increments of nearly 10 % and above. However, it reveals a decrease in areas like Orumba South, Nnewi North and South, Ihiala, and Ekwusigo LGAs. The other areas with a low increase or decrease are the low susceptible areas due to low slope and higher vegetal cover (Figure 4.36 and Table 4. *28*).

Table 4. 28. Mean soil loss per LGA in the State

Towns	2022 (t $ha^{-1}yr^{-1}$)	SSP245 (t $ha^{-1}yr^{-1}$)	Changes a	SSP585 (t $ha^{-1}yr^{-1}$)	Changes b
Aguata	55.74	54.25	-1.49	55.12	-0.62
Anambra East	31.62	43.31	11.69	44.15	12.53
Anambra West	4.34	7.82	3.48	7.97	3.63
Anaocha	50.88	72.03	21.15	73.41	22.53
Awka North	11.19	15.55	4.36	15.93	4.74
Awka South	47.76	74.81	27.05	76.46	28.70
Ayamelum	5.75	8.52	2.77	8.72	2.97
Dunukofia	30.86	40.91	10.05	41.78	10.92
Ekwusigo	30.75	30.06	-0.69	30.45	-0.30
Idemili North	53.09	66.99	13.9	68.14	15.05
Idemili South	41.40	45.56	4.16	46.29	4.89
Ihiala	29.29	27.82	-1.47	28.09	-1.20
Njikoka	47.11	74.08	26.97	75.61	28.50
Nnewi North	59.99	57.78	-2.21	58.56	-1.43
Nnewi South	48.22	44.20	-4.02	44.77	-3.45
Ogbaru	6.78	5.52	-1.26	5.56	-1.22
Onitsha North	37.11	46.28	9.17	46.98	9.87
Onitsha South	5.66	8.18	2.52	8.29	2.63
Orumba North	34.45	48.46	14.01	49.41	14.96
Orumba South	33.25	28.70	-4.55	29.15	-4.10
Oyi	69.60	89.96	20.36	91.69	22.09

*a is changes between 2022 and SSP245, b is between 2022 and SSP585 2060.

The soil loss per LULCC is shown in Table 4. 29. It shows that erosion remains higher on bare surfaces and built-areas followed by croplands (Table 4. 29).

Table 4. 29. Soil erosion per land cover class

Class	SSP245 t ha^{-1} yr^{-1}	SSP585 t ha^{-1} yr^{-1}
water	0.79	0.80
Open forest	9.49	9.63
flooded vegetation	2.38	2.43
cropland	18.32	18.63
Built-areas	64.05	65.22
Bareland	77.72	78.61
Rangeland	8.79	8.97

4.3.2.6 Soil erosion risk zones in Anambra State

Soil erosion risk zones in Anambra State are shown in Figure 4.37. It shows that the severe erosion risk zone predominates the central to southern parts of the State, especially in areas like Onitsha, Ideani, Oko-Ekwulobia, Nanka-Aguleri, Awka, and the southeastern tip (Figure 4.37). The moderate zone is seen in patches around several parts of the State though it is still more concentrated in the central part of the State. The low class covers the greater part of the State on the eastern and western flank and the northern part of the State (Figure 4.37). In 2060, the low class will decline while the moderate and severe classes will spread to low-class areas in the eastern part and south of Awka town and the northwestern tip of the State (Figure 4.37). It shows that soil erosion is a severe threat to agriculture and the environment in the State. The severe erosion areas are the location with mean slopes above 2 degrees, higher elevation, sparse vegetal cover, and increasing human occupation. Thus, erosion risk in the area is aggravated by slope, high erosivity, and human occupation arising from land use change that leads to vegetation depletion. Therefore, as the population increases as well as urban spaces, larger bare surfaces will be created which will aggravate erosion in the future (Figure 4.37).

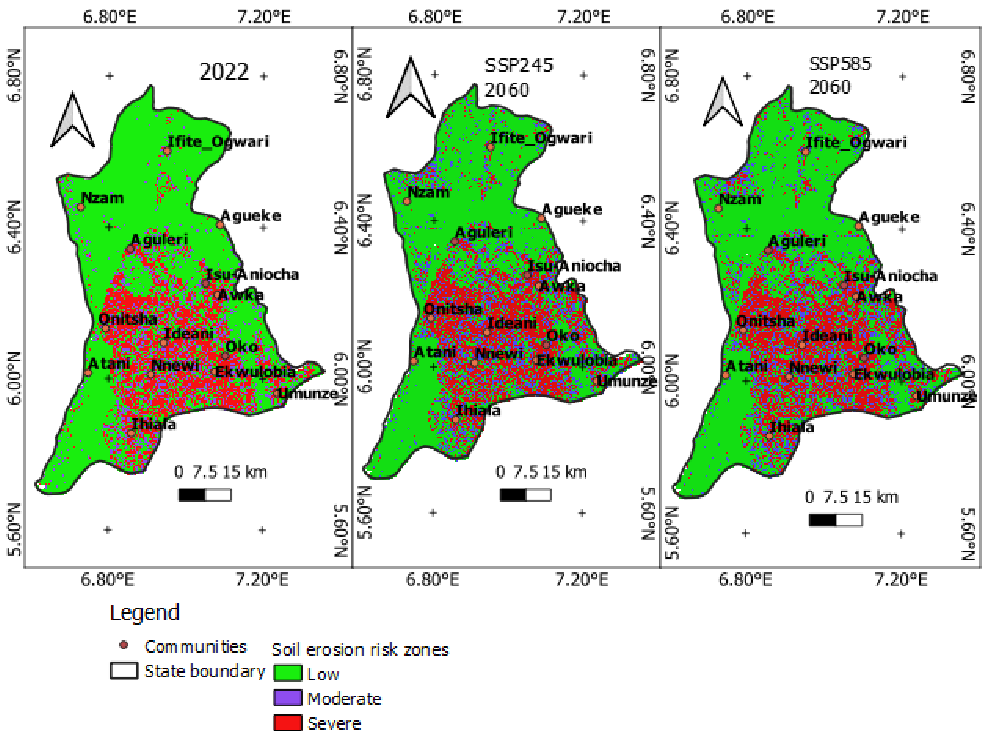

Figure 4.37. Soil erosion susceptibility map in Anambra State

4.1 Farmers' adaptation to soil erosion in Anambra State, Nigeria.

4.1.1 Socio-demographic characteristics of the farmers

The farmers comprised 53.00 % males and 47.00 % females. More on this is shown in Table 4.30. This showed that men have more access to capital than women. Men are entrusted with land and not women except where the husband is deceased. This is in line with Abubakari and Abubakari (2014) that men have more access to capital than women in their community in Eastern Ghana.

Table 4.30. Socio-demographic characteristics of the farmers in percentage

	Class	Percent %		Class	Percent
Gender	Male	53.00	Education	None	26.00
	Female	47.00		Primary	34.00
Age	< 30	9.00		Secondary	31.00
	31 – 40	17.00		Tertiary	9.00
	41 – 50	25.00		1-5 persons	41.00
	51 – 60	24.00		6-10	54.00
	> 60	25.00		11-15	2.00
Marital status	Married	75.00	Household size	> 20	3.00
	Single	4.00			
	Divorced	2.00			
	Widow	19.00			

The socio-demographic attributes of the respondents showed that married farmers and aged farmers dominated the trade (Table 4.30). That is, 74.00 % of the farmers were aged above 40 years. This shows that the youth has taken to other businesses such as education, commerce, and similar activities in several urban centres in the State and beyond. The majority of the farmers own the lands they farm (97.00 %) while 3.00 % rent the lands they farm on. The respondents recognized rainfall as the major cause of soil erosion (Table 4.31). They also perceived that their soils are very susceptible to erosion due to their high erodibility (Table 4.32). Other factors of importance are urbanisation, inadequate knowledge, and attribution to God. However, based on closed-ended questions, over 90 % of the farmers believed that heavy rain, erodible soils, and the absence of soil conservation measures principally caused soil erosion. Other important factors of soil erosion included increasing population, deforestation, and high slopes (> 70%). The farmers disagreed that improper cultivation was a cause of soil erosion in the area. That is, they believed that their conventional method of cultivation did not encourage soil erosion.

Table 4.31. Perceptions on causes of soil erosion based on open-ended questions

causes	percentage
rain	76.00
God/end-time	5.00
don't know	6.00
buildings/urbanisation	7.00
poor drainage	2.00
herbicide	1.00
CC/deforestation	2.00
undecided	1.00

*CC is climate change

Table 4.32. Perceptions on causes of soil erosion based on close-ended questions (percentage)

	improper cultivation	high slope	deforestation	heavy rain
Yes	47.00	73.00	73.00	98.00
No	52.00	26.00	25.00	1.00
undecided	1.00	1.00	2.00	1.00
	Absence of conservation	erodible soil	high population	sand mining
Yes	92.00	92.00	78.00	43.00
No	6.00	6.00	20.00	55.00
undecided	2.00	2.00	2.00	2.00

Table 4.33. Perceptions of the evidence/indicators of soil erosion (percentage)

	environmental Problem	more frequent	erodes farm	shallow soil depth	declining yield
Yes	87.00	84.00	80.00	64.00	63.00
No	12.00	15.00	20.00	35.00	36.00
undecided	1.00	1.00	0.00	1.00	1.00
	soil washed	soil colour	Loss of manure	Rill/gullies	exposed root
Yes	76.00	67.00	77.00	27.00	73.00
No	23.00	32.00	23.00	73.00	26.00
undecided	1.00	1.00	0.00	0.00	1.00

A greater percentage (87.00 %) of the farmers accepted that soil erosion is an environmental and agricultural problem (Table 4.33). Also, 84.00 % of the farmers agreed that the soil erosion menace has become more frequent (Table 4.33). The indicators of soil erosion in the farms include eroded farmlands, shallow soil depth, low yield, change in soil colour, and exposed crop or plant roots each of which recorded over 70 % (Table 4.33). Table 4.33 also showed 27.00 % of the respondents identify the presence of channel erosion (rill/gully) in their farms. This shows that the dominant soil erosion in the area is interill erosion with few severe soil erosion problems in a few farmlands. This is in contrasts to findings in Eastern Ghana that gullies are the main indicators of soil erosion (Abubakari and Abubakari, 2015), and in Ethiopia (Belay, 2014). Gullies are associated with badlands which will less likely be used as farmlands. Also, the conventional heaps/mounds tillage systems might be good soil and water conservation measures that limit erosion growth to rills and gullies.

4.1.2 Adaptation strategies to soil erosion

There were several measures that the farmers have adopted to enable them to live with soil erosion, recover from its effects, and/or absorb the shock without any permanent damage or loss to the farmers. These measures range from mixed cropping to having a secondary job or business (Table 4.34).

Table 4.34. Adaptation strategies of the farmers (percentage)

	mixed crop	Cover crops	few plots	zero tillage	resilient crops	remittance
Yes	91.00	66.00	48.00	14.00	32.00	17.00
No	8.00	33.00	50.00	84.00	66.00	81.00
undecided	1.00	1.00	2.00	2.00	2.00	2.00
	nonfarm job	mulching	CP	RD	SB	
Yes	41.00	34.00	41.00	52.00	32.00	
No	57.00	64.00	57.00	46.00	67.00	
undecided	2.00	2.00	2.00	2.00	1.00	
	hedging	Check dams	CS	NSB	PP	STR
Yes	13.00	20.00	20.00	7.00	24.00	78.00
No	85.00	77.00	79.00	91.00	74.00	20.00
undecided	2.00	3.00	1.00	2.00	2.00	2.00

*CP is contour ploughing, RD is runoff diversion, SB is solid bunds, CS is a cooperative society, PP is planting pit, STR is straw retention, NSB is no slash and burn

It showed that the majority of the farmers practised mixed cropping systems (91.00 %) and 66.00 % plant cover crops which are good at binding soils together and limiting runoff generation (Table 4.34). Also, straw retention in the farm was highly practised (78.00 %) which is good to replenish humus in the soil and improve the SOM and SOC. Studies show that SOM and SOC limit soil erosion and so are good soil conservation measures (Keesstra *et al*., 2016; Petito *et al*., 2022).

However, Table 4.35 showed that the farmers' adaptations to soil erosion were low. Only a very few (20.00 %) belonged to cooperative societies, 91.00 % still practise slash and burn agriculture which is detrimental to soil microbes and soil health, and only 14.00 % practice zero tillage agriculture. Thus, Adaptation is low which is invariably a result of a low level of education. Only 9.00 % of the farmers had a tertiary education and 31.00 % had secondary school level education. From interviews and discussions with the farmers, it was observed that the highly educated ones also had more capital for the farming business, also had remittances from their children and relatives they had helped train in schools, they also practised more soil conservation measures because they know the implication of leaving the soil open to erosion and had more capital. They dug check-pits to hold back runoff and nutrients it had carried (Figure 4.38). This was in line with studies that the adoption of conservation agriculture correlates with education and access to credit (Abdulai, 2016; Abdulai and Abdulai, 2017). The check-pit was to control erosion in a mixed crop farm that had corn, vegetables, cassava and cocoyam but for the shorter growing season of the vegetables and corn, they had been harvested (corn residues were left in the field, Figure 4.38).

Figure 4.38. Checkpits in Orumba North LGA in a mixed crop farm.

There were so many challenges the farmers faced that limited their adaptation strategies to erosion in the State. Some of these limitations included a lack of modern farming systems and tools, low capital, insufficient government support, lack of climate change adaptation, invasive weeds, and food insecurity (Table 4.35).

Table 4.35. Limitations to the farmers' adaptation strategies (percentage)

	low capital	NWF	PA	lack CCA	modern farm	YM
Yes	96.00	93.00	95.00	90.00	90.00	59.00
No	2.00	5.00	3.00	8.00	8.00	38.00
undecided	2.00	2.00	2.00	2.00	2.00	3.00
	deforestation	IGS	DCY	FI	IW	FU
Yes	62.00	96.00	74.00	81.00	50.00	75.00
No	36.00	2.00	24.00	17.00	48.00	23.00
undecided	2.00	2.00	2.00	2.00	2.00	2.00

*NWF is no weather forecast, PA is poor agronomy, IGS is insufficient government support, DCY is declining crop yield, FI is food insecurity, FU is farming becoming unattractive, YM is youth migration, IW is invasive weed

The farmers added that the government support was insufficient and often when it arrived, it was late. The government does not respect their seasons and timing, such that when some of the government support reached them, they had no use for them. For instance, they cited an instance when the government brought improved rice species to them when the time for planting had pretty much passed the planting time. Also, the technicalities involved in planting and nursing some of the government-brought breeds were so tasking for them to follow especially using manual power. Thus, they added that the government should assist them with ploughing, planting and weeding machines at subsidised rates. Some of the farmers argue that soil erosion per se was not their most challenging problem but government support and funding. Food insecurity is increasing because output was getting lower due to insufficient funds and power. In any case, they added that food insecurity is a problem of society because when output was low, the farmers secure them for their use and the next cropping season, implying less quantity for sale. They also added that youth migration was a big challenge to them as it made the cost of labour high as they relied on migrant labourers who in most cases charged higher prices due to competing jobs and demands. Should they have tractors and other equipment from the government at very subsidised prices, they would have increased outputs. Thus, the greatest factors limiting their adaptations were insufficient capital and inadequate government support followed by a lack of weather forecast (Table 4.35). This is in line with findings elsewhere that insufficient credit limits farmers' adaptations to soil erosion (Abubakari and Abubakari, 2014; Belay, 2014; Abubakari and Abubakari, 2015; Abdulai, 2016). A new adaptation strategy adopted by quite a few of the farmers is growing yams in sacks filled with soil. They argue that insecurity has made them resort to growing yams in sacks around their homes which also grow free from soil erosion and the outputs are encouraging. It is yet to be fully and widely practised in the State.

5. GENERAL DISCUSSION

Soil erosion is a serious land degradation problem in Anambra State, Nigeria. Soil erosion problem is increasing in Anambra State as highlighted by the study.

The results show that there is an increasing trend in monthly and annual rainfall in the area, however, they were not significant statistically. Also, there was an increasing trend in the seasonal rainfall except for the MAM season. They were also not significant. This implied a likelihood of increasing erosivity in the area and hence a high potential for increased erosion. Thus, low rainfall and decreasing trend in the MAM season is an indication of decrease in erosion. Similar findings were replete in the literature that there is a decrease in rainfall in the MAM season (Gebrechorkos *et al*., 2023, 2019; Nicholson, 2018). A high rising trend in the SON season would significantly impact soil erosion as erosion is severest in the SON season in the area. Over 50 – 90 % of the recorded soil loss was obtained in the SON season. However, studies in the drier regions showed higher erosion at the onset (Fang *et al*., 2015; Mounirou *et al*., 2022). This might be because the drier lands have little protection before the onset of the rainy season and the soils were highly disturbed, unlike the rainforest areas where the soils have vegetal cover even during the dry season.

The soils of the area have low erodibility due to high quantities of sand and SOM/SOC. However, its susceptibility was worsened by the high slopes, intense rainfall, and vegetation loss. The southern soils are more problematic due to higher quantities of fines and lower MDD. The positive linear relationship between soil loss and soil pH, and SOC is contrary to the results that erosion increases with decreasing SOM and SOC (Arunrat *et al*., 2022; Keesstra *et al*., 2016). Also, soil bulk density had a negative relationship with CaCO3, slope, and soil loss. This is in line with studies by Ostovari *et al*. (2019) and Hassan (2012). The negative relationship of BD with erodibility is corroborated by other studies (Chaudhari *et al*., 2013; Deng *et al*., 2016; Peng *et al*., 2022). This is because in areas of high bulk density, the compact nature of the soil limits erosion but runoff is high due to low infiltration. Thus, Peng *et al*. (2022) point out that the detachment of soil decreased exponentially with increasing bulk density.

This can be aggravated by farm machine use which increases soil strength due to compaction, limiting infiltration, and aggravating runoff (Hamza and Anderson, 2005; Woldeyohannis *et al*., 2022) and likely downslope erosion due to the runoff build-up. Thus, farm machine use alters soils' physicochemical properties causes low crop yield due to poor SOM and root penetration (Hamza and Anderson, 2005) and can worsen erosion due to accelerated build-up of runoff.

The soil loss in the area shows that erosion is higher in Oko followed by Aguleri and then lowest in Isu. The erosion in Aguleri was low initially due to the high permeability of the soil but toward the end of the rainy season when the soils became saturated the soil loss increased astronomically. Miller (1994) showed that soil loss is limited in areas with fine drainage due to increased soil permeability. Furthermore, soil loss is lower in vegetated plots than in bare plots in Isu (Appendix 5, Table 4. *17*). This shows that vegetation provides cover to the soil and inhibits soil loss. This is in line with studies that soil loss decreases in areas with soil conservation measures and vegetal cover (Keesstra *et al*., 2016; López-Vicente *et al*., 2021, 2020). Thus, low soil erosion rates occur in scrublands and agricultural lands with sustainable land management practices and pose less danger to ecosystem health (López-Vicente *et al*., 2017, 2020, 2021; Fernández-Raga *et al*., 2017). Bare lands experience higher runoff and soil loss than covered soils (Fang *et al*., 2017; Mounirou *et al*., 2022; Oza *et al*., 2022).

Also, the importance of rainfall intensity, antecedent soil moisture, and vegetation was demonstrated by the plots in the area. About 59.38 % of the rainfall generated runoff and soil loss in the Isu big plot but it was 42.19 % in the vegetated fallow that generated runoff and soil loss. The soil loss per unit of rain in the big bare plot was nearly 6 times that on the big vegetated plot (42.98 g/mm against 7.45 g/mm). Soil loss decreased from the inception of the study to September in both plots. It increased in October but the increase in the bare fallow was over 8 times that of vegetated fallow (47.66 % against 5.62 %). A similar trend was exhibited by the small plots in Isu. However, in Aguleri and Oko, the soil loss increased progressively from inception to the end of the season. Thus, buttressing the findings of Boix-Fayos *et al*. (2006) that plots suffered exhaustion over the years, the Isu plot demonstrated that exhaustion can manifest in a season in plots located on less erodible soils. Thus, higher soil loss would be experienced in the early periods following the initial soil disturbances but decreases with time unless where a severe storm prevailed. It also showed that though erosion increases with increasing intensity (Ziadat and Taimeh, 2013), it is moderated and weakened by the presence of vegetation cover and SOM. The bulk of the soil loss was recorded in the last month of the season. For instance, in the big plots at Oko, it was 94.66 %, at Aguleri (95.27 %), and at Isu bare (52.86 %). The severe soil loss at this period underscores the importance of antecedent soil moisture and intense rainfall that characterize the post-little dry season rainfall in the State.

Hence, the bulk of the soil loss was recorded in the last month of the season. However, the rate is highest in Aguleri, followed by Oko but least in Isu implying the impact of slope and geology on the soil loss. Isu which is on a low slope and on the Imo clay shale had the lowest rate among the three locations. The Isu plot was having a decreasing trend of soil loss with time till the last month when it increased while runoff was increasing till the end of the season. However, at other locations, the trend was increasing with time till the end of the season, though the rate of increase was astronomical in the last month of the season signifying the impact of rain intensity and antecedent soil moisture. Additionally, in Aguleri, the soil loss was increasing with time but was low until when the soil became saturated toward the end of the season such that the last month generated so much soil loss (over 95 %). Aguleri soil is shown to be susceptible to erosion but its susceptibility is hidden or latent until it reaches saturation toward the end of the season.

Soil erosion is increasing in the State. It increased from 2017 to 2022. The results show that the C-factor which has a direct link with human impact on the environment drives the temporal variations in soil erosion in the State. It showed that erosion was increasing with increasing human occupation arising from vegetation loss and soil disturbances. This is corroborated by studies that land cover change drives soil erosion (Belay *et al*., 2020; El Jazouli *et al*., 2019; Keesstra *et al*., 2016; Nut *et al*., 2021;

Palliyaguru *et al*., 2023; Tadesse *et al*., 2017; Usman *et al*., 2023; Yaswanth *et al*., 2022). Rainfall is a key driver of soil erosion but its role is minimal in determining the spatiotemporal variations in soil loss in the State. This does not imply that erosivity is unimportant because there cannot be soil erosion by water without rain in the humid tropics. However, it shows that though a driver of soil erosion, its role in variations of soil erosion is limited as the C-factor driven by land cover changes was paramount. That is, while there are very high spatiotemporal variations in the C-factor and slope, only a little variation exists in the rainfall distribution because the whole State fall under the same climatic belt. Thus, soil erosion management should place more priority on rainfall and vegetation dynamics in the State, especially at locations above 2 ^{o} slope. This is critical as erosion is predicted to increase in most parts of the State in 2060.

The farmers identified rainfall as the major cause of soil erosion. This was in line with earlier studies (Nwobodo *et al*., 2018). Also, Chinweze (2017) found that climate change, human impact, and sand mining aggravate soil erosion. Similarly, our results showed that there was low education attainment in the area and which likely limited their adaptation to soil erosion. This was corroborated in the study by Angela and Ezeomedo (2018) that the Akpo area of the State has low education. Also, Abubakari and Abubakari (2015) added that low education limited the farmers' access to capital in the Upper East region of Ghana. Adaptation strategies to erosion are low in the area and are limited by insufficient government support, lack of capital, and climate information.

6. CONCLUSIONS AND RECOMMENDATIONS

6.1 Conclusions

Soil erosion is a severe land degradation that threatens sustainable agricultural production in Anambra State. Anambra is one of the most susceptible States to soil erosion in Nigeria. Thus, large quantum of soil is washed downslope into rivers thereby polluting the water system and heightening the risk of flooding. Moreover, climate and land use change are projected to worsen soil erosion in many parts of the world especially the humid tropics. The soil degradation problems have agitated research in soil erosion and water conservation from different fields including Agriculture, economics, hydrology, geomorphology, and climate change scientists. As such, several studies have employed modelling. However, models are based on assumptions that may hamper their ability in solving the soil erosion problems especially in developing world where data for validation are scarce. Therefore, the study carried out a comprehensive assessment of soil erosion risks and farmers' adaptation strategies in Anambra State, Nigeria to improve soil erosion management and conservation planning in the area. This helped to build a reliable soil erosion model for the State.

The study focused on the following research questions: 1. Have there been any variations in the seasonal and annual rainfall of Anambra State? 2. what is the rate of soil erosion? 3. Can the soil erosion rate be determined with a RUSLE model and to what extent have the erosion features changed over the years? and 4. What are the farmers' adaptation strategies to soil erosion?

The results showed that there were rainfall variations in Anambra State with higher rising rainfall trends in the south than in the north. Rainfall is higher in the south than in the north with a likelihood of more intense rains in the 2060s across the State. Soil loss increases with increasing rainfall.

The mean annual soil loss in the State from the field assessment was 27.76 t ha^{-1} yr^{-1} with higher soil loss in Oko and Aguleri than Isu. The State's soils are susceptible to erosion due to low SOC and SOM worsened by high slopes with higher susceptibility on Nanka sands. The alluvial soils are also susceptible but its susceptibility is concealed by its good drainage until the SON season. Field investigations showed that infiltration-excess-related runoff and erosion prevailed on the high slopes while saturation-excess-related erosion dominated the gentle slopes. Hence, there were ubiquitous signs of ponding and deposition on Isu plots on low slopes while signs of scouring dominate the high slopes at Oko. The field assessment has provided us with first-hand information on soil erosion rates in the Anambra State of Nigeria.

Soil erosion rates in Anambra can be estimated with the RUSLE model since it has a low error metric (a mean bias error of -3.00 t ha^{-1} yr^{-1}). It predicted a mean annual soil loss of 25.25 t ha^{-1} yr^{-1} and showed that erosion will be severer in the future with a mean annual soil erosion rate of 31.22/31.79 t ha^{-1} yr^{-1} in 2060. The severe erosion class will increase from 18.09 % (2017) to 25.30 % (2060). However, it underestimated the high erosion areas. It showed that vegetation dynamics highly influenced temporal changes in soil erosion more than erosivity. Soil erosion is high in the State, especially in the southern, central, and Awka areas due to high slopes and land cover changes. This is aggravated by the low-level implementation of soil conservation measures.

The farmers' adaptation strategies to soil erosion include cover cropping, straw retention, and runoff diversion. There were still high percentage practices of conventional tillage, slash and burn agriculture, low use of planting pits, mulching, hedging, check-pit, resilient crops, and membership of cooperative societies. However, a few of the farmers are currently adopting measures that permit farming with minimal to no soil erosion by growing root crops like yams in sacks.

The study has contributed to data for soil erosion assessment in the State. It is the first-time erosion model was validated with field data in the State. It highlighted the importance of time in soil erosion incidences. The spatiotemporal assessment is critical for effective soil erosion management for it will guide farmers and policy makers on where and when erosion is severest. Soil exhaustion on a plot can occur at a short time on less erodible soils. It unveiled the low farmers' adaptation strategies in Anambra.

Finally, there is the need for collaboration among private-public sectors and other stakeholders as a multidisciplinary and participatory approach would lead to effective solutions. Erosion mitigation should be integrated into high school curriculum and much awareness created among all citizens as greater attention to soil conservation is critical to achieving the United Nations' sustainable development goals (SDGs) and the African Union's Agenda 2063 of hunger eradication and increased agricultural productivity. This is vital for an unhealthy soil implies unhealthy people because most human basic needs come from agriculture that relies on fertile soils.

6.2 Recommendations

Recommendations for policy and stakeholders

Capacity building for farmers: NGOs, agricultural organisations and extension services should organise workshops, training sessions, and demonstrations to build farmers' capacity to implement erosion control techniques effectively.

Promote local knowledge: Encourage the integration of effective traditional and local knowledge about land management and erosion control into modern practices. Farmers have valuable insights that contribute to successful adaptation strategies like root-crop farming in sacks and cover cropping.

Invest in infrastructure: Public and private stakeholders should invest in infrastructure development such as terracing, check dams, vegetative barriers, and irrigation facilities. These can effectively reduce erosion on a larger scale. The irrigation will permit early planting and early harvest before the SON season when rain and erosion are intense.

Market access for sustainable products: create markets for sustainably produced goods, which can incentivise farmers to adopt erosion control practices. Certification systems can help customers identify and support environmentally compliant products. Such incentives can motivate the farmers to adopt effective erosion control measures.

Legislation: Aggressive reforestation including urban greening should be enforced by law. Urban developers should integrate surface greening since settlement and bare lands are the most susceptible to erosion.

Farmers should adopt minimal tillage agriculture and ensure the soil always covered and protected. However, on high slopes, a dynamic integrated approach that complements it with other measures like check-pit is recommended.

Recommendations for future research

Long-term impact assessment: Conduct long-term studies to assess the effectiveness of different erosion adaptation strategies over extended periods. This can provide insights into their sustainability under changing climate.

Climate change-erosion-economic-interaction: Investigate the interaction between climate change and soil erosion. Consider how changing rainfall patterns, temperature shifts, and extreme weather events might affect erosion rates. Also, take into account the economic loss to the State due to soil erosion. Research should look into quantifying SOC loss due to soil erosion in Anambra State.

Research should consider using more plots with existing and replanted vegetation comprising diverse species on the runoff plots. This will help establish the impact of diverse vegetation species, vegetation density, and age (perennial or annual plants) on soil erosion. The temporal scale of the study should also be extended to five years to highlight different scenarios in time both anticipated and unexpected.

Multi-scale studies: Undertake research at various scales (local to regional) to better understand the context-specific nature of soil erosion risks and adaptation needs. Innovative technologies: Explore the potential of innovative technologies like drones and artificial intelligence for monitoring, mitigating, and predicting erosion risks. These technologies can provide real-time data, monitoring and simulations.

REFERENCES

Abdelsamie, E.A., Abdellatif, M.A., Hassan, F.O., El Baroudy, A.A., Mohamed, E.S., Kucher, D.E., Shokr, M.S., 2022. Integration of RUSLE Model, Remote Sensing and GIS Techniques for Assessing Soil Erosion Hazards in Arid Zones. Agriculture 13, 35. https://doi.org/10.3390/agriculture13010035

Abdi, E., Babapour, S., Majnounian, B., Amiri, G.Z., Deljouei, A., 2018. How does organic matter affect the physical and mechanical properties of forest soil? Journal of forestry research 29, 657–662. https://doi.org/10.1007/s11676-017-0494-4

Abdulai, A.N., 2016. Impact of conservation agriculture technology on household welfare in Zambia. Agricultural economics 47, 729–741. https://doi.org/10.1111/agec.12269

Abdulai, A.-N., Abdulai, A., 2017. Examining the impact of conservation agriculture on environmental efficiency among maize farmers in Zambia. Environment and Development Economics 22, 177–201. https://doi.org/10.1017/S1355770X16000309

Abubakari, Farida, Abubakari, Fariya, 2015. Farmers' Perception on Soil Erosion Problems and Conservation Methods among Rural Farmers in Talensi-Nabdam Districts of Upper East Region of Ghana. Academic Research Journal of Agricultural Science and Research, Forthcoming.

Abubakari, Farida, Abubakari, Fariya, 2014. Analysis of Production and Marketing Constraints of Tomato among Rural Farmers in Talensi Nabdam District of Upper East Region of Ghana. IJASRT in EESs 4.

Adediji, A., Tukur, A.M., Adepoju, K.A., 2010. Assessment of revised universal soil loss equation (RUSLE) in Katsina area, Katsina state of Nigeria using remote sensing (RS) and geographic information system (GIS). Iranica Journal of Energy & Environment 1, 255–264.

Adhikary, P.P., Tiwari, S.P., Mandal, D., Lakaria, B.L., Madhu, M., 2014. Geospatial comparison of four models to predict soil erodibility in a semi-arid region of Central India. Environmental earth sciences 72, 5049–5062. https://doi.org/10.1007/s12665-014-3374-7

Adornado, H.A., Yoshida, M., Apolinares, H.A., 2009. Erosion vulnerability assessment in REINA, Quezon Province, Philippines with raster-based tool built within GIS environment. Agricultural Information Research 18, 24–31. https://doi.org/10.3173/air.18.24

Ajibade, F.O., Nwogwu, N.A., Adelodun, B., Abdulkadir, T.S., Ajibade, T.F., Lasisi, K.H., Fadugba, O.G., Owolabi, T.A., Olajire, O.O., 2020. Application of RUSLE integrated with GIS and remote sensing techniques to assess soil erosion in Anambra State, South-Eastern Nigeria. Journal of Water and Climate Change 11, 407–422. https://doi.org/10.2166/wcc.2020.222

Alewell, C., Borrelli, P., Meusburger, K., Panagos, P., 2019. Using the USLE: Chances, challenges and limitations of soil erosion modelling. International soil and water conservation research 7, 203–225. https://doi.org/10.1016/j.iswcr.2019.05.004

Alewell, C., Manderscheid, B., 1998. Use of objective criteria for the assessment of biogeochemical ecosystem models. Ecological modelling 107, 213–224. https://doi.org/10.1016/S0304-3800(97)00218-4

Alexakis, D.D., Manoudakis, S., Agapiou, A., Polykretis, C., 2021. Towards the Assessment of Soil-Erosion-Related C-Factor on European Scale Using Google Earth Engine and Sentinel-2 Images. Remote Sensing 13, 5019. https://doi.org/10.3390/rs13245019

Al-Madhhachi, A.-S.T., Hanson, G.J., Fox, G.A., Tyagi, A.K., Bulut, R., 2013. Measuring soil erodibility using a laboratory “mini” JET. Transactions of the ASABE 56, 901–910.

Almagro, A., Thomé, T.C., Colman, C.B., Pereira, R.B., Junior, J.M., Rodrigues, D.B.B., Oliveira, P.T.S., 2019. Improving cover and management factor (C-factor) estimation using remote sensing approaches for tropical regions. International Soil and Water Conservation Research 7, 325–334. https://doi.org/10.1016/j.iswcr.2019.08.005

Al-Shammary, A.A.G., Kouzani, A.Z., Kaynak, A., Khoo, S.Y., Norton, M., Gates, W., 2018. Soil bulk density estimation methods: A review. Pedosphere 28, 581–596. https://doi.org/10.1016/S1002-0160(18)60034-7

Andreoli, R., 2018. Modeling erosion risk using the RUSLE equation. QGIS and Applications in Water and Risks 4, 245–282. https://doi.org/10.1002/9781119476726.ch8

Angela, A., Ezeomedo, I.C., 2018. Changing Climate and the Effect of Gully Erosion on Akpo Community Farmers in Anambra State, Nigeria. J. Ecol. Nat. Resour 2, 000147.

Arabameri, A., Pourghasemi, H.R., 2019. Spatial modeling of gully erosion using linear and quadratic discriminant analyses in GIS and R, in: Spatial Modeling in GIS and R for Earth and Environmental Sciences. Elsevier, pp. 299–321.

Arabameri, A., Pradhan, B., Rezaei, K., Conoscenti, C., 2019a. Gully erosion susceptibility mapping using GIS-based multi-criteria decision analysis techniques. Catena 180, 282–297. https://doi.org/10.1016/j.catena.2019.04.032

Arabameri, A., Rezaei, K., Cerdà, A., Conoscenti, C., Kalantari, Z., 2019b. A comparison of statistical methods and multi-criteria decision making to map flood hazard susceptibility in Northern Iran. Science of the Total Environment 660, 443–458. https://doi.org/10.1016/j.scitotenv.2019.01.021

Arnold, J.G., Moriasi, D.N., Gassman, P.W., Abbaspour, K.C., White, M.J., Srinivasan, R., Santhi, C., Harmel, R.D., Van Griensven, A., Van Liew, M.W., 2012. SWAT: Model use, calibration, and validation. Transactions of the ASABE 55, 1491–1508. https://doi.org/10.13031/2013.42256

Arora, K.R., 2008. Soil mechanics and foundation engineering (geotechnical engineering). Standard Publishers Distributors, Nai Sarak, Delhi, 953p.

Arunrat, N., Sereenonchai, S., Kongsurakan, P., Hatano, R., 2022. Soil organic carbon and soil erodibility response to various land-use changes in northern Thailand. Catena 219, 106595. https://doi.org/10.1016/j.catena.2022.106595

ASTM, 2005. American Society for Tesing Materials Standard Test Methods for Liquid Limit, Plastic Limit, and Plasticity Index of Soils, ASTM D4318-05, West Coshohocken, PA.

ASTM, 1996. ASTM C136-96a Standard Test Method for Sieve Analysis of Fine and Coarse Aggregates, American Society for Testing and Materials, West Conshohocken, PA.

ASTM, 1987. American Society for Tesing of Materials Standard Test for Cone Penetration Testing:D3441-75T. Annual Book of ASTM Standards V.04.08., New York.

Atiah, W.A., Amekudzi, L.K., Aryee, J.N.A., Preko, K., Danuor, S.K., 2020. Validation of satellite and merged rainfall data over Ghana, West Africa. Atmosphere 11, 859. https://doi.org/10.3390/atmos11080859

Ayalew, D.A., Deumlich, D., Šarapatka, B., Doktor, D., 2020. Quantifying the sensitivity of NDVI-based C factor estimation and potential soil erosion prediction using Spaceborne earth observation data. Remote Sensing 12, 1136. https://doi.org/10.3390/rs12071136

Ayanlade, A., Jeje, O.D., Nwaezeigwe, J.O., Orimoogunje, O.O.I., Olokeogun, O.S., 2021. Rainfall seasonality effects on vegetation greenness in different ecological zones. Environmental Challenges 4, 100144. https://doi.org/10.1016/j.envc.2021.100144

Ayele, G.K., Gessess, A.A., Addisie, M.B., Tilahun, S.A., Tebebu, T.Y., Tenessa, D.B., Langendoen, E.J., Nicholson, C.F., Steenhuis, T.S., 2016. A biophysical and economic assessment of a community-based rehabilitated gully in the Ethiopian Highlands. Land Degradation & Development 27, 270–280. https://doi.org/10.1002/ldr.2425

Bagarello, V., Di Stefano, C., Ferro, V., Giordano, G., Iovino, M., Pampalone, V., 2012. Estimating the USLE soil erodibility factor in Sicily, South Italy. Applied Engineering in Agriculture 28, 199–206. https://doi.org/10.13031/2013.41347

Bagarello, V., Di Stefano, C., Ferro, V., Kinnell, P.I.A., Pampalone, V., Porto, P., Todisco, F., 2011. Predicting soil loss on moderate slopes using an empirical model for sediment concentration. Journal of hydrology 400, 267–273. https://doi.org/10.1016/j.jhydrol.2011.01.029

Bagherzadeh, A., 2014. Estimation of soil losses by USLE model using GIS at Mashhad plain, Northeast of Iran. Arabian Journal of Geosciences 7, 211–220. https://doi.org/10.1007/s12517-012-0730-3

Bahadur, A.V., Ibrahim, M., Tanner, T., 2010. The resilience renaissance? Unpacking of resilience for tackling climate change and disasters.

Bamutaze, Y., Mukwaya, P., Oyama, S., Nadhomi, D., Nsemire, P., 2021. Intersecting RUSLE modelled and farmers perceived soil erosion risk in the conservation domain on mountain Elgon in Uganda. Applied Geography 126, 102366. https://doi.org/10.1016/j.apgeog.2020.102366

Barman, B.K., Rao, K.S., Sonowal, K., Prasad, N.S.R., Sahoo, U.K., 2020. Soil erosion assessment using revised universal soil loss equation model and geo-spatial technology: A case study of upper Tuirial river basin, Mizoram, India. AIMS Geosciences 6, 525–545. https://doi.org/10.3934/geosci.2020030

Baroud, H., Ramirez□Marquez, J.E., Barker, K., Rocco, C.M., 2014. Stochastic measures of network resilience: Applications to waterway commodity flows. Risk Analysis 34, 1317–1335. https://doi.org/10.1111/risa.12175

Batista, P.V., Davies, J., Silva, M.L., Quinton, J.N., 2019. On the evaluation of soil erosion models: Are we doing enough? Earth-Science Reviews 197, 102898. https://doi.org/10.1016/j.earscirev.2019.102898

Beasley, D.B., Huggins, L.F., Monke, ampEJ, 1980. ANSWERS: A model for watershed planning. Transactions of the ASAE 23, 938–0944. https://doi.org/10.13031/2013.34692

Behera, D.K., Jamal, S., Ahmad, W.S., Taqi, M., Kumar, R., 2023. Estimation of Soil Erosion Using RUSLE Model and GIS Tools: A Study of Chilika Lake, Odisha. Journal of the Geological Society of India 99, 406–414. https://doi.org/10.1007/s12594-023-2324-y

Belay, H.T., Malede, D.A., Geleta, F.B., 2020. Erosion Risk Potential Assessment Using GIS and RS for Soil and Water Resource Conservation Plan: The Case of Yisir Watershed, Northwestern Ethiopia. Agric. Fish 9.

Belay, T.T., 2014. Perception of farmers on soil erosion and conservation practices in Dejen District, Ethiopia. International Journal of Environmental Protection and Policy 2, 224–229. https://doi.org/10.11648/j.ijepp.20140206.15

Bell, F.G., 2007. Engineering geology. Elsevier.

Bell, F.G., 2004. Engineering geology and construction. CRC Press.

Benavidez, R., Jackson, B., Maxwell, D., Norton, K., 2018. A review of the (Revised) Universal Soil Loss Equation ((R) USLE): with a view to increasing its global applicability and improving soil loss estimates. Hydrol. Earth Syst. Sci 22, 6059–6086. https://doi.org/10.5194/hess-22-6059-2018

Benkobi, L., Trlica, M.J., Smith, J.L., 1994. Evaluation of a refined surface cover subfactor for use in RUSLE. https://doi.org/10.2307/4002845

Bensekhria, A., Bouhata, R., 2022. Assessment and Mapping Soil Water Erosion Using RUSLE Approach and GIS Tools: Case of Oued el-Hai Watershed, Aurès West, Northeastern of Algeria. ISPRS International Journal of Geo-Information 11, 84. https://doi.org/10.3390/ijgi11020084

Beretta, A.N., Carrasco-Letelier, L., 2017. USLE/RUSLE K-factors allocated through a linear mixed model for Uruguayan soils. Ciencia e investigación agraria: revista latinoamericana de ciencias de la agricultura 44, 100–112.

Beven, K.J., 2001. Rainfall–Runoff Modeling: The Primer Wiley. Chichester, UK.

Bichet, A., Diedhiou, A., 2018. Less frequent and more intense rainfall along the coast of the gulf of Guinea in West and central Africa (1981 2014). Climate Research 76, 191–201. https://doi.org/10.3354/cr01537

Biddoccu, M., Opsi, F., Cavallo, E., 2014. Relationship between runoff and soil losses with rainfall characteristics and long-term soil management practices in a hilly vineyard (Piedmont, NW Italy). Soil science and plant nutrition 60, 92–99. https://doi.org/10.1080/00380768.2013.862488

Biondi, D., Freni, G., Iacobellis, V., Mascaro, G., Montanari, A., 2012. Validation of hydrological models: Conceptual basis, methodological approaches and a

proposal for a code of practice. Physics and Chemistry of the Earth, Parts a/b/c 42, 70–76. https://doi.org/10.1016/j.pce.2011.07.037
Bircher, P., Liniger, H.P., Kupferschmied, P., Prasuhn, V., 2021. Tools for USLE-CP-factor calculation and actual erosion risk on field block level for Switzerland. MethodsX 8, 101569. https://doi.org/10.1016/j.mex.2021.101569
Birkmann, J., 2007. Risk and vulnerability indicators at different scales: Applicability, usefulness and policy implications. Environmental hazards 7, 20–31. https://doi.org/10.1016/j.envhaz.2007.04.002
Biscontin, G., Pestana, J.M., Nadim, F., 2004. Seismic triggering of submarine slides in soft cohesive soil deposits. Marine Geology 203, 341–354. https://doi.org/10.1016/S0025-3227(03)00314-1
Boardman, J., Favis-Mortlock, D., 2016. 3.5. 3 The use of erosion pins in geomorphology.
Boix-Fayos, C., Martínez-Mena, M., Arnau-Rosalén, E., Calvo-Cases, A., Castillo, V., Albaladejo, J., 2006. Measuring soil erosion by field plots: Understanding the sources of variation. Earth-Science Reviews 78, 267–285. https://doi.org/10.1016/j.earscirev.2006.05.005
Boix-Fayos, C., Martínez-Mena, M., Calvo-Cases, A., Arnau-Rosalén, E., Albaladejo, J., Castillo, V., 2007. Causes and underlying processes of measurement variability in field erosion plots in Mediterranean conditions. Earth Surface Processes and Landforms: The Journal of the British Geomorphological Research Group 32, 85–101. https://doi.org/10.1002/esp.1382
Bormann, H., 2013. Tools for water quality management at the catchment scale: Geostatistics and erosion modelling, in: During Two Expert Seminars in Year 2012 the Chair of "Water Resources Management" of the University Siegen Has Focused on Both Sides of the Water Story, on the Water Abstraction and Sustainable Water Supply (Seminar on "Wassergewinnung", Hof, Germany) on the One Hand and on Water Pollution through Diverse Uses (Seminar on "Water Pollution by Agriculture", Santa Maria, Brazil) on the Other Hand. p. 57.
Borrelli, P., 2011. Risk assessment of human-induced accelerated soil erosion processes in the intermountain watersheds of Central Italy: A Case Study of the Upper Turano Watershed (Latium-Abruzzi). (PhD Thesis).
Borrelli, P., Meusburger, K., Ballabio, C., Panagos, P., Alewell, C., 2018. Object-oriented soil erosion modelling: A possible paradigm shift from potential to actual risk assessments in agricultural environments. Land degradation & development 29, 1270–1281. https://doi.org/10.1002/ldr.2898
Borrelli, P., Paustian, K., Panagos, P., Jones, A., Schütt, B., Lugato, E., 2016. Effect of good agricultural and environmental conditions on erosion and soil organic carbon balance: a national case study. Land use policy 50, 408–421. https://doi.org/10.1016/j.landusepol.2015.09.033
Borselli, L., Torri, D., Poesen, J., Iaquinta, P., 2012. A robust algorithm for estimating soil erodibility in different climates. Catena 97, 85–94. https://doi.org/10.1016/j.catena.2012.05.012

Bosco, C., de Rigo, D., 2013. Land cover and soil erodibility within the e-RUSLE model. Sci. Top. Focus, MRI-11b13, Maieutike Research Initiative, doi 10, m9.
Bosco, C., de Rigo, D., Dewitte, O., Poesen, J., Panagos, P., 2015. Modelling soil erosion at European scale: towards harmonization and reproducibility. Natural Hazards and Earth System Sciences 15, 225–245. https://doi.org/10.5194/nhess-15-225-2015
Bosco, C., Rusco, E., Montanarella, L., Panagos, P., 2009. Soil erosion in the Alpine area: risk assessment and climate change. Studi Trentini di scienze naturali 85, 117–123.
Bras, R.L., Tucker, G.E., Teles, V., 2003. Six myths about mathematical modeling in geomorphology. MASSACHUSETTS INST OF TECH CAMBRIDGE DEPT OF CIVIL AND ENVIRONMENTAL ENGINEERING.
Bryan, R.B., 2000. Soil erodibility and processes of water erosion on hillslope. Geomorphology 32, 385–415. https://doi.org/10.1016/S0169-555X(99)00105-1
Budnik, S.V., 2019. Change of Erosive Activity in the Context of Change of the Climate, in: Climate Change Impacts on Hydrological Processes and Sediment Dynamics: Measurement, Modelling and Management. Springer, pp. 16–28.
Bufalini, M., Materazzi, M., Martinello, C., Rotigliano, E., Pambianchi, G., Tromboni, M., Paniccià, M., 2022. Soil Erosion and Deposition Rate Inside an Artificial Reservoir in Central Italy: Bathymetry versus RUSLE and Morphometry. Land 11, 1924. https://doi.org/10.3390/land11111924
Carter, M.R., 2002. Soil quality for sustainable land management: organic matter and aggregation interactions that maintain soil functions. Agronomy journal 94, 38–47.
Casagrande, A., Fadum, R.E., 1940. Notes on soil testing for engineering purposes.
Cassol, E.A., Silva, T.S. da, Eltz, F.L.F., Levien, R., 2018. Soil erodibility under natural rainfall conditions as the K factor of the universal soil loss equation and application of the nomograph for a subtropical Ultisol. Revista Brasileira de Ciência do Solo 42. https://doi.org/10.1590/18069657rbcs20170262
Castillo, C., Gómez, J.A., 2016. A century of gully erosion research: Urgency, complexity and study approaches. Earth-Science Reviews 160, 300–319. https://doi.org/10.1016/j.earscirev.2016.07.009
Castillo, C., Pérez, R., James, M.R., Quinton, J.N., Taguas, E.V., Gómez, J.A., 2012. Comparing the accuracy of several field methods for measuring gully erosion. Soil Science Society of America Journal 76, 1319–1332. https://doi.org/10.2136/sssaj2011.0390
Cerato, A.B., 2001. Influence of specific surface area on geotechnical characteristics of fine-grained soils. Unpublished MSc Thesis, Department of Civil and Environmental Engineering, University of Massachusetts.
Cerdà, A., 2000. Aggregate stability against water forces under different climates on agriculture land and scrubland in southern Bolivia. Soil and Tillage Research 57, 159–166. https://doi.org/10.1016/S0167-1987(00)00155-0
Cerdan, O., Landemaine, V., Laignel, B., Evrard, O., Salavador-Blanes, S., Grangeon, T., Vandromme, R., Laceby, P., 2019. The scale dependency of erosion and

runoff for two agricultural catchments in the Western Paris Basin, France., in: Geophysical Research Abstracts.
Cerdan, O., Souchère, V., Lecomte, V., Couturier, A., Le Bissonnais, Y., 2002. Incorporating soil surface crusting processes in an expert-based runoff model: sealing and transfer by runoff and erosion related to agricultural management. Catena 46, 189–205. https://doi.org/10.1016/S0341-8162(01)00166-7
Chang, Y.-F., Lin, C.-J., Chyan, J.M., Chen, I.M., Chang, J.-E., 2007. Multiple regression models for the lower heating value of municipal solid waste in Taiwan. Journal of environmental management 85, 891–899. https://doi.org/10.1016/j.jenvman.2006.10.025
Chaudhari, P.R., Ahire, D.V., Ahire, V.D., Chkravarty, M., Maity, S., 2013. Soil bulk density as related to soil texture, organic matter content and available total nutrients of Coimbatore soil. International Journal of Scientific and Research Publications 3, 1–8.
Chen, B., Sun, D., Yun-shi, H., 2020. Experimental study on strength characteristics and microscopic mechanism of marine soft clays. Marine Georesources & Geotechnology 38, 570–582. https://doi.org/10.1080/1064119X.2019.1604917
Chen, H., Zhang, X., Abla, M., Lü, D., Yan, R., Ren, Q., Ren, Z., Yang, Y., Zhao, W., Lin, P., 2018. Effects of vegetation and rainfall types on surface runoff and soil erosion on steep slopes on the Loess Plateau, China. Catena 170, 141–149. https://doi.org/10.1016/j.catena.2018.06.006
Chen, J., Zhu, X., Vogelmann, J.E., Gao, F., Jin, S., 2011. A simple and effective method for filling gaps in Landsat ETM+ SLC-off images. Remote sensing of environment 115, 1053–1064. https://doi.org/10.1016/j.rse.2010.12.010
Chen, S., Zha, X., 2016. Evaluation of soil erosion vulnerability in the Zhuxi watershed, Fujian Province, China. Natural Hazards 82, 1589–1607. https://doi.org/10.1007/s11069-016-2258-4
Chinweze, C., 2019. Traditional Knowledge and Climate Change Challenges: Anambra State, Nigeria Case Study. The Perils of Climate Risk: The People and the Science 115.
Chinweze, C., 2017. Erosion and Climate Change Challenges: Anambra State, Nigeria Case Study.
Choi, J., Choi, Y.-H., Lim, K.-J., Shin, Y.-C., 2005. Soil erosion measurement and control techniques. Food and Fertilizer Technology Center.
Chorley, R.J., Kennedy, B.A., 1971. Physical geography: a systems approach. Prentice Hall.
Chorley, R.J., Schumm, S.A., Sugden, D.E., 1984. Geomorphology London: Methuen & Co. Ltd.
Choudhury, B.U., Nengzouzam, G., Islam, A., 2022. Runoff and soil erosion in the integrated farming systems based on micro-watersheds under projected climate change scenarios and adaptation strategies in the eastern Himalayan mountain ecosystem (India). Journal of Environmental Management 309, 114667. https://doi.org/10.1016/j.jenvman.2022.114667

Conforti, M., Aucelli, P.P., Robustelli, G., Scarciglia, F., 2011. Geomorphology and GIS analysis for mapping gully erosion susceptibility in the Turbolo stream catchment (Northern Calabria, Italy). Natural hazards 56, 881–898. https://doi.org/10.1007/s11069-010-9598-2

Conforti, M., Buttafuoco, G., Rago, V., Aucelli, P.P., Robustelli, G., Scarciglia, F., 2016. Soil loss assessment in the Turbolo catchment (Calabria, Italy). Journal of Maps 12, 815–825. https://doi.org/10.1080/17445647.2015.1077168

Corral-Pazos-de-Provens, E., Rapp-Arrarás, Í., Domingo-Santos, J.M., 2023. The USLE soil erodibility nomograph revisited. International Soil and Water Conservation Research 11, 1–13. https://doi.org/10.1016/j.iswcr.2022.07.001

Costantini, E.A.C., Agnelli, A.E., Fabiani, A., Gagnarli, E., Mocali, S., Priori, S., Simoni, S., Valboa, G., 2015. Short-term recovery of soil physical, chemical, micro-and mesobiological functions in a new vineyard under organic farming. Soil 1, 443–457. https://doi.org/10.5194/soil-1-443-2015

Coulomb, C.A., 1773. Essai sur une application des regles de maximis et minimis a quelques problemes de statique relatifs a l'architecture. Mem. Div. Sav. Acad.

Cutter, S.L., 1996. Vulnerability to environmental hazards. Progress in human geography 20, 529–539. https://doi.org/10.1177/030913259602000407

David, W.P., 1988. Soil and water conservation planning: policy issues and recommendations. Philippine Institute for Development Studies.

de Hipt, F.O., Diekkrüger, B., Steup, G., Yira, Y., Hoffmann, T., Rode, M., Näschen, K., 2019. Modeling the effect of land use and climate change on water resources and soil erosion in a tropical West African catch-ment (Dano, Burkina Faso) using SHETRAN. Science of the Total Environment 653, 431–445. https://doi.org/10.1016/j.scitotenv.2018.10.351

de León, J.C.V., 2006. Vulnerability assessment: The sectoral approach. Measuring Vulnerability to Natural Hazards: Towards Disaster Resilient Societies 300–315.

de León, J.C.V., Bogardi, J., Dannenmann, S., Basher, R., 2006. Early warning systems in the context of disaster risk management. Entwicklung and Ländlicher Raum 2, 23–25.

De Vente, J., Poesen, J., Verstraeten, G., Govers, G., Vanmaercke, M., Van Rompaey, A., Arabkhedri, M., Boix-Fayos, C., 2013. Predicting soil erosion and sediment yield at regional scales: where do we stand? Earth-Science Reviews 127, 16–29.

Deng, Y., Dong, X.I.A., CAI, C., DING, S., 2016. Effects of land uses on soil physic-chemical properties and erodibility in collapsing-gully alluvial fan of Anxi County, China. Journal of integrative agriculture 15, 1863–1873. https://doi.org/10.1016/S2095-3119(15)61223-0

Desmet, P.J.J., Govers, G., 1996. A GIS procedure for automatically calculating the USLE LS factor on topographically complex landscape units. Journal of soil and water conservation 51, 427–433.

DHI, 1999. SEAGIS:Soil erosion assessment using GIS version 1.0. Documentation and user guide. Horsholm, Denmark: Danish Hydraulic Institute.

Diaz-Sarachaga, J.M., Jato-Espino, D., 2020. Analysis of vulnerability assessment frameworks and methodologies in urban areas. Natural Hazards 1–21.
Dilley, M., Chen, R.S., Deichmann, U., Lerner-Lam, A.L., Arnold, M., 2005. Natural disaster hotspots: a global risk analysis. The World Bank.
Diodato, N., Knight, J., Bellocchi, G., 2013. Reduced complexity model for assessing patterns of rainfall erosivity in Africa. Global and Planetary Change 100, 183–193. https://doi.org/10.1016/j.gloplacha.2012.10.016
Diodato, N., Ljungqvist, F.C., Bellocchi, G., 2020. Historical predictability of rainfall erosivity: a reconstruction for monitoring extremes over Northern Italy (1500–2019). npj climate and atmospheric science 3, 46.
Diop, M., Chirinda, N., Beniaich, A., El Gharous, M., El Mejahed, K., 2022. Soil and Water Conservation in Africa: State of Play and Potential Role in Tackling Soil Degradation and Building Soil Health in Agricultural Lands. Sustainability 14, 13425. https://doi.org/10.3390/su142013425
Doetterl, S., Van Oost, K., Six, J., 2012. Towards constraining the magnitude of global agricultural sediment and soil organic carbon fluxes. Earth Surface Processes and Landforms 37, 642–655. https://doi.org/10.1002/esp.3198
Dosio, A., Panitz, H.-J., 2016. Climate change projections for CORDEX-Africa with COSMO-CLM regional climate model and differences with the driving global climate models. Climate Dynamics 46, 1599–1625. https://doi.org/10.1007/s00382-015-2664-4
Dosio, A., Turner, A.G., Tamoffo, A.T., Sylla, M.B., Lennard, C., Jones, R.G., Terray, L., Nikulin, G., Hewitson, B., 2020. A tale of two futures: contrasting scenarios of future precipitation for West Africa from an ensemble of regional climate models. Environmental Research Letters 15, 064007. https://doi.org/10.1088/1748-9326/ab7fde
Du, X., Jian, J., Du, C., Stewart, R.D., 2022. Conservation management decreases surface runoff and soil erosion. International soil and water conservation research 10, 188–196. https://doi.org/10.1016/j.iswcr.2021.08.001
Duley, F.L., Ackerman, F.G., 1934. Runoff and erosion from plots of different lengths. Journal of agricultural research 48, 505–510.
Dumas, P., Printemps, J., Mangeas, M., Luneau, G., 2010. Developing erosion models for integrated coastal zone management: A case study of The New Caledonia west coast. Marine Pollution Bulletin 61, 519–529. https://doi.org/10.1016/j.marpolbul.2010.06.013
Duncan, J.M., Wright, S.G., Brandon, T.L., 2014. Soil strength and slope stability. John Wiley & Sons.
Dunne, T., Leopold, L.B., 1978. Water in environmental planning. WH Freeman and Company. San Francisco, California.
Duraes, M.F., Sirtoli, A.E., dos Santos, J.S., 2020. Effects of DEM resolution on the RUSLE-LS factor and its implications on soil and water management policies through the land cover seasonality. African Journal of Agricultural Research 16, 1755–1765. https://doi.org/10.5897/AJAR2020.15002
Durigon, V.L., Carvalho, D.F., Antunes, M.A.H., Oliveira, P.T.S., Fernandes, M.M., 2014. NDVI time series for monitoring RUSLE cover management factor in a

tropical watershed. International Journal of Remote Sensing 35, 441–453. https://doi.org/10.1080/01431161.2013.871081
Ebabu, K., Tsunekawa, A., Haregeweyn, N., Tsubo, M., Adgo, E., Fenta, A.A., Meshesha, D.T., Berihun, M.L., Sultan, D., Vanmaercke, M., 2022. Global analysis of cover management and support practice factors that control soil erosion and conservation. International Soil and Water Conservation Research 10, 161–176. https://doi.org/10.1016/j.iswcr.2021.12.002
Ebrahimi, M., Nejadsoleymani, H., Sadeghi, A., Mansouri Daneshvar, M.R., 2021. Assessment of the soil loss-prone zones using the USLE model in northeastern Iran. Paddy and Water Environment 19, 71–86. https://doi.org/10.1007/s10333-020-00820-9
Efthimiou, N., 2020. The new assessment of soil erodibility in Greece. Soil and Tillage Research 204, 104720. https://doi.org/10.1016/j.still.2020.104720
Efthimiou, N., 2018. The importance of soil data availability on erosion modeling. Catena 165, 551–566. https://doi.org/10.1016/j.catena.2018.03.002
Egboka, B.C., Orji, A.E., Nwankwoala, H.O., 2019. Gully Erosion and Landslides in Southeastern Nigeria: Causes, Consequences and Control Measures.
Egboka, B.E., Okpoko, E.I., 1984. gully erosion in the Agulu-Nanka region of Anambra State, Nigeria. IAHS-AISH publication 335–347.
Egbueri, J.C., Igwe, O., 2020. The impact of hydrogeomorphological characteristics on gullying processes in erosion-prone geological units in parts of southeast Nigeria. Geology, Ecology, and Landscapes 1–14.
Egbueri, J.C., Igwe, O., Ifediegwu, S.I., 2022. Erosion risk mapping of Anambra State in southeastern Nigeria: soil loss estimation by RUSLE model and geoinformatics. Bulletin of Engineering Geology and the Environment 81, 91. https://doi.org/10.1007/s10064-022-02589-z
El Jazouli, A., Barakat, A., Khellouk, R., Rais, J., El Baghdadi, M., 2019. Remote sensing and GIS techniques for prediction of land use land cover change effects on soil erosion in the high basin of the Oum Er Rbia River (Morocco). Remote Sensing Applications: Society and Environment 13, 361–374. https://doi.org/10.1016/j.rsase.2018.12.004
Elhakim, A.F., 2016. Estimation of soil permeability. Alexandria Engineering Journal 55, 2631–2638. https://doi.org/10.1016/j.aej.2016.07.034
El-Swaify, S.A., 1990. Research needs and applications to reduce erosion and sedimentation in the tropics. International Association of Hydrological Sciences Publication 192, 3–13.
El-Swaify, S.A., Dangler, E.W., 1982. Rainfall Erosion in the Tropics: A State-of-the-Art. Soil erosion and conservation in the tropics 43, 1–25.
Eltaif, N.I., Gharaibeh, M.A., 2008. Impact of alum on crust prevention and aggregation of calcareous soil: laboratory studies. Soil use and management 24, 424–426. https://doi.org/10.1111/j.1475-2743.2008.00177.x
Emeribeole, A.C., Iheaturu, C.J., 2015. Mapping of potential soil erosion risk areas in Imo State using the Revised Universal Soil Loss Equation (RUSLE). Remote Sensing (RS) and Geospatial Information System (GIS) techniques.

International Journal for Research in Emerging Science and Technology 2, 36–44.
Emesiobi, F.C., 2000. Testing and quality control of materials in civil and highway engineering. The BluePrint Limited, Port Harcourt, Nigeria.
Engle, N.L., 2011. Adaptive capacity and its assessment. Global environmental change 21, 647–656. https://doi.org/10.1016/j.gloenvcha.2011.01.019
Eswaran, H., Lal, R., Reich, P.F., 2019. Land degradation: an overview. Response to land degradation 20–35. https://doi.org/10.1201/9780429187957-4
Evans, R., 2017. Factors controlling soil erosion and runoff and their impacts in the upper Wissey catchment, Norfolk, England: A ten year monitoring programme. Earth Surface Processes and Landforms 42, 2266–2279. https://doi.org/10.1002/esp.4182
Evans, R., Brazier, R., 2005. Evaluation of modelled spatially distributed predictions of soil erosion by water versus field-based assessments. Environmental Science & Policy 8, 493–501. https://doi.org/10.1016/j.envsci.2005.04.009
Evans, R., Collins, A.L., Zhang, Y., Foster, I.D., Boardman, J., Sint, H., Lee, M.R.F., Griffith, B.A., 2017. A comparison of conventional and 137Cs-based estimates of soil erosion rates on arable and grassland across lowland England and Wales. Earth-Science Reviews 173, 49–64. https://doi.org/10.1016/j.earscirev.2017.08.005
Evelpidou, N., Cordier, S., Merino, A., Figueiredo, T. de, Centeri, C., 2013. Runoff erosion.
Ezeh, C.U., Obeta, M.C., Anyadike, R.N., 2016. Variations in the sequences of daily rainfall across Nigeria. Arabian Journal of Geosciences 9, 681. https://doi.org/10.1007/s12517-016-2719-9
Ezeh, C.U., Preko, K., Igwe, O., Adjei, K., Schönbrodt-Stitt, S., Asare, M.Y., 2021. Assessment of gully erosion: A review. Parana J. Sci. Edu 7, 251–275. https://doi.org/9.http://tiny.cc/PJSE24476153v7i6p251-275
F Hassan, K., 2012. Effects of Calcium Carbonate on The Erodibility of Some Calcareouse Soils by Water Erosion. Mesopotamia Journal of Agriculture 40, 11–19. https://doi.org/10.33899/magrj.2012.60183
Fagbohun, B.J., Anifowose, A.Y., Odeyemi, C., Aladejana, O.O., Aladeboyeje, A.I., 2016. GIS-based estimation of soil erosion rates and identification of critical areas in Anambra sub-basin, Nigeria. Modeling Earth Systems and Environment 2, 1–10. https://doi.org/10.1007/s40808-016-0218-3
Fang, H., Sun, L., Tang, Z., 2015. Effects of rainfall and slope on runoff, soil erosion and rill development: an experimental study using two loess soils. Hydrological processes 29, 2649–2658. https://doi.org/10.1002/hyp.10392
Fang, N.F., Wang, L., Shi, Z.H., 2017. Runoff and soil erosion of field plots in a subtropical mountainous region of China. Journal of Hydrology 552, 387–395. https://doi.org/10.1016/j.jhydrol.2017.06.048
Farauta, B.K., Egbule, C.L., Agwu, A.E., Idrisa, Y.L., Onyekuru, N.A., 2012. Farmers' adaptation initiatives to the impact of climate change on agriculture in northern Nigeria. Journal of Agricultural Extension 16, 132–144.

Farhadi-Machekposhti, M., Valdes-Abellan, J., Pla, C., Benavente, D., Pachepsky, Y., 2020. Impact of marble powder amendment on hydraulic properties of a sandy soil. International Agrophysics 34. https://doi.org/10.31545/intagr/118245
Farooq, K., Khalid, U., Mujtaba, H., 2016. Prediction of compaction characteristics of fine-grained soils using consistency limits. Arabian Journal for Science and Engineering 41, 1319–1328. https://doi.org/10.1007/s13369-015-1918-0
Fasinmirin, J.T., Olorunfemi, I.E., Olakuleyin, F., 2018. Strength and hydraulics characteristics variations within a tropical Alfisol in Southwestern Nigeria under different land use management. Soil and Tillage Research 182, 45–56. https://doi.org/10.1016/j.still.2018.04.017
Faye, A., Akinsanola, A.A., 2022. Evaluation of extreme precipitation indices over West Africa in CMIP6 models. Climate Dynamics 58, 925–939. https://doi.org/10.1007/s00382-021-05942-2
Feddema, J.J., 1998. Estimated impacts of soil degradation on the African water balance and climate. Climate Research 10, 127–141. https://doi.org/10.3354/cr010127
Fenta, A.A., Tsunekawa, A., Haregeweyn, N., Tsubo, M., Yasuda, H., Kawai, T., Ebabu, K., Berihun, M.L., Belay, A.S., Sultan, D., 2021. Agroecology-based soil erosion assessment for better conservation planning in Ethiopian river basins. Environmental research 195, 110786. https://doi.org/10.1016/j.envres.2021.110786
Fenta, A.A., Yasuda, H., Shimizu, K., Haregeweyn, N., Kawai, T., Sultan, D., Ebabu, K., Belay, A.S., 2017. Spatial distribution and temporal trends of rainfall and erosivity in the Eastern Africa region. Hydrological Processes 31, 4555–4567. https://doi.org/10.1002/hyp.11378
Fenta, A.A., Yasuda, H., Shimizu, K., Haregeweyn, N., Negussie, A., 2016. Dynamics of soil erosion as influenced by watershed management practices: a case study of the Agula watershed in the semi-arid highlands of northern Ethiopia. Environmental management 58, 889–905. https://doi.org/10.1007/s00267-016-0757-4
Fenta, A.A., Yasuda, H., Shimizu, K., Ibaraki, Y., Haregeweyn, N., Kawai, T., Belay, A.S., Sultan, D., Ebabu, K., 2018. Evaluation of satellite rainfall estimates over the Lake Tana basin at the source region of the Blue Nile River. Atmospheric Research 212, 43–53. https://doi.org/10.1016/j.atmosres.2018.05.009
Fernández-Raga, M., Gutiérrez, E.G., Keesstra, S.D., Tárrega, R., Nunes, J.P., Marcos, E., Rodrigo-Comino, J., 2021. Determining the potential impacts of fire and different land uses on splash erosion in the margins of drylands. Journal of Arid Environments 186, 104419. https://doi.org/10.1016/j.jaridenv.2020.104419
Fernández-Raga, M., Palencia, C., Keesstra, S., Jordán, A., Fraile, R., Angulo-Martínez, M., Cerdà, A., 2017. Splash erosion: A review with unanswered questions. Earth-Science Reviews 171, 463–477. https://doi.org/10.1016/j.earscirev.2017.06.009
Fiener, P., Wilken, F., Auerswald, K., 2019. Filling the gap between plot and landscape scale–eight years of soil erosion monitoring in 14 adjacent watersheds under

soil conservation at Scheyern, Southern Germany. Advances in Geosciences 48, 31–48. https://doi.org/10.5194/adgeo-48-31-2019
Figueiredo, T. de, 2013. Measuring present runoff erosion. Runoff Erosion 72–118.
Fishman, G.S., Kiviat, P.J., 1968. The statistics of discrete-event simulation. Simulation 10, 185–195. https://doi.org/10.1177/003754976801000406
Foster, G.R., 1982. Relation of USLE factors to erosion on rangeland, in: Proc. Workshop on Estimating Erosion and Sediment Yield on Rangelands. USDA-ARS, ARM-W. pp. 17–35.
Foster, G.R., Lane, L.J., Nowlin, J.D., Laflen, J.M., Young, R.A., 1981. Estimating erosion and sediment yield on field-sized areas. Transactions of the ASAE 24, 1253–1262. https://doi.org/10.13031/2013.34429
Frąc, M., Lipiec, J., Usowicz, B., Oszust, K., Brzezińska, M., 2020. Structural and functional microbial diversity of sandy soil under cropland and grassland. PeerJ 8, e9501. https://doi.org/10.7717/peerj.9501
Francaviglia, R., Almagro, M., Vicente-Vicente, J.L., 2023. Conservation agriculture and soil organic carbon: principles, processes, practices and policy options. Soil Systems 7, 17. https://doi.org/10.3390/soilsystems7010017
Francis, C.F., Thornes, J.B., 1990. Runoff hydrographs from three Mediterranean vegetation cover types. Vegetation and erosion. Processes and environments. 363–384.
Funk, C., Peterson, P., Landsfeld, M., Pedreros, D., Verdin, J., Shukla, S., Husak, G., Rowland, J., Harrison, L., Hoell, A., 2015. The climate hazards infrared precipitation with stations—a new environmental record for monitoring extremes. Scientific data 2, 1–21. https://doi.org/10.1038/sdata.2015.66
Ganasri, B.P., Ramesh, H., 2016. Assessment of soil erosion by RUSLE model using remote sensing and GIS-A case study of Nethravathi Basin. Geoscience Frontiers 7, 953–961. https://doi.org/10.1016/j.gsf.2015.10.007
Gao, Y., Sun, D., Zhou, A., 2016. Hydromechanical behaviour of unsaturated soil with different specimen preparations. Canadian Geotechnical Journal 53, 909–917. https://doi.org/10.1139/cgj-2015-0381
Gashaw, T., Tulu, T., Argaw, M., 2018. Erosion risk assessment for prioritization of conservation measures in Geleda watershed, Blue Nile basin, Ethiopia. Environmental Systems Research 6, 1–14. https://doi.org/10.1186/s40068-016-0078-x
Ge, Y., Zhao, L., Chen, J., Li, X., Li, H., Wang, Z., Ren, Y., 2023. Study on Soil Erosion Driving Forces by Using (R) USLE Framework and Machine Learning: A Case Study in Southwest China. Land 12, 639. https://doi.org/10.3390/land12030639
Gebrechorkos, S.H., Hülsmann, S., Bernhofer, C., 2019. Long-term trends in rainfall and temperature using high-resolution climate datasets in East Africa. Scientific reports 9, 11376. https://doi.org/10.1038/s41598-019-47933-8
Gebrechorkos, S.H., Taye, M.T., Birhanu, B., Solomon, D., Demissie, T., 2023. Future changes in climate and hydroclimate extremes in East Africa. Earth's Future e2022EF003011. https://doi.org/10.1029/2022EF003011

Ghosal, K., Bhattacharya, S.D., 2020. A Review of RUSLE Model. Journal of the Indian Society of Remote Sensing 48, 689–707. https://doi.org/10.1007/s12524-019-01097-0

Ghosh, A., Rakshit, S., Tikle, S., Das, S., Chatterjee, U., Pande, C.B., Alataway, A., Al-Othman, A.A., Dewidar, A.Z., Mattar, M.A., 2023. Integration of GIS and Remote Sensing with RUSLE Model for Estimation of Soil Erosion. Land 12, 116. https://doi.org/10.3390/land12010116

Gobin, A.M., Campling, P., Deckers, J.A., Poesen, J., Feyen, J., 1999. Soil erosion assessment at the Udi-Nsukka Cuesta (southeastern Nigeria). Land degradation & development 10, 141–160. https://doi.org/10.1002/(SICI)1099-145X(199903/04)10:2<141::AID-LDR325>3.0.CO;2-N

Gongora, V.R.M., Secco, D., Bassegio, D., de Marins, A.C., Chang, P., Savioli, M.R., 2022. Impact of cover crops on soil physical properties, soil loss and runoff in compacted Oxisol of southern Brazil. Geoderma Regional 31, e00577. https://doi.org/10.1016/j.geodrs.2022.e00577

Grahmann, K., Dellepiane, V.R., Terra, J.A., Quincke, J.A., 2020. Long-term observations in contrasting crop-pasture rotations over half a century: statistical analysis of chemical soil properties and implications for soil sampling frequency. Agriculture, Ecosystems & Environment 287, 106710. https://doi.org/10.1016/j.agee.2019.106710

Grahmann, K., Rubio, V., Perez-Bidegain, M., Quincke, J.A., 2022. Soil use legacy as driving factor for soil erosion under conservation agriculture. Frontiers in Environmental Science 101. https://doi.org/10.3389/fenvs.2022.822967

Grove, A.T., 1951. Soil erosion and population problems in south-east Nigeria. The Geographical Journal 117, 291–304. https://doi.org/10.2307/1791853

Gupta, A., Paul, B., 2016. Augmenting the stability of OB dump by using fly ash: a geo technical approach to sustainably manage OB dump at Jharia Coalfield, India. Current World Environment 11, 204–211. https://doi.org/10.12944/CWE.11.1.25

Gupta, G.S., 2019. Land degradation and challenges of food security. Rev. Eur. Stud. 11, 63. https://doi.org/10.5539/res.v11n1p63

Gwapedza, D., Slaughter, A., Hughes, D., Mantel, S., 2018. Regionalising MUSLE factors for application to a data-scarce catchment. Proceedings of the International Association of Hydrological Sciences 377, 19–24. https://doi.org/10.5194/piahs-377-19-2018

Hagras, A., 2023. Estimating water erosion in the EL-Mador Valley Basin, South-West Matrouh City, Egypt, using revised universal soil loss equation (RUSLE) model through GIS. Environmental Earth Sciences 82, 47. https://doi.org/10.1007/s12665-022-10722-0

Halder, J.C., 2023. The integration of RUSLE-SDR lumped model with Remote Sensing and GIS for soil loss and sediment yield estimation. Advances in Space Research. https://doi.org/10.1016/j.asr.2023.01.008

Hamad, J., Younis, W., 2016. Origin of soil and grain size: soil particle size. Islamic university of Gaza,Civil Engineering Department.

Hamed, K.H., 2011. The distribution of Kendall's tau for testing the significance of cross-correlation in persistent data. Hydrological sciences journal 56, 841–853. https://doi.org/10.1080/02626667.2011.586948

Hamed, K.H., Rao, A.R., 1998. A modified Mann-Kendall trend test for autocorrelated data. Journal of hydrology 204, 182–196. https://doi.org/10.1016/S0022-1694(97)00125-X

Hameso, S., 2015. Perceptions, vulnerability and adaptation to climate change in Ethiopia: The case of smallholder farmers in Sidama (PhD Thesis). University of East London.

Hammad, A.A., Lundekvam, H., Børresen, T., 2004. Adaptation of RUSLE in the eastern part of the Mediterranean region. Environmental Management 34, 829–841. https://doi.org/10.1007/s00267-003-0296-7

Hamza, M.A., Anderson, W.K., 2005. Soil compaction in cropping systems: A review of the nature, causes and possible solutions. Soil and tillage research 82, 121–145. https://doi.org/10.1016/j.still.2004.08.009

Han, Y., Wang, Q., Xia, W., Liu, J., Wang, J., Chen, Y., Shen, J., 2020. Experimental study on the hydraulic conductivity of unsaturated dispersive soil with different salinities subjected to freeze-thaw. Journal of Hydrology 583, 124297. https://doi.org/10.1016/j.jhydrol.2019.124297

Hancock, G.R., Kunkel, V., Wells, T., Martinez, C., 2019. Soil organic carbon and soil erosion–understanding change at the large catchment scale. Geoderma 343, 60–71. https://doi.org/10.1016/j.geoderma.2019.02.012

Hancock, G.R., Lowry, J.B.C., Dever, C., Braggins, M., 2015. Does introduced fauna influence soil erosion? A field and modelling assessment. Science of the Total Environment 518, 189–200. https://doi.org/10.1016/j.scitotenv.2015.02.086

Haregeweyn, N., Tsunekawa, A., Poesen, J., Tsubo, M., Meshesha, D.T., Fenta, A.A., Nyssen, J., Adgo, E., 2017. Comprehensive assessment of soil erosion risk for better land use planning in river basins: Case study of the Upper Blue Nile River. Science of the Total Environment 574, 95–108. https://doi.org/10.1016/j.scitotenv.2016.09.019

Harmon, R.S., Doe III, W.W., Doe, W.W., 2001. Landscape erosion and evolution modeling. Springer Science & Business Media.

Hassan, A., Ijaz, S.S., Lal, R., Ali, S., Hussain, Q., Ansar, M., Khattak, R.H., Baloch, M.S., 2016. Depth distribution of soil organic carbon fractions in relation to tillage and cropping sequences in some dry lands of Punjab, Pakistan. Land Degradation & Development 27, 1175–1185. https://doi.org/10.1002/ldr.2345

Hayward, J.A., 1967. PLOTS FOR EVALUATING THE CATCHMENT CHARACTERISTICS AFFECTING SOIL LOSS: 2—Review of Plot Studies. Journal of Hydrology (New Zealand) 120–137.

Hessel, R., Van den Bosch, R., Vigiak, O., 2006. Evaluation of the LISEM soil erosion model in two catchments in the East African Highlands. Earth Surface Processes and Landforms: The Journal of the British Geomorphological Research Group 31, 469–486. https://doi.org/10.1002/esp.1280

Holtz, R.D., Krizek, R.J., 1970. Properties of slightly organic topsoils. Journal of the Construction Division 96, 29–43. https://doi.org/10.1061/JCCEAZ.0000266

Horn, R., Albrechts, C., 2002. Stress strain effects in structured unsaturated soils on coupled mechanical and hydraulic processes, in: 2002 ASAE Annual Meeting. American Society of Agricultural and Biological Engineers, p. 1.

Horton, R.E., 1933. The role of infiltration in the hydrologic cycle. Eos, Transactions American Geophysical Union 14, 446–460. https://doi.org/10.1029/TR014i001p00446

Hrabalikova, M., Janeček, M., 2017. Comparison of different approaches to LS factor calculations based on a measured soil loss under simulated rainfall. Soil and water research 12, 69–77. https://doi.org/10.17221/222/2015-SWR

Hsieh, Y.P., Grant, K.T., Bugna, G.C., 2009. A field method for soil erosion measurements in agricultural and natural lands. Journal of soil and water conservation 64, 374–382. https://doi.org/10.2489/jswc.64.6.374

Huang, F., Chen, J., Yao, C., Chang, Z., Jiang, Q., Li, S., Guo, Z., 2020. Susle: A slope and seasonal rainfall-based rusle model for regional quantitative prediction of soil erosion. Bulletin of Engineering Geology and the Environment 79, 5213–5228. https://doi.org/10.1007/s10064-020-01886-9

Hudson, N.W., 1995. Soil Conservation (3e). BT Batsford, London.

Hudson, N.W., 1993. Field Measurement of soil erosion and runoff. Prepared for the FAO. FAO, Bedford United Kingdom.

Hurni, H., 1985. Erosion-productivity-conservation systems in Ethiopia.

Huynh, C.V., Pham, T.G., Nguyen, T.Q., Nguyen, L.H.K., Tran, P.T., Le, Q.N.P., Nguyen, M.T.H., 2020. Understanding indigenous farming systems in response to climate change: an investigation into soil erosion in the mountainous regions of central vietnam. Applied Sciences 10, 5091. https://doi.org/10.3390/app10155091

Ifesinachi, K., Adibe, R., Wogu, C., 2015. The management of ecological fund and natural-resource conflicts in northern Nigeria, 2009-2013. European Scientific Journal, ESJ 11, 25.

Igbokwe, J.I., Akinyede, J.O., Dang, B., Alaga, T., Ono, M.N., Nnodu, V.C., Anike, L.O., 2008. Mapping and monitoring of the impact of gully erosion in Southeastern Nigeria with satellite remote sensing and Geographic Information System. The International Archives of the Photogrammetry, Remote Sensing and Spatial Information Sciences 37, 865–872.

Igwe, O., 2018. The mechanisms of enlargement and hydrogeological characteristics of Nanka Gully, Southeast Nigeria. Journal of the Geological Society of India 92, 227–234. https://doi.org/10.1007/s12594-018-0985-8

Igwe, O., Egbueri, J.C., 2018. The characteristics and the erodibility potentials of soils from different geologic formations in Anambra State, Southeastern Nigeria. Journal of the Geological Society of India 92, 471–478. https://doi.org/10.1007/s12594-018-1044-1

Iro, S., 2018. Determining causes of gully erosion and associated rates of change in south-east Nigeria, using a remote sensing and GIS methodology (PhD Thesis). University of Brighton.

Isikwue, M.O., Abutu, C., Onoja, S.B., 2012. Erodibility of Soils of the South West Benue State, Nigeria. Pacific Jour. Sci. Tech 3, 437–447.

Issaka, S., Ashraf, M.A., 2017. Impact of soil erosion and degradation on water quality: a review. Geology, Ecology, and Landscapes 1, 1–11. https://doi.org/10.1080/24749508.2017.1301053

Jia, L., Zhao, W., Zhai, R., Liu, Y., Kang, M., Zhang, X., 2019. Regional differences in the soil and water conservation efficiency of conservation tillage in China. Catena 175, 18–26. https://doi.org/10.1016/j.catena.2018.12.012

Johnson, A.I., 1963. Application of laboratory permeability data. US Geological Survey.

Jones, A., Panagos, P., Barcelo, S., Bouraoui, F., Bosco, C., Dewitte, O., Gardi, C., Erhard, M., Hervás, J., Hiederer, R., 2012. The state of soil in Europe. A Contribution of the JRC to the European Environment Agency's Environment State and Outlook Report.(European Commission: Luxembourg) Available at.

Jones, B.G., Gyawali, B.R., Zourarakis, D., Gebremedhin, M., Antonious, G., 2022. Soil Loss Analysis of an Eastern Kentucky Watershed Utilizing the Universal Soil Loss Equation. Environments 9, 126. https://doi.org/10.3390/environments9100126

Kalambukattu, J., Kumar, S., 2017. Modelling soil erosion risk in a mountainous watershed of Mid-Himalaya by integrating RUSLE model with GIS. Eurasian Journal of Soil Science 6, 92–105.

Karásek, P., Pochop, M., Konečná, J., Podhrázská, J., 2022. Comparison of the Methods for LS Factor Calculation when Evaluating the Erosion Risk in a Small Agricultural Area Using the USLE Tool. Journal of Ecological Engineering 23. https://doi.org/10.12911/22998993/143977

Karydas, C.G., Panagos, P., Gitas, I.Z., 2014. A classification of water erosion models according to their geospatial characteristics. International Journal of Digital Earth 7, 229–250. https://doi.org/10.1080/17538947.2012.671380

Kayet, N., Pathak, K., Chakrabarty, A., Sahoo, S., 2018. Evaluation of soil loss estimation using the RUSLE model and SCS-CN method in hillslope mining areas. International Soil and Water Conservation Research 6, 31–42. https://doi.org/10.1016/j.iswcr.2017.11.002

Kebede, Y.S., Endalamaw, N.T., Sinshaw, B.G., Atinkut, H.B., 2021. Modeling soil erosion using RUSLE and GIS at watershed level in the upper beles, Ethiopia. Environmental Challenges 2, 100009. https://doi.org/10.1016/j.envc.2020.100009

Keesstra, S., Pereira, P., Novara, A., Brevik, E.C., Azorin-Molina, C., Parras-Alcántara, L., Jordán, A., Cerdà, A., 2016. Effects of soil management techniques on soil water erosion in apricot orchards. Science of the Total Environment 551, 357–366. https://doi.org/10.1016/j.scitotenv.2016.01.182

Keller, J.B., 2017. Darcy's law for flow in porous media and the two-space method, in: Nonlinear Partial Differential Equations in Engineering and Applied Science. Routledge, pp. 429–443.

Kendall, M.G., 1975. Rank Correlation Methods; Griffin: London, UK, 1975. Google Scholar.

Khaledi Darvishan, A., Sadeghi, S.H., Homaee, M., Arabkhedri, M., 2014. Measuring sheet erosion using synthetic color-contrast aggregates. Hydrological Processes 28, 4463–4471. https://doi.org/10.1002/hyp.9956

Khan, F., Hayat, Z., Ahmad, W., Ramzan, M., Shah, Z., Sharif, M., Mian, I.A., Hanif, M., 2013. Effect of slope position on physico-chemical properties of eroded soil. Soil Environ 32, 22–28.

Kidane, M., Bezie, A., Kesete, N., Tolessa, T., 2019. The impact of land use and land cover (LULC) dynamics on soil erosion and sediment yield in Ethiopia. Heliyon 5, e02981. https://doi.org/10.1016/j.heliyon.2019.e02981

Kinnell, P.I.A., 2019. A review of the science and logic associated with approach used in the universal soil loss equation family of models. Soil systems 3, 62. https://doi.org/10.3390/soilsystems3040062

Kinnell, P.I.A., 2016. A review of the design and operation of runoff and soil loss plots. catena 145, 257–265. https://doi.org/10.1016/j.catena.2016.06.013

Kinnell, P.I.A., 2010. Event soil loss, runoff and the Universal Soil Loss Equation family of models: A review. Journal of hydrology 385, 384–397. https://doi.org/10.1016/j.jhydrol.2010.01.024

Kirkby, M., Jones, R.J., Irvine, B., Gobin, A.G.G., Cerdan, O., van Rompaey, J.J., Le Bissonais, Y., Daroussin, J., King, D., Montanarella, L., 2004. Pan-European Soil Erosion Risk Assessment for Europe: the PESERA map, version 1 October 2003. Explanation of Special Publication Ispra 2004 No. 73 (SPI 04.73). Office for Official Publications of the European Communities.

Kirkby, M.J., 1985. Hillslope hydrology. Hydrological Forecasting, John Wiley and Sons, New York, New York 1985. p 37-75, 21 fig, 1 tab, 42 ref.

Kodiwo, M.O., Oindo, B.O., Ang'awa, F.O., 2014. Intensity of farmland cultivated and soil bulk density in different physiographic units in Nyakach district.

Koirala, P., Thakuri, S., Joshi, S., Chauhan, R., 2019. Estimation of soil erosion in Nepal using a RUSLE modeling and geospatial tool. Geosciences 9, 147. https://doi.org/10.3390/geosciences9040147

Koppen, W., 1936. Das geographische system der klimat. Handbuch der klimatologie 46.

Kou, M., Jiao, J., Yin, Q., Wang, N., Wang, Z., Li, Y., Yu, W., Wei, Y., Yan, F., Cao, B., 2016. Successional trajectory over 10 years of vegetation restoration of abandoned slope croplands in the hill-gully region of the Loess Plateau. Land Degradation & Development 27, 919–932. https://doi.org/10.1002/ldr.2356

Kruk, E., 2021. Use of Chosen Methods for Determination of the USLE Soil Erodibility Factor on the Example of Loess Slope. Journal of Ecological Engineering 22. https://doi.org/10.12911/22998993/128861

KS, C., Chew, Y.M., Osman, M.H., SK, M.G., 2015. Estimating maximum dry density and optimum moisture content of compacted soils, in: International Conference on Advances in Civil and Environmental Engineering. pp. 1–8.

Kumar, M., Sahu, A.P., Sahoo, N., Dash, S.S., Raul, S.K., Panigrahi, B., 2022. Global-scale application of the RUSLE model: a comprehensive review. Hydrological Sciences Journal 67, 806–830. https://doi.org/10.1080/02626667.2021.2020277

Kumar, S.V., Vanajakshi, L., 2015. Short-term traffic flow prediction using seasonal ARIMA model with limited input data. European Transport Research Review 7, 1–9. https://doi.org/10.1007/s12544-015-0170-8
Lal, R., 2003. Soil erosion and the global carbon budget. Environment international 29, 437–450. https://doi.org/10.1016/S0160-4120(02)00192-7
Lal, R., 1990. Soil erosion and land degradation: the global risks. Advances in Soil Science: Soil Degradation Volume 11 129–172.
Lal, R., Kimble, J.M., 2001. Importance of soil bulk density and methods of its importance. Assessment methods for soil carbon 31–44.
Lanckriet, S., Frankl, A., Mesfin, G., Descheemaeker, K., Nyssen, J., 2015. Gully cut-and-fill cycles as related to agro-management: a historical curve number simulation in the Tigray Highlands. Earth Surface Processes and Landforms 40, 796–808. https://doi.org/10.1002/esp.3687
Lange, A., Siebert, R., Barkmann, T., 2015. Sustainability in land management: An analysis of stakeholder perceptions in rural northern Germany. Sustainability 7, 683–704. https://doi.org/10.3390/su7010683
Lassu, T., Rodrigo Comino, J., Seeger, M., Ries, J.B., 2015. Monitoring soil erosion processes: The erosion plots at the Geocampus, University of Trier, in: EGU General Assembly Conference Abstracts. p. 14338.
Lee, S., Chu, M.L., Guzman, J.A., Flanagan, D.C., 2022. Modeling soil erodibility and critical shear stress parameters for soil loss estimation. Soil and Tillage Research 218, 105292. https://doi.org/10.1016/j.still.2021.105292
Li, Z., Fang, H., 2016. Impacts of climate change on water erosion: A review. Earth-Science Reviews 163, 94–117. https://doi.org/10.1016/j.earscirev.2016.10.004
Lilja, D.J., 2016. Linear Regression Using R: An Introduction to Data Modeling. University of Minnesota Libraries Publishing.
Littleboy, M., Silburn, D.M., Freebairn, D.M., Woodruff, D.R., Hammer, G.L., Leslie, J.K., 1992. Impact of soil erosion on production in cropping systems. I. Development and validation of a simulation model. Soil Research 30, 757–774.
Liu, Hanbing, Lyu, X., Wang, J., He, X., Zhang, Y., 2020. The dependence between shear strength parameters and microstructure of subgrade soil in seasonal permafrost area. Sustainability 12, 1264. https://doi.org/10.3390/su12031264
Liu, Hua, Zhao, W., Liu, Y., 2020. Assessment on the Soil retention service of water Erosion in the Nile River Basin considering vegetation factor variance from 1982 to 2013. Water 12, 2018. https://doi.org/10.3390/w12072018
López-Vicente, M., Calvo-Seas, E., Álvarez, S., Cerdà, A., 2020. Effectiveness of cover crops to reduce loss of soil organic matter in a rainfed vineyard. Land 9, 230. https://doi.org/10.3390/land9070230
López-Vicente, M., Kramer, H., Keesstra, S., 2021. Effectiveness of soil erosion barriers to reduce sediment connectivity at small basin scale in a fire-affected forest. Journal of Environmental Management 278, 111510. https://doi.org/10.1016/j.jenvman.2020.111510
López-Vicente, M., Nadal-Romero, E., Cammeraat, E.L., 2017. Hydrological connectivity does change over 70 years of abandonment and afforestation in

the Spanish Pyrenees. Land degradation & development 28, 1298–1310. https://doi.org/10.1002/ldr.2531
Luvai, A., Obiero, J., Omuto, C., 2022. Soil Loss Assessment Using the Revised Universal Soil Loss Equation (RUSLE) Model. Applied and Environmental Soil Science 2022. https://doi.org/10.1155/2022/2122554
Ma, B., Yu, X., Ma, F., Li, Z., Wu, F., 2014. Effects of crop canopies on rain splash detachment. PLoS One 9, e99717. https://doi.org/10.1371/journal.pone.0099717
Macedo, P.M.S., Oliveira, P.T.S., Antunes, M.A.H., Durigon, V.L., Fidalgo, E.C.C., de Carvalho, D.F., 2021. New approach for obtaining the C-factor of RUSLE considering the seasonal effect of rainfalls on vegetation cover. International soil and water conservation research 9, 207–216. https://doi.org/10.1016/j.iswcr.2020.12.001
Mah, M.G.C., Douglas, L.A., Ringrose-Voase, A.J., 1992. Effects of crust development and surface slope on erosion by rainfall. Soil Science 154, 37–43. https://doi.org/10.1097/00010694-199207000-00005
Mahamud, M.A., Saad, N.A., Zainal Abidin, R., Yusof, M.F., Zakaria, N.A., Mohd Amiruddin Arumugam, M.A.R., Mat Desa, S., Md. Noh, M.N., 2021. Determination of Cover and Land Management Factors for Soil Loss Prediction in Cameron Highlands, Malaysia. Agriculture 12, 16. https://doi.org/10.3390/agriculture12010016
Maidment, R., Black, E., Young, M., 2017. TAMSAT Daily Rainfall Estimates (Version 3.0).
Maidment, R.I., Grimes, D., Black, E., Tarnavsky, E., Young, M., Greatrex, H., Allan, R.P., Stein, T., Nkonde, E., Senkunda, S., 2017. A new, long-term daily satellite-based rainfall dataset for operational monitoring in Africa. Scientific data 4, 1–19.
Mann, H.B., 1945. Nonparametric tests against trend. Econometrica: Journal of the Econometric Society 245–259. https://doi.org/10.2307/1907187
Martin, P.H., 1996. Physics of stamp-collecting? Thoughts on ecosystem model design. The Science of the Total Environment 183, 7–15. https://doi.org/10.1016/S0048-9697(95)90001-2
McCauley, A., Jones, C., Jacobsen, J., 2009. Soil pH and organic matter. Nutrient management module 8, 1–12.
McCool, D.K., Brown, L.C., Foster, G.R., Mutchler, C.K., Meyer, L.D., 1987. Revised slope steepness factor for the Universal Soil Loss Equation. Transactions of the ASAE 30, 1387–1396. https://doi.org/10.13031/2013.30576
McCool, D.K., Foster, G.R., Weesies, G.A., 1997. Slope length and steepness factors (LS). Predicting soil erosion by water: A guide to conservation planning with the revised universal soil loss equation (RUSLE) 101–141.
McFarlane, D., Delroy, N., Van Vreeswyk, S., 1991. Water erosion of potato land in Western Australia, 1. Factors affecting soil loss and the effect of soil loss on productivity. Australian Journal of Soil and Water Conservation (Australia).
McGlade, J., Bankoff, G., Abrahams, J., Cooper-Knock, S.J., Cotecchia, F., Desanker, P., Erian, W., Gencer, E., Gibson, L., Girgin, S., 2019. Global Assessment

Report on Disaster Risk Reduction 2019. UN Office for Disaster Risk Reduction.
Mello, C.R. de, Norton, L.D., Pinto, L.C., Beskow, S., Curi, N., 2016. Modelagem em bacias hidrográficas agrícolas: uma revisão para hidrologia e processos de erosão do solo. Ciência e Agrotecnologia 40, 7–25. https://doi.org/10.1590/S1413-70542016000100001
Mengie, M.A., Hagos, Y.G., Malede, D.A., Andualem, T.G., 2022. Assessment of soil loss rate using GIS–RUSLE interface in Tashat Watershed, Northwestern Ethiopia. Journal of Sedimentary Environments 7, 617–631. https://doi.org/10.1007/s43217-022-00112-8
Mentlik, P., Stacke, V., 2015. Role of fieldwork in Geomorphology. Presented at the Annual Conference of the Czech Association of Geomorphologists, Vydala: Západočeská univerzita v Plzni 2015, Plzen CZ.
Merchán, L., Martínez-Graña, A.M., Alonso Rojo, P., Criado, M., 2023. Water Erosion Risk Analysis in the Arribes del Duero Natural Park (Spain) Using RUSLE and GIS Techniques. Sustainability 15, 1627. https://doi.org/10.3390/su15021627
Merritt, W.S., Letcher, R.A., Jakeman, A.J., 2003. A review of erosion and sediment transport models. Environmental Modelling & Software 18, 761–799. https://doi.org/10.1016/S1364-8152(03)00078-1
Mhangara, P., Kakembo, V., Lim, K.J., 2012. Soil erosion risk assessment of the Keiskamma catchment, South Africa using GIS and remote sensing. Environmental Earth Sciences 65, 2087–2102. https://doi.org/10.1007/s12665-011-1190-x
Michalopoulou, M., Depountis, N., Nikolakopoulos, K., Boumpoulis, V., 2022. The Significance of Digital Elevation Models in the Calculation of LS Factor and Soil Erosion. Land 11, 1592. https://doi.org/10.3390/land11091592
Miller, S., 1994. Handbook for agrohydrology. Natural Resources Institute (NRI).
Miller, S.N., Semmens, D.J., Goodrich, D.C., Hernandez, M., Miller, R.C., Kepner, W.G., Guertin, D.P., 2007. The automated geospatial watershed assessment tool. Environmental Modelling & Software 22, 365–377. https://doi.org/10.1016/j.envsoft.2005.12.004
Millington, K., Cleland, J., 2017. Counting people and making people count: Key sources of population projections.
Minasny, B., McBratney, A.B., 2018. Limited effect of organic matter on soil available water capacity. European journal of soil science 69, 39–47. https://doi.org/10.1111/ejss.12475
Miró, J.J., Estrela, M.J., Corell, D., Gómez, I., Luna, M.Y., 2023. Precipitation and drought trends (1952–2021) in a key hydrological recharge area of the eastern Iberian Peninsula. Atmospheric Research 106695. https://doi.org/10.1016/j.atmosres.2023.106695
Mitas, L., Mitasova, H., 1998. Distributed soil erosion simulation for effective erosion prevention. Water resources research 34, 505–516. https://doi.org/10.1029/97WR03347
Mitasova, H., Brown, W.M., Johnston, D., Mitas, L., 1996. GIS tools for erosion/deposition modelling and multidimensional visualization. Part III:

Process based erosion simulation. Geographic Modelling and Systems Laboratory, University of Illinois.
Mitter, H., Kirchner, M., Schmid, E., Schönhart, M., 2014. The participation of agricultural stakeholders in assessing regional vulnerability of cropland to soil water erosion in Austria. Regional Environmental Change 14, 385–400. https://doi.org/10.1007/s10113-013-0506-7
Mohamadi, M.A., Kavian, A., 2015. Effects of rainfall patterns on runoff and soil erosion in field plots. International soil and water conservation research 3, 273–281. https://doi.org/10.1016/j.iswcr.2015.10.001
Mondal, A., Khare, D., Kundu, S., 2016. Change in rainfall erosivity in the past and future due to climate change in the central part of India. International soil and water conservation research 4, 186–194. https://doi.org/10.1016/j.iswcr.2016.08.004
Mondal, A., Khare, D., Kundu, S., Meena, P.K., Mishra, P.K., Shukla, R., 2015. Impact of climate change on future soil erosion in different slope, land use, and soil-type conditions in a part of the Narmada River Basin, India. Journal of Hydrologic Engineering 20, C5014003. https://doi.org/10.1061/(ASCE)HE.1943-5584.0001065
Moore, I.D., Burch, G.J., 1986a. Modelling erosion and deposition: topographic effects. Transactions of the ASAE 29, 1624–1630. https://doi.org/10.13031/2013.30363
Moore, I.D., Burch, G.J., 1986b. Physical basis of the length-slope factor in the universal soil loss equation. Soil Science Society of America Journal 50, 1294–1298. https://doi.org/10.2136/sssaj1986.03615995005000050042x
Moore, I.D., Nieber, J.L., 1989. Landscape assessment of soil erosion and nonpoint source pollution. Journal of the Minnesota Academy of Science 55, 18–25.
Morgan, R.P.C., 2009. Soil erosion and conservation. John Wiley & Sons.
Morgan, R.P.C., Morgan, D.D.V., Finney, H.J., 1984. A predictive model for the assessment of soil erosion risk. Journal of agricultural engineering research 30, 245–253. https://doi.org/10.1016/S0021-8634(84)80025-6
Morgan, R.P.C., Quinton, J.N., Smith, R.E., Govers, G., Poesen, J.W.A., Auerswald, K., Chisci, G., Torri, D., Styczen, M.E., 1998. The European Soil Erosion Model (EUROSEM): a dynamic approach for predicting sediment transport from fields and small catchments. Earth Surface Processes and Landforms: The Journal of the British Geomorphological Group 23, 527–544. https://doi.org/10.1002/(SICI)1096-9837(199806)23:6<527::AID-ESP868>3.0.CO;2-5
Mounirou, L.A., Yonaba, R., Tazen, F., Ayele, G.T., Yaseen, Z.M., Karambiri, H., Yacouba, H., 2022. Soil Erosion across Scales: Assessing Its Sources of Variation in Sahelian Landscapes under Semi-Arid Climate. Land 11, 2302. https://doi.org/10.3390/land11122302
Mugagga, F., Kakembo, V., Buyinza, M., 2012. A characterisation of the physical properties of soil and the implications for landslide occurrence on the slopes of Mount Elgon, Eastern Uganda. Natural hazards 60, 1113–1131. https://doi.org/10.1007/s11069-011-9896-3

Mullan, D., 2013. Managing soil erosion in Northern Ireland: a review of past and present approaches. Agriculture 3, 684–699. https://doi.org/10.3390/agriculture3040684
Murphy, C.A., Foster, B.L., Ramspott, M.E., Price, K.P., 2004. Grassland management effects on soil bulk density. Transactions of the Kansas Academy of Science 107, 45–54. https://doi.org/10.1660/0022-8443(2004)107[0045:GMEOSB]2.0.CO;2
Mutchler, C.K., Greer, J.D., 1980. Effect of slope length on erosion from low slopes. Transactions of the ASAE 23, 866–0869. https://doi.org/10.13031/2013.34678
Naipal, V., Reick, C., Pongratz, J., Van Oost, K., 2015. Improving the global applicability of the RUSLE model–adjustment of the topographical and rainfall erosivity factors. Geoscientific Model Development 8, 2893–2913. https://doi.org/10.5194/gmd-8-2893-2015
Nakil, M., Khire, M., 2016. Effect of slope steepness parameter computations on soil loss estimation: review of methods using GIS. Geocarto international 31, 1078–1093. https://doi.org/10.1080/10106049.2015.1120349
Nearing, M.A., 1998. Why soil erosion models over-predict small soil losses and under-predict large soil losses. Catena 32, 15–22. https://doi.org/10.1016/S0341-8162(97)00052-0
Nearing, M.A., Foster, G.R., Lane, L.J., Finkner, S.C., 1989. A process-based soil erosion model for USDA-Water Erosion Prediction Project technology. Transactions of the ASAE 32, 1587–1593. https://doi.org/10.13031/2013.31195
Nearing, M.A., Pruski, F.F., O'neal, M.R., 2004. Expected climate change impacts on soil erosion rates: a review. Journal of soil and water conservation 59, 43–50.
Nelson, K., Gillespie-Marthaler, L., Baroud, H., Abkowitz, M., Kosson, D., 2019. An integrated and dynamic framework for assessing sustainable resilience in complex adaptive systems. Sustainable and Resilient Infrastructure 1–19.
Nelson, K.S., 2018. Towards quantitative assessment of vulnerability, resilience, and the effects of adaptation on social-environmental systems (PhD Thesis). Vanderbilt University.
Nelson, P.H., 1994. Permeability-porosity relationships in sedimentary rocks. The log analyst 35.
NEWMAP, 2015. Nigeria Erosion and Watershed Management Project (NEWMAP) draft report on Environmental and Social Management Plan (ESMP) for the Amachalla Gully Erosion Site, Anambra State (E2924 V8), prepared for the State Project Management Unit (SPMU).
Nicholson, S.E., 2018. Climate of the Sahel and West Africa, in: Oxford Research Encyclopedia of Climate Science.
Nill, D., Schwertmann, U., Sabel-Koschella, U., Bernhard, M., Breuer, J., 1996. Soil erosion by water in Africa: Principle, predictions and protection. >eutsche Gescllschaft fiir Technische Zusammen:ir-lxit (GTZ) G 1lll3H 1'ostk~ch 5 180 D-05726 Esch1x)rn 291.
Nut, N., Mihara, M., Jeong, J., Ngo, B., Sigua, G., Prasad, P.V., Reyes, M.R., 2021. Land use and land cover changes and its impact on soil erosion in Stung

Sangkae catchment of Cambodia. Sustainability 13, 9276. https://doi.org/10.3390/su13169276
Nwobodo, C.E., Otunwa, S., Ohagwu, V.A., Okechukwu, E.D., 2018. Farmers use of erosion control measures in Anambra State Nigeria. Journal of Agricultural Extension 22, 174–184. https://doi.org/10.4314/jae.v22i3.17
Obia, A., Cornelissen, G., Martinsen, V., Smebye, A.B., Mulder, J., 2020. Conservation tillage and biochar improve soil water content and moderate soil temperature in a tropical Acrisol. Soil and Tillage Research 197, 104521. https://doi.org/10.1016/j.still.2019.104521
Obiadi, I.I., Nwosu, C.M., Ajaegwu, N.E., Anakwuba, E.K., Onuigbo, N.E., Akpunonu, E.O., Ezim, O.E., 2011. Gully erosion in Anambra State, south east Nigeria: Issues and solution. International Journal of Environmental Sciences 2, 795–804.
Ofomata, G.E.K., 2002. Relief, Drainage and Landforms, in: A Survey of Igbo Nation. Africana Publishers Ltd, pp. 83–98.
Ofomata, G.E.K., Egboka, M.O., 1986. Factors Controlling The Growth And Development of Gullies In South Eastern Nigeria', in: Proceedings of the National Workshop on Sec, Land Cleaning and Soil Testing Techniques. Unpublished Centre for Rural Development and Cooperatives, University in Nigeria, Nsukka, Nigeria. pp. 856–870.
Ogungbenro, S.B., Morakinyo, T.E., 2014. Rainfall distribution and change detection across climatic zones in Nigeria. Weather and Climate Extremes 5, 1–6. https://doi.org/10.1016/j.wace.2014.10.002
O'KEEFE, P., 1976. Taking the" Naturalness" out of" Natural Disaster". Nature (London) 260, 566–567. https://doi.org/10.1038/260566a0
Okoli, C.S., 2014. HYDRAULICS OF SLOPE EROSION BY OVERLAND FLOW (A Case Study of Nnobi-Onitsha Hillslope Site, Anambra State SE Nigeria.). scientiairanica 21, 251–262.
Okoloye, C.U., Aisiokuebo, N.I., Ukeje, J.E., Anuforom, A.C., Nnodu, I.D., 2013. Rainfall variability and the recent climate extremes in Nigeria. Journal of meteorology and climate science 11, 49–57.
Okoyeh, E.I., Akpan, A.E., Egboka, B.C.E., Okeke, H.I., 2014. An assessment of the influences of surface and subsurface water level dynamics in the development of gullies in Anambra State, southeastern Nigeria. Earth Interactions 18, 1–24. https://doi.org/10.1175/2012EI000488.1
Olaniya, M., Bora, P.K., Das, S., Chanu, P.H., 2020. Soil erodibility indices under different land uses in Ri-Bhoi district of Meghalaya (India). Scientific Reports 10, 1–13. https://doi.org/10.1038/s41598-020-72070-y
Olatunji, O.O., Akinlabi, S., Madushele, N., Adedeji, P.A., Felix, I., 2019. Multilayer perceptron artificial neural network for the prediction of heating value of municipal solid waste. AIMS Energy 7, 944–956. https://doi.org/10.3934/energy.2019.6.944
Oldeman, L.R., 1994. The global extent of soil degradation, p. 99-118. Soil resilience and sustainable land use. CAB International, Wallingford, Oxon, United Kingdom.

Olesen, J.E., Trnka, M., Kersebaum, K.C., Skjelvåg, A.O., Seguin, B., Peltonen-Sainio, P., Rossi, F., Kozyra, J., Micale, F., 2011. Impacts and adaptation of European crop production systems to climate change. European journal of agronomy 34, 96–112. https://doi.org/10.1016/j.eja.2010.11.003
Oliveira, J.D.A., Dominguez, J.M.L., Nearing, M.A., Oliveira, P.T., 2015. A GIS-based procedure for automatically calculating soil loss from the universalsoil loss equation: Gisus-m. Applied Engineering in Agriculture 31, 907.
O'loughlin, E.M., 1986. Prediction of surface saturation zones in natural catchments by topographic analysis. Water Resources Research 22, 794–804. https://doi.org/10.1029/WR022i005p00794
Olson, K.R., Al-Kaisi, M., Lal, R., Cihacek, L., 2016. Impact of soil erosion on soil organic carbon stocks. Journal of Soil and water Conservation 71, 61A-67A. https://doi.org/10.2489/jswc.71.3.61A
Onyeka, J.O., Obi, L.E., Uwanugo, R.G.U., 2019. Erosion Control in the Erosion-Ravaged Area of Nanka – Adazi- Nnukwu – Agulu Axis of Anambra State, Nigeria 5, 11.
Osadebe, C.C., Abam, T.K.S., Obiora, F.I., Sani, R.O., 2014. Evaluating the Stability of Gully Walls in Agulu-Nanka-Oko gully erosion complex area of Anambra State, Nigeria, using empirical approach. Advancement in scientific and Engineering Research, vol2 (1) 35–43.
Ostovari, Y., Ghorbani-Dashtaki, S., Bahrami, H.-A., Naderi, M., Dematte, J.A.M., 2017. Soil loss estimation using RUSLE model, GIS and remote sensing techniques: A case study from the Dembecha Watershed, Northwestern Ethiopia. Geoderma regional 11, 28–36. https://doi.org/10.1016/j.geodrs.2017.06.003
Ostovari, Y., Ghorbani-Dashtaki, S., Kumar, L., Shabani, F., 2019. Soil erodibility and its prediction in semi-arid regions. Archives of Agronomy and Soil Science 65, 1688–1703. https://doi.org/10.1080/03650340.2019.1575509
Ostovari, Y., Moosavi, A.A., Mozaffari, H., Poppiel, R.R., Tayebi, M., Demattê, J.A., 2022. Soil erodibility and its influential factors in the Middle East, in: Computers in Earth and Environmental Sciences. Elsevier, pp. 441–454.
Oza, K.P., Sharma, G.R., Dwivedi, D.K., 2022. Effect of Different Cropping Patterns on Runoff and Soil Loss for Junagadh Region. Managing Land Degradation for Enhancing Farm Productivity 113.
Pal, S.C., Shit, M., 2017. Application of RUSLE model for soil loss estimation of Jaipanda watershed, West Bengal. Spatial Information Research 25, 399–409. https://doi.org/10.1007/s41324-017-0107-5
Palliyaguru, C., Basnayake, V., Makumbura, R.K., Gunathilake, M.B., Muttil, N., Wimalasiri, E.M., Rathnayake, U., 2023. Evaluation of the Impact of Land Use Changes on Soil Erosion in the Tropical Maha Oya River Basin, Sri Lanka. Land 12, 107. https://doi.org/10.3390/land12010107
Panagos, P., Ballabio, C., Borrelli, P., Meusburger, K., Klik, A., Rousseva, S., Tadić, M.P., Michaelides, S., Hrabalíková, M., Olsen, P., 2015a. Rainfall erosivity in Europe. Science of the Total Environment 511, 801–814. https://doi.org/10.1016/j.scitotenv.2015.01.008

Panagos, P., Borrelli, P., Meusburger, K., 2015b. A new European slope length and steepness factor (LS-Factor) for modeling soil erosion by water. Geosciences 5, 117–126. https://doi.org/10.3390/geosciences5020117

Panagos, P., Borrelli, P., Poesen, J., Ballabio, C., Lugato, E., Meusburger, K., Montanarella, L., Alewell, C., 2015c. The new assessment of soil loss by water erosion in Europe. Environmental science & policy 54, 438–447. https://doi.org/10.1016/j.envsci.2015.08.012

Panagos, P., Meusburger, K., Ballabio, C., Borrelli, P., Alewell, C., 2014. Soil erodibility in Europe: A high-resolution dataset based on LUCAS. Science of the total environment 479, 189–200. https://doi.org/10.1016/j.scitotenv.2014.02.010

Parras-Alcántara, L., Lozano-García, B., Keesstra, S., Cerdà, A., Brevik, E.C., 2016. Long-term effects of soil management on ecosystem services and soil loss estimation in olive grove top soils. Science of the Total Environment 571, 498–506. https://doi.org/10.1016/j.scitotenv.2016.07.016

Patakamuri, S.K., O'Brien, N., Patakamuri, M.S.K., 2021. Package 'modifiedmk.'

Peng, L., Tang, C., Zhang, X., Duan, J., Yang, L., Liu, S., 2022. Quantifying the Effects of Root and Soil Properties on Soil Detachment Capacity in Agricultural Land Use of Southern China. Forests 13, 1788. https://doi.org/10.3390/f13111788

Petito, M., Cantalamessa, S., Pagnani, G., Degiorgio, F., Parisse, B., Pisante, M., 2022. Impact of Conservation Agriculture on Soil Erosion in the Annual Cropland of the Apulia Region (Southern Italy) Based on the RUSLE-GIS-GEE Framework. Agronomy 12, 281. https://doi.org/10.3390/agronomy12020281

Phinzi, K., Ngetar, N.S., 2019. The assessment of water-borne erosion at catchment level using GIS-based RUSLE and remote sensing: A review. International Soil and Water Conservation Research 7, 27–46. https://doi.org/10.1016/j.iswcr.2018.12.002

Pimentel, D., Burgess, M., 2013. Soil erosion threatens food production. Agriculture 3, 443–463. https://doi.org/10.3390/agriculture3030443

Pitt, R., 2004. Module 4: Erosion Mechanisms and the Revised Universal Soil Loss Equation (RUSLE). Retrieved 1, 35.

Pohlert, T., 2020. Non-parametric trend tests and change-point detection. CC BY-ND 4.

Polakowski, C., Ryżak, M., Sochan, A., Beczek, M., Mazur, R., Bieganowski, A., 2021. Particle size distribution of various soil materials measured by laser diffraction—the problem of reproducibility. Minerals 11, 465. https://doi.org/10.3390/min11050465

Polidori, E., 2007. Relationship between the Atterberg limits and clay content. Soils and foundations 47, 887–896. https://doi.org/10.3208/sandf.47.887

Prasuhn, V., 2022. Experience with the assessment of the USLE cover-management factor for arable land compared with long-term measured soil loss in the Swiss Plateau. Soil and Tillage Research 215, 105199. https://doi.org/10.1016/j.still.2021.105199

Prasuhn, V., Liniger, H., Gisler, S., Herweg, K., Candinas, A., Clément, J.-P., 2013. A high-resolution soil erosion risk map of Switzerland as strategic policy support

system. Land use policy 32, 281–291. https://doi.org/10.1016/j.landusepol.2012.11.006
Prosdocimi, M., Tarolli, P., Cerdà, A., 2016. Mulching practices for reducing soil water erosion: A review. Earth-Science Reviews 161, 191–203. https://doi.org/10.1016/j.earscirev.2016.08.006
Qin, W., Guo, Q., Zuo, C., Shan, Z., Ma, L., Sun, G., 2016. Spatial distribution and temporal trends of rainfall erosivity in mainland China for 1951–2010. Catena 147, 177–186. https://doi.org/10.1016/j.catena.2016.07.006
Rahmati, O., Haghizadeh, A., Pourghasemi, H.R., Noormohamadi, F., 2016. Gully erosion susceptibility mapping: the role of GIS-based bivariate statistical models and their comparison. Natural Hazards 82, 1231–1258. https://doi.org/10.1007/s11069-016-2239-7
Rao, S.M., 1996. Role of apparent cohesion in the stability of Dominician allophane soil slopes. Engineering Geology 43, 265–279. https://doi.org/10.1016/S0013-7952(96)00036-1
Reeher, L.J., Hughes, A.N., Davis, G.H., Kemeny, J.M., Ferrill, D.A., 2023. Finding the right place in Mohr circle space: Geologic evidence and implications for applying a non-linear failure criterion to fractured rock. Journal of Structural Geology 166, 104773. https://doi.org/10.1016/j.jsg.2022.104773
Regazzoni, P.-L., Hanson, G., Wahl, T., Marot, D., Courivaud, J.-R., Fry, J.-J., 2008. The influence of some engineering parameters on the erosion of soils, in: Proceedings 4th International Conference on Scour and Erosion (ICSE-4). November 5-7, 2008, Tokyo, Japan. pp. 442–446.
Renard, K.G., Foster, G.R., Weesies, G.A., McCool, D.K., Yoder, D.C., 1997. Predicting soil erosion by water: A guide to conservation planning with the Revised Universal Soil Loss Equation (RUSLE). Agriculture handbook 703, 407.
R-Instant, 2022. R-Instant software. Available at https://r-instat.org/.
Risse, L.M., Nearing, M.A., Laflen, J.M., Nicks, A.D., 1993. Error assessment in the universal soil loss equation. Soil Science society of America journal 57, 825–833. https://doi.org/10.2136/sssaj1993.03615995005700030032x
Roels, J.M., 1985. Estimation of soil loss at a regional scale based on plot measurements—some critical considerations. Earth Surface Processes and Landforms 10, 587–595. https://doi.org/10.1002/esp.3290100606
Römkens, M.J.M., Young, R.A., Poesen, J.W.A., McCool, D.K., El-Swaify, S.A., Bradford, J.M., 1997. Soil erodibility factor (K). Compilers) In: Renard KG, Foster GR, Weesies GA, McCool DK, Yoder DC, editors. Predicting soil erosion by water: a guide to conservation planning with the Revised Universal Soil Loss Equation (RUSLE). Washington, DC, USA: Agric. HB 65–99.
Romshoo, S.A., Bhat, S.A., Rashid, I., 2012. Geoinformatics for assessing the morphometric control on hydrological response at watershed scale in the Upper Indus Basin. Journal of Earth System Science 121, 659–686. https://doi.org/10.1007/s12040-012-0192-8

Roose, E., 1971. Influence des modifications du milieu naturel sur l'érosion, le bilan hydrique et chimique suite à la mise en culture sous climat tropical: synthèse des observations en Côte d'Ivoire et Haute Volta.
Roose, E.J., 1977. Use of the universal soil loss equation to predict erosion in West Africa, in: Soil Erosion: Prediction and Control. Soil Conservation Society of America Ankeny, Iowa, pp. 60–74.
Roose, E.J., 1975. Natural mulch or chemical conditioner for reducing soil erosion in humid tropical areas. Soil Conditioners 7, 131–138.
Rozos, D., Skilodimou, H.D., Loupasakis, C., Bathrellos, G.D., 2013. Application of the revised universal soil loss equation model on landslide prevention. An example from N. Euboea (Evia) Island, Greece. Environmental Earth Sciences 70, 3255–3266. https://doi.org/10.1007/s12665-013-2390-3
Rubio, V., Diaz-Rossello, R., Quincke, J.A., van Es, H.M., 2021. Quantifying soil organic carbon's critical role in cereal productivity losses under annualized crop rotations. Agriculture, Ecosystems & Environment 321, 107607. https://doi.org/10.1016/j.agee.2021.107607
Ruehlmann, J., Körschens, M., 2009. Calculating the effect of soil organic matter concentration on soil bulk density. Soil Science Society of America Journal 73, 876–885. https://doi.org/10.2136/sssaj2007.0149
Sachs, E., Sarah, P., 2017. Effect of raindrop temperatures on soil runoff and erosion in dry and wet soils. A laboratory experiment. Land Degradation & Development 28, 1549–1556. https://doi.org/10.1002/ldr.2682
Sadeghi, S.H.R., Hazbavi, Z., 2015. Trend analysis of the rainfall erosivity index at different time scales in Iran. Natural Hazards 77, 383–404. https://doi.org/10.1007/s11069-015-1607-z
Sadeghi, S.H.R., Moghadam, E.S., Darvishan, A.K., 2016. Effects of subsequent rainfall events on runoff and soil erosion components from small plots treated by vinasse. Catena 138, 1–12. https://doi.org/10.1016/j.catena.2015.11.007
Saffih-Hdadi, K., Défossez, P., Richard, G., Cui, Y.-J., Tang, A.-M., Chaplain, V., 2009. A method for predicting soil susceptibility to the compaction of surface layers as a function of water content and bulk density. Soil and Tillage Research 105, 96–103. https://doi.org/10.1016/j.still.2009.05.012
Saha, S., Sarkar, D., Mondal, P., 2022. Assessing and mapping soil erosion risk zone in Ratlam District, central India. Regional Sustainability 3, 373–390. https://doi.org/10.1016/j.regsus.2022.11.005
Sakin, E., 2012. Organic carbon organic matter and bulk density relationships in arid-semi arid soils in Southeast Anatolia region. African journal of biotechnology 11, 1373–1377.
Samanta, S., Koloa, C., Pal, D.K., Palsamanta, B., 2016. Estimation of potential soil erosion rate using RUSLE and E 30 model. Modeling Earth Systems and Environment 2, 149. https://doi.org/10.1007/s40808-016-0206-7
Sanogo, S., Fink, A.H., Omotosho, J.A., Ba, A., Redl, R., Ermert, V., 2015. Spatio-temporal characteristics of the recent rainfall recovery in West Africa. International Journal of Climatology 35, 4589–4605. https://doi.org/10.1002/joc.4309

Schmidt, J., Werner, M.V., Michael, A., 1999. Application of the EROSION 3D model to the CATSOP watershed, The Netherlands. Catena 37, 449–456. https://doi.org/10.1016/S0341-8162(99)00032-6

Selmy, S.A., Abd Al-Aziz, S.H., Jiménez-Ballesta, R., García-Navarro, F.J., Fadl, M.E., 2021. Modeling and assessing potential soil erosion hazards using usle and wind erosion models in integration with gis techniques: Dakhla oasis, egypt. Agriculture 11, 1124. https://doi.org/10.3390/agriculture11111124

Sen, P.K., 1968. Estimates of the regression coefficient based on Kendall's tau. Journal of the American statistical association 63, 1379–1389.

Shamshad, A., Azhari, M.N., Isa, M. al, Hussin, W.W., Parida, B.P., 2008. Development of an appropriate procedure for estimation of RUSLE EI30 index and preparation of erosivity maps for Pulau Penang in Peninsular Malaysia. Catena 72, 423–432. https://doi.org/10.1016/j.catena.2007.08.002

Sharma, S.B., 2022. Trend setting impacts of organic matter on soil physico-chemical properties in traditional vis-a-vis chemical-based amendment practices. PLOS Sustainability and Transformation 1, e0000007. https://doi.org/10.1371/journal.pstr.0000007

Sherka, T.D., 2023. Factors affecting women's participation in soil & water conservation in abeshege district Southern Ethiopia. Cogent Economics & Finance 11, 2192455. https://doi.org/10.1080/23322039.2023.2192455

Shi, P., Li, P., Li, Z., Sun, J., Wang, D., Min, Z., 2022. Effects of grass vegetation coverage and position on runoff and sediment yields on the slope of Loess Plateau, China. Agricultural Water Management 259, 107231. https://doi.org/10.1016/j.agwat.2021.107231

Shruthi, R.B., Kerle, N., Jetten, V., Abdellah, L., Machmach, I., 2015. Quantifying temporal changes in gully erosion areas with object oriented analysis. Catena 128, 262–277. https://doi.org/10.1016/j.catena.2014.01.010

Simpson, F., 2010. Prevention and control of gullying processes in diverse climatic settings: lessons for the age of global climate change, in: 2nd Joint Federal Interagency Conference, Las Vegas, NV.

Sinshaw, B.G., Belete, A.M., Mekonen, B.M., Wubetu, T.G., Anley, T.L., Alamneh, W.D., Atinkut, H.B., Gelaye, A.A., Bilkew, T., Tefera, A.K., 2021. Watershed-based soil erosion and sediment yield modeling in the Rib watershed of the Upper Blue Nile Basin, Ethiopia. Energy Nexus 3, 100023. https://doi.org/10.1016/j.nexus.2021.100023

Smit, B., Wandel, J., 2006. Adaptation, adaptive capacity and vulnerability. Global environmental change 16, 282–292. https://doi.org/10.1016/j.gloenvcha.2006.03.008

Smith, D.D., Wischmeier, W.H., 1957. Factors affecting sheet and rill erosion. Eos, Transactions American Geophysical Union 38, 889–896.

Smith, R.E., 1981. A kinematic model for surface mine sediment yield. Transactions of the ASAE 24, 1508–1514. https://doi.org/10.13031/2013.34482

Sowers, G.B., Sowers, G.F., 1970. Introductory soil mechanics and foundations, revised. ed. LWW.

Stern, R., Parsons, D., Stern, D., Torgbor, F., 2020. R-Instant Climatic Guide.

Stock, J.D., Montgomery, D.R., 1999. Geologic constraints on bedrock river incision using the stream power law. Journal of Geophysical Research: Solid Earth 104, 4983–4993. https://doi.org/10.1029/98JB02139

Stone, R.P., Hilborn, D., 2011. Universal Soil Loss Equation (USLE) Factsheet Order No. 12-051. Ministry of Agriculture, Food and Rural Affairs, Ontario, Canada, ISSN 1198–712.

Stroosnijder, L., 2005. Measurement of erosion: is it possible? Catena 64, 162–173. https://doi.org/10.1016/j.catena.2005.08.004

Supandi, S., Saputra, Y.H.E., Nugroho, Y., Suyanto, S., Rudy, G.S., Wirabuana, P.Y.A.P., 2023. The influence of land cover variation on soil erosion vulnerability around coal mining concession areas in South Borneo. Journal of Degraded and Mining Lands Management 10, 4289–4295. https://doi.org/10.15243/jdmlm.2023.102.4289

Sverdrup, H., Warfvinge, P., Blake, L., Goulding, K., 1995. Modelling recent and historic soil data from the Rothamsted Experimental Station, UK using SAFE. Agriculture, Ecosystems & Environment 53, 161–177. https://doi.org/10.1016/0167-8809(94)00558-V

Swanson, D.A., 2015. On the relationship among values of the same summary measure of error when used across multiple characteristics at the same point in time: an examination of MALPE and MAPE. Review of Economics and Finance 5.

Symeonakis, E., 2001. Soil erosion modelling over sub Saharan Africa using remote sensing and geographical information systems. University of London.

Tadesse, L., Suryabhagavan, K.V., Sridhar, G., Legesse, G., 2017. Land use and land cover changes and Soil erosion in Yezat Watershed, North Western Ethiopia. International soil and water conservation research 5, 85–94. https://doi.org/10.1016/j.iswcr.2017.05.004

Talchabhadel, R., Prajapati, R., Aryal, A., Maharjan, M., 2020. Assessment of rainfall erosivity (R-factor) during 1986–2015 across Nepal: a step towards soil loss estimation. Environmental monitoring and assessment 192, 1–17. https://doi.org/10.1007/s10661-020-8239-9

Tamta, S., Kumar, A., Kushwaha, D.P., 2023. Potential of roots and shoots of Napier grass for arresting soil erosion and runoff of mollisols soils of Himalayas. International Soil and Water Conservation Research. https://doi.org/10.1016/j.iswcr.2023.02.001

Tan, Ö., 2006. Investigation of soil parameters affecting the stability of homogeneous slopes using the Taguchi method. Eurasian Soil Science 39, 1248–1254. https://doi.org/10.1134/S1064229306110135

Tanveera, A., Kanth, T.A., Tali, P.A., Naikoo, M., 2016. Relation of soil bulk density with texture, total organic matter content and porosity in the soils of Kandi Area of Kashmir valley, India. Int. Res. J. Earth Sci 4, 1–6.

Tanyaş, H., Kolat, Ç., Süzen, M.L., 2015. A new approach to estimate cover-management factor of RUSLE and validation of RUSLE model in the watershed of Kartalkaya Dam. Journal of Hydrology 528, 584–598. https://doi.org/10.1016/j.jhydrol.2015.06.048

Taye, G., Vanmaercke, M., Poesen, J., Van Wesemael, B., Tesfaye, S., Teka, D., Nyssen, J., Deckers, J., Haregeweyn, N., 2018. Determining RUSLE P-and C-factors for stone bunds and trenches in rangeland and cropland, North Ethiopia. Land Degradation & Development 29, 812–824. https://doi.org/10.1002/ldr.2814

Terzaghi, K., Peck, R.B., Mesri, G., 1996. Soil mechanics in engineering practice. John wiley & sons.

Tetzlaff, B., Wendland, F., 2012. Modelling sediment input to surface waters for German states with MEPhos: methodology, sensitivity and uncertainty. Water resources management 26, 165–184. https://doi.org/10.1007/s11269-011-9911-1

Thapa, P., 2020. Spatial estimation of soil erosion using RUSLE modeling: a case study of Dolakha district, Nepal. Environmental Systems Research 9, 1–10. https://doi.org/10.1186/s40068-020-00177-2

Thomas, K., Hardy, R.D., Lazrus, H., Mendez, M., Orlove, B., Rivera□Collazo, I., Roberts, J.T., Rockman, M., Warner, B.P., Winthrop, R., 2019. Explaining differential vulnerability to climate change: A social science review. Wiley Interdisciplinary Reviews: Climate Change 10, e565. https://doi.org/10.1002/wcc.565

Tiruwa, D.B., Khanal, B.R., Lamichhane, S., Acharya, B.S., 2021. Soil erosion estimation using Geographic Information System (GIS) and Revised Universal Soil Loss Equation (RUSLE) in the Siwalik Hills of Nawalparasi, Nepal. Journal of Water and Climate Change 12, 1958–1974. https://doi.org/10.2166/wcc.2021.198

Tiwari, K., Chong, N.Y., 2019. Multi-robot Exploration for Environmental Monitoring: The Resource Constrained Perspective. Academic Press.

Todisco, F., Brocca, L., Termite, L.F., Wagner, W., 2015. Coupling rainfall observations and satellite soil moisture for predicting event soil loss in Central Italy, in: EGU General Assembly Conference Abstracts. p. 12179.

Toy, T.J., Foster, G.R., Renard, K.G., 1999. RUSLE for mining, construction and reclamation lands. Journal of Soil and Water Conservation 54, 462–467.

Trenberth, K.E., 2011. Changes in precipitation with climate change. Climate Research 47, 123–138. https://doi.org/10.3354/cr00953

Trigunasih, N.M., Saifulloh, M., 2023. Investigation of Soil Erosion in Agro-Tourism area: Guideline for Environmental Conservation Planning.

Trimble, S.W., Crosson, P., 2000. US soil erosion rates–myth and reality. Science 289, 248–250. https://doi.org/10.1126/science.289.5477.248

Trucano, T.G., Swiler, L.P., Igusa, T., Oberkampf, W.L., Pilch, M., 2006. Calibration, validation, and sensitivity analysis: What's what. Reliability Engineering & System Safety 91, 1331–1357. https://doi.org/10.1016/j.ress.2005.11.031

Tsegaye, L., Bharti, R., 2021. Soil erosion and sediment yield assessment using RUSLE and GIS-based approach in Anjeb watershed, Northwest Ethiopia. SN Applied Sciences 3, 1–19. https://doi.org/10.1007/s42452-021-04564-x

Tsige, M.G., Malcherek, A., Seleshi, Y., 2022. Improving the Modified Universal Soil Loss Equation by Physical Interpretation of Its Factors. Water 14, 1450. https://doi.org/10.3390/w14091450

USDA_ARS, 2004. Revised Universal Soil Loss Equation RUSLE. Retrieved at https://www.ars.usda.gov/southeast-area/oxford-ms/national-sedimentation-laboratory/watershed-physical-processes-research/docs/revised-universal-soil-loss-equation-rusle-welcome-to-rusle-1-and-rusle-2/ on February 22nd 2023.
Usman, K., Deribew, K.T., Alemu, G., Hailu, S., 2023. Spatial modeling of soil loss as a response to land use-land cover change in Didessa sub-basin, the agricultural watershed of Ethiopia. Heliyon. https://doi.org/10.1016/j.heliyon.2023.e14590
Van, D.K., Jones, R., Montanarella, L., 2000. Soil erosion risk assessment in Europe. Luxembourg: Office for Official Publications of the European Communities.
Van Rompaey, A.J., Verstraeten, G., Van Oost, K., Govers, G., Poesen, J., 2001. Modelling mean annual sediment yield using a distributed approach. Earth Surface Processes and Landforms 26, 1221–1236. https://doi.org/10.1002/esp.275
Vanmaercke, M., Maetens, W., Poesen, J., Jankauskas, B., Jankauskiene, G., Verstraeten, G., de Vente, J., 2012. A comparison of measured catchment sediment yields with measured and predicted hillslope erosion rates in Europe. Journal of Soils and Sediments 12, 586–602. https://doi.org/10.1007/s11368-012-0479-z
Vanmaercke, M., Poesen, J., Broeckx, J., Nyssen, J., 2014. Sediment yield in Africa. Earth-Science Reviews 136, 350–368. https://doi.org/10.1016/j.earscirev.2014.06.004
Vicente-Serrano, S.M., Beguería, S., López-Moreno, J.I., 2010. A multiscalar drought index sensitive to global warming: the standardized precipitation evapotranspiration index. Journal of climate 23, 1696–1718. https://doi.org/10.1175/2009JCLI2909.1
Vieira, D.C.S., Serpa, D., Nunes, J.P.C., Prats, S.A., Neves, R., Keizer, J.J., 2018. Predicting the effectiveness of different mulching techniques in reducing post-fire runoff and erosion at plot scale with the RUSLE, MMF and PESERA models. Environmental Research 165, 365–378. https://doi.org/10.1016/j.envres.2018.04.029
Villarino, S.H., Studdert, G.A., Baldassini, P., Cendoya, M.G., Ciuffoli, L., Mastrángelo, M., Piñeiro, G., 2017. Deforestation impacts on soil organic carbon stocks in the Semiarid Chaco Region, Argentina. Science of the total environment 575, 1056–1065. https://doi.org/10.1016/j.scitotenv.2016.09.175
Vincent, L.A., Wang, X.L., Milewska, E.J., Wan, H., Yang, F., Swail, V., 2012. A second generation of homogenized Canadian monthly surface air temperature for climate trend analysis. Journal of Geophysical Research: Atmospheres 117. https://doi.org/10.1029/2012JD017859
Volpe, E., Ciabatta, L., Salciarini, D., Camici, S., Cattoni, E., Brocca, L., 2021. The impact of probability density functions assessment on model performance for slope stability analysis. Geosciences 11, 322. https://doi.org/10.3390/geosciences11080322
Vrieling, A., 2006. Satellite remote sensing for water erosion assessment: A review. Catena 65, 2–18. https://doi.org/10.1016/j.catena.2005.10.005

Walter, M.T., Mehta, V.K., Marrone, A.M., Boll, J., Gérard-Marchant, P., Steenhuis, T.S., Walter, M.F., 2003. Simple estimation of prevalence of Hortonian flow in New York City watersheds. Journal of Hydrologic Engineering 8, 214–218. https://doi.org/10.1061/(ASCE)1084-0699(2003)8:4(214)

Wang, B., Zheng, F., Guan, Y., 2016. Improved USLE-K factor prediction: A case study on water erosion areas in China. International Soil and Water Conservation Research 4, 168–176. https://doi.org/10.1016/j.iswcr.2016.08.003

Wang, G., Innes, J., Yusheng, Y., Shanmu, C., Krzyzanowski, J., Jingsheng, X., Wenlian, L., 2012. Extent of soil erosion and surface runoff associated with large-scale infrastructure development in Fujian Province, China. Catena 89, 22–30.

Wang, J., He, Q., Zhou, P., Gong, Q., 2019. Test of the RUSLE and Key Influencing Factors Using GIS and Probability Methods: A Case Study in Nanling National Nature Reserve, South China. Advances in Civil Engineering 2019. https://doi.org/10.1155/2019/7129639

Wang, S., Xu, X., Huang, L., 2023. Spatial and Temporal Variability of Soil Erosion in Northeast China from 2000 to 2020. Remote Sensing 15, 225. https://doi.org/10.3390/rs15010225

Wang, X.L., Chen, H., Wu, Y., Feng, Y., Pu, Q., 2010. New techniques for the detection and adjustment of shifts in daily precipitation data series. Journal of Applied Meteorology and Climatology 49, 2416–2436. https://doi.org/10.1175/2010JAMC2376.1

Wang, Y., Cheng, C., Xie, Y., Liu, B., Yin, S., Liu, Y., Hao, Y., 2017. Increasing trends in rainfall-runoff erosivity in the Source Region of the Three Rivers, 1961–2012. Science of the Total Environment 592, 639–648. https://doi.org/10.1016/j.scitotenv.2017.02.235

Wang, Y.Q., Shao, M.A., 2013. Spatial variability of soil physical properties in a region of the Loess Plateau of PR China subject to wind and water erosion. Land Degradation & Development 24, 296–304. https://doi.org/10.1002/ldr.1128

Wati, S.E., Hastuti, T., Widjojo, S., Pinem, F., 2010. Landslide susceptibility mapping with heuristic approach in mountainous area: A case study in Tawangmangu sub district Central Java, Indonesia. International archives of the photogrammetry, remote sensing and spatial information science 38.

Wawer, R., Nowocien, E., Podolski, B., 2005. Eal and calculated kusle erobility factor for selected Polish soils. Polish Journal of Environmental Studies 14, 655–658.

Webb, N.P., Stokes, C.J., 2012. Climate change scenarios to facilitate stakeholder engagement in agricultural adaptation. Mitigation and Adaptation Strategies for Global Change 17, 957–973. https://doi.org/10.1007/s11027-011-9355-1

Wei, H., Zhang, Y., Wang, F., Che, G., Li, Q., 2018. Experimental research on resilient modulus of silty clay modified by oil shale ash and fly ash after freeze-thaw cycles. Applied Sciences 8, 1298. https://doi.org/10.3390/app8081298

Wendt, R.C., Alberts, E.E., Hjelmfelt Jr, A.T., 1986. Variability of runoff and soil loss from fallow experimental plots. Soil Science Society of America Journal 50, 730–736. https://doi.org/10.2136/sssaj1986.03615995005000030035x

Wener, C.G., 1981. Soil Conservation In Kenya, Nairobi. Ministry of Agriculture, Soil Conservation Extension Unit.
White, G.W., Fox, M.H., Rooney, C., Cahill, A., 2007. Assessing the impact of Hurricane Katrina on persons with disabilities. Research and Training Center on Independent Living, University of Kansas.
Williams, J.R., Renard, K.G., Dyke, P.T., 1983. EPIC: A new method for assessing erosion's effect on soil productivity. Journal of Soil and water Conservation 38, 381–383.
Wischmeier, W.H., Mannering, J.V., 1969. Relation of soil properties to its erodibility. Soil science society of America journal 33, 131–137. https://doi.org/10.2136/sssaj1969.03615995003300010035x
Wischmeier, W.H., Smith, D.D., 1978. Predicting rainfall erosion losses: a guide to conservation planning. Department of Agriculture, Science and Education Administration.
Wischmeier, W.H., Smith, D.D., 1958. Rainfall energy and its relationship to soil loss. Eos, Transactions American Geophysical Union 39, 285–291. https://doi.org/10.1029/TR039i002p00285
Woldeyohannis, Y.S., Hiremath, S.S., Tola, S., Wako, A., 2022. Investigation of Soil Physiochemical Properties Effects on Soil Compaction for a Long Year Tilled Farmland. Applied and Environmental Soil Science 2022. https://doi.org/10.1155/2022/8626200
Wu, G.-L., Liu, Y.-F., Cui, Z., Liu, Y., Shi, Z.-H., Yin, R., Kardol, P., 2020. Trade-off between vegetation type, soil erosion control and surface water in global semi-arid regions: A meta-analysis. Journal of Applied Ecology 57, 875–885. https://doi.org/10.1111/1365-2664.13597
Wu, Q., Chen, Y., Wilson, J.P., Tan, H., Chu, T., 2021. A new approach for calculating the slope length factor in the Revised Universal Soil Loss Equation. Journal of Soil and Water Conservation 76, 153–165. https://doi.org/10.2489/jswc.2021.00085
Wu, Y., Li, X., Yu, L., Wang, T., Wang, J., Liu, T., 2022. Review of soil heavy metal pollution in China: Spatial distribution, primary sources, and remediation alternatives. Resources, Conservation and Recycling 181, 106261. https://doi.org/10.1016/j.resconrec.2022.106261
Xiong, M., Sun, R., Chen, L., 2019. A global comparison of soil erosion associated with land use and climate type. Geoderma 343, 31–39. https://doi.org/10.1016/j.geoderma.2019.02.013
Yang, S., Luo, D., Han, H., Jin, Z., 2023. Soil erosion differences in paired grassland and forestland catchments on the Chinese Loess Plateau. Journal of Mountain Science 20, 1336–1348. https://doi.org/10.1007/s11629-022-7623-z
Yang, X., 2015. Digital mapping of RUSLE slope length and steepness factor across New South Wales, Australia. Soil Research 53, 216–225. https://doi.org/10.1071/SR14208
Yaswanth, K., Kona, M., Andra, S.K., Rathinasamy, M., 2022. Understanding the impact of changes in land-use land-cover and rainfall patterns on soil erosion rates using the RUSLE model and GIS techniques: A study on the Nagavali

River basin. Journal of Water and Climate Change 13, 2648–2670. https://doi.org/10.2166/wcc.2022.016
Yigez, B., Xiong, D., Zhang, B., Yuan, Y., Baig, M.A., Dahal, N.M., Guadie, A., Zhao, W., Wu, Y., 2021. Spatial distribution of soil erosion and sediment yield in the Koshi River Basin, Nepal: a case study of Triyuga watershed. Journal of Soils and Sediments 21, 3888–3905. https://doi.org/10.1007/s11368-021-03023-9
Yoder, D.C., Foster, G.R., Weesies, G.A., Renard, K.G., McCool, D.K., Lown, J.B., 2001. Evaluation of the RUSLE soil erosion model. Agricultural non-point source water quality model: their use and application. Dans: Parsons et al 107–117.
Yoshida, Y., Kuwano, J., Kuwano, R., 1991. Effects of saturation on shear strength of soils. Soils and foundations 31, 181–186. https://doi.org/10.3208/sandf1972.31.181
Young, R.A., Onstad, C.A., Bosch, D.D., Anderson, W.P., 1989. AGNPS: A nonpoint-source pollution model for evaluating agricultural watersheds. Journal of soil and water conservation 44, 168–173.
Yu, C., Wang, H., Zhou, A., Cai, X., Wu, Z., 2019. Experimental study on strength and microstructure of cemented soil with different suctions. Journal of Materials in Civil Engineering 31, 04019082. https://doi.org/10.1061/(ASCE)MT.1943-5533.0002717
Yuan, L., Yue, K., Gu, Z., Chen, H., Chi, Y., 2021. Analysis of Rainfall Factors and Soil Erosion in Different Soil and Water Conservation Measures in the Karst Plateau-Mountain. Polish Journal of Environmental Studies 30. https://doi.org/10.15244/pjoes/135824
Yue, S., Wang, C., 2004. The Mann-Kendall test modified by effective sample size to detect trend in serially correlated hydrological series. Water resources management 18, 201–218. https://doi.org/10.1023/B:WARM.0000043140.61082.60
Yue, S., Wang, C.Y., 2002. Applicability of prewhitening to eliminate the influence of serial correlation on the Mann-Kendall test. Water resources research 38, 4–1. https://doi.org/10.1029/2001WR000861
Zabihi, M., Mirchooli, F., Motevalli, A., Darvishan, A.K., Pourghasemi, H.R., Zakeri, M.A., Sadighi, F., 2018. Spatial modelling of gully erosion in Mazandaran Province, northern Iran. Catena 161, 1–13. https://doi.org/10.1016/j.catena.2017.10.010
Zakour, M.J., Gillespie, D.F., 2013. Vulnerability theory, in: Community Disaster Vulnerability. Springer, pp. 17–35.
Zanchin, M., Moura, M.M. de, Nunes, M.C.M., Beskow, S., Miguel, P., Lima, C.L.R. de, Bressiani, D. de A., 2021. Soil loss estimated by means of the RUSLE model in a subtropical climate watershed. Revista Brasileira de Ciência do Solo 45. https://doi.org/10.36783/18069657rbcs20210050
Zerihun, M., Mohammedyasin, M.S., Sewnet, D., Adem, A.A., Lakew, M., 2018. Assessment of soil erosion using RUSLE, GIS and remote sensing in NW Ethiopia. Geoderma regional 12, 83–90. https://doi.org/10.1016/j.geodrs.2018.01.002

Zhang, B., Zhao, Q.G., Horn, R., Baumgartl, T., 2001. Shear strength of surface soil as affected by soil bulk density and soil water content. Soil and tillage research 59, 97–106. https://doi.org/10.1016/S0167-1987(01)00163-5

Zhang, H., Wei, J., Yang, Q., Baartman, J.E., Gai, L., Yang, X., Li, S., Yu, J., Ritsema, C.J., Geissen, V., 2017a. An improved method for calculating slope length (λ) and the LS parameters of the Revised Universal Soil Loss Equation for large watersheds. Geoderma 308, 36–45. https://doi.org/10.1016/j.geoderma.2017.08.006

Zhang, H., Yang, Q., Li, R., Liu, Q., Moore, D., He, P., Ritsema, C.J., Geissen, V., 2013. Extension of a GIS procedure for calculating the RUSLE equation LS factor. Computers & Geosciences 52, 177–188. https://doi.org/10.1016/j.cageo.2012.09.027

Zhang, H., Yao, Z., Yang, Q., Li, S., Baartman, J.E., Gai, L., Yao, M., Yang, X., Ritsema, C.J., Geissen, V., 2017b. An integrated algorithm to evaluate flow direction and flow accumulation in flat regions of hydrologically corrected DEMs. Catena 151, 174–181. https://doi.org/10.1016/j.catena.2016.12.009

Zhang, X., Yang, F., 2004. RClimDex 10 user manual Climate Research Branch Environment Canada. P22.

Zhao, L., Fang, Q., Hou, R., Wu, F., 2021. Effect of rainfall intensity and duration on soil erosion on slopes with different microrelief patterns. Geoderma 396, 115085. https://doi.org/10.1016/j.geoderma.2021.115085

Zhu, F., Cheng, J., 2022. Comparison of the effects of litter decomposition process on soil erosion under simulated rainfall. Scientific Reports 12, 20929. https://doi.org/10.1038/s41598-022-25035-2

Zhu, Y., Li, W., Wang, D., Wu, Z., Shang, P., 2022. Spatial Pattern of Soil Erosion in Relation to Land Use Change in a Rolling Hilly Region of Northeast China. Land 11, 1253. https://doi.org/10.3390/land11081253

Ziadat, F.M., Taimeh, A.Y., 2013. Effect of rainfall intensity, slope, land use and antecedent soil moisture on soil erosion in an arid environment. Land Degradation & Development 24, 582–590. https://doi.org/10.1002/ldr.2239

Zingg, A.W., 1940. Degree and length of land slope as it affects soil loss in run-off. Agric. Engng. 21, 59–64.

Zornoza, R., Acosta, J.A., Bastida, F., Domínguez, S.G., Toledo, D.M., Faz, A., 2015. Identification of sensitive indicators to assess the interrelationship between soil quality, management practices and human health. Soil 1, 173–185. https://doi.org/10.5194/soil-1-173-2015

APPENDIX 1. SAMPLE OF THE SURVEY QUESTIONNAIRE

A. Quantitative- Household survey questions

Questionnaire for the inhabitants

I am Christopher Uche, a research student at Kwame Nkrumah University of Science and Technology, Kumasi Ghana studying soil erosion risks and farmers' adaptation strategies in your State.

The research seeks to assess the risks of erosion and farmers' adaptation strategies to soil erosion by exploring how the menace is perceived (awareness), the risks and what you do to adapt to it.

Your responses will be treated as confidential and will only be used for research purposes.

Thank you in anticipation for your willingness to attend to the questions. Below are the questions posed to you:

1. Household head: Name of village:
2. Date of the interview: Name of enumerator:
3. Age:

Section A: Demographic and Social Characteristics (Tick the right ones)

Code	Question	Answer (cross)
GENDR	Gender	1. Male 2. Female
MARIT	Marital status	1. Married 2. Single 3. Divorced 4. widow
RELIG	Religion	1. Catholic

		2. Anglican 3. Protestant 4. Muslim 5. ATR 6. Others
EDUCA	Education	1. None 2. Primary 3. Secondary 4. Tertiary 5. Others
OCCUP	Occupation	1. Small-scale farmer 2. Civil servant 3. Student 4. Artisan 5. Trader 6. Driver/Mechanic 7. Unemployed 8. Others

Section B.

B.1. Family and family size

How many people live in your house? ………….

Number of males	Number of females	The household head*	Age of the household head

Section B2

Land ownership

1. Please, do you own farm land? Yes, No
2. If yes, what is the average size and main crops grown?
3. Quantity of harvest last season

Main crops	Area grown in hectares	Quantity harvested
1		
2		
3		
4		
5		
Others		

4. Compared to previous years, is harvest increasing now?

Section B3

Perception of Climate Change and soil erosion

1.Have you heard of climate change?

2.What do you understand by climate change?

3. How is climate change affecting your farming activities?

4 What are the causes of climate change?

5.Does it affect your agricultural practices and productivity?

6. Do extension service workers visit you regularly?

Section C. Farmers' perception of soil erosion

C.1. Noticed erosion and climate change related events

1. Do you know soil erosion?

2. Has it increased in recent years?

3. What do you think is causing the increasing problem of erosion?....................

	Your perception of the following in the past years	Yes	No
	Do you think erosion is an environmental problem?		
Indicators of soil erosion	Has soil erosion become a bigger problem and frequent now?		
	Has flooding become more frequent?		
	How do you notice erosion? Rills on farm		
	Shallow soil depth		
	Declining productivity		
	Soil washed away from farmland		
	Change in soil colour		
	Shallow soil depth		
	Loss of manure/fertilizer		
	Gullies		
	Sediments in ditches and washing off seedlings		
	Exposed plant roots		
	Is rain of high intensity nowadays?		
	Does heavy rainfall of long duration occur now?		
	Does rainy season start early?		
	Does rainy season end late?		
	Is temperature higher nowadays?		
	Has rainfall become unreliable and unpredictable?		
	Does rainy season seem to be shorter?		
	Do you think nights are becoming warmer now than before?		
Others			

5. What are the causes of soil erosion?

Factors	Yes	No
Improper or over-cultivation		
High slope		
Deforestation		
Heavy rainfall		
Absence of SWC practices		
Easily erodible soils		
High population/more corrugated houses		
Sand mining and nonchalance		

Adaptation Strategies

Statement	yes	no
You practice mixed cropping		
You grow more leguminous crops		
You cultivate fewer plots		
You practice no-tillage		
You grow more resilient crops		
You depend on remittances now		
You depend more on non-farm activities now than in the past years		
You do mulching		
You do terracing		
You practice contour farming		
Runoff diversion		
Solid bunds (embankment) and sand bags		
Hedging or shelterbelts/tree planting		
You construct check dams or detention pits		
Insufficient funds and no cooperative society		
Stopped slash and burn agriculture		

You use planting pits		
Straw and residue retention after harvest		
Others, specify		

Limitations to adaptation

Statement	Yes	No
Increasing climate variability		
Low financial capacity		
Unavailability of the weather forecast		
Poor agronomic activities		
Poor knowledge of climate change adaptation mechanisms		
Non-adaptability of modern farming practices		
Youth migration		
Increased deforestation		
Insufficient government support		
Others		

Have you observed the following soil erosion and climate change impacts in the past 5 years?

Erosion related impacts/shocks	Yes	No
A decline in crop yields/poor harvest		
Food insecurity or shortage		
Increased or invasive weeds		
Farming becoming unattractive due to poor yield		
Others		

F.1. Information sources

Do you use the following information sources?	Yes	No
Radio		

Television		
Newspaper		
Leaflets/posters		
Extension workers		
Others, specify		

F. 2. Rating weather-related information

How do you rate weather-related information ?	1=Poor, 2=Average, 3=Good
Is the information timely and adequate?	
Is the information useful?	

Thank you participating

APPENDIX 2. RELATIONSHIP BETWEEN COHESION, SHEAR STRESS AND ANGLE OF INTERNAL FRICTION

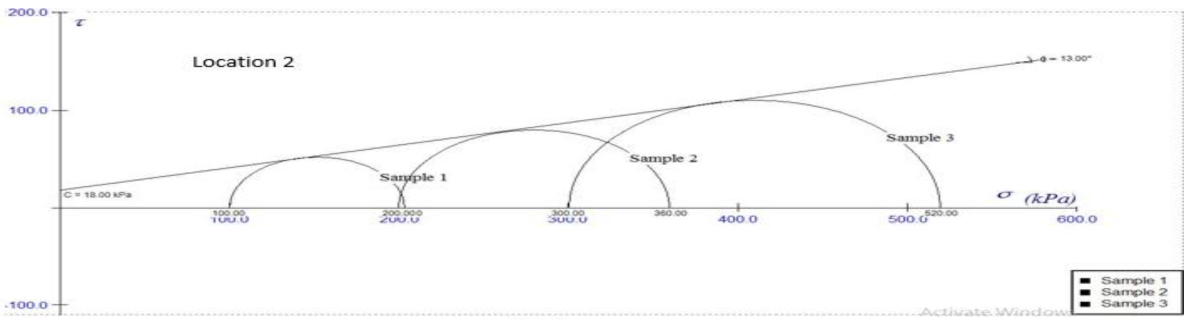

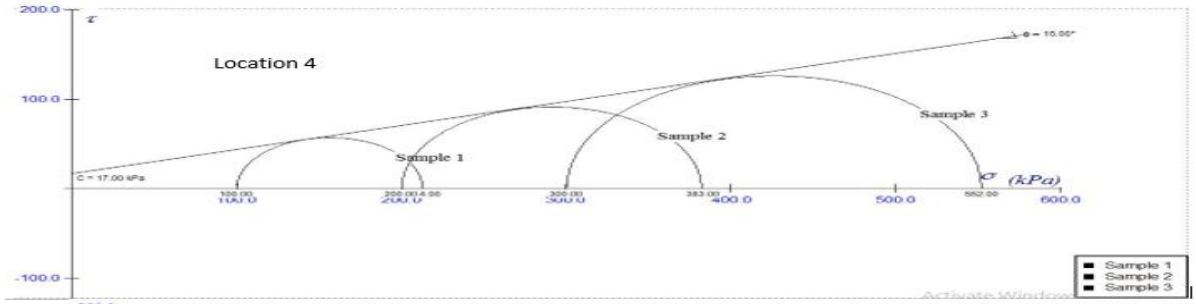

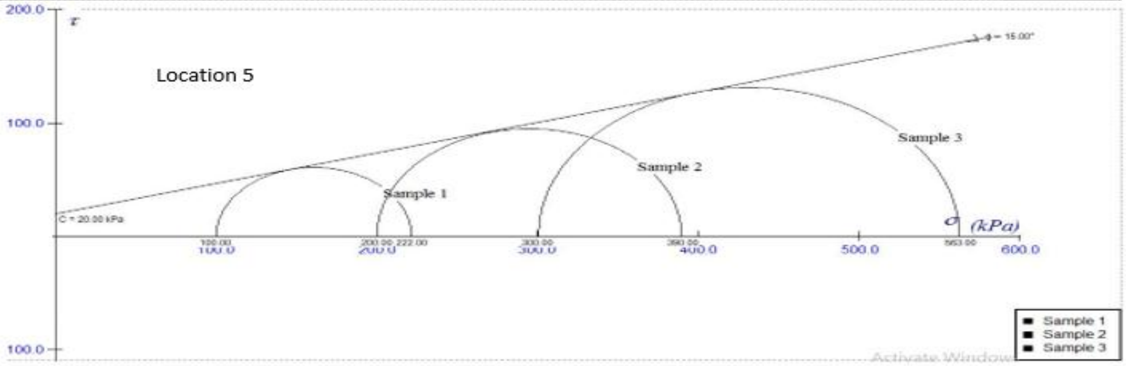

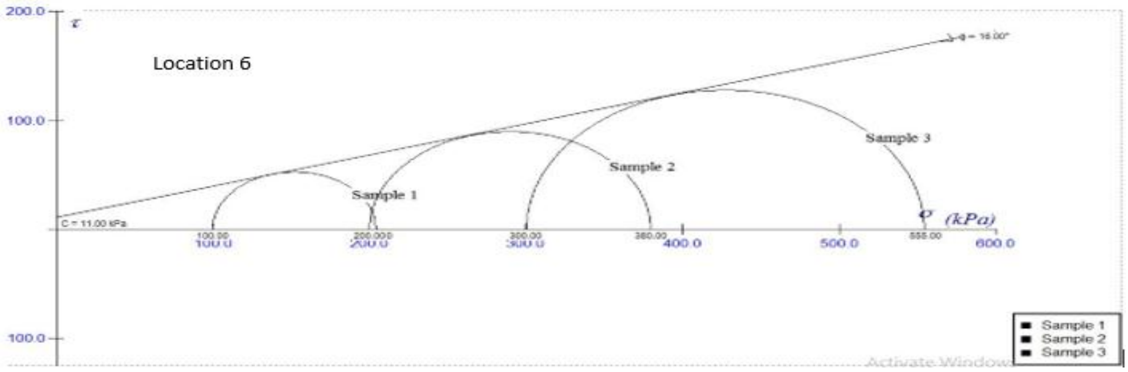

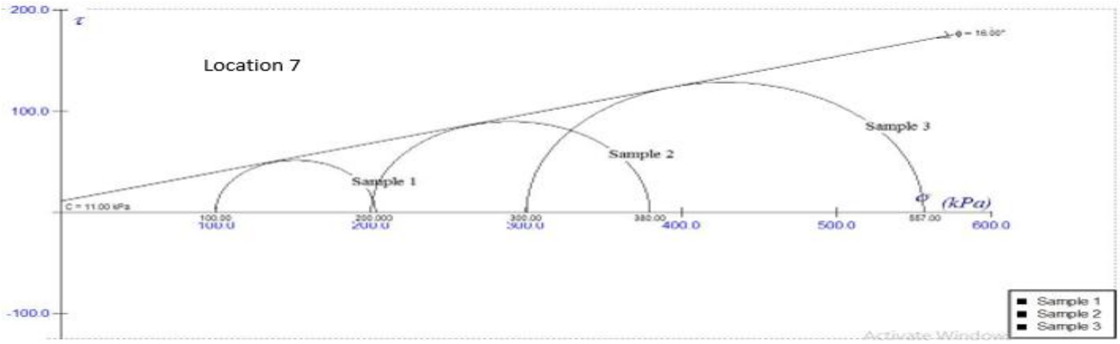
200.0
100.0
-100.0
τ
Location 7
φ = 16.00°
Sample 1
Sample 2
Sample 3
C = 11.00 kPa
100.00
200.000
300.00
380.00
557.00
σ (kPa)
100.0
200.0
300.0
400.0
500.0
600.0
Sample 1
Sample 2
Sample 3

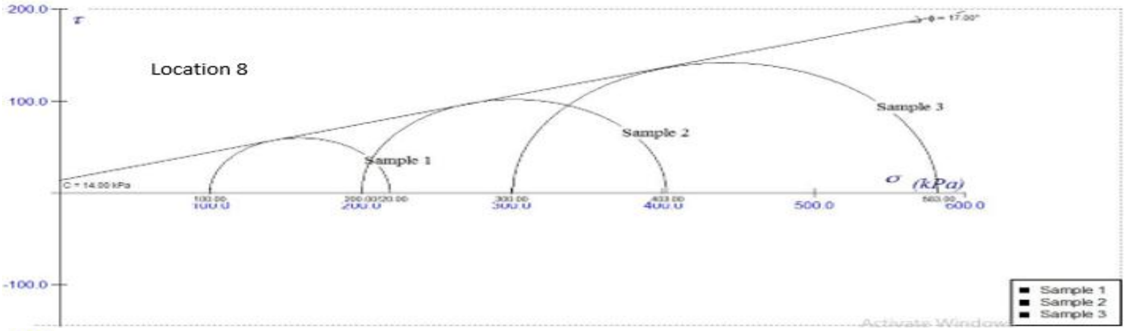
200.0
100.0
-100.0
τ
Location 8
φ = 17.00°
Sample 1
Sample 2
Sample 3
C = 14.00 kPa
σ (kPa)
100.0
200.0
300.0
400.0
500.0
600.0
Sample 1
Sample 2
Sample 3

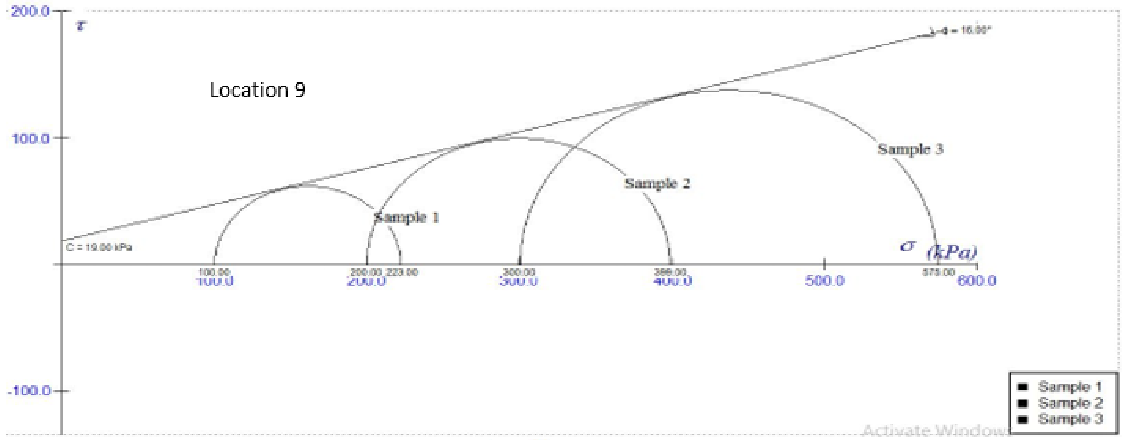
200.0
100.0
-100.0
τ
Location 9
φ = 16.00°
Sample 1
Sample 2
Sample 3
C = 19.00 kPa
100.00
200.00 223.00
300.00
399.00
575.00
σ (kPa)
100.0
200.0
300.0
400.0
500.0
600.0
Sample 1
Sample 2
Sample 3

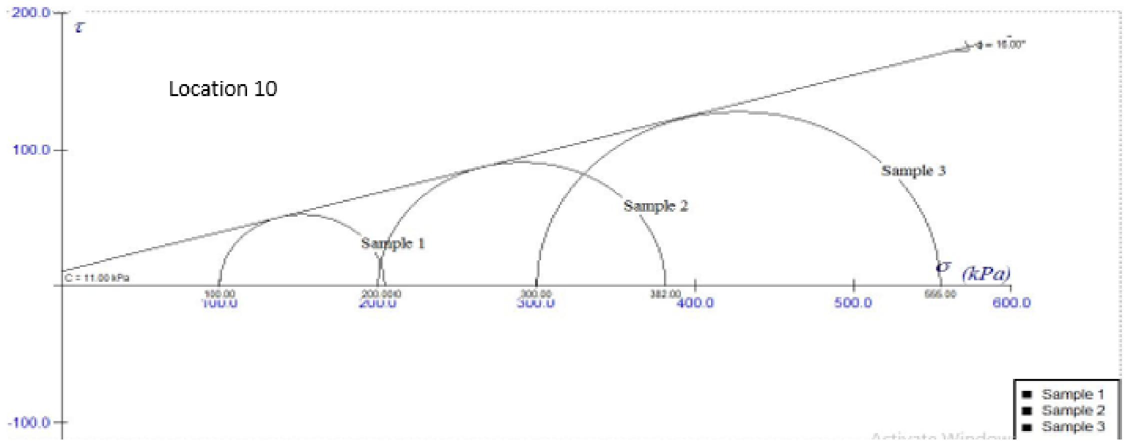
200.0
100.0
-100.0
τ
Location 10
Sample 1
Sample 2
Sample 3
C = 11.00 kPa
100.00
300.00
382.00
565.00
σ (kPa)
100.0
200.0
300.0
400.0
500.0
600.0
Sample 1
Sample 2
Sample 3

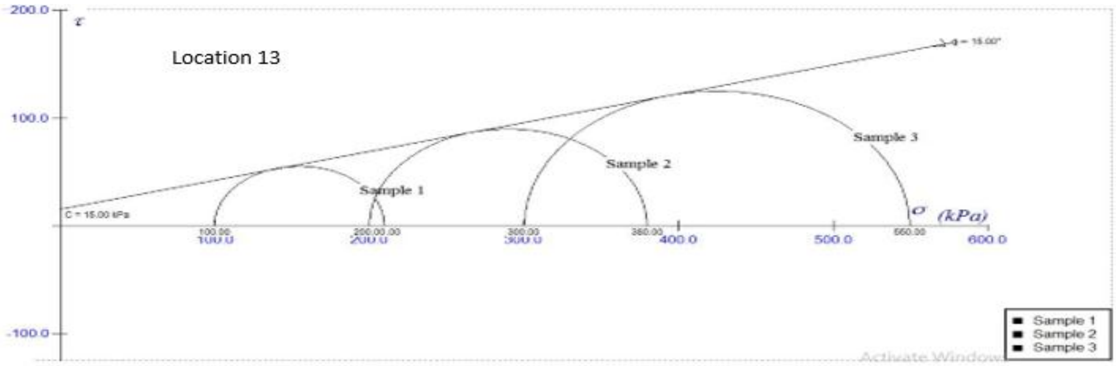
Location 13
τ
200.0
100.0
-100.0
φ = 15.00°
C = 15.00 kPa
Sample 1
Sample 2
Sample 3
100.0
200.0
300.0
400.0
500.0
600.0
σ (kPa)
Sample 1
Sample 2
Sample 3

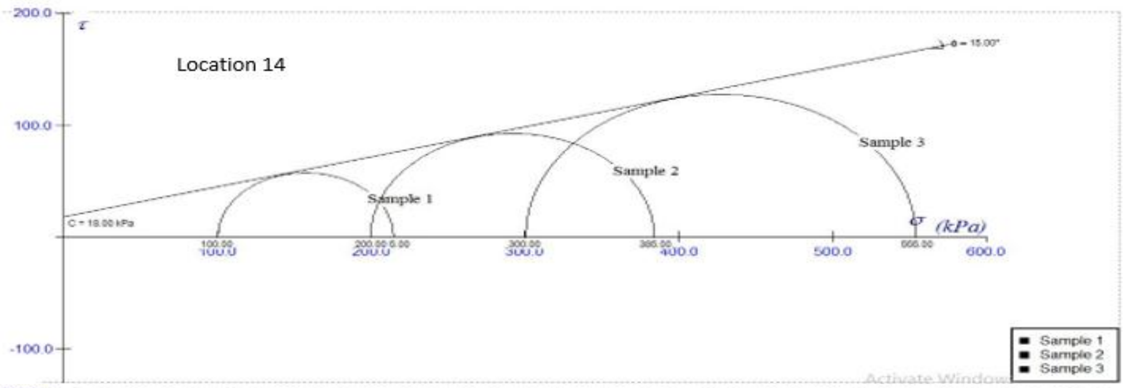
Location 14
τ
200.0
100.0
-100.0
φ = 15.00°
C = 18.00 kPa
Sample 1
Sample 2
Sample 3
100.0
200.0
300.0
400.0
500.0
600.0
σ (kPa)
Sample 1
Sample 2
Sample 3

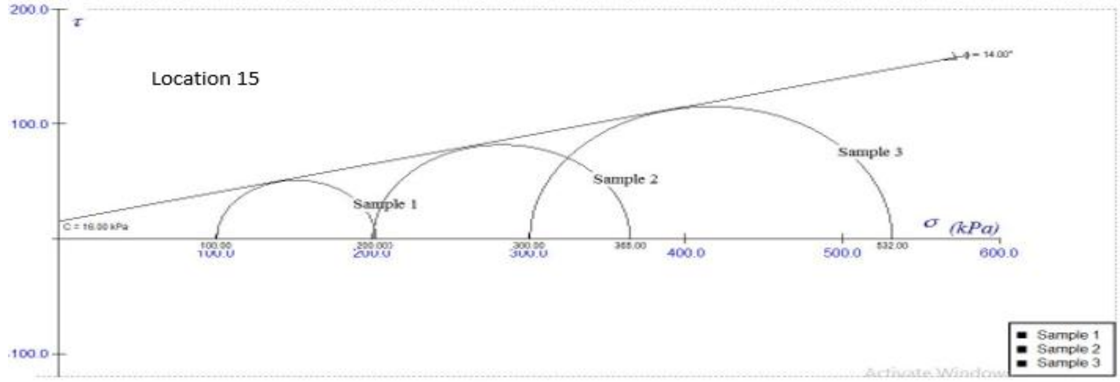
Location 15
τ
200.0
100.0
-100.0
φ = 14.00°
C = 16.00 kPa
Sample 1
Sample 2
Sample 3
100.0
200.0
300.0
400.0
500.0
600.0
σ (kPa)
Sample 1
Sample 2
Sample 3

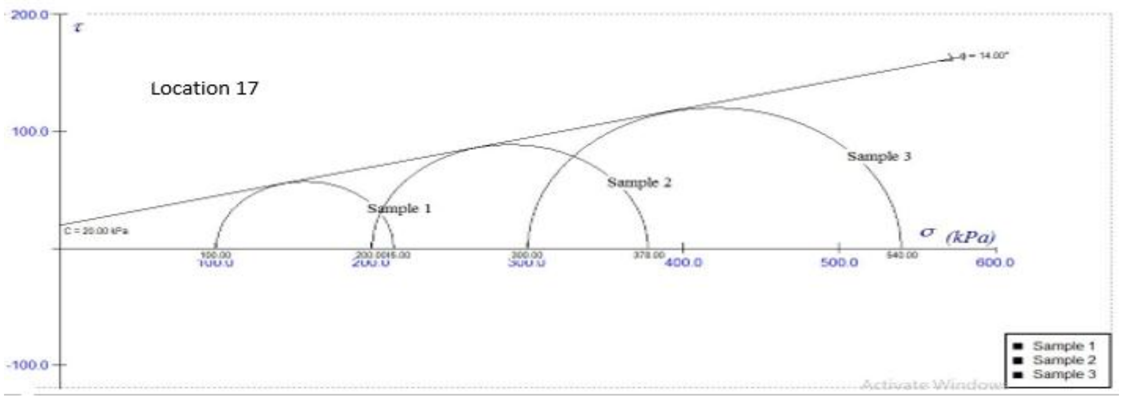
Location 17
τ
200.0
100.0
-100.0
φ = 14.00°
C = 20.00 kPa
Sample 1
Sample 2
Sample 3
100.0
200.0
300.0
400.0
500.0
600.0
σ (kPa)
Sample 1
Sample 2
Sample 3

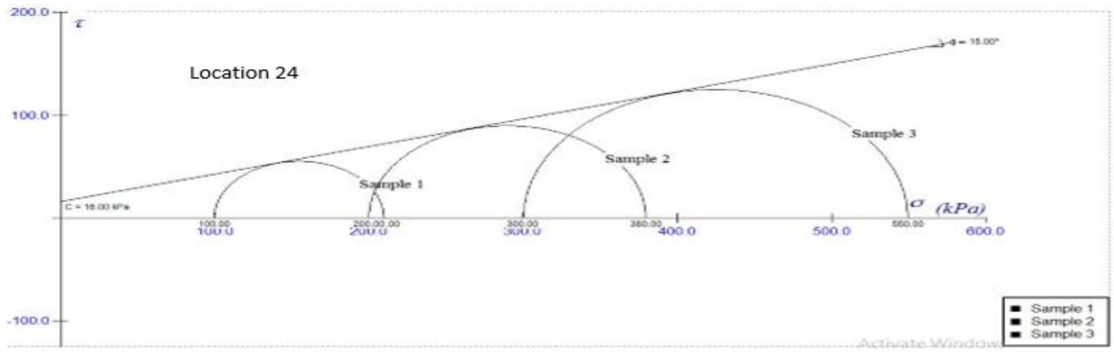
Location 24
200.0
100.0
-100.0
τ
σ (kPa)
C = 16.00 kPa
Sample 1
Sample 2
Sample 3
100.00
200.00
300.00
380.00
560.00
100.0
200.0
300.0
400.0
500.0
600.0
Sample 1
Sample 2
Sample 3

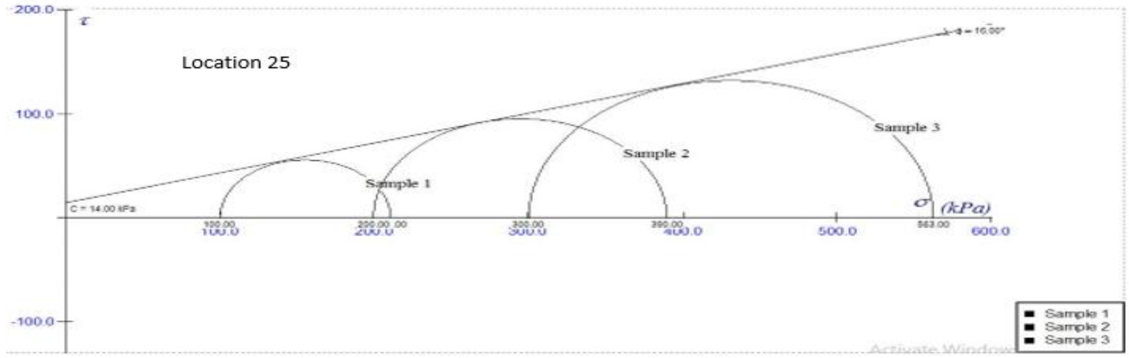
Location 25
200.0
100.0
-100.0
τ
σ (kPa)
C = 14.00 kPa
Sample 1
Sample 2
Sample 3
100.00
200.00
300.00
390.00
563.00
100.0
200.0
300.0
400.0
500.0
600.0
Sample 1
Sample 2
Sample 3

APPENDIX 3. RELATIONSHIP BETWEEN OMC AND MDD

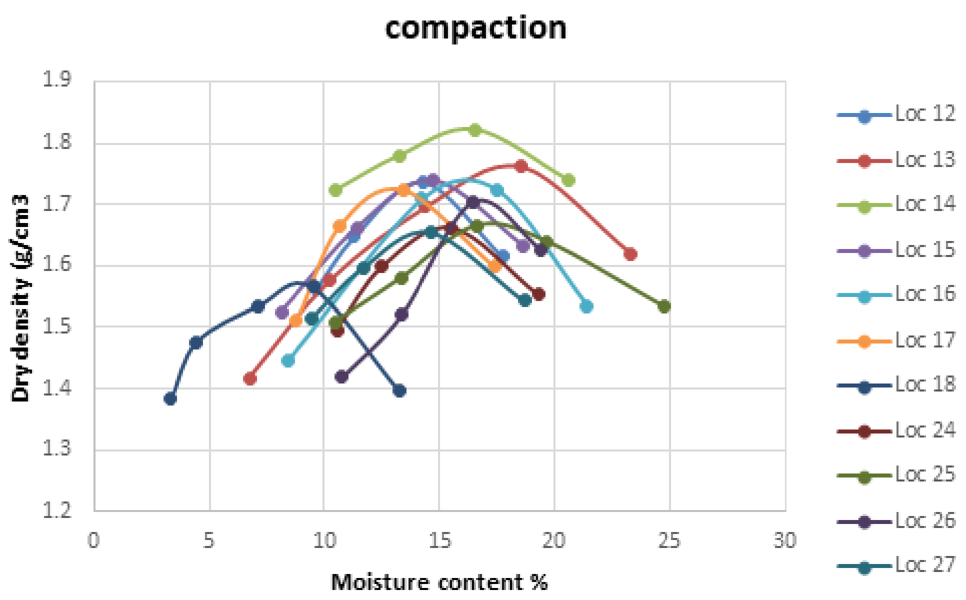

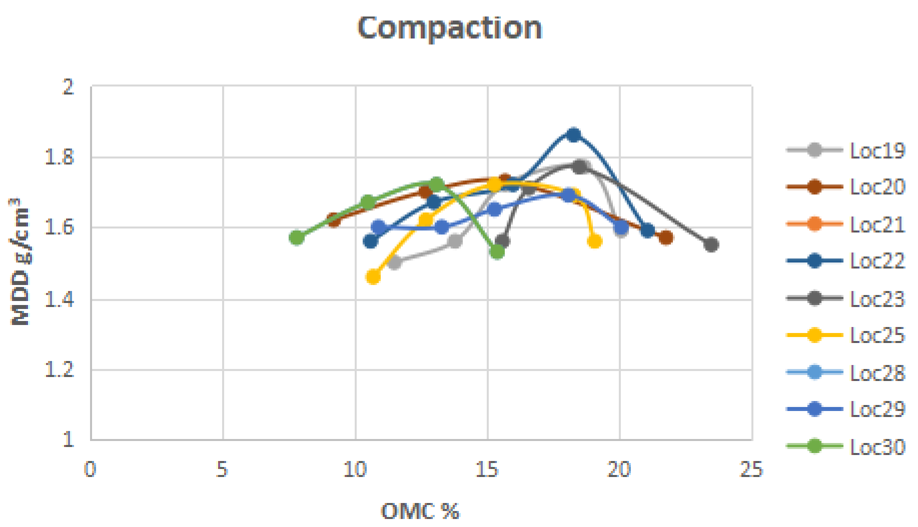

APPENDIX 4 TRIAXIAL AND ATTERBERG TESTS

SAMPLE NO.	DIRECT SHEAR BOX TEST			CONSISTENCY LIMITS TEST.			
	C (KN/M^2)	∅ (°)	γ (KN/M^3)	LL (%)	PL (%)	PI (%)	LS (%)
1	-	-	-	38.00	23.61	14.39	16.43
2	-	-	-	30.00	22.88	7.12	9.29
3	-	-	-	28.00	19.99	8.01	9.29
4	-	-	-	36.00	23.70	12.30	9.29
5	-	-	-	32.00	21.74	10.26	9.29
6	-	-	-	29.00	18.83	10.17	8.57
7	-	-	-	30.00	20.83	9.17	7.86
8	-	-	-	28.00	19.25	8.75	7.14
9	-	-	-	34.00	19.77	14.23	9.29
10	-	-	-	28.00	18.18	9.82	7.86
11	7	15	19.98	NP	NP	NP	NP
12	-	-	-	27.00	15.39	11.61	8.57
13	-	-	-	32.00	21.24	10.76	10.00
14	-	-	-	29.00	22.47	6.53	6.43
15	-	-	-	36.00	21.89	14.11	10.00
16	4	17	20.41	NP	NP	NP	NP
17	-	-	-	32.00	21.58	11.42	7.86
18	2	17	19.98	NP	NP	NP	NP
24	-	-	-	33.00	20.61	12.39	8.57
25	-	-	-	34.00	22.71	11.29	10.00
26	-	-	-	32.00	18.71	13.29	7.14

27	-	-	-	36.00	20.34	15.66	9.29
19	-	-	-	41.00	22.87	18.13	
20	-	-	-	27.00	20.90	6.10	
21	-	-	-	26.00	22.10	3.90	
22	-	-	-	31.00	22.50	8.50	
23	-	-	-	28.00	18.70	9.30	
24	-	-	-	30.00	10.60	19.40	
25	-	-	-	28.00	10.60	17.40	
30	-	-	-	27.00	21.21	5.79	

APPENDIX 5. RELATIONSHIP BETWEEN SOIL LOSS AND RUNOFF

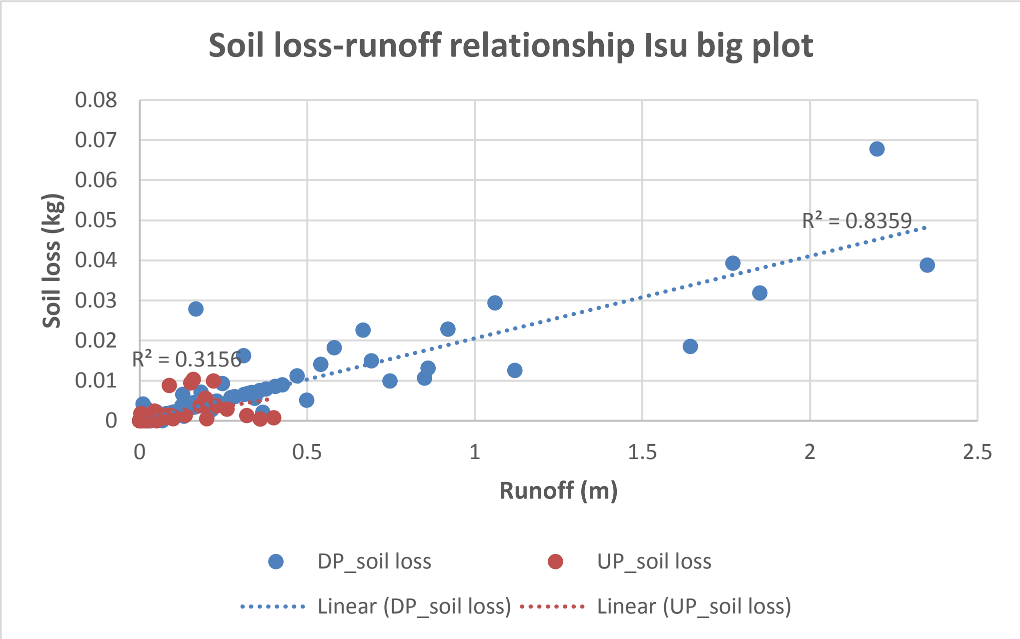

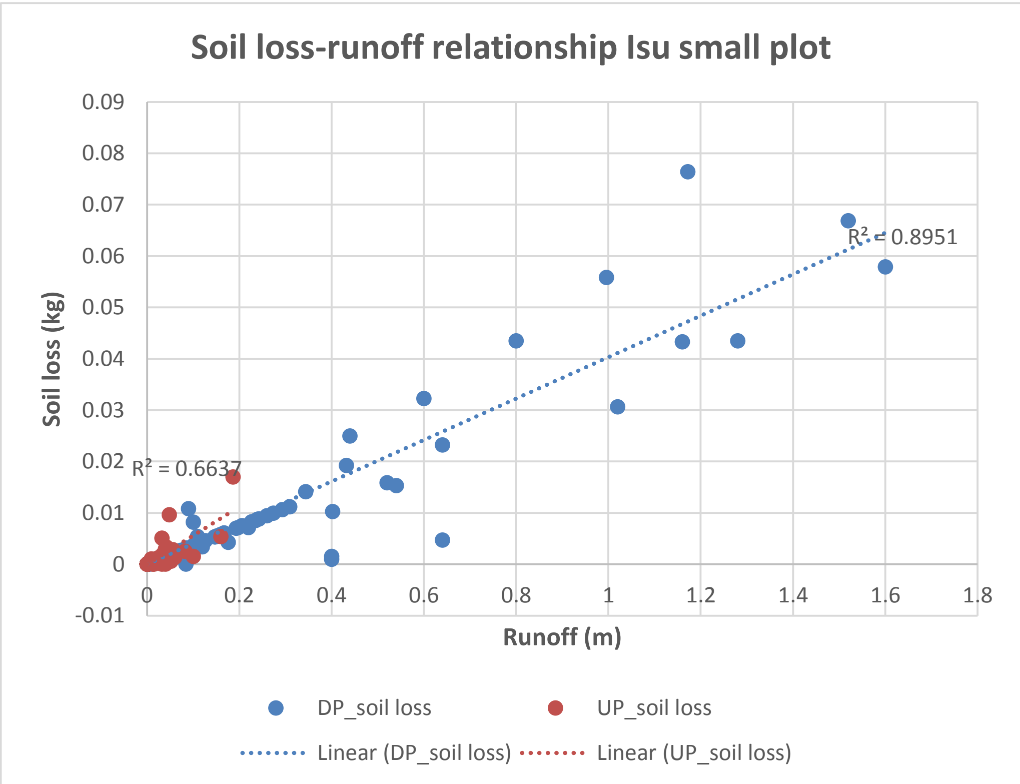

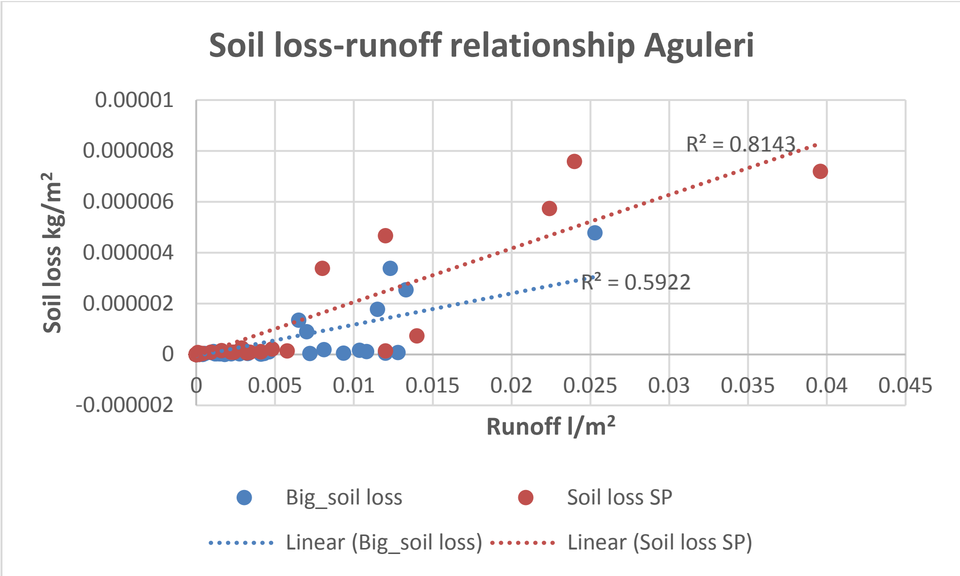
Soil loss-runoff relationship Aguleri
Soil loss kg/m²
0.00001
0.000008
0.000006
0.000004
0.000002
0
-0.000002
0
0.005
0.01
0.015
0.02
0.025
0.03
0.035
0.04
0.045
Runoff l/m²
R² = 0.8143
R² = 0.5922
Big_soil loss
Soil loss SP
Linear (Big_soil loss)
Linear (Soil loss SP)